



UNIVERSIDADE DE BRASÍLIA
INSTITUTO DE CIÊNCIAS BIOLÓGICAS
DEPARTAMENTO DE FITOPATOLOGIA
PROGRAMA DE PÓS-GRADUAÇÃO EM FITOPATOLOGIA

IVAIR JOSÉ DE MORAIS JÚNIOR

**Exploring the genomic diversity of potato virus Y and its
interaction with hosts**

BRASÍLIA – DF
2024

IVAIR JOSÉ DE MORAIS JÚNIOR

**Exploring the genomic diversity of potato virus Y and its
interaction with hosts**

Tese de doutorado apresentada ao Programa de Pós-Graduação em Fitopatologia da Universidade de Brasília, para obtenção do título de Doutor em Fitopatologia.

Orientador: Profa. Dra. Alice Kazuko Inoue Nagata

Coorientador: Prof. Dr. Santiago F. Elena Fito

BRASÍLIA – DF
2024

AGRADECIMENTOS

Nem sempre foi fácil, mas também não foi sempre difícil. Ficaria triste se essa tese fosse medida apenas pelos meus esforços ou pelos resultados obtidos, pois muito do que consegui não teria sido possível sozinho. Muitas pessoas cruzaram meu caminho ao longo desses anos; algumas chegaram e ficaram, trazendo risos e uma companhia que muito apreciei. Outras, por sua vez, tornaram a jornada um pouco mais desafiadora. A todas elas, meu sincero obrigado. Por bem ou por mal, cada uma contribuiu para que eu chegasse até aqui.

Esta tese não foi escrita por uma única mão (ou cérebro), mas pelas mãos de muitas pessoas, fruto dos esforços coletivos. Em especial, agradeço aos meus orientadores. Nunca tive a infelicidade de encontrar um mau orientador; pelo contrário, todos foram excelentes e me ensinaram a enxergar a ciência com entusiasmo.

À Alice Nagata, que não só me orientou, mas também me ajudou a crescer, estando ao meu lado em todos os momentos. Ela sempre sorriu com minhas pequenas conquistas e me impulsionou rumo ao desconhecido e promissor futuro que vivenciei no doutorado.

A Santiago Elena, que em va acollir, acompanyar, orientar i em va posar a la meua disposició tot el que estava al seu abast perquè poguera realitzar un treball excel·lent.

A Paqui de la Iglesia, sense la qual encara estaria fent les meues primeres passes; aquest treball mai hauria estat possible sense la seua ajuda.

Agradeço também, de forma especial, aos meus amigos do Laboratório de Virologia da Embrapa Hortaliças: Dorian, Jonas, Yanca, Bárbara, Gabriela, Valdemir, Malu, AnaLis, Erich e Wandressa. I als companys del Laboratório de Virología Evolutiva y de Sistemas, que em van ajudar en una adaptació que no va ser fàcil.

Aos meus pais, que jamais imaginaram ter um filho Doutor, mas que me apoiaram em todos os meus caminhos, por mais incertos que fossem.

Aos meus amigos Lais e Maike, que me ofereceram suporte emocional nos momentos mais difíceis.

Aos que permaneceram ao meu lado e que amo mais que tudo, meus queridos Cacao e Neve, e aos que se foram, especialmente Ada e Darwin.

Muitos nomes, todos lembrados com gratidão e felicidade.

A todos que me viram chorar e sorrir, enlouquecer e progredir, meu mais profundo agradecimento.

Resumo

O potyvirus potato virus Y (PVY) já foi considerado um dos cinco vírus mais importantes entre os vírus de plantas, devido à sua capacidade de infectar uma ampla gama de hospedeiros, ser transmitido por várias espécies de afídeos e causar prejuízos significativos em culturas de importância agrônômica. Sua rápida adaptação a novos ambientes, altas taxas de mutação e recombinação resultam em uma nuvem de mutantes conhecida como vírus *quasispecies*, capazes de se adaptar a condições diversas sobrevivendo no ambiente e se dispersando a novas regiões. Embora no passado alguns programas de melhoramento tenham focado no desenvolvimento de materiais com resistência à infecção por PVY, ainda existe uma grande lacuna de conhecimento sobre a interação do vírus com diferentes hospedeiros e as alterações genômicas resultantes dessa interação.

Para abordar essas questões, iniciamos a análise de isolados de PVY coletados em campos de produção de tomate (PVYSl), batata (PVYSt) e pimentão (PVYCa). Desenvolvemos um protocolo de sequenciamento genômico utilizando a tecnologia Nanopore de modo a sequenciar simultaneamente os genomas de PVYCa, PVYSt e PVYSl, reduzindo significativamente os custos operacionais. Foi também realizada uma avaliação de resistência a infecção por PVY de cultivares de tomate, pimentão e linhagens de *Solanum* spp. do Banco de Germoplasma do Instituto Agrônomo de Campinas. Observamos que nenhuma das cultivares de tomate, pimentão e acessos de banco de germoplasma avaliados apresentou resistência à infecção por PVY, indicando a necessidade urgente de busca por materiais com algum nível de resistência para o mercado e para programas de melhoramento.

Para a análise da influência do hospedeiro nas modificações genômicas, um experimento foi realizado com dois isolados virais (PVYNb, coletado em *Nicotiana benthamiana*, e PVYSt) com 10 passagens virais sucessivas por inoculação mecânica em plantas de *N. benthamiana*, tomateiro e batateira. PVYNb e PVYSt mostraram comportamentos distintos: diminuição e extinção da infecção viral em tomateiro, aumento expressivo em *N. benthamiana* e manutenção moderada em batateira. PVYNb apresentou maior especialização com mais SNPs fixados, indicando maior capacidade adaptativa a novos ambientes e hospedeiros, enquanto PVYSt se mostrou mais generalista com menos SNPs fixados. Além disso, investigamos a geração e

manutenção de genomas defectivos virais (GDVs) em diferentes populações de PVY. Foram identificados GDVs nas populações de PVY, cuja produção foi dependente do isolado viral, modo de transmissão, órgão da planta, passagem realizada e hospedeiro. Nossos achados fornecem informações para a elaboração de novas abordagens de recomendações de manejo e controle do PVY, promovendo avanços na sustentabilidade da produção agrícola.

Palavras-chaves: Alteração genômica, Ecologia de vírus, Evolução de vírus, Genomas defectivos virais (GDVs), Interação vírus-hospedeiro, Sequenciamento Nanopore, Suplantação de resistência

Exploring the genomic complexity of potato virus Y and its interaction with hosts

Abstract

The potyvirus potato virus Y (PVY) has been considered one of the five most important plant viruses due to its ability to infect a wide range of hosts, be transmitted by various aphid species, and cause significant damage to crops. Its rapid adaptation to new environments, high mutation and recombination rates result in a cloud of mutants known as *viral quasispecies*, capable of adapting to diverse conditions, surviving in the environment, and spreading to new regions. Although some breeding programs in the past focused on developing materials resistant to PVY infection, there remains a substantial gap in knowledge about the virus' interaction with different hosts and the resulting genomic alterations from this interaction.

To address these issues, we initiated the analysis of PVY isolates collected from tomato (PVYSl), potato (PVYSt), and pepper (PVYCa) production fields. A genomic sequencing protocol was developed using Nanopore technology so we could simultaneously sequence the genomes of PVYCa, PVYSt, and PVYSl, significantly reducing operational costs. We also evaluated the resistance to PVY infection of tomato and pepper cultivars, and *Solanum* spp. lines from the Germplasm Bank of the Instituto Agronômico de Campinas. None of the evaluated tomato, pepper cultivars, and germplasm bank accessions showed resistance to PVY infection, indicating an urgent need to find materials with some level of resistance for the market and breeding programs.

To analyze the host influence on genomic modifications, an experiment was conducted with two viral isolates (PVYNb, collected from *Nicotiana benthamiana*, and PVYSt) with 10 successive viral passages through mechanical inoculation in *N. benthamiana*, tomato, and potato plants. PVYNb and PVYSt exhibited different behaviors, displaying a decrease and extinction of viral infection in tomato plants, a significant increase in *N. benthamiana*, and moderate maintenance in potato plants. PVYNb showed greater specialization with more fixed SNPs, indicating a higher adaptive capacity to new environments and hosts, while PVYSt was more generalist with fewer fixed SNPs. Additionally, we investigated the generation and maintenance of defective viral genomes (DVGs) in different PVY populations. DVGs were identified in PVY

populations, whose production depended on the viral isolate, transmission mode, plant organ, passage performed, and host.

Our findings provide valuable information for developing new management and control recommendations for PVY, promoting advances in the sustainability of agricultural production.

Keywords: Genomic variation, Defective viral genomes (DVGs), Virus ecology, Virus evolution, Virus-host interaction, Nanopore sequencing, Overcoming resistance

1	Summary	
2	Introduction	1
3	References	8
4	General objective	12
5	Specific objectives:	12
6	UNRAVELING THE DYNAMICS OF HOST SPECIFICITY AND RESISTANCE RESPONSES TO	
7	POTATO VIRUS Y, AND IMPLICATIONS FOR CROP MANAGEMENT	13
8	Abstract	14
9	Main text	15
10	References	27
11	DETECTING AND SEQUENCING THE WHOLE-GENOME OF DISTINCT POTATO VIRUS Y	
12	ISOLATES USING A PCR-NANOPORE APPROACH	38
13	Abstract	38
14	Introduction	40
15	Materials and methods	42
16	Virus isolates collection	42
17	Nanopore primer design	43
18	Amplification of target region with PCR	43
19	ONT sequencing strategy	44
20	Sequencing analysis and genome assembly	44
21	Total RNA purification and Illumina sequencing	45
22	Genome analysis	45
23	Design and evaluation of PVY-specific primers	46
24	Results	46
25	Field collection and identification of PVY isolates	46
26	Nanopore primer design and evaluation	47

27	Nanopore sequencing results	49
28	Illumina sequencing results	54
29	Genome comparison and phylogenetics	54
30	PVY-specificity primers	56
31	Discussion	57
32	References	62
33	EXPERIMENTAL EVOLUTION OF HOST RANGE FOR TWO ISOLATES OF <i>POTYVIRUS</i>	
34	<i>YITUBEROSI</i>	80
35	Abstract	80
36	Introduction	81
37	Materials and methods	83
38	Plants and growth environment	83
39	Isolates, inoculation and collection	84
40	Primer design and RNA amplification	84
41	Evolution experiment	86
42	Transmission rate experiment	87
43	HTS and sequence analyses	88
44	Results	89
45	Test of transmission efficiency across host species	89
46	Variation of viral loads along the passage through the plants	92
47	Infectivity of evolved lineages depends on both the evolved environment and the test host	95
48	Changes in virulence and symptomatology	96
49	Genome alterations	99
50	Discussion	105
51	References	110
52	<i>IN SILICO</i> EVIDENCES FOR THE PRESENCE OF DEFECTIVE VIRAL GENOMES (DVGs) IN	
53	POTATO VIRUS <i>Y</i>-INFECTED PLANTS	123
54	Abstract	123

55	Introduction	125
56	Materials and methods	127
57	Datasets	127
58	DVGs identification	128
59	DVG analysis	129
60	Results	129
61	DVGs profile	129
62	Clustering DVGs	134
63	DVGs formation and distribution	136
64	DVGs diversity	139
65	Discussion	141
66	References	145
67	Concluding remarks	162
68		
69		

1 Introduction

2

3 Since Virology emerged as a scientific field in the late 19th and early 20th centuries
4 (Burrell et al. 2017), our understanding of viruses as pathogens affecting all kinds of
5 organisms has evolved dramatically. Early studies relied on physical, biological, and
6 electron microscopy techniques (Zuo et al. 2024). Today, methods such as genetic
7 engineering and deep sequencing have accelerated the advances in the field. For
8 example, we can now edit genomes, gain insights into viral infection dynamics and host
9 responses through single-cell sequencing, and visualize high-resolution 3D structures of
10 viral particles using Cryo-EM. Technology facilitated the development of antiviral
11 drugs targeting various stages of the viral infection cycle. Recombinant DNA
12 technology and mRNA vaccine platforms have further helped vaccine development, as
13 evidenced by the rapid creation of COVID-19 vaccines (Karikó et al. 2005; Baden et al.
14 2021; Polack et al. 2021).

15 While initial virus research primarily focused on plants, the significant impact of
16 viruses on human health often overshadows plant virology. However, plant viruses may
17 also cause huge damages, exemplified by important diseases such as tobacco mosaic
18 virus (TMV) in tobacco (Chen et al. 2014), potato virus Y (PVY) in potatoes (Nolte et
19 al. 2004), African cassava mosaic virus (ACMV) in cassava (Legg et al. 2011), barley
20 yellow dwarf virus (BYDV) in cereals (Choudhury et al. 2018), rice tungro virus (RTV)
21 in rice (Hibino et al. 1991), tomato yellow leaf curl virus (TYLCV) in tomatoes
22 (Papayiannis et al. 2011), banana bunchy top virus (BBTV) in bananas (Dale 1987),
23 plum pox virus (PPV) in stone fruits (Németh 1994), and papaya ringspot virus (PRSV)
24 in papaya (Jain et al. 2004). These viruses not only reduce crop quality and yield but
25 also impact food security and livelihoods in affected regions.

26 To mitigate these impacts, we must implement strategies such as enhanced
27 surveillance and implement diagnostics, quarantine and sanitation measures, breeding
28 for resistance, and integrated pest management (Strange and Scott 2005). Yet, there are
29 numerous questions missing of appropriate answers. We are within a small bubble of
30 knowledge that, despite recent advances, still holds many mysteries. Our innate
31 curiosity drives us to explore and seek for answers to many questions. Numerous
32 questions remain unanswered in Virology: What is the exact origin of viruses? How do

33 they evolve so rapidly? Why do some viruses cause severe diseases while others do not?
34 What determines their host range? How do viruses manipulate host cellular machinery
35 so effectively? What drives the emergence and re-emergence of viral diseases? How do
36 viruses cross species barriers enabling them to infect new hosts? And what unknown
37 viruses live in unexplored habitats?

38 Driven by these questions, our research aims to fill gaps in the overall
39 comprehension of the virus genome and host range, starting from collection of virus
40 isolates in commercial fields for detailed analysis of genome alterations during
41 host-virus interactions. Our work, conducted over four years, focused on potato virus Y
42 (PVY; species *Potyvirus yituberosi*, genus *Potyvirus*, family *Potyviridae*), a pathogen
43 often associated with substantial crop losses (Kerlan et al. 2008) having caused
44 significant impacts in the past on tomato and pepper crops in Brazil. But since the
45 1960s, concerns about PVY in these crops have diminished due to the development of
46 resistant cultivars. As a result, a few studies have been conducted on PVY in crops other
47 than its primary host, the potato.

48 Looking the database available in GenBank, out of 585 PVY genomes available,
49 only 18 viruses were isolated from tomatoes (*Solanum lycopersicum*), six from peppers
50 (*Capsicum annuum*), while the isolates from potatoes (*Solanum tuberosum*) add up to
51 466 items of this list. Thus, it is evident that studies on potatoes have been prioritized.
52 The other isolates on the list include those collected from *Capsicum baccatum* ($n = 1$),
53 *Datura metel* ($n = 1$), *Nicotiana tabacum* ($n = 67$), *Physalis peruviana* ($n = 7$), *S.*
54 *americanum* ($n = 1$), *S. bataveum* ($n = 7$), *S. nigrum* ($n = 7$), *S. phureja* ($n = 1$), *S.*
55 *quitoenses* ($n = 1$), *S. sisymbriifolium* ($n = 1$), and *Curcubita pepo* ($n = 1$).

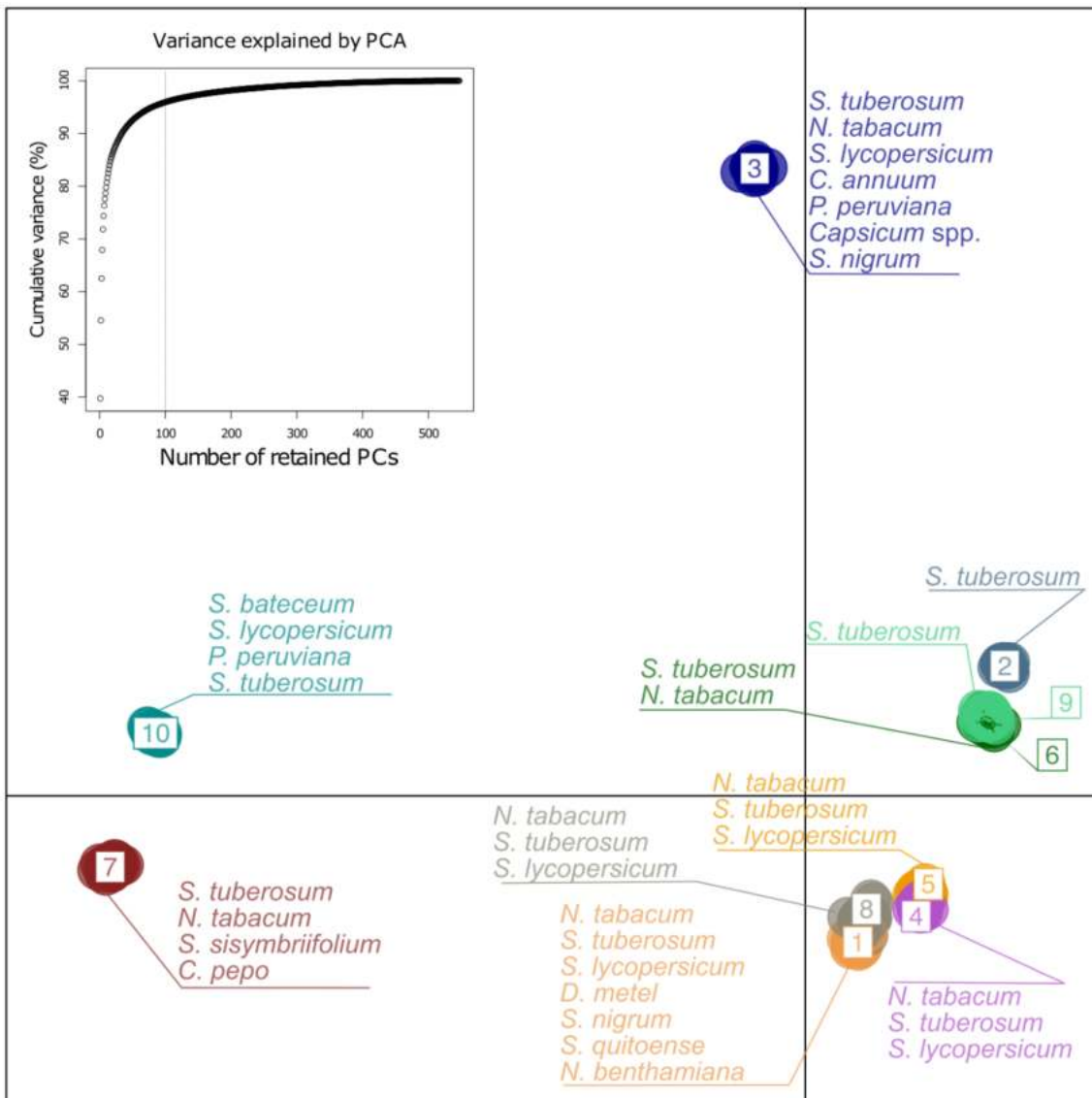
56 In a way, it is understandable that numerous studies have been conducted on
57 potatoes, since currently there are no cultivars with strong resistance to PVY, and it can
58 significantly reduce production both qualitatively (Nolte et al. 2004) and quantitatively
59 (Beczner et al. 1984). However, despite the predominance of large-scale agricultural
60 systems for potato production, other vegetable crops cultivated nearby may act as PVY
61 reservoirs for potato plants.

62 In recent years, during field trips of our group, necrotic symptoms were observed
63 in tomato plants. The disease is known as "Mexican fire" disease. This symptom was
64 then demonstrated to be associated to PVY infection (Lucena et al. 2024). The most

65 concerning aspect is that this symptom is increasingly being found in tomato plants,
66 which could represent a threat to tomato cultivation. This has raised an alert about the
67 potential risks that PVY could pose to these crops which are often grown by small-scale
68 and low-income producers.

69 Due to this, we sought to fill the gap left by breeding programs by testing widely
70 used tomato and pepper cultivars in production fields. In a preliminary discriminant
71 analysis of principal components (DAPC) using all available genomes in GenBank that
72 have the annotation of the host from which the isolate was collected ($n = 492$), we
73 observed that the host in which the PVY was collected have influenced the clustering
74 (Fig 1.). Isolates from peppers and tomatoes tend to be in the same group, separated
75 from the potato isolates. This genetic differentiation highlighted by DAPC prompted us
76 to question the role and forces that the host might exert on distinct PVY populations.

77



78

79 **Fig 1.** Scatter plot of Discriminant Analysis of Principal Components (DAPC) based on
 80 492 potato virus Y (PVY) genomes obtained from GenBank. Only isolates with known
 81 host information were included in the analysis. The dataset was divided into 10 distinct
 82 subpopulations, each represented by a different color. Arrows within each cluster point
 83 to the specific host species from which the isolates were collected.

84

85 From this, we hypothesized that the host could alter the evolutionary course of
 86 PVY populations. Understanding that isolates collected from different crops may be
 87 distinct and that these differences cannot be detected by tools such as ELISA or
 88 RT-PCR, one of our objectives was to develop a quick, easy, and affordable way to
 89 sequence the entire genome of isolates using Nanopore sequencing.

90 Still trying to understand how the virus-host interaction works, we hypothesized
91 that during the passage of the virus through different hosts, these hosts would modulate
92 the composition and fitness of the viral population, leading to viral specialization and
93 fixation of few haplotypes, or the contrary, an expansion of the genetic variability
94 associated to generalism. In pilot trials, we observed that some isolates collected from
95 different crops were not able to infect certain plant species, which could be related to
96 genomic changes or selection mechanisms. From this, we decided to study how the
97 adaptation of two PVY isolates collected from two different plant species evolve in
98 distinct hosts.

99 Indeed, due to the wide host range of PVY, the virus faces significant tradeoffs in
100 fitness when infecting different hosts (Elena et al. 2014). For instance, adaptations that
101 enhance PVY fitness in one host, such as the evolution of resistance-breaking strains in
102 potato (*Solanum tuberosum*), may come at the expense of reduced fitness when the virus
103 infects other solanaceous hosts like tomato (*Solanum lycopersicum*). This phenomenon
104 underscores the importance of host-specific adaptations in PVY evolution. PVY
105 classification has often been linked to symptomatology and infectivity in different hosts,
106 suggesting a correlation between viral isolates and host range properties (Quenouille et
107 al. 2013). For example, some PVY isolates that are infectious to potato tend to be
108 poorly infectious to pepper (Romero et al. 2001), while isolates from Chile show limited
109 infectivity to potatoes and are predominantly restricted to that region (Moury 2010).

110 The adaptability of PVY is further enhanced by its RNA-dependent RNA
111 polymerase (RdRp), which is particularly error-prone, leading to high mutation rates
112 (Drake 1993; Sanjuán 2012). These high mutation rates are among the highest observed
113 in nature and contribute significantly to the rapid evolution and adaptability of RNA
114 viruses (Sanjuán and Domingo-Calap 2016), enabling them to swiftly evade host
115 immune responses and develop resistance to antiviral treatments. Moreover, RNA
116 viruses, including PVY, mutate more rapidly than DNA viruses (Drake et al. 1998).
117 Single-stranded RNA viruses exhibit higher mutation rates than their double-stranded
118 counterparts, and there is a negative correlation between genome size and mutation rate.
119 This suggests that viral genetic diversity is influenced by both virus- and
120 host-dependent factors and evolves in response to selective pressures (Sanjuán and
121 Domingo-Calap 2016).

122 Recombination also plays a critical role in the evolutionary process of PVY.
123 Recombination is responsible of generating variability that can drive adaptation or even
124 the emergence of new species (Padidam et al. 1999; Inoue-Nagata et al. 2006;
125 Fiallo-Olivé et al. 2019; Lal et al. 2022). In RNA viruses, the recombination occurs
126 when the RdRp associated with a nascent transcript dissociates from one template and
127 associates with another (Kirkegaard and Baltimore 1986), Together with mutation, these
128 evolutionary parameters, influenced by past selection, work to maintain a
129 mutation-selection balance, an equilibrium where the population remains resilient
130 against deleterious mutations. This balance, shaped by the interplay of limited genetic
131 capacity, high mutation rates, and population size dynamics, forges a close relationship
132 between the biology of RNA viruses like PVY and their evolutionary dynamics (Dolan
133 et al. 2018).

134 In large viral populations like those of PVY, the diversity generated by these high
135 mutation rates results in a network of mutant genotypes surrounding a dominant
136 sequence. This network enables various interactions among the viral variants, such as
137 antagonism, cooperation, and recombination. During transmission bottlenecks, the
138 phenomenon of en bloc transmission helps preserve population size and diversity,
139 facilitating coinfection and mitigating the effects of genetic drift (Dolan et al. 2018).

140 As a result, PVY populations are constantly generating mutants with varying
141 levels of infectivity. The high mutation rates in these populations regularly give rise to
142 such variants, each with its own potential impact on the virus's overall fitness (Holland
143 et al. 1982). The concept of quasispecies, first proposed in the 1970s for bacteriophage
144 Q β replicating in *Escherichia coli*, is crucial for understanding this diversity. It refers to
145 a model where a viral population exists not as a single, homogeneous entity but as a
146 cloud of genetically diverse variants centered around a consensus or "master" sequence
147 (Eigen 1971; Eigen and Schuster 1977). Within this quasispecies cloud, individual
148 variants can interact through mechanisms like recombination, complementation, and
149 selection, enabling the viral population to maintain its fitness despite the accumulation
150 of deleterious mutations. Although initially described for bacteriophages, the
151 quasispecies concept has since become fundamental to understanding RNA virus
152 evolution and adaptability.

153 Indeed, the selection pressure have been shaping the PVY population from its
154 emergence in the Andes of South America to its introduction in Europe in the 16th
155 century (Torrance and Talianksy 2020), making PVY an important viruses in
156 agricultural systems. The fitness landscape for PVY is thus intricately shaped by its
157 interactions with different plant hosts, mutation rates, and the genetic diversity of the
158 viral population. As a quasispecies, PVY comprises numerous coexisting variants
159 within a population. These variants explore the fitness landscape, with some mutations
160 leading to increased fitness. The rugged nature of this fitness landscape allows PVY to
161 rapidly adapt to new environmental conditions, such as shifts in host species or changes
162 in agricultural practices.

163 Based on all that we know about viral variability, we became curious to
164 understand other factors that might be involved in the success or failure of the
165 virus-host interaction, such as the effect of defective genomes (DVGs) in the wild-type
166 virus replication process. For potato cultivation, tubers are usually used, which are often
167 propagated over several generations. Our hypothesis is that DVGs are pervasively
168 generated in PVY populations, particularly in potatoes that are vegetatively propagated,
169 considering that they have fewer selective bottlenecks compared to those transmitted by
170 aphid vectors. Therefore, we sought to identify the DVGs component of PVY
171 populations maintained under different transmission protocols. Specifically, we
172 examined populations isolated from potato tubers or leaves, inoculated via aphid vector
173 or mechanically, maintained in different hosts, and after consecutive viral passages.

174 This thesis has been divided into four chapters, all centered on PVY and its
175 interaction with different hosts. In the first chapter, we performed a screening for PVY
176 resistance in commercial tomato and pepper cultivars, and also in tomato accessions
177 used in breeding programs at the Instituto Agronômico de Campinas (IAC). In the
178 second chapter, we developed a methodology for PVY genome sequencing using
179 Nanopore MinION. In the third chapter, we performed a viral passage evolution
180 experiment with different hosts and two different viral isolates. Finally, in the fourth
181 chapter, we evaluated the emergence and maintenance of defective viral genomes
182 (DVGs) in different viral populations and their potential impact on PVY population
183 modulation.

184 Together, our experiments aimed to deepen our understanding of PVY genetic
185 diversity and adaptability in different host environments. By leveraging advanced
186 sequencing technologies and rigorous experimental approaches, we seek to unravel the
187 complexities of virus-host interactions, uncovering the mechanisms that drive viral
188 evolution and specialization. In summary, in this thesis we managed to: (i) identify host
189 preferences and genetic variability by screening a range of tomato and pepper cultivars,
190 we determined the host preferences of different PVY isolates and explored the genetic
191 variability among these isolates; (ii) develop rapid genome sequencing methods
192 establishing a streamlined, cost-effective methodology for sequencing PVY genomes
193 using Nanopore MinION technology, facilitating rapid and accurate genomic analysis;
194 (iii) investigate viral replication dynamics through viral passage experiments, we
195 evaluated how different hosts influence PVY replication rates and the genetic
196 bottlenecks that shape viral populations; and (iv) examine the role of defective viral
197 genomes (DVGs) studying the emergence and impact of DVGs on PVY populations,
198 particularly in relation to their role in modulating viral replication and host adaptation.

199 References

200

201 Baden LR, Sahly HME, Essink B, et al (2021) Efficacy and Safety of the mRNA-1273
202 SARS-CoV-2 Vaccine. *New England Journal of Medicine*, 384, 5, 403-416.
203 <http://dx.doi.org/10.1056/nejmoa2035389>.

204

205 Beczner L, Horváth J, Romhányi I, et al (1984) Studies on the etiology of tuber necrotic
206 ringspot disease in potato. *Potato Research*, 27, 339–352.
207 <https://doi.org/10.1007/BF02357646>

208

209 Burrell CJ, Howard CR, Murphy FA (2017) History and impact of virology. In: Fenner
210 and White's *Medical Virology*. Elsevier, pp 3–14.
211 <https://doi.org/10.1016/B978-0-12-375156-0.00001-1>

212

213 Chen W, Liu W, Jiao H, et al (2014) Development of a concentration method for
214 detection of tobacco mosaic virus in irrigation water. *Virologica Sinica* 29:155-161.
215 <https://doi.org/10.1007/s12250-014-3461-7>

216

217 Choudhury S, Larkin P, Meinke H et al. (2018) *Barley yellow dwarf virus* infection
218 affects physiology, morphology, grain yield and flour pasting properties of wheat. *Crop*
219 *& Pasture Science* 70:16-25. <https://doi.org/10.1071/CP18364>

220

221 Dale JL (1987) Banana bunchy top: an economically important tropical plant virus
222 disease. *Advances in virus research* 33:301-325.
223 [https://doi.org/10.1016/s0065-3527\(08\)60321-8](https://doi.org/10.1016/s0065-3527(08)60321-8)

224

225 Dolan PT, Whitfield ZJ, Andino R (2018) Mechanisms and concepts in RNA virus
226 population dynamics and evolution. *Annual Review of Virology* 5:69–92.
227 <https://doi.org/10.1146/annurev-virology-101416-041718>

228

229 Drake JW (1993) Rates of spontaneous mutation among RNA viruses. Proceedings of
230 the National Academy of Sciences 90:4171–4175.
231 <https://doi.org/10.1073/pnas.90.9.4171>
232

233 Drake JW, Charlesworth B, Charlesworth D, Crow JF (1998) Rates of spontaneous
234 mutation. Genetics, 148:1667-86. <https://doi.org/10.1093/genetics/148.4.1667>
235

236 Eigen M (1971) Selforganization of matter and the evolution of biological
237 macromolecules. Naturwissenschaften 58:465–523.
238 <https://doi.org/10.1007/BF00623322>
239

240 Eigen M, Schuster P (1977) A principle of natural self-organization.
241 Naturwissenschaften 64:541–565. <https://doi.org/10.1007/BF00450633>
242

243 Elena SF, Fraile A, García-Arenal F (2014) Evolution and emergence of plant viruses.
244 Advances in Virus Research 88:161-191. <https://doi.org/10.1016/B978-0-12-800098-4.00003-9>
245

246

247 Fiallo-Olivé E, Trenado HP, Louro D, Navas-Castillo J (2019) Recurrent speciation of a
248 tomato yellow leaf curl geminivirus in Portugal by recombination. Scientific Reports
249 9:1332. <https://doi.org/10.1038/s41598-018-37971-z>
250

251 Hibino H, Ishikawa K, Omura T (1991) Characterization of rice tungro bacilliform and
252 rice tungro spherical viruses. Phytopathology 81:1130-1132.
253

254 Holland J, Spindler K, Horodyski F, et al (1982) Rapid evolution of RNA genomes.
255 Science (1979) 215:1577–1585. <https://doi.org/10.1126/science.7041255>
256

257 Inoue-Nagata AK, Martin DP, Boiteux LS, et al (2006) New species emergence via
258 recombination among isolates of the Brazilian tomato infecting Begomovirus complex.
259 Pesquisa Agropecuária Brasileira 41:1329–1332.
260 <https://doi.org/10.1590/S0100-204X2006000800018>

261

262 Jain RK, Nasiruddin KM, Sharma KM, et al (2004) First report of occurrence of Papaya
263 ring spot virus infecting Papaya in Bangladesh. *Plant disease* 88:221.
264 <https://doi.org/10.1094/PDIS.2004.88.2.221C>

265

266 Karikó K, Buckstein M, Ni H, Weissman D (2005) Suppression of RNA recognition by
267 toll-like receptors: the impact of nucleoside modification and the evolutionary origin of
268 RNA. *Immunity* 23:165–175. <https://doi.org/10.1016/j.immuni.2005.06.008>

269

270 Kerlan C, Moury B (2008) Potato virus Y. *Encyclopedia of Virology*, 4, 287-296.

271

272 Kirkegaard K, Baltimore D (1986) The mechanism of RNA recombination in
273 poliovirus. *Cell* 47:433–443. [https://doi.org/10.1016/0092-8674\(86\)90600-8](https://doi.org/10.1016/0092-8674(86)90600-8)

274

275 Lal A, Kil E-J, Vo TTB, et al (2022) Interspecies recombination-led speciation of a
276 novel geminivirus in Pakistan. *Viruses* 14:2166. <https://doi.org/10.3390/v14102166>

277

278 Legg JP, Jerimiah SC, Obiero HM, et al (2011) Comparing the regional epidemiology of
279 the cassava mosaic and cassava brown streak virus pandemics in Africa. *Virus Research*
280 159:161-170. <https://doi.org/10.1016/j.virusres.2011.04.018>

281

282 Lucena VS, Nakasu EYT, Pereira JL, et al (2024) Emergence of potato virus Y
283 outbreaks in tomatoes in Brazil, the disease and spread. *bioRxiv*.
284 <https://doi.org/10.1101/2024.05.17.594728>

285

286 Moury B (2010) A new lineage sheds light on the evolutionary history of Potato virus Y.
287 *Molecular Plant Pathology* 11:161–168.
288 <https://doi.org/10.1111/j.1364-3703.2009.00573.x>

289

290 Neméth M (1994) History and importance of plum pox in stone-fruit production.
291 *Bulletin OEPP EPPO Bulletin* 24:525-536.
292 <https://doi.org/10.1111/j.1365-2338.1994.tb01065.x>

293

294 Nolte P, Whitworth JL, Thornton MK, McIntosh CS (2004). Effect of seedborne potato
295 virus Y on performance of russet burbank, russet norkotah, and shepody potato. *Plant*
296 *Disease*, 88 (3), 248-252. <https://doi.org/10.1094/PDIS.2004.88.3.248>

297

298 Padidam M, Sawyer S, Fauquet CM (1999) Possible emergence of new geminiviruses
299 by frequent recombination. *Virology* 265:218–225.
300 <https://doi.org/10.1006/viro.1999.0056>

301

302 Quenouille J, Vassilakos N, Moury B (2013) Potato virus Y: a major crop pathogen that
303 has provided major insights into the evolution of viral pathogenicity. *Molecular Plant*
304 *Pathology* 14:439–452. <https://doi.org/10.1111/mpp.12024>

305

306 Romero A, Blanco-Urgoiti B, Soto MJ, et al (2001) Characterization of typical
307 pepper-isolates of PVY reveals multiple pathotypes within a single genetic strain. *Virus*
308 *Research* 79:71–80. [https://doi.org/10.1016/S0168-1702\(01\)00300-8](https://doi.org/10.1016/S0168-1702(01)00300-8)

309

310 Sanjuán R (2012) From molecular genetics to phylodynamics: evolutionary relevance of
311 mutation rates across viruses. *PLoS Pathogens* 8:e1002685.
312 <https://doi.org/10.1371/journal.ppat.1002685>

313

314 Sanjuán R, Domingo-Calap P (2016) Mechanisms of viral mutation. *Cellular and*
315 *Molecular Life Sciences* 73:4433–4448. <https://doi.org/10.1007/s00018-016-2299-6>

316

317 Strange RN, Scott PR (2005) Plant Disease: a threat to global food security. *Annual*
318 *Review of Phytopathology* 43:83–116.
319 <https://doi.org/10.1146/annurev.phyto.43.113004.133839>

320

321 Papayiannis LC, Katis NI, Idris AM, Brown JK (2011) Identification of weed hosts of
322 tomato yellow leaf curl virus in Cyprus. *Plant Disease* 95:120-125.
323 <https://doi.org/10.1094/PDSI-05-10-0346>

324

325 Polack FP, Thomas SJ, Kitchin N, et al (2020) Safety and Efficacy of the BNT162b2
326 mRNA Covid-19 Vaccine. *New England Journal of Medicine*, 383, 27, 2603-2615.
327 <http://doi.org/10.1056/nejmoa2034577>

328

329 Torrance L, Talianksy ME (2020) Potato Virus Y Emergence and evolution from the
330 Andes of South America to become a major destructive pathogen of potato and other
331 solanaceous crops worldwide. *Viruses* 12. <https://doi.org/10.3390/V12121430>

332

333 Zuo K, Gao W, Wu Z, et al (2024) Evolution of virology: science history through
334 milestones and technological advancements. *Viruses* 16:374.
335 <https://doi.org/10.3390/v16030374>

1 General objective

2

3 Study the effects of the host on the evolution of PVY by analyzing aspects of infectivity,
4 host specificity, transmissibility, and genome variation.

5

6 Specific objectives:

7

8 Chapter I

9 1. Assess the infectivity of PVY isolates across distinct host species.

10 2. Evaluate the resistance of commercial tomato and pepper cultivars, along with
11 germplasm bank accessions, against PVY infection.

12

13 Chapter II

14 3. Design and validate specific primers for the detection of PVY using RT-PCR.

15 4. Develop a cost-effective sequencing protocol utilizing the Nanopore technology.

16

17 Chapter III

18 5. Monitor and quantify the infection ability of two PVY isolates across multiple
19 host combinations in a viral passage experiment.

20 6. Investigate the genomic alterations on PVY isolates as they infect different hosts
21 at selected passage points.

22 7. Evaluate the impact of distinct PVY isolates on the phenotype of infected plants
23 during successive viral passages through the hosts.

24 8. Determine the role of host species in driving the generation of viral genomic
25 variability.

26

27 Chapter IV

28 9. Identify and characterize the formation of defective viral genomes (DVGs) using
29 data from Chapter III and those available in databases.

30 10. Detect the generation of DVGs according to the interaction of the PVY
31 strains/isolates with diverse hosts, with different transmission modes and plant organs,
32 and after mechanically passaging under distinct experimental conditions.

1

2

3 **Unraveling the dynamics of host specificity and resistance responses to** 4 **potato virus Y, and implications for crop management**

5

6 Ivair José de Moraes^{1,2}, Dorian Yest Melo Silva^{1,2}, Barbara Mavie Camargo¹, André Luiz
7 Lourenção³, Alice Kazuko Inoue-Nagata²

8

9 ¹Departamento de Fitopatologia, Instituto de Ciências Biológicas, Universidade de
10 Brasília (UnB), 70910-900, Brasília, Distrito Federal, Brazil

11 ²Embrapa Hortaliças, 70351-970, Brasília, Distrito Federal, Brazil

12 ³Departamento de Entomologia e Acarologia, Escola Superior de Agricultura “Luiz de
13 Queiroz” (ESALQ), Universidade de São Paulo, 13418-900, Piracicaba, São Paulo,
14 Brazil

15

16 Corresponding author: Alice Kazuko Inoue-Nagata

17 e-mail: alice.nagata@embrapa.br

18

19 *Submitted to Tropical Plant Pathology*

20 Abstract

21

22 Potato virus Y (PVY), a virus member of the family *Potyviridae*, poses a significant
23 threat to global agriculture, affecting crops such as potato, tomato, pepper, and tobacco.
24 Despite its economic importance, there remains a critical gap in understanding the
25 dynamics of PVY-host interactions and the development of effective management
26 strategies. This study aimed to comprehensively characterize PVY isolates from sweet
27 pepper, potato, and tomato plants, elucidating their infectivity and adaptation across
28 diverse host species and cultivars. Initially, using antigen-trapped ELISA, we
29 determined the optimal detection timeframe and leaf sampling strategy for detection of
30 PVY by serological assays, showing that some hosts require a minimum incubation
31 period and leaf selection for a reliable virus detection. By comparing PVY isolates from
32 distinct hosts, we demonstrated that the choice of the isolate is crucial for resistance
33 evaluations. Additionally, inoculation trials across various plant species elucidated
34 differences in infectivity and adaptation among PVY isolates. Resistance trials in
35 commercial cultivars of tomato and pepper plants and wild *Solanum* spp. accessions
36 revealed susceptibility across all tested materials, challenging previous assumptions of
37 resistant cultivars and accessions. These findings underscore the urgency of addressing
38 PVY spread and understanding host-virus interactions to identify resistant genotypes for
39 commercial use and for developing breeding programs directed to PVY isolates present
40 in Brazil.

41

42 **Keywords:** host range, plant breeding, *Potyviridae*, *Potyvirus*, resistance screening,
43 viral adaptation

44 Main text

45

46 According to the latest update from the International Committee on Taxonomy of
47 Viruses, potato Y virus (PVY) is classified as species *Potyvirus yituberosi* (genus
48 *Potyvirus*, family *Potyviridae*). It possesses a positive single-stranded RNA genome of
49 approximately 9.7 kb in length, encoding 11 mature proteins (Inoue-Nagata et al. 2022).
50 Ten proteins, P1, HC-Pro, P3, 6K1, CI (cylindrical inclusion), 6K2, NIa, VPg, NIb
51 (viral polymerase), and CP (capsid protein), are derived from the cleavage of a larger
52 polyprotein by viral proteases. One protein, PIPO, is generated by a polymerase
53 slippage mechanism and is expressed as the trans-frame protein P3N-PIPO. PVY stands
54 as a serious viral threat in global agriculture, affecting crops such as potato, tomato,
55 pepper, and tobacco (Quenouille et al. 2013). In fact, PVY has been considered a major
56 threat to global potato production due to its high prevalence and ability to rapidly spread
57 through fields (Karasev and Gray 2013). Its detrimental impact on crop yield is also
58 relevant in tomato and pepper crops, underscoring the necessity for comprehensive
59 research to identify resistant cultivars amidst its high prevalence and rapid spread in
60 fields (Karasev and Gray 2013). Despite its importance, the current tomato portfolio of
61 cultivars lacks a comprehensive description of resistance against PVY, thereby requiring
62 further investigation.

63 Studies have revealed the substantial economic losses PVY can induce, with
64 sweet pepper crops experiencing yield reductions ranging from 20 to 70% upon
65 infection, particularly severe during early stages (Avilla et al. 1997). While the exact
66 economic impact on tomato crops remains unquantified, its significant effects are
67 well-documented (Quenouille et al. 2013). Thus, PVY remains a relevant concern to
68 agriculture, threatening both yield and economic stability.

69 Historically, PVY posed a significant threat to Brazilian agriculture during the
70 1960s and 1970s. However, the development of resistant tomato cultivars, such as those
71 in the Ângela group, and hybrid peppers has substantially mitigated its impact (Nagai
72 and Costa 1969; Nagai 1971). The rare reports of PVY occurrence in Brazilian tomato
73 and pepper fields further diminished its economic significance in these crops (Meissner
74 et al., 1990). Yet, recent observations suggesting a new disease named “Mexican Fire”
75 in plants infected with PVY, highlight the resurgence of PVY in tomato fields,

76 underscoring the potential re-emergence of this virus as a serious threat in Brazil
77 (Lucena et al. 2024).

78 PVY is a generalist virus and exhibits a broad host range, experimentally infecting
79 over 400 species across 30 families (Edwardson and Christie 1997; Jeffries 1998) and
80 understanding the host range of viruses is crucial for virus diagnosis (Dijkstra 1992;
81 McLeish et al. 2019). However, the determinants of host range in plant virus genomes
82 and their implications for virus fitness and pathogenicity remain largely unknown.
83 Despite this, it is known that the inability of a virus to infect a particular plant host may
84 arise from various factors, including the failure to complete essential steps of the
85 infection cycle, such as replication or systemic movement, or the presence of active and
86 specific resistance mechanisms within the plant (Kang et al. 2005). Additionally, host
87 range expansion is a common phenomenon among plant viruses, often at the cost of
88 reduced fitness in the original host (Agudelo-Romero and Elena 2008; Bedhomme et al.
89 2012; García-Arenal and Fraile 2013). Furthermore, after serial passages in a specific
90 host, the infectivity in the original host can diminish, suggesting potential constraints on
91 a virus adapted to one host's ability to infect another one within its host range (Yarwood
92 1979). This implies that a virus adapted to one host may not necessarily be able to infect
93 another host within its host range.

94 Nevertheless, even among generalist viruses, significant host-virus associations
95 exist, with host specialization emerging as a successful strategy for increased prevalence
96 (Malpica et al. 2006). Such specialization often involves genetic changes within the
97 virus genome, potentially leading to alterations in host range. Additionally, host
98 jumping and adaptation within plant species are not sporadic events in plant virus
99 evolution but rather significant drivers of viral emergence (Vassilakos et al. 2016).
100 These events carry epidemiological consequences, impacting viral survival and spread.
101 Therefore, elucidating virus-host interactions holds immediate implications for control
102 measures.

103 PVY exists as a complex of strains, delineated based on host range, serological
104 properties and molecular characteristics (Singh et al. 2008). These strains are generally
105 classified as PVY^C, PVY^O, and PVY^N. Studies investigating different PVY strains have
106 revealed exceptional nucleotide diversification through mutation and/or recombination,
107 enabling adaptation to new cultivars or diverse environments and resulting in varying

108 degrees of infectivity (Karasev and Gray 2013; Nigam et al. 2019). PVY^O and PVY^N
109 predominantly comprise potato isolates, which are less adept at infecting peppers, while
110 PVY^C primarily consists of pepper isolates with limited adaptation to potato (Moury
111 2010). However, it is noteworthy that the PVY^C clade also includes potato-infecting
112 isolates (Dullemans et al. 2011). Interestingly, in tomato fields, a PVY^C isolate from
113 commercial tomato production was grouped within the same clade as potato-infecting
114 isolates but exhibited an inability to infect potatoes (Chikh-Ali et al. 2016). In addition
115 to the C, O, and N strains, a large number of recombinants can be easily found,
116 particularly in potato production fields, where they are more prevalent than
117 non-recombinant strains (Galvino-Costa et al. 2012; Karasev et al. 2011). This
118 prevalence poses a challenge for developing PVY-resistant potatoes, as there are
119 currently no resistant cultivars available.

120 Phylogenetically, the host species appears to significantly influence the
121 distribution of PVY, as evidenced by studies demonstrating differential infectivity
122 among isolates across hosts (Cuevas et al. 2012). This effect becomes apparent when
123 certain isolates successfully infect one host while failing to do so in others (Green et al.
124 2017).

125 Therefore, our study aims to address basic concepts of virus-hosts interaction at a
126 mechanically inoculation and detection level, filling this gap in knowledge by
127 understanding (1) the dynamics between three PVY isolates, identified in three distinct
128 host species, and (2) the capacity to infect its original host and other hosts. We also
129 consider the recent increase in incidence of PVY in tomato crops (Lucena et al. 2024)
130 and search for resistant commercial sweet pepper and tomato cultivars, alongside wild
131 solanum lines utilized in breeding programs. Our findings yield valuable insights that
132 can contribute to breeding programs and help understanding the intricate dynamics of
133 PVY-host interactions.

134 First, we used three PVY isolates collected from different hosts: PVYCa collected
135 from a sweet pepper (*Capsicum annuum*) plant, PVYSt from a potato (*Solanum*
136 *tuberosum*) plant and PVYSl from tomato (*Solanum lycopersicum*), all of them from the
137 district of PAD-DF, close to Brasília, the Federal District in Brazil. Seeds were sown in
138 polystyrene trays containing 128 cells and subsequently transplanted to 500 mL pots,
139 containing organic potting mix and substrate (1:1 ratio), and kept in a greenhouse.

140 For all trials, the detection was done by antigen-trapped ELISA in nitrocellulose
141 membranes (dot-ELISA) using a house made polyclonal antibody at a concentration of
142 1 µg/mL, as described in Nagata et al. (1995). This antibody detects both PVY^O and
143 PVY^N strains (Inoue-Nagata et al., 2001; Fonseca et al., 2005). The crude sap diluted in
144 0.5x PBS of each sample was applied on a nitrocellulose filter and treated with 1 µg/mL
145 anti-PVY after blocking with skimmed milk, and later with anti-rabbit IgG alkaline
146 phosphatase-conjugated antibody produced in goat (Sigma-Aldrich), diluted 1:30,000.
147 Samples were considered positive if a purple color developed after incubation with a
148 solution with nitro blue tetrazolium (NBT) and 5-bromo-4-chloro-3-indolyl-phosphate
149 (BCIP) by visual inspection.

150 In a pilot test, the detection of PVY in sweet pepper cv. Ikeda, our model cultivar,
151 by serology proved to be challenging due low level of detection in early
152 post-inoculation stages (*data not shown*). Due to this, the optimal time for inoculum
153 collection was determined by testing the second and third leaves of plants 3, 5, 7, 9, 11,
154 and 13 days post-inoculation (d.p.i.) of cv. Ikeda, using 10 plants each. Our aim was to
155 determine which leaves, and the minimal time to collect samples to avoid false negative
156 results. The inoculation was done using leaves of infected plants ground (~1:10) in 0.05
157 M phosphate buffer, pH 7.0, in plants with 2-4 true leaves. At this stage, we used the
158 PVYCa and PVYSt isolates due to their ability to infect pepper plants (*data not shown*).

159 The serological test demonstrated that PVY remained undetectable until 13 d.p.i.
160 under the tested conditions, regardless of the PVY isolate. This implies that the virus
161 remains below detection levels in the plant until at least 11 d.p.i. Notably, no infections
162 were observed until 11 d.p.i., with positive detections emerging only two days later
163 (Sup. Fig. 1). While the dot-ELISA method is commonly employed due to its
164 cost-effectiveness and suitability as an initial screener for a large number of plants, our
165 results suggest that PVY detection is only reliably possible after at least 13 d.p.i.,
166 indicating a narrow window for serological detection within this timeframe considering
167 the sweet pepper cultivar Ikeda. Consequently, screening plants for PVY during the
168 early stages of infection may yield false negative results, as the virus may be present in
169 the field but remain undetectable at these early stages.

170 In serological tests, a single leaf, preferably the youngest, is typically collected for
171 detection. We conducted experiments to determine which of the younger leaves is most

172 suitable for the detection test. For PVYCa, the virus was detected in the second
173 youngest leaf in 4 out of 5 inoculated plants, and in the third leaf in 2 out of the same 5
174 plants. For PVYSl, 4 positives out of 5 were detected in the second leaf, while 1 out of 5
175 were detected using the third leaf (Sup. Fig. 1). The detection test was performed at 13
176 d.p.i. In conclusion, our findings suggest that for the detection of PVY in sweet pepper
177 plants using dot-ELISA, testing should be conducted at least 13 d.p.i., preferably using
178 the second youngest leaf. Note that our experiments were exclusively conducted with
179 Ikeda peppers, as detection in tomato and potato cultivars posed no challenges during
180 previous laboratory tests (*data not shown*). Therefore, all PVY detections in our
181 experiments were performed with at least 13 d.p.i. and using the second youngest leaf.

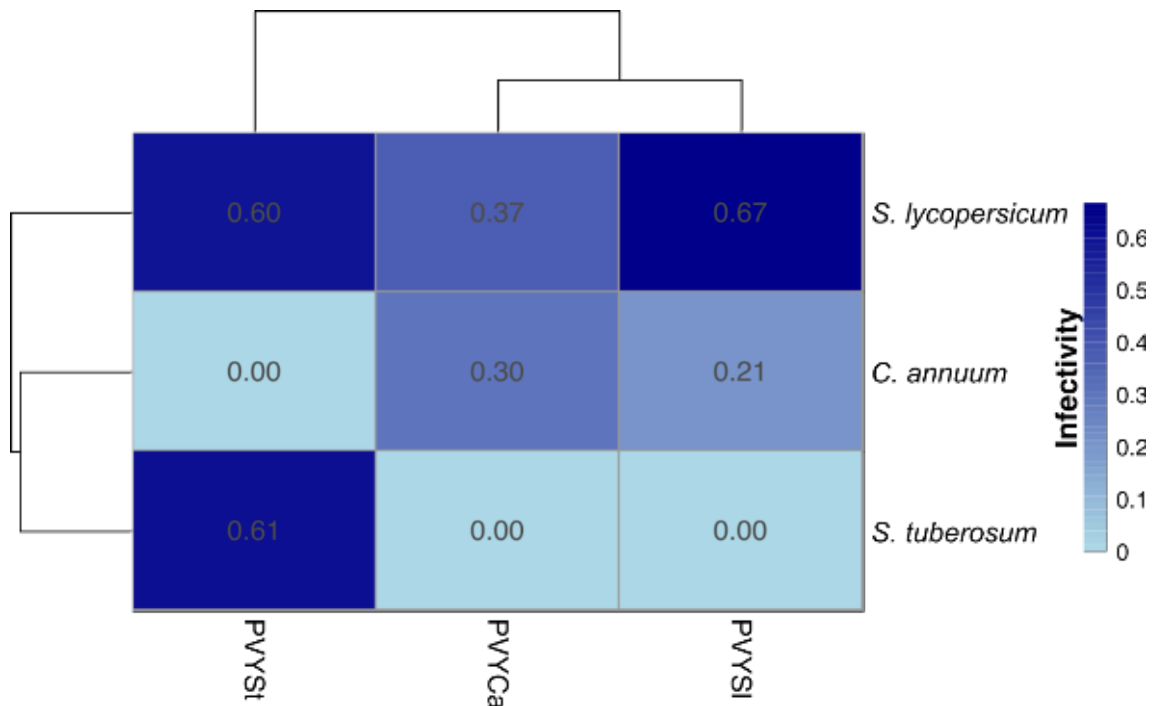
182 To investigate whether the host from which the PVY isolate originated influences
183 resistance responses, PVYCa, PVYSt and PVYSl were used for inoculation of 27-30
184 plants of sweet pepper cv. Ikeda, potato cv. Atlantic and tomato cv. Santa Clara.

185 Sweet pepper plants were infected with PVYCa (8 positives out of 27, Infection
186 Rate (IR) of 30%) and PVYSl (6/29, IR=21%), but not with PVYSt. Tomato plants were
187 infected by all isolates: PVYCa (11/30, IR=37%), PVYSt (18/30, IR=60%) and PVYSl
188 (20/30, IR=67%). Potato plants were infected by PVYSt (17/28, IR=61%), but neither
189 PVYCa nor PVYSl infected them. This suggested a strong specificity of the isolates to
190 the hosts (Gebre Selassie et al. 1985; Fereres et al. 1993; Romero et al. 2001; Moury
191 2010). None of the combinations yielded a 100% IR. Interestingly, PVYCa was unable
192 to establish infection in potato plants, while PVYSt failed to infect sweet pepper plants,
193 indicating a clear distinct interaction between these two viruses and hosts. Actually, the
194 responses of pepper and tomato plants against the inoculation of PVYCa and PVYSl
195 were similar, and clearly differed from the ones of PVYSt.

196 A Generalized Linear Model (GLM) with a binomial distribution was fitted to
197 assess the interaction effects of species, virus isolate, and host on the infection
198 proportion. The significance of the model coefficients was evaluated to determine the
199 effect of each factor and their interactions on the infectivity. The model showed that the
200 original hosts generally had higher infection proportions compared to non-original
201 hosts, with some exceptions, such as tomato infected with PVYSt (Fig. 1). It was also
202 possible to detect three different patterns in non-original hosts, in which pepper plants
203 could be infected by PVYCa and PVYSl, tomatoes by all isolates and potatoes only by

204 PVYSt. This is consistent with the expectation that viruses are better adapted to their
205 original hosts.

206



207

208 **Fig 1.** Infectivity proportions of the three plant species for each PVY isolate. Darker
209 blue shades represent a higher number of infected plants, while lighter shades represent
210 fewer infected plants.

211

212 Further studies could explore the mechanisms behind the observed infection
213 patterns, such as differences in plant immune responses or viral replication efficiency in
214 original versus non-original hosts. Understanding these underlying factors could
215 improve the prediction of viral spread and the development of resistant plant cultivars.
216 In conclusion, our findings confirm the importance of considering isolate specificity in
217 screening and management strategies for disease control (reviewed in Karasev and Gray
218 2013).

219 Our systematic evaluation of diverse host-pathogen interactions aimed to uncover
220 potential cross-species transmission patterns of PVY and their implications for disease
221 spread and management strategies. We observed that hosts (genotype, physiology and
222 phenology) may influence and shape the PVY population, with certain isolates showing
223 limited impact on specific hosts upon initial infection. This phenomenon suggests the

224 presence of antagonistic pleiotropy, wherein mutations beneficial in one host may be
225 detrimental in another (Whitlock 1996). Furthermore, phylogenetic analysis revealed a
226 strong correlation between PVY phylogeny and host species origin, with pepper isolates
227 clustering together and no specificity observed for PVY isolates in tomatoes
228 (Quenouille et al. 2013). Based on the evidence that the choice of the isolate is crucial
229 for screening purposes, we selected PVYCa to test sweet pepper cultivars and PVYSI to
230 test tomato cultivars. We did not screen potato cultivars for resistance to PVY as all
231 commercial cultivars are known to be susceptible (Karasev and Gray 2013).

232 Seeds of commercial cultivars of sweet pepper ($n = 5$) and tomato ($n = 18$) were
233 searched in the market and subjected to inoculation trials, conducted twice, in Autumn
234 and Summer, to ensure consistent results. Inoculations were performed and symptoms
235 recorded, both in a greenhouse environment. Based on paired t-test (-1.2371, p -value
236 0.2297), Wilcoxon signed-rank test (29.5, p -value 0.2781), and Cohen's d (-0.264),
237 there was no statistically significant difference rates between 1st and 2nd repetitions. The
238 results from both trials were similar, prompting the calculation of the IR based on
239 combined data.

240 Sweet pepper cultivars were inoculated with PVYCa, resulting in infection across
241 all five cultivars. The IR ranged from 45% to 82%, averaging 74% (Fig. 2, green bars).
242 Notably, severe symptoms such as blistering and interveinal chlorosis, along with leaf
243 abscission and severe damage, were observed, particularly in cv. Ikeda (Sup. Fig. 2).
244 Despite displaying strong symptoms, cv. Ikeda exhibited the lowest infection rate
245 among all cultivars (45% IR).

246 The absence of resistant sweet pepper cultivars contradicts the description of these
247 cultivars as resistant to PVY infection, according to the seed company. This discrepancy
248 underscores the importance of using multiple isolates during cultivar screening,
249 considering potential infection barriers. Indeed, previous studies have demonstrated
250 such barriers, such as the findings that isolates from potatoes poorly infect pepper
251 plants, consistent with our results (Blanco-Urgoiti et al. 1998; Romero et al. 2001;
252 Moury 2010).

253 Tomato cultivars (18 in total) were mechanically inoculated with PVYSI in the
254 greenhouse, with all cultivars displaying susceptibility to the virus. The infection rates

255 were even higher compared to sweet peppers, with ten cultivars exhibiting 100% IR,
256 and the lowest rate at 88%, averaging 96% for all cultivars (Fig. 2, blue bars).

257 Despite the high infection rates, tomato cultivars exhibited mild symptoms (Sup.
258 Fig. 3). This raised concerns about the detection of PVY in tomato fields, as visual
259 inspections may miss strains inducing mild or no symptoms, potentially serving as
260 undetected inoculum sources.

261 There are no studies that elucidate these questions in commercial cultivars,
262 primarily because PVY is well studied in potatoes but not in other crops. In these cases,
263 ELISA detection methodology can be used, ruling out false negatives based on
264 symptomatology. Although the observation of mild symptoms in tomato plants has
265 already been reported (Costa et al. 1960) and is in agreement with the results found
266 here, the appearance of strong symptoms of necrosis caused by PVY, present in the
267 middle third of the plant in tomato production fields, cannot be ruled out (Lucena et al.
268 2024). This means that the symptoms development may be related to the viral isolate,
269 the cultivar, environment aspects, simultaneous mixed infections (for example the
270 combination of PVY and potato virus X (Vance 1991) or PVY and potato spindle tuber
271 viroid (PSTVd) (Qiu et al. 2014) or a combination of them or unknown factors.

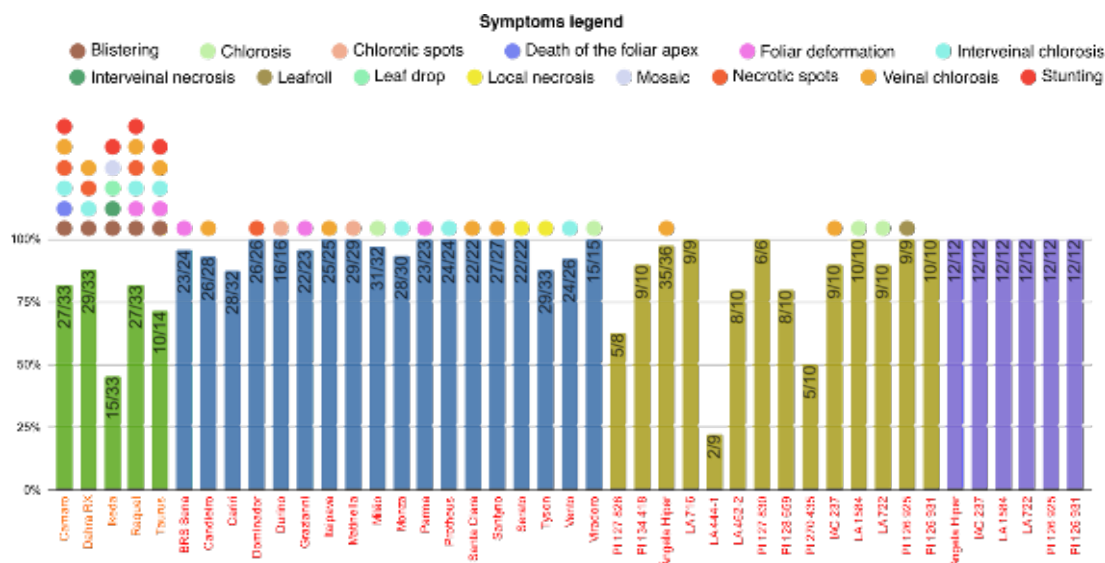
272 Although there is no information regarding the resistance to PVY infection in any
273 of these 18 tomato cultivars, they were chosen due to the agronomic characteristics they
274 possess, but more importantly to the resistance to other pathogens. Altogether, they are
275 resistant to bacteria, fungi, nematode or even virus infection. This includes the
276 resistance of BRS Sena to begomoviruses, Itaipava and Viradoro to tospoviruses,
277 Grazianni and Vento to tobamoviruses, Serato to tospoviruses and tobamoviruses and
278 Cariri, Candieiro, Durino, Milão, Monza, Parma, Protheus, Santyno, and Tyson to
279 begomoviruses, tobamoviruses and tospoviruses.

280 However, our tests revealed that none of the commercial sweet pepper or tomato
281 cultivars exhibited resistance to the tested PVY isolates, highlighting the necessity of
282 seeking new materials through breeding programs. This emphasizes the urgency of
283 addressing PVY susceptibility in commercial cultivars to mitigate potential production
284 losses and ensure crop health. Note that these cultivars, when infected, may serve as a
285 reservoir of the PVY isolates.

286 As no commercial cultivar was resistant to PVY infection, wild lines of *Solanum*
 287 spp. accessions were screened in an attempt to obtain potential resistance sources.
 288 Fourteen wild tomato materials from the Instituto Agronômico de Campinas
 289 Germplasm Collection of *Solanum* species were screened: *Solanum pimpinellifolium* (PI
 290 126 931, LA 722, LA 1584 and PI 126 925), *S. habrochaites* (PI 134 418 and PI 127
 291 826), *S. lycopersicum* (Ângela Hiper), *S. pennellii* (LA 716) and *S. peruvianum* (LA
 292 462-2, PI 127 830, PI 270 435, IAC 237, LA 444-1 and PI 128 659). The wild tomato
 293 species were tested once, due to limited seed availability, with Ângela Hiper being the
 294 exception and tested three times.

295 All accessions were susceptible to PVY infection with IR between 22% to 100%:
 296 *S. pimpinellifolium* ($n = 4$) presented 97% of IR, *S. lycopersicum* ($n = 1$) presented 97%,
 297 *S. habrochaites* ($n = 2$) presented 77%, *S. pennellii* ($n = 1$) presented 100% and *S.*
 298 *peruvianum* ($n = 6$) presented 69% of IR (Fig. 3, golden bars). The only material that
 299 showed low IR was LA444-1 (*S. peruvianum*) with 22%. Although some accessions
 300 exhibited chlorosis, veinal chlorosis and leafroll, most of them exhibited no symptoms
 301 at all, suggesting tolerance of these accessions (Sup. Fig. 4). Despite their susceptibility,
 302 these accessions may still be important in the search for resistance against PVY due to
 303 the lower IR compared to other tomato cultivars (Tukey`s HSD = 0.1, p-value=0.041).

304



305

306 **Fig 3.** Comparative infection rates of tomato and pepper cultivars, and wild *Solanum*
 307 spp. accessions. Sweet pepper cultivars are represented by green bars, tomato cultivars

308 by blue bars, wild *Solanum* spp. accessions by golden bars, and their second-generation
309 plants by purple bars. The number inside each bar indicates the number of plants
310 positive for PVY infection followed by a slash and the total number of tested plants.
311 Sweet pepper and tomato cultivars were evaluated in two different seasons in the
312 greenhouse, with the number of plants representing the sum of positive and tested
313 plants. The isolate used for inoculation is indicated by distinct colors on the x-axis:
314 PVYCa in orange and PVYSl in red. Colored circles above the graph denote the
315 presence of symptoms, with an absence of a circle indicating no symptoms.

316

317 Previous studies had identified the wild tomato LA444-1 as resistant against PVY
318 based on the absence of symptoms using visual evaluation (Lourenção et al. 2005). Our
319 findings demonstrate that while LA444-1 may serve as a potential source of resistance
320 to PVY due to its lower IR, though it remains susceptible to PVY. This underscores the
321 challenge of selecting the isolates for resistance tests, and also of relying solely on
322 visual cues to determine resistance, especially when infected plants exhibit only mild or
323 no symptoms, as described previously in others wild tomato accessions (Palazzo et al.
324 2008).

325 Interestingly, the cultivar Ângela Hiper, historically valued for its resistance to
326 PVY, displayed unexpectedly high IR of 98%. Since the 1960s, significant efforts had
327 been made to introgress PVY resistance into the tomato cultivar Santa Cruz, which was
328 highly susceptible to this important disease. In the 1970s, through backcrossing between
329 Santa Cruz and PI 126410 (*S. peruvianum*), a new cultivar called Ângela (Nagai and
330 Costa 1969) was released. It was quickly adopted by tomato growers due to its
331 resistance to PVY, *Fusarium oxysporum* f. sp. lycopersici race 1, and *Stemphylium*
332 *solani*, as well as its high yield. Between 1975 and 1988, it was used on 75-80% of the
333 total stalked (fresh market) tomato acreage. This initial success spurred the development
334 of new cultivars, such as Ângela Hiper (Nagai et al. 1992), derived from the original.
335 However, despite its past success, our extensive testing consistently revealed high levels
336 of susceptibility (averaging 98%).

337 This result aligns with previous studies on screening wild tomato species for
338 resistance, in which 19 *Solanum* spp. accessions were found to be susceptible to PVY,
339 sometimes showing symptoms and other times remaining asymptomatic (Palazzo et al.

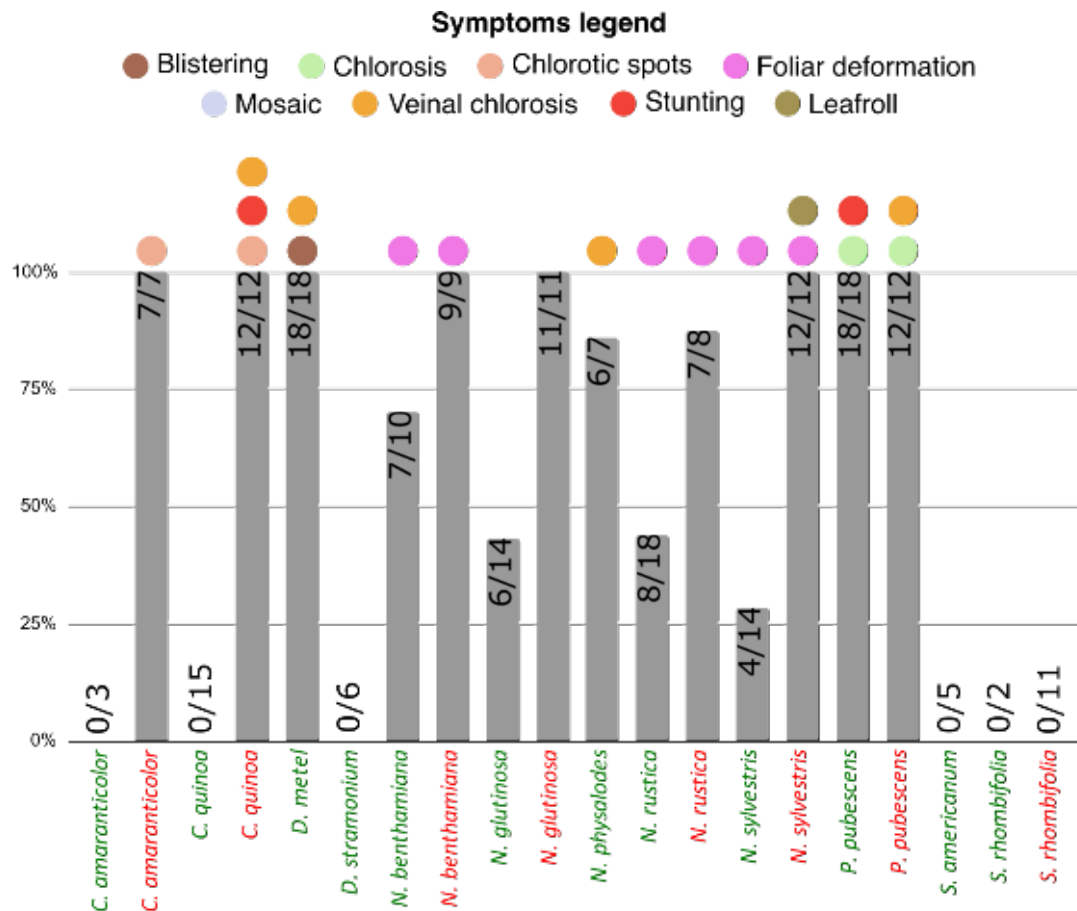
340 2008). However, the results obtained here indicate a higher level of susceptibility
341 among the accessions, with a greater number of positive plants, suggesting that this
342 virus isolate PVYSI has a potential to infect other tomato cultivars believed to be
343 resistant to PVY infection.

344 To validate our findings and rule out the possibility of genetic segregation, we
345 conducted an additional experiment with wild tomato accessions. We generated seeds
346 from six autopollinated non-infected wild tomato plants, including one *S. lycopersicum*,
347 one *S. peruvianum*, and four *S. pimpinellifolium* accessions. These seeds were then
348 sown and subjected to PVY inoculation. All six cultivars exhibited a minimum IR of
349 90%, mirroring the parental generation's susceptibility. After mechanical inoculation
350 with PVYSI, all first-generation plants displayed 100% IR, consistent with the parental
351 generation, indicating no genetic segregation (Fig. 2, purple bars). As observed in the
352 previous trial, no symptoms were observed in any of these plants. Thus, the
353 susceptibility was confirmed for all commercial and wild tomato accessions to PVY
354 infection. These findings collectively suggest that, although some may present escapes
355 of infection, there are currently no known sources of resistance to the isolate PVYSI in
356 tomatoes.

357 Based on the previously inoculation trials, PVYCa and PVYSI have similar
358 infectivity properties, so PVYSt and PVYSI were tested in inoculation trials of various
359 plant species. Our tests encompassed plant species from the Solanaceae family (*Datura*
360 *metel*, *D. stramonium*, *Nicotiana benthamiana*, *N. glutinosa*, *N. rustica*, *N. sylvestris*,
361 *Nicandra physalodes*, *Physalis pubescens* and *Solanum americanum*), Amaranthaceae
362 (*Chenopodium amaranticolor* and *C. quinoa*) and Malvaceae (*Sida rhombifolia*). Due to
363 low seed availability, not all hosts were tested with both isolates.

364 Our data show evidence that PVY infected hosts within the Solanaceae and
365 Amaranthaceae families (Fig. 3), consistent with previous reports cataloging these
366 plants as hosts of PVY (Edwardson and Christie 1997). However, *S. rhombifolia*
367 (Malvaceae family) plants were not infected with PVY, corroborating existing reports
368 that malvaceous plants are not hosts of PVY (Coutts and Jones 2014). PVYSI and
369 PVYSt differed in the rate of IR in the tested hosts, in which PVYSI demonstrated to be
370 more adapted to different hosts, compared to PVYSt (Fig. 3).

371



372

373 **Fig 3.** Experiments for determination of infection rates in indicator plants using PVYSt
 374 and PVYSI isolates from potato and tomato, respectively. Each PVY isolate is depicted
 375 by a distinct color on the x-axis: PVYSt in green and PVYSI in red. The number inside
 376 each bar indicates the number of plants positive for PVY infection followed by a slash
 377 and the total number of tested plants. Colored circles positioned above the graph denote
 378 the presence of symptoms, with an absence of a circle indicating no symptoms.

379

380 While both PVY isolates successfully infected most tested plants, the two
 381 exceptions were *C. amaranticolor* and *C. quinoa* plants. These two indicator plants are
 382 commonly used as test plants due to the production of easily countable local lesions
 383 after mechanical inoculation (Hollings 1956). They displayed unique symptoms upon
 384 inoculation with PVYSI. Initially, chlorotic spots with a red halo appeared on older
 385 leaves, which gradually evolved into systemic symptoms spreading throughout the plant
 386 (Sup. Fig. 6). This result contradicts previous knowledge of the local infection caused
 387 by PVY (Palazzo et al. 2008), demonstrating a concern with the use of model plants and

388 their applications. Importantly, this result was only observed when using PVYSl, while
389 PVYSt was not able to infect this host, once again proving the importance of isolate
390 choice. According to our results, it is crucial to exercise caution when performing
391 detection tests, preferably conducting pilot tests to minimize the risk of false negative
392 results and ensure accuracy.

393 While extensive research was conducted to elucidate the interactions between
394 potato and PVY, such as transgenic approaches overexpressing PVY-derived coat
395 protein, PVY-specific dsRNA (for RNAi), modified plant eIF4E, clustered regularly
396 interspaced short palindromic repeats (CRISPR/Cas) and spray-induced gene silencing
397 (SIGS) (Romano et al. 2001; Zimnoch-Guzowska et al. 2013; Valkonen et al. 2017;
398 Torrance and Talianksy 2020), other crops such as tomatoes and peppers have received
399 comparatively less attention. This highlights the need for increased research focus on
400 tomato and pepper to develop effective PVY management strategies.

401 The absence of resistant materials from commercial or breeding programs
402 underscores the urgency of addressing the spread of PVY in tomato and pepper
403 production fields, as it allows the virus to persist. Furthermore, our findings highlight
404 the variability in host range adaptation among different isolates of the same species,
405 emphasizing the need for thorough testing using diverse isolates.

406 Organisms continually evolve and adapt to new environments, resulting in the
407 emergence of new characteristics, including changes in their ability to infect hosts.
408 Therefore, a more dynamic approach to understanding the interaction between the virus
409 and its host is essential.

410 A comprehensive understanding of PVY and its adaptation across various host
411 systems is vital for developing effective control strategies against this pathogen.
412 Integration of advanced molecular techniques with a deep understanding of viral
413 dynamics across diverse hosts is key to mitigating the impact of PVY and safeguarding
414 global agricultural systems from its detrimental effects.

415 References

416

417 Agudelo-Romero P, Elena SF (2008) The degree of plant resilience to infection
418 correlates with virus virulence and host-range. Spanish Journal of Agricultural Research
419 6:160. <https://doi.org/10.5424/sjar/200806S1-384>

420

421 Avilla C, Collar JL, Duque M, Fereres A (1997) Yield of bell pepper (*Capsicum*
422 *annuum*) inoculated with CMV and/or PVY at different time intervals. Journal of Plant
423 Diseases and Protection 104:1–8

424

425 Bedhomme S, Lafforgue G, Elena SF (2012) Multihost experimental evolution of a
426 plant RNA virus reveals local adaptation and host-specific mutations. Molecular
427 Biology Evolution 29:1481–1492. <https://doi.org/10.1093/molbev/msr314>

428

429 Blanco-Urgoiti B, Sánchez F, Román CPS, et al (1998) Potato virus Y group C isolates
430 are a homogeneous pathotype but two different genetic strains. Journal of General
431 Virology 79:2037–2042. <https://doi.org/10.1099/0022-1317-79-8-2037>

432

433 Chikh-Ali M, Vander Pol D, Nikolaeva OV, et al (2016) Biological and molecular
434 characterization of a tomato isolate of potato virus Y (PVY) of the PVYCA lineage.
435 Archives of Virology 161:3561–3566. <https://doi.org/10.1007/s00705-016-3071-9>

436

437 Costa AS, Carvalho AMB, Kitajima EW (1960) Risca do tomateiro em São Paulo,
438 causada por estirpe do vírus Y. Bragantia 19:1111–1128.
439 <https://doi.org/10.1590/S0006-87051960000100067>

440

441 Coutts BA, Jones RAC (2014) Potato virus Y: contact transmission, stability,
442 inactivation, and infection sources. Plant Disease 99:387–394.
443 <https://doi.org/10.1094/PDIS-07-14-0674-RE>

444

445 Cuevas JM, Delaunay A, Visser JC, et al (2012) Phylogeography and molecular
446 evolution of potato virus Y. PLoS One 7:e37853.
447 <https://doi.org/10.1371/journal.pone.0037853>
448

449 Dijkstra J (1992) Importance of host ranges and other biological properties for the
450 taxonomy of plant viruses. Archives of Virology pp 173–176.
451 https://doi.org/10.1007/978-3-7091-6920-9_14
452

453 Dullemans AM, Cuperus C, Verbeek M, van der Vlugt RAA (2011) Complete
454 nucleotide sequence of a potato isolate of strain group C of Potato virus Y from 1938.
455 Archives of Virology 156:473–477. <https://doi.org/10.1007/s00705-010-0853-3>
456

457 Edwardson JR, Christie RG (1997) Viruses infecting peppers and other solanaceous
458 crops. In: Florida Agricultural Experiment Station Monograph Series 18-II. University
459 of Florida, Gainesville. Pp 424-524
460

461 Fereres A, Perez P, Gemeno C, et al (1993) Transmission of a Spanish pepper- and
462 potato-PVY isolates by aphid (Homoptera: Aphididae) vectors: epidemiological
463 implications. Environmental Entomology 22:1260-1265. [https://doi.org/](https://doi.org/10.1093/ee/22.6.1260)
464 [10.1093/ee/22.6.1260](https://doi.org/10.1093/ee/22.6.1260)
465

466 Fonseca LN, Inoue-Nagata AK, Nagata T, et al (2005) Diferenciação de estirpes de
467 Potato virus Y (PVY) por RT-PCR. Horticultura Brasileira, Brasília 4:904-910.
468 <https://doi.org/10.1590/S0102-05362005000400008>
469

470 Galvino-Costa S, dos Reis Figueira A, de Assis Câmara Rabelo-Filho F, et al (2012)
471 Molecular and serological typing of potato virus Y isolates from Brazil reveals a diverse
472 set of recombinant strains. Plant disease 10:1451-1458. [https://doi.org/](https://doi.org/10.1094/PDIS-02-12-0163-RE)
473 [10.1094/PDIS-02-12-0163-RE](https://doi.org/10.1094/PDIS-02-12-0163-RE)
474

475 García-Arenal F, Fraile A (2013) Trade-offs in host range evolution of plant viruses.
476 Plant Pathology 62:2–9. <https://doi.org/10.1111/ppa.12104>

477

478 Gebre Selassie K, Marchoux G, Delecolle B, et al (1985) Variabilité naturelle des
479 souches du virus Y de la pomme de terre dans les cultures de piment du sud-est de la
480 France. Caractérisation et classification en pathotypes. *Agronomie* 5:621-630.
481 [https://doi.org/ 10.1051/agro:19850708](https://doi.org/10.1051/agro:19850708)

482

483 Green KJ, Chikh-Ali M, Hamasaki RT, et al (2017) Potato virus Y (PVY) isolates from
484 *Physalis peruviana* are unable to systemically infect potato or pepper and form a
485 distinct new lineage within the PVY C strain group. *Phytopathology* 107:1433–1439.
486 <https://doi.org/10.1094/PHTO-04-17-0147-R>

487

488 Hollings M (1956) *Chenopodium amaranticolor* as a test plant for plant viruses. *Plant*
489 *Pathology* 5:57–60. <https://doi.org/10.1111/j.1365-3059.1956.tb00085.x>

490

491 Inoue-Nagata AK, Jordan R, Kreuze J, et al (2022) ICTV Virus Taxonomy Profile:
492 *Potyviridae* 2022. *Journal of General Virology* 103:001738.
493 <https://doi.org/10.1099/jgv.0.001738>

494

495 Inoue-Nagata AK, Fonseca MEN, Lobo TOTA, et al (2001) Analysis of the nucleotide
496 sequence of the coat protein and 3'-untranslated region of two Brazilian Potato virus Y
497 isolates. *Fitopatologia Brasileira* 26:45-52.
498 <https://doi.org/10.1590/S0100-41582001000100008>

499

500 Jeffries CJ (1998) FAO/IPGRI Technical guidelines for the safe movement of potato
501 germplasm. Food and Agriculture Organization of the United Nations,
502 Rome/International Plant Genetic Resources Institute, Rome, Italy 19

503

504 Kang BC, Yeam I, Jahn MM (2005) Genetics of plant virus resistance. *Annual Review*
505 of *Phytopathology* 43:581–621.
506 <https://doi.org/10.1146/annurev.phyto.43.011205.141140>

507

508 Karasev AV, Xiaojun H, Brown CJ, et al (2011) Genetic diversity of the ordinary strain
509 of potato virus Y (PVY) and origin of recombinant PVY strains. *Phytopathology*
510 7:778-785. <https://doi.org/10.1094/PHYTO-10-10-0284>
511

512 Karasev AV, Gray SM (2013) continuous and emerging challenges of potato virus Y in
513 potato. *Annual Review of Phytopathology* 51:571–586.
514 <https://doi.org/10.1146/annurev-phyto-082712-102332>
515

516 Lourenção AL, Siqueira WJ, Melo AMT, et al (2005) Resistência de cultivares e
517 linhagens de tomateiro a tomato chlorotic spot virus e a potato virus Y. *Fitopatol*
518 *Brasileira* 30:609–614. <https://doi.org/10.1590/S0100-41582005000600007>
519

520 Lucena VS, Nakasu EYT, Pereira JL, et al (2024) Emergence of potato virus Y
521 outbreaks in tomatoes in Brazil, the disease and spread. *bioRxiv*.
522 <https://doi.org/10.1101/2024.05.17.594728>
523

524 Malpica JM, Sacristán S, Fraile A, García-Arenal F (2006) Association and host
525 selectivity in multi-host pathogens. *PLoS One* 1:e41.
526 <https://doi.org/10.1371/journal.pone.0000041>
527

528 McLeish MJ, Fraile A, García-Arenal F (2019) Evolution of plant-virus interactions:
529 host range and virus emergence. *Current Opinion in Virology* 34:50-55. <https://doi.org/10.1016/j.coviro.2018.12.003>
530
531

532 Meissner PEF, Cupertino FP, Avila AC (1990) Purificacao e serologia de dois isolados
533 do virus Y da batata obtidos de pimentão e de tomate no Distrito Federal. *Fitopatologia*
534 *Brasileira* 15:235-237.
535

536 Moury B (2010) A new lineage sheds light on the evolutionary history of potato virus Y.
537 *Molecular Plant Pathology* 11:161–168.
538 <https://doi.org/10.1111/j.1364-3703.2009.00573.x>
539

540 Nagai H (1971) Novas variedades de pimentão resistentes ao mosaico causado por vírus
541 Y. *Bragantia* 30:91–100. <https://doi.org/10.1590/S0006-87051971000200001>
542

543 Nagai H, Costa AS (1969) Incorporação de resistência ao mosaico Y em tomateiro.
544 *Bragantia* 28:219–226. <https://doi.org/10.1590/S0006-87051969000100017>
545

546 Nagai H, Lourenção AL, Siqueira WJ (1992) Tomato breeding for resistance to diseases
547 and pests in Brazil. *Acta Horticultae* 301:91–97. [https://doi.org/](https://doi.org/10.17660/ActaHortic.1992.301.10)
548 [10.17660/ActaHortic.1992.301.10](https://doi.org/10.17660/ActaHortic.1992.301.10)
549

550 Nagata T, Inoue AK, Dusi A, Kitajima EW (1995) Bidens mosaic potyvirus newly
551 isolated from pea, its characteristics and serological relationship with other potyviruses.
552 *Fitopatologia Brasileira* 20:473-478
553

554 Nigam D, LaTourrette K, Souza PFN, Garcia-Ruiz H (2019) Genome-wide variation in
555 potyviruses. *Frontiers in Plant Science* 10. <https://doi.org/10.3389/fpls.2019.01439>
556

557 Palazzo SRL, Colariccio A, Marchi ATM (2008) Reação de acessos de *Lycopersicon*
558 spp. a um isolado de potato virus y (PVY^o) de tomateiro. *Bragantia* 67:391–399.
559 <https://doi.org/10.1590/S0006-87052008000200015>
560

561 Qiu CL, LV WH, LV DQ et al (2014) Symptoms of four potato varieties infected with
562 Potato spindle tuber viroid (PSTVd). *Journal of Plant Protection Research* 6:159-163
563

564 Quenouille J, Vassilakos N, Moury B (2013) Potato virus Y: a major crop pathogen that
565 has provided major insights into the evolution of viral pathogenicity. *Molecular Plant*
566 *Pathology* 14:439–452. <https://doi.org/10.1111/mpp.12024>
567

568 Romano E, Ferreira AT, Dusi AN, et al (2001) Extreme resistance to two Brazilians
569 strains of potato virus Y (PVY) in transgenic potato cv Achat expressing the PVY^o coat
570 protein gene from argentine PVY^o strain. *Horticultura Brasileira* 2:118-122
571

572 Romero A, Blanco-Urgoiti B, Soto MJ, et al (2001) Characterization of typical
573 pepper-isolates of PVY reveals multiple pathotypes within a single genetic strain. *Virus*
574 *Research* 79:71–80. [https://doi.org/10.1016/S0168-1702\(01\)00300-8](https://doi.org/10.1016/S0168-1702(01)00300-8)
575

576 Singh RP, Valkonen JPT, Gray SM, et al (2008) Discussion paper: The naming of potato
577 virus Y strains infecting potato. *Archives of Virology* 153:1–13.
578 <https://doi.org/10.1007/s00705-007-1059-1>
579

580 Torrance L, Talianksy ME (2020) Potato Virus y emergence and evolution from the
581 Andes of South America to become a major destructive pathogen of potato and other
582 solanaceous crops worldwide. *Viruses* 12. <https://doi.org/10.3390/V12121430>
583

584 Valkonen JPT, Gebhardt C, Zimnoch-Guzowska E, Watanabe KN (2017) Resistance to
585 Potato virus Y in potato. In: *Potato virus Y: biodiversity, pathogenicity, epidemiology*
586 *and management*. Springer International Publishing, Cham, pp 207–241
587

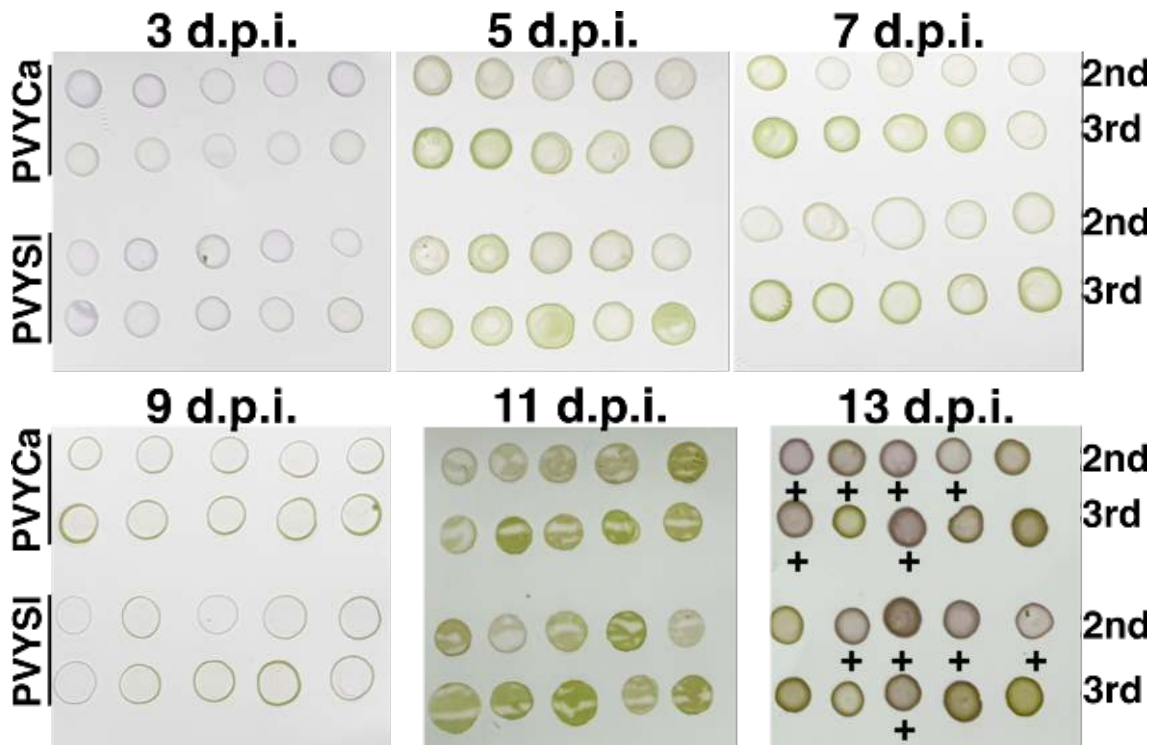
588 Vance BV (1991) Replication of potato virus X RNA is altered in coinfections with
589 potato virus Y. *Virology* 181:486-494. [https://doi.org/10.1016/0042-6822\(91\)90589-4](https://doi.org/10.1016/0042-6822(91)90589-4)
590

591 Vassilakos N, Simon V, Tzima A, et al (2016) Genetic determinism and evolutionary
592 reconstruction of a host jump in a plant virus. *Molecular Biology and Evolution*
593 33:541–553. <https://doi.org/10.1093/molbev/msv222>
594

595 Whitlock MC (1996) The red queen beats the jack-off-all-trades: the limitations on the
596 evolution of phenotypic plasticity and niche breadth. *The American Naturalist*
597 148:S65–S77.
598

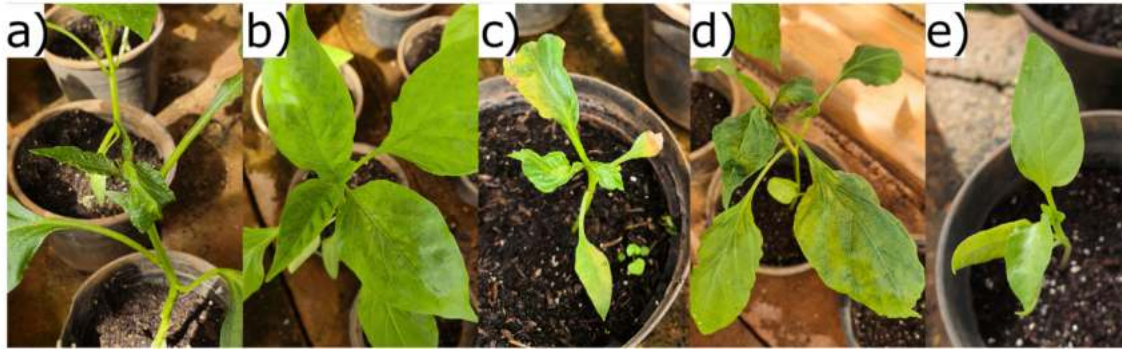
599 Yarwood CE (1979) Host passage effects with plant viruses. *Advances in Virus*
600 *Research* pp 169–190. [https://doi.org/10.1016/s0065-3527\(08\)60570-9](https://doi.org/10.1016/s0065-3527(08)60570-9)
601

602 Zimnoch-Guzowska E, Yin Z, Chrzanowska M, Flis B (2013) sources and effectiveness
603 of potato PVY resistance in ihar's breeding research. American Journal of Potato
604 Research 90:21–27. <https://doi.org/10.1007/s12230-012-9289-5>



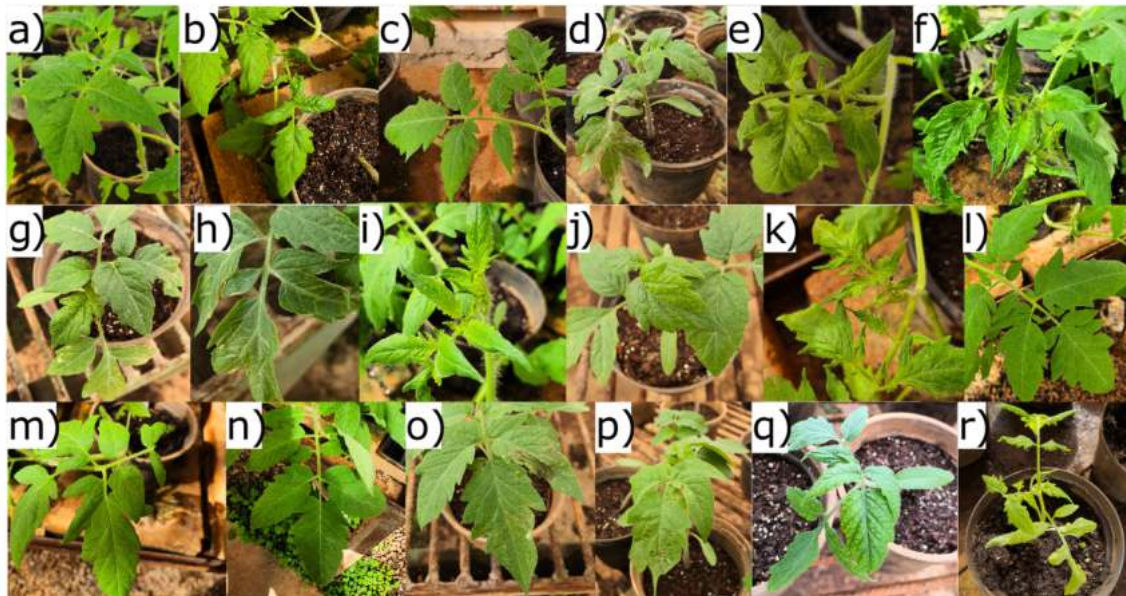
605

606 **Sup. Fig 1.** Dot-ELISA of pepper plants with 3, 5, 7, 9, 11 and 13 days post inoculation
 607 (d.p.i.) using two isolates, PVYCa and PVYSI, and two different leaves, the second
 608 (2nd) and the third (3rd) leaf from the top. The purple color development represents a
 609 positive reaction. Positive samples are marked with + symbol.



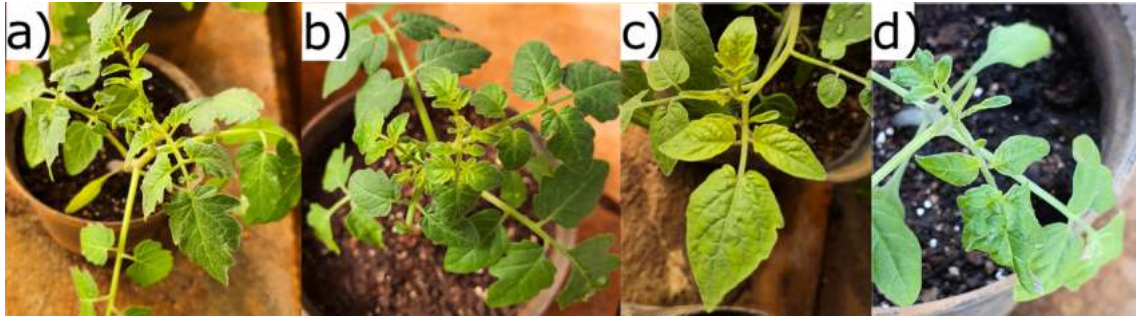
610

611 **Sup Fig 2.** Symptoms observed in sweet pepper cultivars mechanically inoculated with
612 PVYCa: (a) foliar deformation and interveinal chlorosis in Camaro, (b) interveinal and
613 veinal chlorosis in Dahra RX, (c) foliar deformation, stunting and necrotic spots in
614 Ikeda, (d) foliar deformation, interveinal and veinal chlorosis in Raquel, and (e) stunting
615 in Taurus.



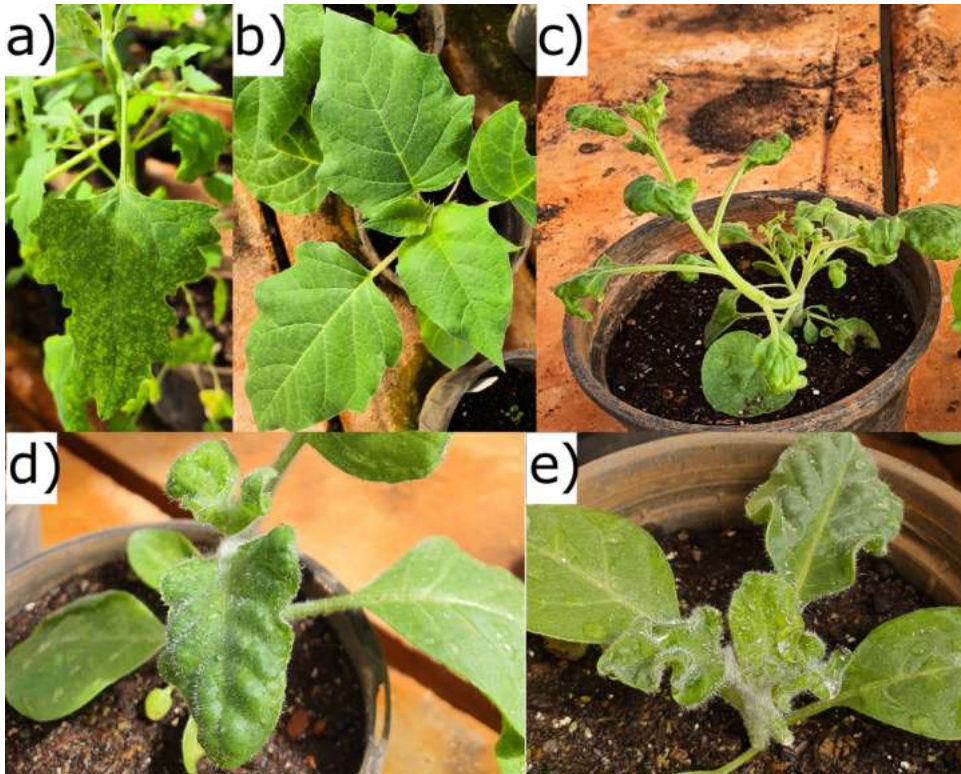
616

617 **Sup Fig 3.** Symptoms observed in tomato cultivars mechanically inoculated with
 618 PVYSl: (a) veinal chlorosis in Ângela Hiper, (b) foliar deformation in BRS Sena, (c)
 619 veinal chlorosis in Candieiro, (d) necrotic spots in Dominador, (e) chlorotic spots in
 620 Durino, (f) foliar deformation in Grazianni, (g) veinal chlorosis in Itaipava, (h) chlorotic
 621 spots in Matinella, (i) chlorosis in Milão, (j) interveinal chlorosis in Monza, (k) foliar
 622 deformation in Parma, (l) interveinal chlorosis in Protheus, (m) veinal chlorosis in Santa
 623 Clara, (n) veinal chlorosis in Santyno, (o) local necrosis in Serato, (p) local necrosis in
 624 Tyson, (q) interveinal chlorosis in Vento and (r) chlorosis in Viradoro. Only cultivars
 625 with symptoms are shown in the figure.



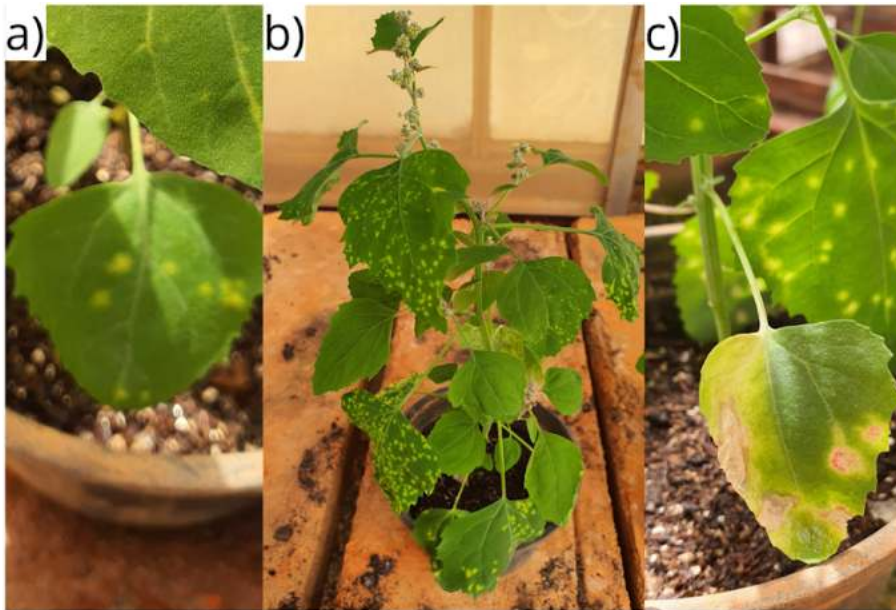
626

627 **Sup Fig 4.** Symptoms observed in wild tomato cultivars mechanically inoculated with
628 PVYSl: (a) veinal chlorosis in IAC 237, (b) chlorosis in LA1584, (c) chlorosis in
629 LA722 and (d) leafroll in PI126925. Only cultivars with symptoms are shown in the
630 figure.



631

632 **Sup Fig 5.** Symptoms observed in indicator plants mechanically inoculated with PVYSt
633 and PVYSt (a) chlorotic spots in *C. quinoa* (PVYSt), (b) veinal chlorosis in *D. metel*
634 (PVYSt), (c) foliar deformation in *N. benthamiana* (PVYSt), (d) foliar deformation in
635 *N. rustica* (PVYSt) and (e) blistering and foliar deformation in *N. sylvestris* (PVYSt).



636

637 **Sup Fig 6.** Evolution of symptoms in *C. amaranticolor* infected with PVYSl, showing
638 (a) the first chlorotic spots on the inoculated leaves, followed by (b) systemic infection
639 with chlorotic spots in young leaves and (c) the appearance of red halos around old
640 lesion.

1

2

3 **Detecting and sequencing the whole-genome of distinct potato virus Y** 4 **isolates using a PCR-Nanopore approach**

5

6

7 **Abstract**

8

9 Potato virus Y (PVY) is a relevant pathogen affecting a range of solanaceous crops,
10 including potatoes, tomatoes, and peppers. This study aimed to develop and validate a
11 robust sequencing approach for PVY genomes using Oxford Nanopore Technologies
12 (ONT). For selecting the virus isolates to be sequenced, a total of 21 PVY-positive
13 samples were collected from infected potato, pepper, and tomato plants. One isolate per
14 host was selected to conduct ONT sequencing: PVYCa (pepper), PVYSt (potato), and
15 PVYSl (tomato). For this purpose, four overlapping primer sets covering the complete
16 viral genome were designed based on conserved regions identified through alignment of
17 a large dataset ($n = 445$). We also used a barcorde kit, able to sequence up to 24 samples
18 in the same flowcell. Although a similar amount of input amplicons was used for
19 sequencing, the obtained read coverage was not uniform along the genome, yet we were
20 able to produce sufficient reads to assemble the genome of all isolates. The number of
21 reads varied according to the samples, but the expected sizes of ~ 1.8 and ~ 3 kb were
22 consistently obtained, including long reads covering the entire genome. Illumina
23 sequencing was used to validate the Nanopore assembly using the isolate PVYCa. By
24 calculating the pairwise nucleotide distance using Tamura-Nei model and performing a
25 phylogenetic analysis, our results demonstrated a high level of identity between both
26 PVYCa genomes, validating the sequence quality obtained by the ONT approach.
27 Furthermore, we developed PVY-specific primers to facilitate specific detection. These
28 primers effectively distinguished PVY from other viruses, including closely related
29 potyviruses. This study highlights the reliability of ONT for sequencing diverse PVY
30 genomes, demonstrating its utility for high-throughput, cost-effective, and rapid viral
31 genome analysis. The successful application of this methodology in sequencing multiple

32 PVY isolates will contribute to a deeper understanding of PVY diversity and host
33 interactions, advancing on both diagnostic and evolutionary studies.

34

35 **Key-words:** High-throughput genome sequencing, Nanopore, Sequencing
36 methodology, Virus detection, Virus epidemiology, Virus sequencing

37 Introduction

38

39 Potato virus Y (PVY) is a positive-sense, single-stranded RNA virus, classified in the
40 family *Potyviridae*, genus *Potyvirus* and species *Potyvirus yituberosi*, with a genome
41 size of approximately 9.7 Kb. It encodes a polyprotein that undergoes autoproteolysis
42 (Inoue-Nagata et al. 2022). PVY can be transmitted in a non-persistent manner by at
43 least 65 species of aphids (Lacomme et al. 2017; Rizk et al. 2020). PVY has a broad
44 host range (Edwardson and Christie 1997; Jeffries 1998) that includes important
45 solanaceous plants, *e.g.*, tomato (*Solanum lycopersicum*), potato (*S. tuberosum*), and
46 pepper (*Capsicum annuum*) (Kerlan et al. 2008). Potato plants are greatly affected by
47 PVY infection, with reported losses of up to 80% (Hane and Hamm 1999) and
48 adversely affecting tuber quality (Le Romancer et al. 1994). Yield reduction of 0.1805
49 Tons/ha has been reported for each 1% increase in PVY incidence (Nolte et al. 2004). In
50 contrast, studies of PVY in tomatoes are limited. These properties rendered to PVY a
51 ranking position of the fifth most important plant virus (Scholthof et al. 2011). This
52 position may not have changed in the last decade.

53 RNA viruses, such as PVY, have high mutation rates of 10^{-6} to 10^{-4}
54 substitutions/nucleotide/replication (Peck and Lauring 2018) due to various
55 mechanisms, such as the lack of 3' exonuclease proofreading activity of the RdRp
56 (Steinhauer et al. 1992), genome size, type, and replication mode (Sanjuán and
57 Domingo-Calap 2016). Notwithstanding, recombination is known to highly modulate
58 PVY populations (Revers et al. 1996). Recombination in viruses mostly happens when
59 two or more virus genomes combine through replicase-driven template switching,
60 resulting in a chimeric genome that may exhibit unique genetic traits compared to their
61 parental viruses. This process is particularly significant in potyviruses, for which the
62 estimated recombination rate is 3.427×10^{-5} per nucleotide site per generation,
63 comparable to the rate of mutation, highlighting the important role of recombination in
64 generating viral diversity (Tromas et al. 2014). Hence, PVY has a high genetic
65 variability, and it exists as a complex of strains, classified based on the symptoms'
66 development in potatoes and tobacco. Initially, PVY was classified in three strains, the
67 ordinary (PVY^O), common (PVYCA) and necrotic (PVY^N) (Jones 1990; Singh et al.
68 2008). Then, many recombinant strains were reported in the last 20 years (Le Romancer

69 et al. 1994; Chikh Ali et al. 2010; Karasev et al. 2011; Funke et al. 2017; Green et al.
70 2017, 2020; Davie et al. 2017; Rodriguez-Rodriguez et al. 2020), which corroborates
71 with the high mutation rates.

72 A broad range of diagnostic tools are available to detect plant viruses, including
73 enzyme-linked immunosorbent assay (ELISA), loop mediated isothermal amplification
74 (LAMP) and the most commonly used polymerase chain reaction (PCR). Also
75 important, genome sequencing is generally used to detect, identify and determine the
76 virus properties. More recently, high throughput sequencing, HTS (or next generation
77 sequencing) became popular for virus identification. Obtaining the complete genome
78 sequence of a virus is still costly and labor-intensive when using the traditional methods
79 of Sanger sequencing or HTS. With the purpose to facilitate and cheapen the sequencing
80 process, Oxford Nanopore Technology (ONT) released an equipment and protocols
81 based on the use of nanopores to determine the base sequences by analyzing the
82 electrical current when the nucleic acid passes through these nanopores (Mikheyev and
83 Tin 2014). ONT sequencing offers various benefits, such as the ability to sequence
84 individual molecules, generate lengthy sequencing reads, achieve fast sequencing
85 speeds, and monitor sequencing data in real-time (Laver et al. 2015; Deamer et al.
86 2016). Likewise, to decrease even more the time and price of sequencing per sample the
87 use of barcodes can be applied, sequencing more than one sample in a single flow-cell.
88 The ONT MinION, the Nanopore sequencing platform, has gained widespread
89 acceptance, and it can be powered through a USB port on a personal computer. This
90 platform is unique among other sequencing technologies because it allows for
91 sequencing and real-time data analysis to be conducted directly on laboratory benches.
92 Since its introduction to the public, ONT has been employed in several plant virus
93 genome studies (Martins et al. 2021; Amoia et al. 2022; Dong et al. 2022), though it
94 remains in its early stages and offer substantial potential for further refinement.
95 Nanopore sequencing offers numerous applications in virus research, including viral
96 detection and surveillance, genome assembly, the discovery of new variants and novel
97 viruses, and the identification of chemical modifications and impose advantages over
98 HTS, such as the capability to produce ultra-long reads, real-time monitoring and
99 analysis, portability, and the ability to directly sequence RNA or DNA molecules (Ji et
100 al. 2024).

101 As explained above, PVY is characterized by a diverse population structure
102 composed of a large number of variant genomes, known as *quasispecies* (Más et al.
103 2010), which arises due to its high mutation rates. This mutant cloud is constantly
104 changing in relative frequency during viral replication. Sequencing the genomes of
105 many isolates, and capturing the diversity present in their genomes are an arduous task,
106 whereas they are essential for population structure and evolution studies. For this
107 reason, we wanted to use PVY as the model virus to evaluate the use of Nanopore
108 sequence for genome sequence studies. Three PVY isolates were selected, one from
109 potato, one from pepper and another one from tomato.

110 Here, we provide a step-by-step guide for a simple strategy to detect and obtain up
111 to 24 PVY whole genome sequences in a single ONT flow-cell. Our methodology is
112 efficient in enriching and amplifying the target sequences, as we designed primers that
113 are highly specific for PVY genomes while also detecting all available variability within
114 the species.

115

116

117 **Materials and methods**

118

119 **Virus isolates collection**

120 PVY isolates were collected from pepper (*Capsicum annuum*), potato (*Solanum*
121 *tuberosum*) and tomato (*S. lycopersicum*) in commercial fields located near each other
122 in the greenbelt of Brasília (16°04'23.1"S 47°21'32.9"W to PVYSt and 15°55'58.8"S
123 47°35'47.1"W to PVYCa and PVYSl), Distrito Federal, Brazil. We randomly collected
124 plants with and without apparent symptoms (Sup. Table 1 and Sup. Fig. 1).

125 All samples ($n = 18$ from pepper, $n = 52$ from potato and $n = 110$ from tomato)
126 were submitted to a serological test (dot-ELISA) with our PVY polyclonal antibody,
127 according to Nagata et al. (1995) (a list of positively detected plants is detailed in Sup.
128 Table 1). The leaves were weighed, homogenized in phosphate-buffered saline (PBS,
129 pH 7.0), and spotted in two dilutions: 1:10 and 1:100. After color development using
130 nitro blue tetrazolium (NBT) and 5-bromo-4-chloro-3-indolyl-phosphate (BCIP), we
131 randomly chose one positive sample from each plant species to proceed to the next

132 steps. The virus isolates were identified as PVYCa (from pepper), PVYSt (from potato)
133 and PVYSl (from tomato).

134

135 **RNA extraction, cDNA synthesis, PCR and Sanger sequencing**

136 Total RNA was extracted using the RNeasy plant mini kit (Qiagen, Hilden,
137 Germany) following the manufacturer protocol. The cDNA was constructed using
138 SuperScript III (ThermoFisher, California, USA) with primers M4T (5'-GTT TTC CCA
139 GTC ACG AC(T₁₅)-3') (Chen et al. 2001) and random hexamers. An incubation at 37
140 °C for 20 min using 2 Units of *Escherichia coli* RNase H (ThermoFisher) was done to
141 remove the RNA strand of the RNA-cDNA hybrid.

142 To confirm the identity of the PVY isolates, their genomes were partially
143 sequenced by Sanger sequencing. PCR was performed with *Taq* DNA recombinant
144 polymerase (ThermoFisher) with M4 (5'-GTT TTC CCA GTC ACG AC-3') and
145 Sprimer (5'-GGX AAY AAY AGY GGX CAZ CC-3') primers (Chen et al. 2001),
146 producing an amplicon of ~1.7 kb. The PCR products were separated on a 1% agarose
147 gel, the agarose gel fragments containing the target DNA were sliced and isolated from
148 the agarose gel using Wizard SV Gel and PCR Clean-up System (Promega, Wisconsin,
149 USA). The amplicons were sequenced using the Sanger method with Sprimer by
150 Macrogen Inc. (South Korea).

151

152 **Nanopore primer design**

153 All complete genomes of PVY available in the GenBank database were downloaded (*n*
154 = 634) in February, 2023. The dataset was analyzed, excluding all dubious and
155 incomplete sequences, aligned and manually adjusted using Muscle (Edgar 2004). Only
156 one representative haplotype was maintained by using DnaSP (Rozas et al. 2017)
157 resulting in a dataset of 445 sequences. Highly conserved regions were searched in the
158 alignment. These regions were selected and candidate primers were designed and
159 evaluated using optimal primer conditions, such as melting temperature, folding and
160 hybridization of strands, GC content and amplicon size using OlygoAnalyzer
161 (Owczarzy et al. 2008).

162 Four sets of degenerated primers with overlapping regions were designed in these
163 highly conserved regions, covering the entire PVY genome (Table 1). Each set of

164 primers was composed of three forward and three reverse primers (A to C) with minor
165 differences, named Y1F to Y4F and Y1R to Y4R for forward and reverse primers,
166 respectively. To avoid any eventual mismatch in the last base of the primer, hence
167 capturing all the genome diversity, an inosine was added at the 3'-termini of all designed
168 primers. For amplification of the 3' terminal end, the M4 primer was used in
169 combination with the Y4F primer mix.

170

171 **Amplification of target region with PCR**

172 PCR amplification was performed using the cDNA with high-fidelity Q5 DNA
173 polymerase (NEB, Massachusetts, USA) according to the manufacturer
174 recommendations. The best temperature and reaction conditions were tested for
175 obtaining the highest amplicon yield. For sequencing, the PCR products were purified
176 using Wizard SV Gel and PCR Clean-up System (Promega, Wisconsin, USA) to remove
177 excess primers and nucleotides.

178

179 **ONT sequencing strategy**

180 Amplified DNA fragments were first quantified by Qubit 3 fluorometer (Invitrogen,
181 Massachusetts, USA), and mixed to obtain equimolar quantities for amplicon and for
182 PVY isolate, according to the recommended protocol.

183 The barcode expansion kit (EXP-NBD 104, NEB) was used to sequence the three
184 viruses at the same time, following the recommendation. The DNA repair and
185 end-preparation were performed without the fragmentation step. After barcoding, the
186 three amplicon pools were measured and diluted again to have the same equimolar
187 quantity in each of the three samples, approximately 600 ng each. The sequencing was
188 done using the Nanopore ligation sequencing kit SQK-LSK109 (NEB) and the prepared
189 library was mixed together and loaded on a MinION with a R9.4.1 flow cell
190 (FLO-MIN106). All other procedure steps of native barcoding genomic DNA Nanopore
191 were followed as described in the recommended protocol.

192

193 **Sequencing analysis and genome assembly**

194 The quality of the reads was assessed both within and between samples using
195 NanoPack2 (De Coster et al. 2018). Three PVY isolates (PVYCa, PVYSt, PVYSl) were

196 subjected to Nanopore sequencing at the same time and in the same flowcell.
197 Sequencing data were analyzed to derive mean and median read lengths, mean and
198 median read quality scores, number of reads, total bases, read length N50, standard
199 deviation (SD) of read lengths, and read quality distribution ($> Q_{10}$, $> Q_{15}$, $> Q_{20}$).
200 Dorado (Oxford Nanopore Technologies) was employed for base calling. It is important
201 to notice that the Q-score for Nanopore and Illumina sequencing are similar, but the
202 cutoff values and achievable accuracies differ because Nanopore works with lower
203 Q-scores, and higher error rates are compensated for by different downstream
204 processing strategies, such as polishing and consensus generation.
205 Subsequently, minimap2 (Li 2018) was used to align reads to the reference PVY
206 genome (X12456) and convert it to SAM file. SAM file was then converted and sorted
207 to BAM using Samtools (Danecek et al. 2021) and used to assemble the consensus
208 genome using Geneious Prime v. 2022.2 (Biomatters). Manual inspection was
209 conducted to validate the assembled genomes, and BLASTn (Johnson et al. 2008) was
210 utilized to compare the three genomes against the GenBank nucleotide sequence
211 database.

212

213 **Total RNA purification and Illumina sequencing**

214 To validate the accuracy of the Nanopore genome sequence and assembly, we selected
215 one isolate, PVYCa, to sequence with the conventional HTS method by using the
216 Illumina platform. Pepper cultivar Ikeda, infected with the original PVYCa, was used to
217 semi-purify the viral particles (Blawid et al. 2017). Total RNA was extracted using the
218 AllPrep DNA/RNA Micro Kit (QIAGEN) and subsequently sequenced on the Illumina
219 Novaseq platform by Macrogen Inc. (Seul, South Korea). Following Illumina
220 sequencing, the reads underwent trimming using BBduk
221 (<https://sourceforge.net/projects/bbmap/>), and the resulting contigs were *de novo*
222 assembled using MEGAHIT (Li et al. 2015). The assembled contigs were aligned and
223 subjected to diamond Blastx (Buchfink et al. 2015) against the nr database (downloaded
224 on the 2024-06-24) to exclude non-PVY contigs. The longest contig was subjected to
225 BLASTn against the nucleotide database to identify the closest isolate (EU563512) and
226 then the reads were aligned to this sequence with BMAP

227 (<https://sourceforge.net/projects/bbmap/>) and the consensus sequence was generated
228 with Geneious Prime v. 2022.2.

229

230 **Genome analysis**

231 In order to compare the assembled consensus genomes, we computed the pairwise
232 distances using the better-fit model with the lowest AIC, Tamura-Nei model with
233 Gamma distributed rates, using MEGAX (Kumar et al. 2018). To this analysis, we
234 included both PVYCa assembled genomes (Illumina and Nanopore) along with PVYSl,
235 PVYSt, and the PVY reference genome (X12456). Pheatmap package (Kolde 2019) on
236 R (R Core Team 2022) was used to generate the heatmap. Furthermore, to confirm the
237 accuracy of the sequencing, we calculated the Pearson correlation coefficient between
238 the distances obtained from Illumina and Nanopore sequencing of PVYCa.

239 In a second approach, we added 49 representative PVY genomes from diverse
240 strains, countries and hosts, together with our sequenced isolates ($n = 53$). Furthermore,
241 we included three outgroup species, namely bidens mosaic virus (BiMV) (Dujovny et
242 al. 1998; Inoue-Nagata et al. 2006b), pepper severe mosaic virus (PSMV) (Ahn et al.
243 2006) and sunflower chlorotic mottle virus (SCMoV) (Dujovny et al. 2000), known to
244 be the closest relatives to PVY. Consequently, our dataset consisted of a total of 56
245 genomes. After construction of the alignment with Muscle (Edgar 2004), a
246 maximum-likelihood (ML) phylogenetic tree was inferred using iq-tree2 (Minh et al.
247 2020) with 10,000 bootstrap replicates. The phylogenetic tree was edited using iTol
248 (Letunic and Bork 2021).

249

250 **Design and evaluation of PVY-specific primers**

251 Two PVY-specific primers, a forward (YSF: 5'-ACT ATG ATT TTT CGT CGA GAA
252 CAA G-3') and a reverse (YSR: 5'-GGC GAG GTT CCA TTT TCA ATG C-3') primer,
253 were designed using the same alignment ($n = 445$) that was used for Nanopore primer
254 design. We searched for regions conserved in PVY genomes, using primer Blast
255 (Johnson et al. 2008).

256 In order to test the efficiency of the primers, they were tested with three PVY
257 isolates. Additionally, we included in our analysis other widespread viruses that infect
258 solanaceous plants: groundnut ringspot virus (GRSV - genus *Orthotospovirus*), pepper

259 yellow mosaic virus (PepYMV - *Potyvirus*), pepper mild mottle virus (PMMoV -
260 *Tobamovirus*), and tomato mosaic virus (ToMV - *Tobamovirus*). Total RNA and the
261 cDNA construction of infected leaves were performed essentially as described above.
262 We also included a non-infected healthy plant in our analyses. The PCR was done using
263 *Taq* DNA recombinant polymerase (ThermoFisher) in a 35-cycling reaction of 95 °C
264 denaturing for 30 sec, 52 °C annealing for 30 sec and 72 °C extension for 1 min with a
265 final extension of 10 min.

266

267

268 **Results**

269

270 **Field collection and identification of PVY isolates**

271 We wanted to establish a protocol for amplification and sequencing of PVY genomes
272 within a wide range of diversity, hence isolates were collected from potato, pepper and
273 tomato plants, expecting they were divergent though coexisting in the same
274 agroecosystem. Leaves of infected plants were collected in different fields and a
275 dot-ELISA procedure using polyclonal PVY antibody was performed as the first
276 detection test. We detected 17 positive samples in the potato crop (Infection Rate (IR) =
277 32.7%), 2 positive samples in pepper (IR = 11.1%) and 2 positive samples in tomatoes
278 (IR = 1.8%) (Supplementary Table 1). Infected plants exhibited blistering, chlorosis,
279 mosaic and necrosis in pepper; chlorosis and necrotic spots in potato; and no symptom
280 in tomato plants. One positive sample was selected from each crop, total RNA was
281 extracted, and used for cDNA construction with a random hexamer and an anchored
282 oligodT primer. The 3' terminal region of the genome was amplified by PCR using the
283 Sprimer, located in the NIb region, and the anchor primer M4, described as universal
284 potyvirus primers (Chen et al. 2001). This fragment was Sanger sequenced and
285 confirmed that all three viruses are isolates of PVY (not shown). They were named
286 PVYCa (pepper isolate), PVYSt (potato isolate) and PVYSl (tomato isolate).

287

288 **Nanopore primer design and evaluation**

289 To design primers able to capture the diversity of the PVY genome, we used all full
290 genome sequences available at the GenBank ($n = 445$) for complete genome alignment

291 and searched for conserved regions. The PVY genome was divided in four regions,
 292 three with ~3 kb and a 3'-end region with ~1.8 kb. Therefore, four primer sets were
 293 designed, each set being composed by three forward and three reverse primers (except
 294 the set 4, which uses M4 as reverse primer) (Fig 1a - Table 1). Some primers were
 295 degenerated (a list of all primers and their characteristics can be found in Table 1). An
 296 inosine was added to the 3' end of the primer to avoid misannealing due to unexpected
 297 divergency in this position.

298 The primers were tested with the three PVY isolates and the optimal Q5 DNA
 299 Polymerase PCR conditions were determined for each set of primers (Table 1). Using
 300 the optimal conditions, a PCR was done for each primer set and each isolate. Some
 301 conditions may include the use of GC enhancer due the presence of rich G-C regions
 302 and a difference in extension time for Set 4. All primers have the same melting
 303 temperature of 55 degrees. All sets of primers successfully amplified all genome regions
 304 for all the three isolates (Fig 1b).

305 The PCR amplification yield was not uniform for all amplicons, consequently
 306 before and after the barcoding ligation, the DNA was measured to ensure the input of
 307 equimolar quantity and then proceed to sequencing (Fig 1c).

308

309 **Tab 1.** Description of the sequencing primers and the PCR conditions for amplification
 310 of the whole-genome of PVY using Q5 DNA polymerase. Each color represents a set of
 311 primers used to sequence each fragment.

Primer	Sequence (5' → 3')	Size	%GC	GC En ^s	ET (min) [#]	MT (°C)*
	AAATTAAAACAACACTCAATACAACAT					
Y1F-A	AAI	28	18			
Y1F-B	AAATTAAAACAACACTCAATACAACAI	25	20			
Y1F-C	AAATTAAAACAACACTCAATACAI	22	18	no	1:45	55
Y1R-A	AACGCCTAAAGATTCTACGAATI	23	35			
Y1R-B	AAACGCCTAAAGAKYSTACGI	22	33			
Y1R-C	GGCAAACGCCTAAARAKYSTAI	22	32			

	ATGGAAAAAAAAAYTATCTARRYCTCT				
Y2F-A	TI	27	26		
Y2F-B	ATGGAAAAAAAAAYTATCTARRYCTCI	25	28		
Y2F-C	TTATGGAAAAAAAAAYTATCTARRYCI	25	24		
Y2R-A	GCYTTRTCRBACCARTCYTI	20	46		
Y2R-B	TTRTCRBACCARTCYTTYCTI	21	39		
Y2R-C	CCARTCYTTYCTRAARTANGCI	22	41	yes	
Y3F-A	CCACTGTTGGTATGGGCAI	19	53		
Y3F-B	CACCACTGTTGGTATGGGI	19	53		
Y3F-C	GGCACCACTGTTGGTATGI	19	53		
Y3R-A	ATGCACCARACCATWAGCCCAI	22	48		
Y3R-B	GCACCARACCATWAGCCCATI	21	50		
Y3R-C	ACCARACCATWAGCCCATTCAI	22	43		
<hr/>					
Y4F-A	GTNGTDGAYAAAYTCYCTYATGGTI	24	41		
Y4F-B	CBGTNGTDGAYAAAYTCYCTYATGI	24	44		
Y4F-C	GTDGAYAAAYTCYCTYATGGTYGTI	24	41	no	1:00
M4	GGNAAYAAAYAGYGGNCARCC	20	55		

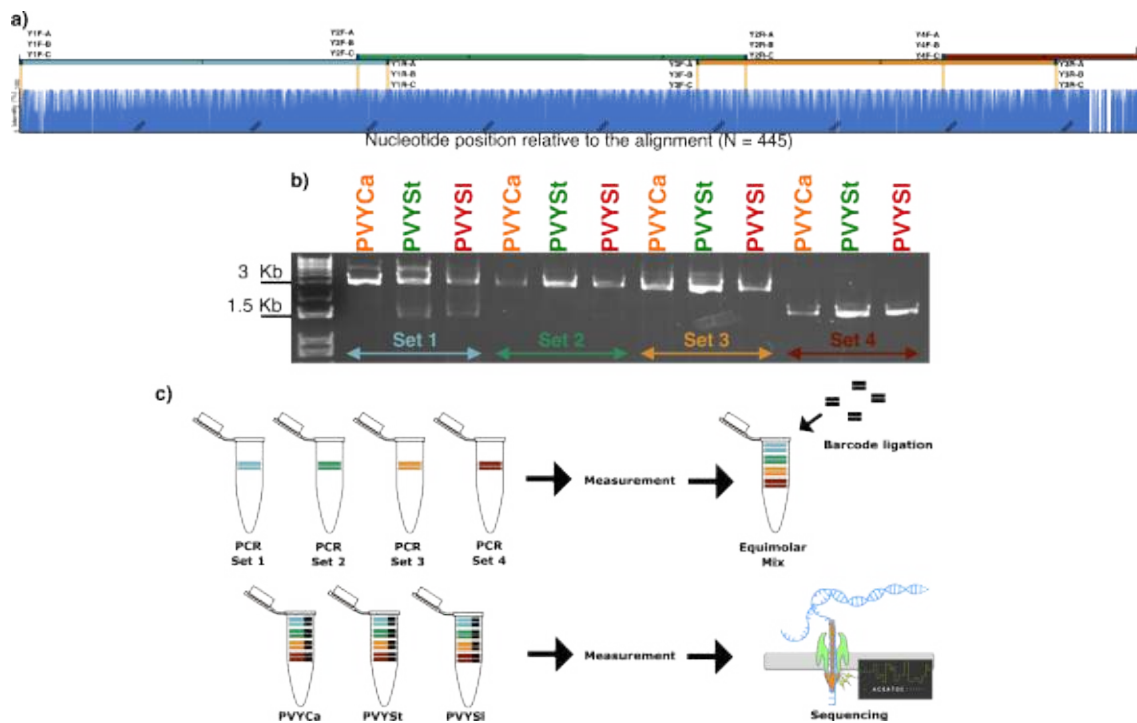
312

313 * Melting temperature

314 # Extension time

315 \$ Usage or GC enhancer from Q5 Polymerase

316



317

318 **Fig 1.** a) Position of primers designed along the PVY alignment ($n = 445$). Four sets of
 319 primers (indicated by different colors) were designed, each composed of 3 forward and
 320 3 reverse primers with small differences, producing amplicons of ~ 3 kb. The exception
 321 is the set 4, for which the anchor primer was used for amplification, and produced an
 322 amplicon of ~ 1.8 kb. b) Agarose gel electrophoresis of the amplicons of the three
 323 isolates, PVYCa, PVYSt and PVYSl, using the 4 sets of primers (1, 2, 3, and 4). Each
 324 well has 1 μ L of the PCR product. c) Schematic view of the sequencing strategy used to
 325 amplify the genome by Nanopore sequencing.

326

327 Nanopore sequencing results

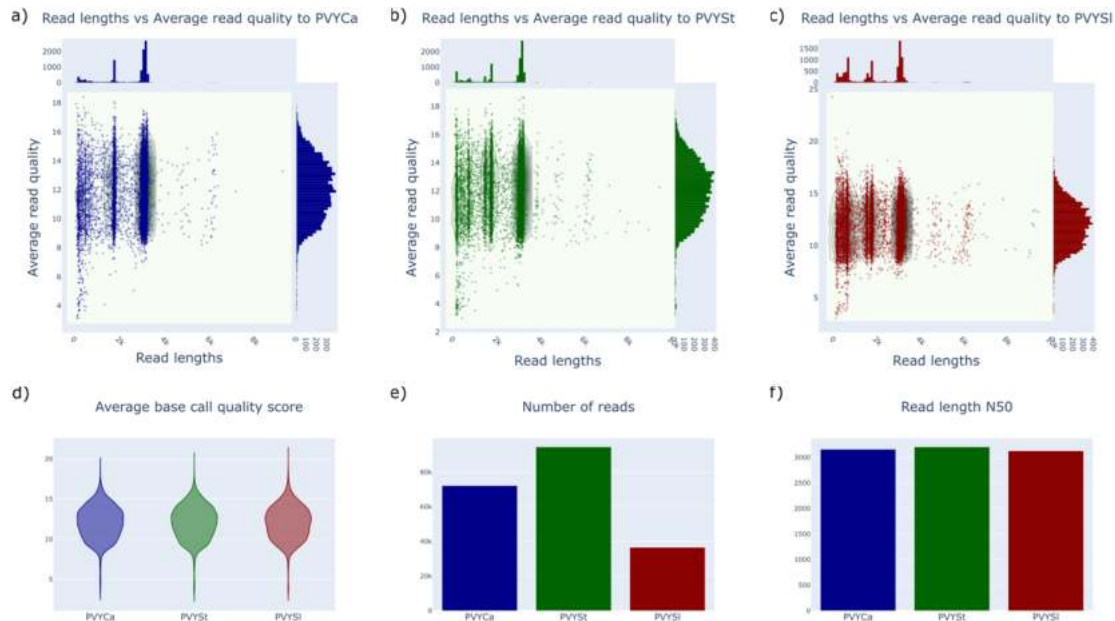
328 This study evaluated the ONT sequencing performance based on the analysis of three
 329 PVY isolates. Key metrics such as read length, read quality, number of reads, total
 330 bases, and quality cutoffs were assessed to determine the sequencing efficacy and data
 331 quality for each sample. The sequencing procedure was conducted for a duration of 2
 332 days, but the number of reads plateaued after approximately 16 hours.

333 We observed two predominant read lengths, approximately 1.8 kb and 3 kb, as
 334 expected (Fig. 2a-c). Both PVYCa and PVYSt sequences exhibited similar mean and
 335 median read lengths and qualities (Fig. 2a-b), whereas PVYSl showed shorter read
 336 lengths (Fig. 2c). All samples produced comparable base call quality scores (Fig. 2d).

337 Specifically, PVYCa had a mean read length of 2,561.5 bases, a median read
 338 length of 3,125.0 bases, a mean read quality of 11.0, and a median read quality of 12.1.
 339 PVYSt had a mean read length of 2,394.4 bases, a median read length of 3,112.0 bases,
 340 a mean read quality of 11.0, and a median read quality of 12.1. PVYSl, on the other
 341 hand, had a mean read length of 2,059.6 bases, a median read length of 1,871.0 bases, a
 342 mean read quality of 11.0, and a median read quality of 12.0.

343 Regarding the number of reads, read length N50, standard deviation (SD) of read
 344 lengths, and total bases, PVYSt yielded the highest values, followed by PVYCa and
 345 PVYSl. PVYCa produced 72,121 reads (Fig. 2e), with 66,698 assembled to the
 346 reference genome, a read length N50 of 3,157 bases (Fig. 2f), a read length SD of 1,021
 347 bases, and a total base count of 184,736,289. PVYSt produced 94,479 reads (Fig. 2e),
 348 with 85,297 assembled to the reference genome, a read length N50 of 3,201 bases (Fig.
 349 2f), a read length SD of 1,131.5 bases, and a total base count of 226,218,980. PVYSl
 350 produced 36,463 reads (Fig. 2e), with 27,668 assembled to the reference genome, a read
 351 length N50 of 3,127 bases (Fig. 2f), a read length SD of 1,248.7 bases, and a total base
 352 count of 75,100,253.

353



354

355 **Fig 2.** Scatter plot graph showing the distribution and clustering of the reads based on
 356 the length and quality for a) PVYCa (blue), b) PVYSt (green) and c) PVYSl (red).

357 Violin plot of the average base call quality score (d) for each library. Barplots showing
 358 the number of reads (e) and read length of N50 (f).

359

360 The longest read lengths and the distribution of reads above quality cutoffs (>Q10
 361 (~90% of base-calling accuracy), >Q15 (~96.8% of accuracy), >Q20 (~99% of
 362 accuracy) are presented in Table 2. PVYCa had a longest read of 10,550 bases, with
 363 59,824 reads (82.9%) above Q10, totaling 155.8 Mb, 4,527 reads (6.3%) above Q15,
 364 totaling 11.4 Mb, and 2 reads (0.0%) above Q20. PVYSt had a longest read of 12,601
 365 bases, with 77,983 reads (82.5%) above Q10, totaling 190.9 Mb, 6,229 reads (6.6%)
 366 above Q15, totaling 15.1 Mb, and 4 reads (0.0%) above Q20. PVYSl had a longest read
 367 of 11,689 bases, with 29,943 reads (82.1%) above Q10, totaling 63.2 Mb, 2,299 reads
 368 (6.3%) above Q15, totaling 4.5 Mb, and 5 reads (0.0%) above Q20.

369 Among the reads longer than 9 kb, we identified 8 reads for PVYCa, 21 reads for
 370 PVYSt, and 21 reads for PVYSl. All the longest reads were compared to GenBank
 371 using BLASTn, showing high identity with PVY genomes (a list of the five longest
 372 reads with BLASTn results is available in Sup. Table 2). An exception was one PVYCa
 373 read of 9,666 bases, which mapped to *Xanthomonas euvesicatoria* (CP018467). This
 374 exception was likely due to residual contamination or a misclassification of a non-target
 375 sequence as part of the PVY dataset. Such anomalies highlight the importance of
 376 stringent quality control measures and careful analysis to ensure the accuracy of
 377 sequencing results and the reliability of data interpretation. Future efforts will focus on
 378 refining the sequencing protocol and enhancing the accuracy of read assignment to
 379 further minimize these issues.

380

381 **Tab 2.** Summary of Nanoplot results to sequenced reads of PVYCa, PVYSt and PVYSl
 382 using ONT Nanopore.

	Mean read length	Mean read quality	Median length	read Median quality
PVYCa	2,561.5	11.0	3,125.0	12.1
PVYSt	2,394.4	11.0	3,112.0	12.1
PVYSl	2,059.6	11.0	1,871.0	12.0

	Number of reads	Read length N50	SD read length	Total bases
PVYCa	72,121.0	3,157.0	1,021.0	184,736,289.0
PVYSt	94,479.0	3,201.0	1,131.5	226,218,980.0
PVYSl	36,463.0	3,127.0	1,248.7	75,100,253.0
	Longest read	>Q10*	>Q15*	>Q20*
		59824 (82.9%)	4527 (6.3%)	
PVYCa	10550 155.8Mb		11.4Mb	2 (0.0%) 0.0Mb
		77983 (82.5%)	6229 (6.6%)	
PVYSt	12601 190.9Mb		15.1Mb	4 (0.0%) 0.0Mb
		29943 (82.1%)		
PVYSl	11689 63.2Mb		2299 (6.3%) 4.5Mb	5 (0.0%) 0.0Mb

*Number, percentage and megabases of reads above quality cutoffs

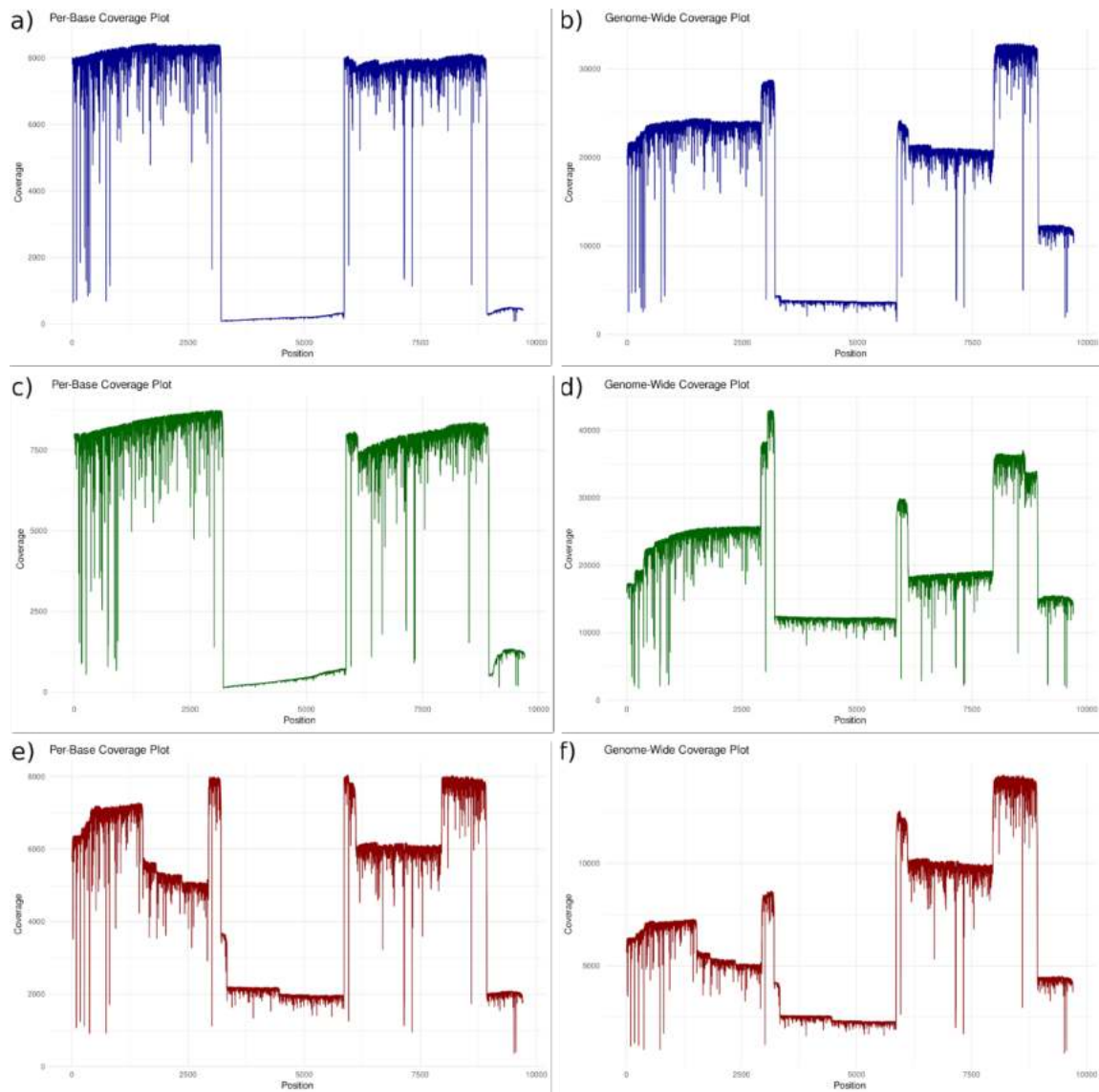
383

384 The reads were mapped against the reference PVY genome, assessing coverage
385 per base and genome coverage. Despite differences in coverage across the genome, we
386 successfully reconstructed and assembled the entire genome for all isolates. Of the 184k
387 bases produced for PVYCa sequencing, 169k were mapped against the reference
388 genome, with coverage ranging from 79 to 8446 reads (Fig. 3a-b). For PVYSt, 197 of
389 226 kb were mapped, with coverage ranging from 123 to 8750 reads (Fig. 3c-d). For
390 PVYSl, 64 of 75 kb were mapped, with coverage ranging from 366 to 8044 reads (Fig.
391 3e-f).

392 Ultimately, we reconstructed the consensus sequence for each isolate. The PVYCa
393 consensus sequence was 9,699 bases long, with an ORF of 9,186 bases, a 5' UTR of 185
394 bases, and a 3' UTR of 328 bases. The PVYSt genome was 9,689 bases long, with a 5'
395 UTR of 188 bases, an ORF of 9,173 bases, and a 3' UTR of 328 bases. The PVYSl
396 genome was 9,699 bases long, with a 5' UTR of 185 bases, an ORF of 9,186 bases, and
397 a 3' UTR of 328 bases. The 3' UTR region excluded the polyadenylated sequence.

398 To determine the closest related genomes, a BLASTn analysis was performed
399 against a reference database. The PVYCa and PVYSl sequences exhibited the highest
400 identities (91.1% and 90.7%, respectively) with the Dutch PVY isolate from 1938
401 (EU563512) collected from potato plants. Additionally, PVYSt showed the highest

402 identity (98.3%) with a potato isolate from Russia obtained in 2021 (accession
403 OR479975).



404

405 **Fig 3.** Number of Nanopore reads that covers each individual nucleotide position in the
406 genome (per-base coverage, left side) to: (a) PVYCa, (c) PVYSt and (e) PVYSl; and
407 number of sequencing reads covering each position across the entire genome
408 (genome-wide coverage, right side) to (b) PVYCa, (d) PVYSt and (f) PVYSl.

409

410 In summary, we were able to determine the sequence of three PVY isolates,
411 demonstrating consistent sequencing performance and data quality metrics such as read
412 length, quality scores, and genome coverage. Despite variation in read lengths and
413 coverage across isolates, complete genome reconstructions were achieved, validating

414 the efficacy of the sequencing approach. While we achieved satisfactory Q-scores, there
415 remains room for improvement in future research to further enhance the overall
416 sequencing accuracy. These findings underscore the reliability and utility of ONT
417 sequencing in PVY infected populations.

418

419 **Illumina sequencing results**

420 While we were able to achieve complete genome coverage for all samples, we
421 encountered challenges in obtaining an equal number of reads along the whole-genome.
422 Starting from the same sample, PVYCa was the sample that presented the smaller
423 genome coverage and number of reads. To evaluate the accuracy of the assembly, we
424 employed HTS as a validation method for the genome with lower coverage obtained
425 through Nanopore sequencing. A total of 57 million reads were generated through HTS,
426 resulting in 8617 million bases. The quality assessment revealed a Q20 score of 97.6%
427 and a Q30 score of 93.7%. After applying BBduk for trimming, we removed 49,000
428 reads (0.09%) or 766 million bases (8.67%), resulting in 57 million reads (7870 million
429 bases) for contig assembly. The consensus sequence was constructed using Geneious
430 assembler and has 9699 nt, a 5'UTR of 185 nt and ORF of 9186 and 3'UTR of 328 nt,
431 exactly the same size and genome organization as the one constructed using Nanopore
432 sequencing. It is important to mention that both PVYCa sequencings were done using
433 the same sample, but to increase the number of viral particles to Illumina sequencing, a
434 single mechanically passage was added using sweet pepper cv. Ikeda. About 30 plants
435 were used to achieve the necessary weight of infected plants for semi-purification. On
436 the other hand, Nanopore sequencing was done using the field collected sample.

437

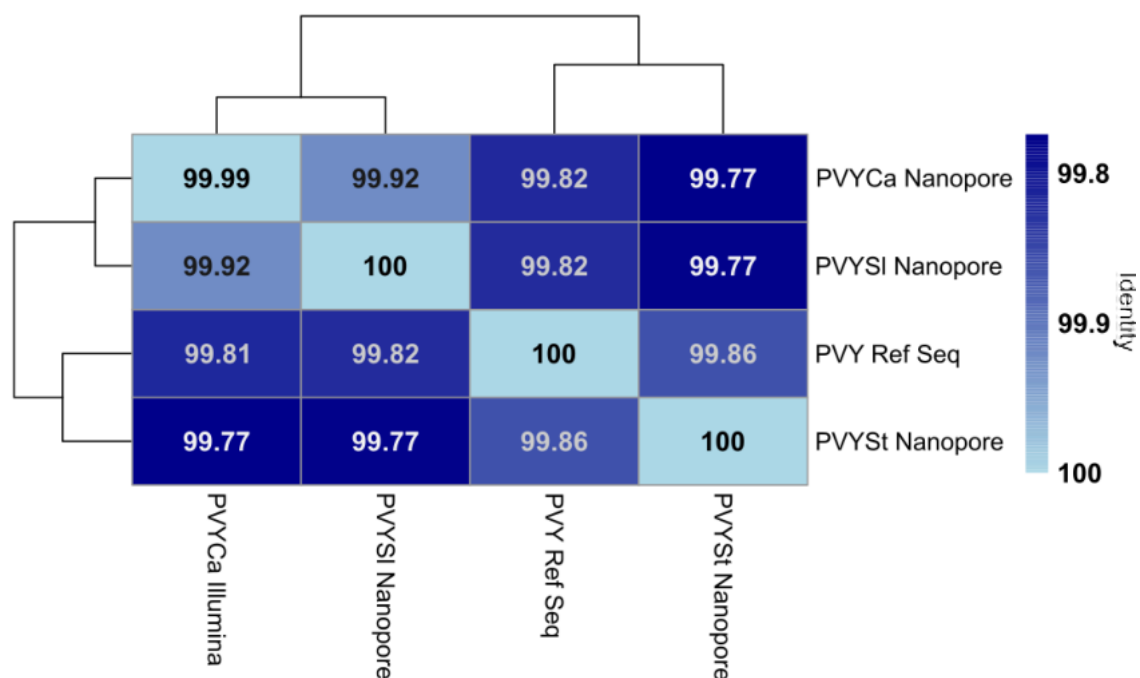
438 **Genome comparison and phylogenetics**

439 We first calculated the pairwise distance between the assembled genomes with the PVY
440 reference genome, shown in Fig 4.

441 Our results revealed that the identity between PVYCa and PVYSt was 99.77%
442 ± 0.007 (± 1 SD). When compared to the reference PVY genome, both PVYCa
443 sequences showed a identity of 99.82% ± 0.006 . In contrast, PVYSt was closer to the
444 reference genome, with a identity of 99.86% ± 0.005 , suggesting it is genetically more
445 similar to the reference sequence, which was isolated from potato. Interestingly, the

446 identity between both PVYCa sequences and PVYSl was the lowest at 99.92% \pm 0.003,
 447 indicating a high level of identity. However, PVYSt and PVYSl exhibited a identity of
 448 99.77% \pm 0.007, similar to the divergence observed between PVYCa and PVYSt. The
 449 comparison between the PVY reference genome and PVYSl resulted in a identity of
 450 99.82% \pm 0.006, similar to the distance between PVYCa and the reference genome.
 451 Furthermore, the comparison between PVYCa sequenced with Nanopore and with
 452 Illumina showed a low distance, with identity of 99.99% \pm 0.000.

453



454

455 **Fig 4.** Pairwise distances (identity) between the four assembled genomes and the
 456 reference genome of PVY using the Tamura-Nei nucleotide substitution model with a
 457 Gamma distribution of sites.

458

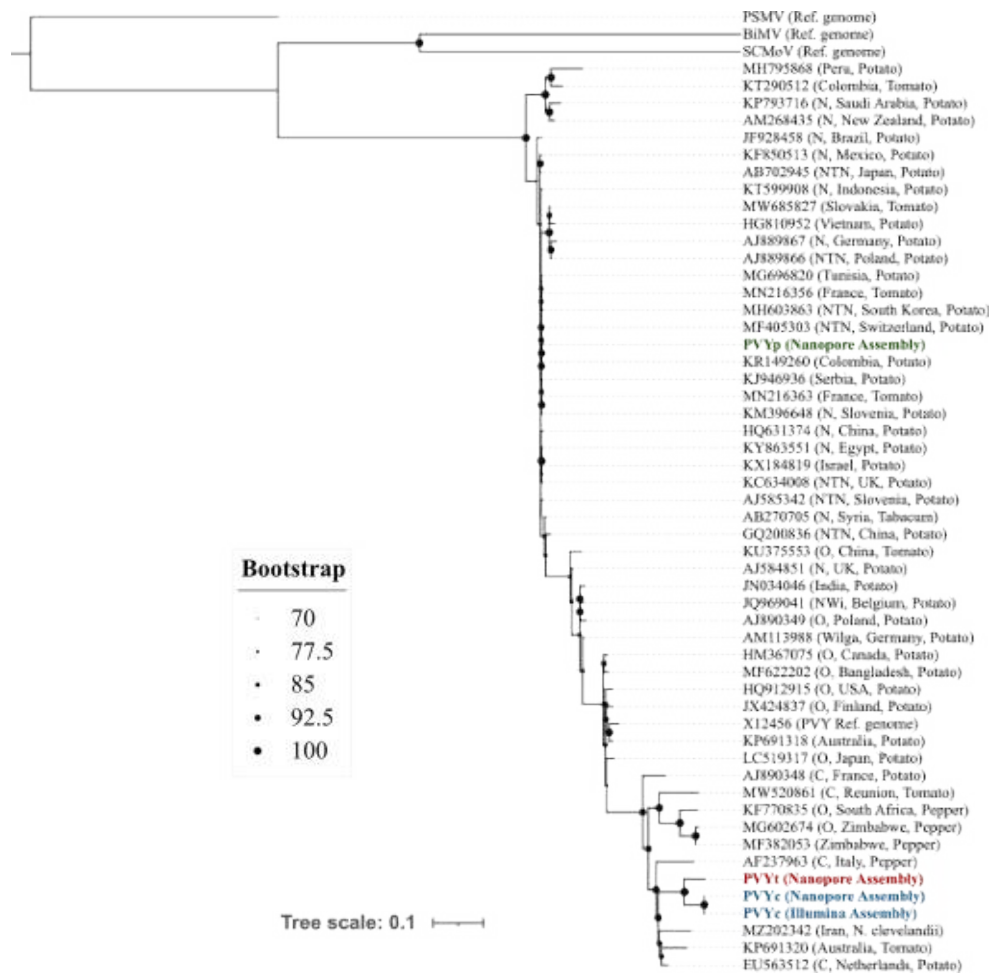
459 The Pearson correlation results demonstrate a correlation coefficient of $r = 0.99$,
 460 which means there is an almost perfect positive correlation between the Illumina and
 461 Nanopore distances (Sup. Fig. 2). This indicates that the distances obtained from both
 462 methods are identical for these comparisons, reinforcing the claim of consistency and
 463 accuracy between the two sequencing technologies.

464 In summary, we demonstrated the relative accuracy of different sequencing
465 technologies. The minimal genetic distance between PVYCa sequenced by Nanopore
466 and Illumina underscores the reliability and consistency of both technologies in
467 accurately detecting variations within the same viral sample, supporting their
468 complementary use in comprehensive genomic analysis across different isolates.

469 For a further analysis, we utilized a representative dataset comprising 49 PVY
470 isolates, in addition to BiMV, PSMV and SCMoV sequences, to reconstruct the
471 ML-phylogenetic tree (Fig. 5). The phylogeny was quite consistent with the pairwise
472 distance, as both PVYCa genomes were clustered in the same clade. PVYSl also
473 appears to have a genetically close relationship with PVYCa, and with other isolates
474 collected from tomato and pepper, primarily corresponding to strains C and O. On the
475 other hand, PVYSt clustered with other isolates collected from potato and of strain N,
476 revealing a separation influenced by the host.

477 Once again, the phylogeny highlights a close proximity between the two PVYCa
478 genomes, underscoring the good sequencing capability of Nanopore.

479



480

481 **Fig 5.** Maximum likelihood (ML) tree of 49 PVY isolates, the four assembled genomes
 482 (PVYCa, in blue, PVYSt in green and PVYSl in red) and three related viruses, BiMV,
 483 PSMV and SCMoV. Each isolate is represented by the GenBank accession, with the
 484 strain, country, and host of origin provided in parentheses, when available.

485

486 PVY-specific primers

487 Capturing the whole variability in a highly variable virus, but without detecting other
 488 species, is a difficult task. The primers need to be specific to the virus but identify all
 489 possible variants within the populations arisen from evolution of this virus. For this
 490 purpose, we designed a pair of primers (UniYF and UniYR), able to detect any PVY
 491 isolate (Fig 6a). The pair of primers were verified by the BLASTn tool and the only hit
 492 was with PVY. We tested the pair of primers using PVYCa, -p and -t and common
 493 viruses such as GRSV, ToMV, PepYMV and PMMoV. We also included a non-infected
 494 plant and a negative control. It is important to note that PepYMV is a potyvirus and our

495 primers were not able to produce amplicons from this virus. The ideal PCR conditions
 496 with *Taq* DNA recombinant polymerase was using an initial denaturation at 95 °C for 1
 497 min followed by 35 cycles of 95 °C for 30 s, 52 °C for 30 s, 72 °C for 1 min and a final
 498 extension with 72 °C for 10 min. An electrophoresis with agarose gel was used to
 499 visualize the PCR products. The primers were able to amplify only PVY samples (Fig
 500 6b). Further analysis using other potyviruses is still necessary to validate the specificity
 501 of the designed primers.

502

a)

Primer	Sequence (5' -> 3')	Size	%GC
YSF	ACTATGATTTTTTCGTCGAGAACAAG	25	36
YSR	GGCGAGGTTCCATTTTCAATGC	22	50

b)



503

504 **Fig 6.** a) PVY-specific primers and PCR conditions using *Taq* DNA-recombinant
 505 polymerase. b) Agarose gel electrophoresis of the PCR amplified products using
 506 PVY-specific primers of the following templates: three PVY isolates, GRSV, PepYMV,
 507 PMMoV and ToMV. A healthy plant (HP) and a negative control (C-) were added to the
 508 analysis.

509

510

511 Discussion

512

513 In our investigation, we collected samples from symptomatic and asymptomatic plants,
 514 with a focus on develop a methodology to detect PVY in the most cultivated
 515 solanaceous plants. Despite the unbalanced plant species sampling, potatoes exhibited a
 516 higher infection rate (IR) compared to tomatoes, which is consistent with potatoes being

517 the most affected and studied host of PVY (Kreuze et al. 2020). We observed that
518 symptom inspection is not a reliable method for confirming PVY infection, especially
519 on tomatoes. It indicates that analysis of the samples by various detection tests is
520 necessary for an accurate diagnosis, including genome sequencing.

521 Detecting and distinguishing different virus species in a sample is crucial for
522 control strategies and genetic improvement programs (Du et al. 2006). However,
523 detecting a single virus with high specificity can also be valuable. Various primers have
524 been developed for PVY detection and classification (Moravec et al. 2003; Glais et al.
525 2005; Chikh Ali et al. 2010; Chikh-Ali et al. 2013). Our approach, using regular
526 RT-PCR primers, differs by focusing on identifying PVY presence in samples using a
527 conservative dataset. This methodology can be extended to other viruses with high
528 genome variability and divergence. Although we sampled viruses commonly found in
529 Brazilian tomato fields, only one potyvirus (PepYMV) was included, necessitating
530 further validation with other potyviruses.

531 After collecting the plants in the field, we used dot-ELISA and Sanger sequencing
532 prior to ONT sequencing to confirm the PVY infection. Serological tests are
533 cost-effective and simple but prone to errors (Hühnlein et al. 2013), related to low
534 sensitivity, and presence of molecules inducing false positive or false negative results.
535 The RT-PCR method provides a sensitive, specific, and reliable diagnostic method
536 (Malgosa et al. 2005; López et al. 2009), and thus it is considered one of the most
537 widely used detection method. This method amplifies cDNA, which is then sequenced
538 after amplicon purification. Although newer techniques allow for direct RNA and
539 cDNA sequencing, PCR-amplified cDNA continues to be widely used RNA sequencing
540 experiments (Bayega et al. 2018; Chen et al. 2021; Garalde et al. 2018). Our method
541 could be advantageous for samples with low viral loads or highly divergent genomes, as
542 it specifically amplifies the target virus, minimizing interference and background noise.

543 Traditional short-read sequencing technologies present important constraints, such
544 as the difficulties in assembly of repetitive regions, which may cause structural
545 variations due to the limitations of the short DNA fragments they analyze (Mak et al.
546 2016). This may result in fragmented genomes and potential biases in alignments
547 (Huang et al. 2013). The efficiency of PCR amplification often decreases for long
548 fragments, leading to smeared gel bands from unamplified truncated products. Illumina

549 can yield a broad overview of the sample composition but may suffer from low
550 coverage or significant noise of non-specific reads. In contrast, our PCR-based approach
551 reduces noise, and while non-specific reads were sequenced, they did not compromise
552 sequencing confidence.

553 For our PCR approach, we divided the PVY genome into four segments. Similar
554 amplification methods with a reduced number of genomes during the primer design and
555 smaller amplicons have been used in other studies (Quick et al. 2017; Stubbs et al.
556 2020), typically following the Primal Scheme methodology (Quick et al. 2017).
557 Multiplex RT-PCR can misidentify new genetic variants, especially rare and
558 recombinant genotypes (Green et al. 2018). Our strategy, however, is more conservative
559 and potentially covers all possible genome variations in an attempt to ensure no
560 genomes are excluded. Despite differences in read numbers among the three sequenced
561 samples, the final read quality was similar before and after base calling, indicating that
562 read quantity does not necessarily correlate with better consensus assembly.

563 Although ONT was previously known for its high error rate (Rang et al. 2018),
564 recent advances in base-calling algorithms have achieved consensus sequences with
565 over 99.9% accuracy (Oxford Nanopore Technologies 2020; Chang et al. 2020). Our
566 study, focusing on three PVY isolates, demonstrated that our methodology can
567 accommodate up to 24 isolates for simultaneous identification and sequencing,
568 facilitating whole-genome construction. We confirmed the identity of our isolates
569 through BLASTn and phylogenetic analyses including closely related virus species as
570 outgroups. This study also contributes to the limited datasets of PVY genomes from
571 tomato and pepper, enhancing our understanding of host species' roles in PVY
572 evolution. While HTS remains expensive and often inaccessible to small laboratories,
573 we show that Nanopore sequencing is efficient, cost-effective when using barcode, and
574 quicker, with simpler preparation (Petersen et al. 2019). We achieved long reads over 9
575 kb, some representing entire viral genomes. This capability enhances the accuracy of
576 identifying complex repetitive or rearranged structures and facilitates the detection of a
577 full spectrum of structural variations (Cretu Stancu et al. 2017; Gong et al. 2018).
578 Although we only sequenced three isolates, our method can be applied to a broader
579 range of viruses or organisms. Future work should focus on testing this approach on a
580 larger number of PVY isolates.

581 Using pairwise distance and a phylogenetic approach, we were able to indirectly
582 compare the assembled genomes, since both platforms use different bioinformatic
583 pipelines. It is important to note that PVYCa and PVYSl are very similar. This genetic
584 distance could be due the geographic barriers, since tomato and pepper plants are
585 usually cultivated side by side, which can facilitate the movement of the virus between
586 these two hosts. Differently, potato fields are often cultivated on large scale farms and
587 away from other crops to avoid the movement of pests and diseases. But this does not
588 appear to be the only cause, since phylogenetically, PVYCa and PVYSl tend to cluster
589 with other isolates from pepper and tomato, and PVYSt is present among other isolates
590 collected from potato. Thus, there appears to be an influence of the host on the
591 evolutionary course of the virus, since the genetic distance between them is positively
592 or negatively affected.

593 Diagnostic methods evolve for reliability, sensitivity and efficiency, meanwhile
594 time and cost are two factors of great concerns. We present here two methods: (1) for a
595 universal detection of PVY; and (2) for rapid sequencing the genome of PVY. The
596 second method is particularly useful for small laboratories and for field studies,
597 requiring minimal bioinformatics and computational skills, thereby reducing sequencing
598 costs and training. Nanopore sequencing can be achieved with a reduced time and
599 equipment costs (Lu et al. 2016; Petersen et al. 2019), offering versatility and simplicity.
600 Studies have shown that Nanopore sequencing is more cost-effective than those
601 provided by PacBio or Illumina platforms (Logsdon et al. 2020; Ranasinghe et al.
602 2022). Sequencing virus genomes is the basis for identifying genetic variation and study
603 virus evolution. Overall, we experienced that the Nanopore technology, emerging from
604 2014, offered a powerful sequencing tool that required minimal preparation time and
605 provided quick results. With the decrease in error rate in Nanopore sequencing (Oxford
606 Nanopore Technologies 2020; Chang et al. 2020), this method is a valuable tool for
607 understanding viral biology and evolution, with applications across various fields,
608 including agricultural pest management.

609 Finally, we were able to detect and sequence three different PVY isolates, which
610 show high genomic diversity among isolates. Moreover, both Illumina and Nanopore
611 consensus assembly of PVYCa were highly similar, indicating the efficacy of our
612 sequencing methodology. By sequencing a highly variable virus and finding results very

613 similar using Nanopore at a lower cost, we will be able to explore the technique for use
614 in other virus-host systems. Although new tools are being generated to decrease the
615 error rate of Nanopore sequencing, this method may have advantages when compared
616 with Illumina if considering the fast result delivery (Garcia-Pedemonte et al. 2023). A
617 direct comparison between Nanopore and Illumina is difficult to perform, but it is
618 important to differentiate the bioinformatics skills required on both platforms, as
619 Nanopore offers fewer steps, making the process simpler and easier.

620 As observed in Sup. Table 1, PVYSl was isolated from an asymptomatic tomato
621 plant in the field, demonstrating that symptom inspection alone is insufficient for
622 accurate PVY detection. Instead, a combination of various detection techniques,
623 including PCR-based methods and Nanopore sequencing, provides a more reliable
624 approach. Our sequencing methodology proved effective in capturing the PVY genome
625 diversity, even with low viral loads or divergent genomes. This approach offers
626 cost-effective, high-throughput sequencing with minimal preparation and bioinformatic
627 skills, presenting a viable alternative to traditional methods like Illumina sequencing.
628 Illumina still remains as the gold standard method of sequencing, but Nanopore
629 sequencing may offer a reasonable performance and reliability.

630 References

631

632 Ahn HI, Yoon JY, Hong JS, et al (2006) The complete genome sequence of pepper
633 severe mosaic virus and comparison with other potyviruses. Archives of Virology
634 151:2037–2045. <https://doi.org/10.1007/s00705-006-0776-1>

635

636 Amoia SS, Minafra A, Nicoloso V, et al (2022) A new jasmine virus C isolate identified
637 by nanopore sequencing is associated to yellow mosaic symptoms of *Jasminum*
638 *officinale* in Italy. Plants (Basel) 11. <https://doi.org/10.3390/PLANTS11030309>

639

640 Bayega A, Wang YC, Oikonomopoulos S, et al (2018) Transcript profiling using
641 long-read sequencing technologies. Methods in Molecular Biology 1783:121–147.
642 https://doi.org/10.1007/978-1-4939-7834-2_6

643

644 Blawid R, Silva JMF, Nagata T (2017) Discovering and sequencing new plant viral
645 genomes by next-generation sequencing: description of a practical pipeline. Annals of
646 Applied Biology 170:301–314. <https://doi.org/10.1111/aab.12345>

647

648 Buchfink B, Xie C, Huson DH (2015) Fast and sensitive protein alignment using
649 DIAMOND. Nature Methods 12:59–60. <https://doi.org/10.1038/nmeth.3176>

650

651 Chang JJM, Ip YCA, Bauman AG, Huang D (2020) MinION-in-ARMS: nanopore
652 sequencing to expedite barcoding of specimen-rich macrofaunal samples from
653 autonomous reef monitoring structures. Frontiers in Marine Science 7:448.
654 <https://doi.org/10.3389/FMARS.2020.00448/BIBTEX>

655

656 Chen J, Chen J, Adams MJ (2001) A universal PCR primer to detect members of the
657 *Potyviridae* and its use to examine the taxonomic status of several members of the
658 family. Archives of Virology 146:757–766. <https://doi.org/10.1007/s007050170144>

659

660 Chen Y, Davidson NM, Wan YK, et al (2021) A systematic benchmark of Nanopore
661 long read RNA sequencing for transcript level analysis in human cell lines. *Nature*
662 *Methods*, 21, 1349-1363. <https://doi.org/10.1101/2021.04.21.440736>

663

664

665 Chikh-Ali M, Maoka T, Natsuaki KT, Natsuaki T (2010) The simultaneous
666 differentiation of Potato virus Y strains including the newly described strain PVY^{NTN-NW}
667 by multiplex PCR assay. *Journal of Virological Methods* 165:15–20.
668 <https://doi.org/10.1016/j.jviromet.2009.12.010>

669

670 Chikh-Ali M, Gray SM, Karasev AV. (2013) An improved multiplex IC-RT-PCR assay
671 distinguishes nine strains of Potato virus Y. *Plant Disease* 97:1370–1374.
672 <https://doi.org/10.1094/PDIS-02-13-0161-SR>

673

674 Cretu Stancu M, van Roosmalen MJ, Renkens I, et al (2017) Mapping and phasing of
675 structural variation in patient genomes using nanopore sequencing. *Nature*
676 *Communications* 8:1326. <https://doi.org/10.1038/s41467-017-01343-4>

677

678 Danecek P, Bonfield JK, Liddle J, et al (2021) Twelve years of SAMtools and BCFtools.
679 *Gigascience* 10. <https://doi.org/10.1093/gigascience/giab008>

680

681 Davie K, Holmes R, Pickup J, Lacomme C (2017) Dynamics of PVY strains in field
682 grown potato: impact of strain competition and ability to overcome host resistance
683 mechanisms. *Virus Research* 241:95–104.
684 <https://doi.org/10.1016/J.VIRUSRES.2017.06.012>

685

686 De Coster W, D’Hert S, Schultz DT, et al (2018) NanoPack: visualizing and processing
687 long-read sequencing data. *Bioinformatics* 34:2666–2669.
688 <https://doi.org/10.1093/bioinformatics/bty149>

689

690 Deamer D, Akeson M, Branton D (2016) Three decades of nanopore sequencing.
691 *Nature Biotechnology* 34:518–524. <https://doi.org/10.1038/NBT.3423>

692

693 Dong ZX, Lin CC, Chen YK, et al (2022) Identification of an emerging cucumber virus
694 in Taiwan using Oxford nanopore sequencing technology. *Plant Methods* 18.
695 <https://doi.org/10.1186/S13007-022-00976-X>

696

697 Du Z, Chen J, Hiruki C (2006) Optimization and Application of a multiplex RT-PCR
698 system for simultaneous detection of five potato viruses using 18S rRNA as an internal
699 control. *Plant Disease* 90:185–189. <https://doi.org/10.1094/PD-90-0185>

700

701 Dujovny G, Sasaya T, Koganesawa H, et al (2000) Molecular characterization of a new
702 potyvirus infecting sunflower. *Archives of Virology* 145:2249–2258.
703 <https://doi.org/10.1007/s007050070018>

704

705 Dujovny G, Usugi T, Shohara K, Lenardon S (1998) Characterization of a potyvirus
706 infecting sunflower in Argentina. *Plant Disease* 82:470–474.
707 <https://doi.org/10.1094/PDIS.1998.82.5.470>

708

709 Edgar RC (2004) MUSCLE: multiple sequence alignment with high accuracy and high
710 throughput. *Nucleic Acids Research* 32:1792–1797. <https://doi.org/10.1093/nar/gkh340>

711

712 Edwardson JR, Christie RG (1997) Viruses infecting peppers and other solanaceous
713 crops. Agricultural Experiment Station, University of Florida, Gainesville.

714

715 Funke CN, Nikolaeva OV, Green KJ, et al (2017) Strain-specific resistance to potato
716 virus y (PVY) in potato and its effect on the relative abundance of PVY strains in
717 commercial potato fields. *Plant Disease* 101:20–28.
718 <https://doi.org/10.1094/PDIS-06-16-0901-RE>

719

720 Garalde DR, Snell EA, Jachimowicz D, et al (2018) Highly parallel direct RNA
721 sequencing on an array of nanopores. *Nature Methods* 2018 15:3 15:201–206.
722 <https://doi.org/10.1038/nmeth.4577>

723

724 Garcia-Pedemonte D, Carcereny A, Gregori J, et al (2023) Comparison of nanopore and
725 synthesis-based next-generation sequencing platforms for SARS-CoV-2 variant
726 monitoring in wastewater. *International Journal of Molecular Science* 24:17184.
727 <https://doi.org/10.3390/ijms242417184>

728

729 Glais L, Tribodet M, Kerlan C (2005) Specific detection of the PVYN-W variant of
730 Potato virus Y. *Journal of Virology Methods* 125:131–136.
731 <https://doi.org/10.1016/j.jviromet.2005.01.007>

732

733 Gong L, Wong CH, Cheng WC, et al (2018) Picky comprehensively detects
734 high-resolution structural variants in nanopore long reads. *Nature Methods* 15:455–460.
735 <https://doi.org/10.1038/s41592-018-0002-6>

736

737 Green KJ, Brown CJ, Gray SM, Karasev AV (2017) Phylogenetic study of recombinant
738 strains of Potato virus Y. *Virology* 507:40–52.
739 <https://doi.org/10.1016/J.VIROL.2017.03.018>

740

741 Green KJ, Brown CJ, Karasev AV (2018) Genetic diversity of potato virus Y (PVY):
742 sequence analyses reveal ten novel PVY recombinant structures. *Archives of Virology*
743 163:23–32. <https://doi.org/10.1007/S00705-017-3568-X>

744

745 Green KJ, Funke CN, Chojnacky J, et al (2020) Potato Virus Y (PVY) isolates from
746 *Solanum betaceum* represent three novel recombinants within the PVYN strain group
747 and are unable to systemically spread in potato. *Phytopathology* 110:1588–1596.
748 <https://doi.org/10.1094/PHYTO-04-20-0111-R>

749

750 Hane DC, Hamm PB (1999) Effects of seedborne potato virus y infection in two potato
751 cultivars expressing mild disease symptoms. *Plant Disease* 83:43–45.
752 <https://doi.org/10.1094/PDIS.1999.83.1.43>

753

754 Huang L, Popic V, Batzoglou S (2013) Short read alignment with populations of
755 genomes. *Bioinformatics* 29:i361–i370.
756 <https://doi.org/10.1093/BIOINFORMATICS/BTT215>
757

758 Hühnlein A, Drechsler N, Steinbach P, et al (2013) Comparison of three methods for the
759 detection of Potato virus Y in seed potato certification. *Journal of Plant Diseases and*
760 *Protection* 120:57–69. <https://doi.org/> <https://doi.org/10.1007/BF03356455>
761

762 Inoue-Nagata AK, Jordan R, Kreuze J, et al (2022) ICTV Virus Taxonomy Profile:
763 *Potyviridae* 2022. *Journal of General Virology* 103:001738.
764 <https://doi.org/10.1099/jgv.0.001738>
765

766 Inoue-Nagata AK, Oliveira PA, Dutra LS, Nagata T (2006) Bidens mosaic virus is a
767 member of the potato virus Y species. *Virus Genes* 33:45–49.
768 <https://doi.org/10.1007/s11262-005-0037-5>
769

770 Jeffries CJ (1998) FAO/IPGRI Technical guidelines for the safe movement of potato
771 germplasm. Food and Agriculture Organization of the United Nations,
772 Rome/International Plant Genetic Resources Institute, Rome, Italy 19.
773

774 Ji CM, Feng XY, Huang YW, Chen RA (2024) The applications of nanopore sequencing
775 technology in animal and human virus research. *Viruses* 16:798.
776 <https://doi.org/10.3390/v16050798>
777

778 Johnson M, Zaretskaya I, Raytselis Y, et al (2008) NCBI BLAST: a better web interface.
779 *Nucleic Acids Res* 36. <https://doi.org/10.1093/NAR/GKN201>
780

781 Jones RAC (1990) Strain group specific and virus specific hypersensitive reactions to
782 infection with potyviruses in potato cultivars. *Annals of Applied Biology* 117:93–105.
783 <https://doi.org/> <https://doi.org/10.1111/j.1744-7348.1990.tb04198.x>
784

785 Karasev A V., Hu X, Brown CJ, et al (2011) Genetic diversity of the ordinary strain of
786 Potato virus Y (PVY) and origin of recombinant PVY strains. *Phytopathology*
787 101:778–785. <https://doi.org/10.1094/PHYTO-10-10-0284>

788

789 Kerlan C, Moury B, Granoff A, Webster RG (2008) *Encyclopedia of virology.*
790 Association of Applied Biologists 287–296.

791

792 Kolde R (2019) Pheatmap: pretty heatmaps version 1.0.12 from CRAN.

793

794 Kreuze JF, Souza-Dias JAC, Jeevalatha A, et al (2020) Viral diseases in potato. In: *The*
795 *Potato Crop.* Springer International Publishing, Cham, pp 389–430.

796

797 Kumar S, Stecher G, Li M, et al (2018) MEGA X: molecular evolutionary genetics
798 analysis across computing platforms. *Molecular Biology Evolution* 35:1547–1549.
799 <https://doi.org/10.1093/molbev/msy096>

800

801 Lacomme C, Glais L, Bellstedt DU, et al (2017) Potato virus Y: biodiversity,
802 pathogenicity, epidemiology and management. Springer International Publishing,
803 Springer Cham. <https://doi.org/10.1007/978-3-319-58860-5>

804

805 Laver T, Harrison J, O’Neill PA, et al (2015) Assessing the performance of the Oxford
806 Nanopore Technologies MinION. *Biomolecular Detection and Quantification* 3:1–8.
807 <https://doi.org/10.1016/J.BDQ.2015.02.001>

808

809 Le Romancer M, Kerlan C, Nedellec M (1994) Biological characterization of various
810 geographical isolates of potato virus Y inducing superficial necrosis on potato tubers.
811 *Plant Pathology* 43:138–144. <https://doi.org/10.1111/j.1365-3059.1994.tb00563.x>

812

813 Letunic I, Bork P (2021) Interactive Tree Of Life (iTOL) v5: an online tool for
814 phylogenetic tree display and annotation. *Nucleic Acids Research* 49:W293–W296.
815 <https://doi.org/10.1093/nar/gkab301>

816

817 Li D, Liu C-M, Luo R, et al (2015) MEGAHIT: an ultra-fast single-node solution for
818 large and complex metagenomics assembly via succinct de Bruijn graph. *Bioinformatics*
819 31:1674–1676. <https://doi.org/10.1093/bioinformatics/btv033>

820

821 Li H (2018) Minimap2: pairwise alignment for nucleotide sequences. *Bioinformatics*
822 34:3094–3100. <https://doi.org/10.1093/bioinformatics/bty191>

823

824 Logsdon GA, Vollger MR, Eichler EE (2020) Long-read human genome sequencing
825 and its applications. *Nature Reviews Genetics* 21:597–614.
826 <https://doi.org/10.1038/s41576-020-0236-x>

827

828 López MM, Llop P, Olmos A, et al (2009) Are molecular tools solving the challenges
829 posed by detection of plant pathogenic bacteria and viruses? *Current Issues Molecular*
830 *Biology* 11(1):13-46. <https://doi.org/10.21775/cimb.011.013>

831

832 Lu H, Giordano F, Ning Z (2016) Oxford Nanopore MinION sequencing and genome
833 assembly. *Genomics Proteomics Bioinformatics* 14:265–279.
834 <https://doi.org/10.1016/j.gpb.2016.05.004>

835

836 Mak ACY, Lai YYY, Lam ET, et al (2016) Genome-wide structural variation detection
837 by genome mapping on nanochannel arrays. *Genetics* 202:351–362.
838 <https://doi.org/10.1534/GENETICS.115.183483>

839

840 Malgosa A, Montiel R, Díaz N, et al (2005) Ancient DNA: a modern look at the
841 infections of the past. In: Pandalai SG (ed) *Recent research developments in*
842 *microbiology*, 1st ed. Trivandrum, pp 213–236.

843

844 Martins TP, Souza TA, da Silva PS, et al (2021) Nanopore sequencing of tomato mottle
845 leaf distortion virus, a new bipartite begomovirus infecting tomato in Brazil. *Archives*
846 *of Virology* 166:3217–3220. <https://doi.org/10.1007/s00705-021-05220-w>

847

848 Más A, López-Galíndez C, Cacho I, et al (2010) Unfinished stories on viral
849 quasispecies and darwinian views of evolution. *Journal of Molecular Biology*
850 397:865–877. <https://doi.org/10.1016/J.JMB.2010.02.005>
851

852 Mikheyev AS, Tin MMY (2014) A first look at the Oxford Nanopore MinION
853 sequencer. *Molecular Ecology Resources* 14:1097–1102.
854 <https://doi.org/10.1111/1755-0998.12324>
855

856 Minh BQ, Schmidt HA, Chernomor O, et al (2020) IQ-TREE 2: new models and
857 efficient methods for phylogenetic inference in the genomic era. *Molecular Biology and*
858 *Evolution* 1;37(5):1530-1534 37:1530–1534. <https://doi.org/10.1093/molbev/msaa015>
859

860 Moravec T, Cerovská N, Boonham N (2003) The detection of recombinant, tuber
861 necrosing isolates of Potato virus Y (PVY^{NTN}) using a three-primer PCR based in the
862 coat protein gene. *Journal of Virological Methods* 109:63–68.
863 [https://doi.org/10.1016/S0166-0934\(03\)00047-8](https://doi.org/10.1016/S0166-0934(03)00047-8)
864

865 Nolte P, Whitworth JL, Thornton MK, McIntosh CS (2004) Effect of seedborne Potato
866 virus Y on performance of russet burbank, russet norkotah, and shepody potato. *Plant*
867 *Disease* 88:248–252. <https://doi.org/10.1094/PDIS.2004.88.3.248>
868

869 Owczarzy R, Tataurov AV., Wu Y, et al (2008) IDT SciTools: a suite for analysis and
870 design of nucleic acid oligomers. *Nucleic Acids Research* 36:W163–W169.
871 <https://doi.org/10.1093/nar/gkn198>
872

873 Oxford Nanopore Technologies (2020) New research algorithms yield accuracy gains
874 for nanopore sequencing. In:
875 [https://nanoporetech.com/news/news-new-research-algorithms-yield-accuracy-gains-na](https://nanoporetech.com/news/news-new-research-algorithms-yield-accuracy-gains-nanopore-sequencing)
876 [nopore-sequencing](https://nanoporetech.com/news/news-new-research-algorithms-yield-accuracy-gains-nanopore-sequencing)
877

878 Peck KM, Lauring AS (2018) Complexities of Viral Mutation Rates. *Journal of*
879 *Virology* 92. <https://doi.org/10.1128/JVI.01031-17>

880

881 Petersen LM, Martin IW, Moschetti WE, et al (2019) Third-generation sequencing in
882 the clinical laboratory: exploring the advantages and challenges of nanopore
883 sequencing. *Journal of Clinical Microbiology* 58. <https://doi.org/10.1128/JCM.01315-19>

884

885 Quick J, Grubaugh ND, Pullan ST, et al (2017) Multiplex PCR method for MinION and
886 Illumina sequencing of Zika and other virus genomes directly from clinical samples.
887 *Nature Protocols* 12:1261–1266. <https://doi.org/10.1038/nprot.2017.066>

888

889 R Core Team (2022) R: A language and environment for statistical computing. R
890 Foundation for Statistical Computing, Vienna, Austria.

891

892 Ranasinghe D, Jayadas TTP, Jayathilaka D, et al (2022) Comparison of different
893 sequencing techniques for identification of SARS-CoV-2 variants of concern with
894 multiplex real-time PCR. *PLoS One* 17:e0265220.
895 <https://doi.org/10.1371/journal.pone.0265220>

896

897 Rang FJ, Kloosterman WP, de Ridder J (2018) From squiggle to basepair:
898 computational approaches for improving nanopore sequencing read accuracy. *Genome*
899 *Biology* 19. <https://doi.org/10.1186/S13059-018-1462-9>

900

901 Revers F, Le Gall O, Candresse T, et al (1996) Frequent occurrence of recombinant
902 potyvirus isolates. *Journal of General Virology* 77:1953–1965.
903 <https://doi.org/10.1099/0022-1317-77-8-1953>

904

905 Rizk MN, Ketta HA, Shabana YM (2020) Potential alternative hosts and
906 transmissibility of potato virus Y. *Journal of Plant Protection and Pathology*
907 11:549–553. <https://doi.org/10.21608/jppp.2020.133232>

908

909 Rodriguez-Rodriguez M, Chikh-Ali M, Johnson SB, et al (2020) The recombinant
910 Potato virus Y (PVY) Strain, PVY^{NTN}, identified in potato fields in Victoria,

911 Southeastern Australia. Plant Disease 104:3110–3114.
912 <https://doi.org/10.1094/pdis-05-20-0961-sc>
913

914 Rozas J, Ferrer-Mata A, Sanchez-DelBarrio JC, et al (2017) DnaSP 6: DNA sequence
915 polymorphism analysis of large data sets. Molecular Biology Evolution 34:3299–3302.
916 <https://doi.org/10.1093/molbev/msx248>
917

918 Sanjuán R, Domingo-Calap P (2016) Mechanisms of viral mutation. Cellular and
919 Molecular Life Sciences 73:4433–4448. <https://doi.org/10.1007/s00018-016-2299-6>
920

921 Scholthof KBG, Adkins S, Czosnek H, et al (2011) Top 10 plant viruses in molecular
922 plant pathology. Molecular Plant Pathology 12:938–954. [https://doi.org/](https://doi.org/10.1111/j.1364-3703.2011.00752.x)
923 [10.1111/j.1364-3703.2011.00752.x](https://doi.org/10.1111/j.1364-3703.2011.00752.x)
924

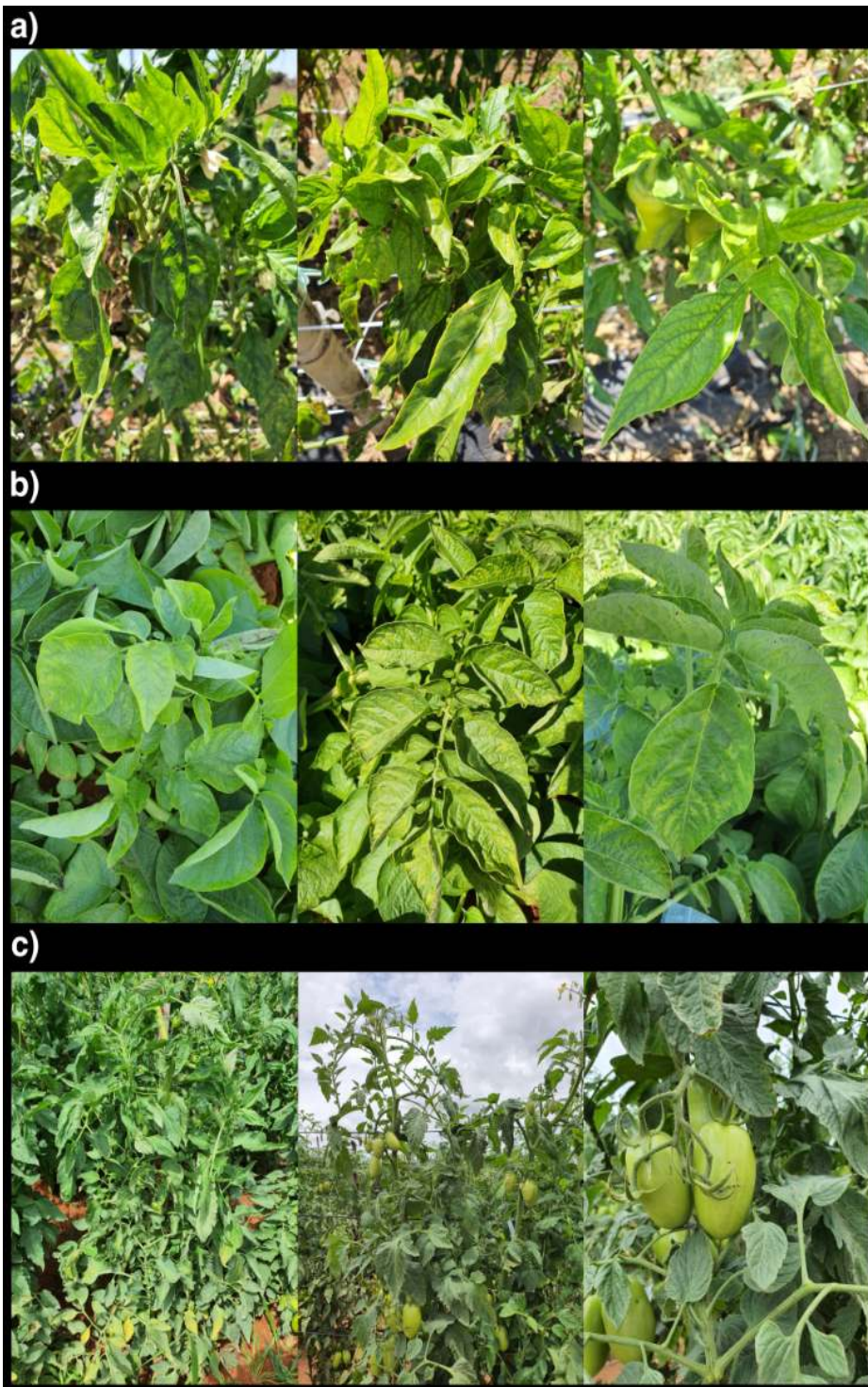
925 Singh RP, Valkonen JPT, Gray SM, et al (2008) Discussion paper: the naming of Potato
926 virus Y strains infecting potato. Archives of Virology 153:1–13.
927 <https://doi.org/10.1007/s00705-007-1059-1>
928

929 Steinhauer DA, Domingo E, Holland JJ (1992) Lack of evidence for proofreading
930 mechanisms associated with an RNA virus polymerase. Gene 122:281–288.
931 [https://doi.org/10.1016/0378-1119\(92\)90216-C](https://doi.org/10.1016/0378-1119(92)90216-C)
932

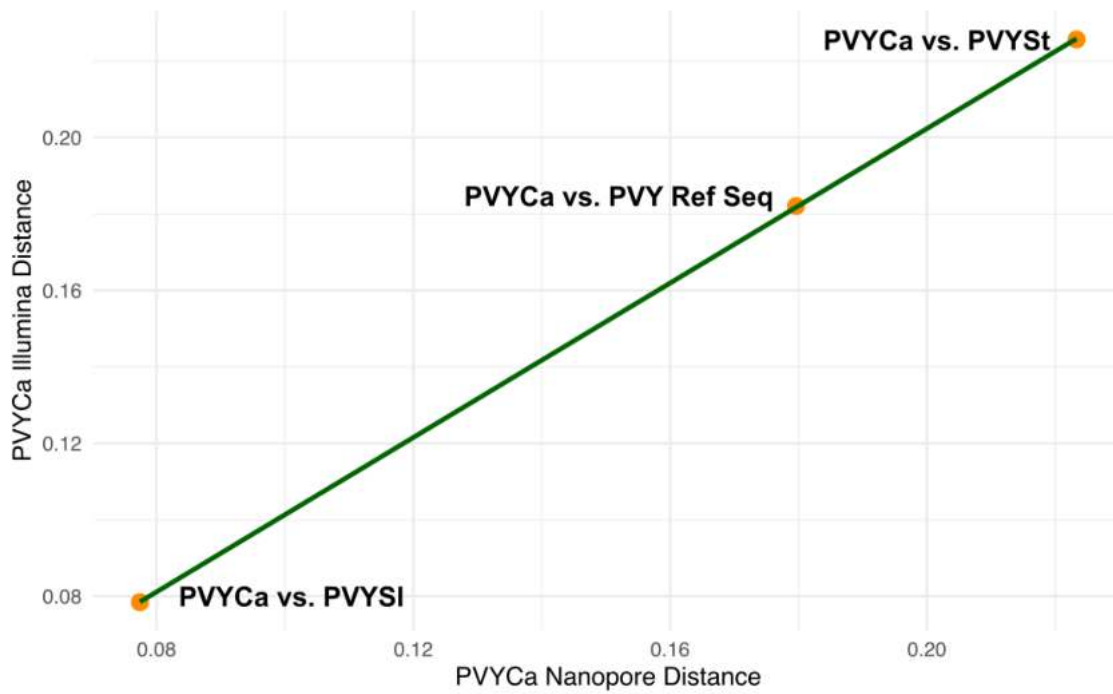
933 Stubbs SCB, Blacklaws BA, Yohan B, et al (2020) Assessment of a multiplex PCR and
934 Nanopore-based method for dengue virus sequencing in Indonesia. Virology Journal
935 17:24. <https://doi.org/10.1186/s12985-020-1294-6>
936

937 Tromas N, Zwart MP, Maité P, Elena SF (2014) Estimation of the in vivo recombination
938 rate for a plant RNA virus. Journal of General Virology 95:724–732.
939 <https://doi.org/10.1099/vir.0.060822-0>

940 **Sup. Fig 1.** Photograph of plant samples collected in the field: pepper plants (a) with
941 blistering, mosaic and interveinal chlorosis; potato (b) plants showing chlorosis,
942 mottling and necrotic spots; and tomato (c) plants with leafroll and necrotic spots.



943



944

945 **Sup. Fig 2.** Scatter plot comparing pairwise distances between PVYCa sequences
 946 obtained from Illumina and Nanopore sequencing technologies. Each point represents
 947 the distance between PVYCa and other PVY isolates (PVYSt, PVYSl, and the reference
 948 genome). The orange points indicate the pairwise distances, while the green line
 949 represents the linear regression fit ($r = 0.99$).

950 **Sup. Table 1.** Description of the samples.

Code	Plant species	Symptoms found	Collection date
1.1	Potato	Foliar chlorosis and necrotic spots	Aug 12, 2021
1.2	Potato	Foliar chlorosis	Aug 12, 2021
1.3	Potato	Foliar chlorosis	Aug 12, 2021
1.4	Potato	Foliar chlorosis	Aug 12, 2021
1.5	Potato	Foliar chlorosis	Aug 12, 2021
1.6	Potato	Foliar chlorosis	Aug 12, 2021
1.7	Potato	Foliar chlorosis	Aug 12, 2021
1.8	Potato	Foliar chlorosis and necrosis	Aug 12, 2021
1.9	Potato	Foliar chlorosis	Aug 12, 2021
1.10	Potato	Nervous chlorosis	Aug 12, 2021
1.11	Potato	Necrotic spots	Aug 12, 2021
1.12	Potato	Foliar chlorosis	Aug 12, 2021
1.13	Potato	Foliar chlorosis and necrotic spots	Aug 12, 2021
1.14	Potato	Foliar chlorosis and necrotic spots	Aug 12, 2021
1.15	Potato	Foliar chlorosis and necrotic spots	Aug 12, 2021
1.16	Potato	Foliar chlorosis	Aug 12, 2021
1.17	Potato	Foliar chlorosis	Aug 12, 2021
1.18	Potato	Foliar chlorosis	Aug 12, 2021
1.19	Potato	Necrotic spots	Aug 12, 2021
1.20	Potato	Necrotic spots	Aug 12, 2021
1.21	Potato	Necrotic spots	Aug 12, 2021
1.22	Potato	Foliar chlorosis	Aug 12, 2021
1.23	Potato	Foliar chlorosis	Aug 12, 2021
1.24	Potato	Foliar chlorosis and necrotic spots	Aug 12, 2021
1.25	Potato	Necrotic spots	Aug 12, 2021
1.26	Potato	Necrotic spots and stunting	Aug 12, 2021
1.27	Potato	Necrosis	Aug 12, 2021
1.28	Potato	Mottle and stunting	Aug 12, 2021
1.29	Potato	Necrosis	Aug 12, 2021
1.30	Potato	Necrosis	Aug 12, 2021
1.31	Potato	Necrosis	Aug 12, 2021
1.32	Potato	Necrosis	Aug 12, 2021
1.33	Potato	Mottle and leaf distortion	Aug 12, 2021
1.34	Potato	Chlorosis	Aug 12, 2021
1.35	Potato	Necrotic spots	Aug 12, 2021
1.36	Potato	Veinal necrosis	Aug 12, 2021
1.37	Potato	no symptoms	Aug 12, 2021
1.38	Potato	Chlorosis	Aug 12, 2021
1.39	Potato	Chlorosis	Aug 12, 2021

1.40	Potato	Chlorosis	Aug 12, 2021
1.41	Potato	Necrotic spots and stunting	Aug 12, 2021
1.42	Potato	Necrotic spots and stunting	Aug 12, 2021
1.43	Potato	Leafroll, stunting and veinal chlorosis	Aug 12, 2021
1.44	Potato	Leafroll and necrotic spots	Aug 12, 2021
1.45	Potato	Necrotic spots	Aug 12, 2021
1.46	Potato	Necrotic spots	Aug 12, 2021
1.47	Potato	Chlorosis and crinkling	Aug 12, 2021
1.48	Potato	Necrotic spots	Aug 12, 2021
1.49	Potato	Necrotic spots and small leaves	Aug 12, 2021
1.50	Potato	Necrotic spots, stunting and small leaves	Aug 12, 2021
1.51	Potato	Necrotic spots and stunting	Aug 12, 2021
1.52	Potato	Necrotic spots	Aug 12, 2021
2.1	Tomato	Interveinal chlorosis	Aug 23, 2021
2.2	Tomato	Interveinal chlorosis and necrosis	Aug 23, 2021
2.3	Tomato	Interveinal chlorosis and necrosis	Aug 23, 2021
2.4	Tomato	Interveinal chlorosis	Aug 23, 2021
2.5	Tomato	Interveinal chlorosis and necrosis	Aug 23, 2021
2.6	Tomato	Interveinal chlorosis and small leaves	Aug 23, 2021
2.7	Tomato	Interveinal chlorosis	Aug 23, 2021
2.8	Tomato	Interveinal chlorosis	Aug 23, 2021
2.9	Tomato	Wrinkled leaves	Aug 23, 2021
2.10	Tomato	Interveinal chlorosis	Aug 23, 2021
2.11	Tomato	Interveinal chlorosis	Aug 23, 2021
2.12	Tomato	Stunting	Aug 23, 2021
2.13	Tomato	Leafroll and stunting	Aug 23, 2021
2.14	Tomato	Chlorosis, leaf deformation and necrotic spots	Aug 23, 2021
2.15	Tomato	Chlorosis, leafroll and stunting	Aug 23, 2021
2.16	Tomato	Leafroll and stunting	Aug 23, 2021
2.17	Tomato	Yellowing	Aug 23, 2021
2.18	Tomato	Chlorosis and yellowing	Aug 23, 2021
2.19	Tomato	Chlorosis	Aug 23, 2021
2.20	Tomato	Stunting	Aug 23, 2021
3.1	Pepper	Chlorosis and stunting	Aug 23, 2021
3.2	Pepper	Chlorosis, leafroll and stunting	Aug 23, 2021
3.3	Pepper	Leafroll	Aug 23, 2021
3.4	Pepper	Blistering and stunting	Aug 23, 2021
2.21	Tomato	Stunted growth	Aug 23, 2021
2.22	Tomato	Stunted growth	Aug 23, 2021
2.23	Tomato	Chlorosis, mottle, necrosis and yellowing	Aug 23, 2021
2.24	Tomato	Yellowing	Aug 23, 2021
2.25	Tomato	Interveinal chlorosis and necrotic spots	Aug 23, 2021

2.26	Tomato	Chlorosis	Aug 23, 2021
2.27	Tomato	Chlorotic and necrotic spots	Aug 23, 2021
3.5	Pepper	Blistering, foliar chlorosis and necrotic spots	Aug 23, 2021
3.6	Pepper	Blistering and foliar chlorosis	Aug 23, 2021
3.7	Pepper	Foliar chlorosis and necrosis	Aug 23, 2021
3.8	Pepper	Blistering, foliar chlorosis and necrotic spots	Aug 23, 2021
3.9	Pepper	Interveinal chlorosis	Aug 23, 2021
3.10	Pepper	Blistering, foliar chlorosis and necrotic spots	Aug 23, 2021
3.11	Pepper	Mosaic, necrosis and veinal blistering	Aug 23, 2021
3.12	Pepper	Chlorotic spots and necrosis	Aug 23, 2021
3.13	Pepper	Chlorosis, interveinal chlorosis and veinal blistering	Aug 23, 2021
3.14	Pepper	Chlorotic spots and necrosis	Aug 23, 2021
3.15	Pepper	Chlorotic spots, small leaves and necrosis	Aug 23, 2021
3.16	Pepper	Chlorosis and interveinal necrosis	Aug 23, 2021
3.17	Pepper	Chlorotic spots and necrosis	Aug 23, 2021
3.18	Pepper	Chlorosis, interveinal and necrotic spots	Aug 23, 2021
2.28	Tomato	Chlorosis, leafroll and necrotic spots	Aug 23, 2021
2.29	Tomato	Necrotic spots and stunting	Aug 23, 2021
2.30	Tomato	No symptoms	Aug 23, 2021
2.31	Tomato	No symptoms	Aug 23, 2021
2.32	Tomato	No symptoms	Aug 23, 2021
2.33	Tomato	No symptoms	Aug 23, 2021
2.34	Tomato	No symptoms	Aug 23, 2021
2.35	Tomato	No symptoms	Aug 23, 2021
2.36	Tomato	No symptoms	Aug 23, 2021
2.37	Tomato	No symptoms	Aug 23, 2021
2.38	Tomato	Necrosis	Aug 23, 2021
2.39	Tomato	Chlorosis	Aug 23, 2021
2.40	Tomato	Chlorotic spots	Aug 23, 2021
2.41	Tomato	Chlorosis	Aug 23, 2021
2.42	Tomato	Chlorotic spots	Aug 23, 2021
2.43	Tomato	Chlorosis	Aug 23, 2021
2.44	Tomato	Chlorosis	Aug 23, 2021
2.45	Tomato	No symptoms	Aug 23, 2021
2.46	Tomato	No symptoms	Aug 23, 2021
2.47	Tomato	Chlorosis	Aug 23, 2021
2.48	Tomato	Chlorosis	Aug 23, 2021
2.49	Tomato	No symptoms	Aug 23, 2021
2.50	Tomato	No symptoms	Aug 23, 2021
2.51	Tomato	No symptoms	Aug 23, 2021
2.52	Tomato	No symptoms	Aug 23, 2021

2.53	Tomato	No symptoms	Aug 23, 2021
2.54	Tomato	No symptoms	Aug 23, 2021
2.55	Tomato	No symptoms	Aug 23, 2021
2.56	Tomato	No symptoms	Aug 23, 2021
2.57	Tomato	No symptoms	Aug 23, 2021
2.58	Tomato	No symptoms	Aug 23, 2021
2.59	Tomato	No symptoms	Aug 23, 2021
2.60	Tomato	No symptoms	Aug 23, 2021
2.61	Tomato	No symptoms	Aug 23, 2021
2.62	Tomato	No symptoms	Aug 23, 2021
2.63	Tomato	No symptoms	Aug 23, 2021
2.64	Tomato	No symptoms	Aug 23, 2021
2.65	Tomato	No symptoms	Aug 23, 2021
2.66	Tomato	Chlorosis	Aug 23, 2021
2.67	Tomato	Chlorosis	Aug 23, 2021
2.68	Tomato	Chlorosis	Aug 23, 2021
2.69	Tomato	Interveinal chlorosis	Aug 23, 2021
2.70	Tomato	Chlorosis	Aug 23, 2021
2.71	Tomato	Chlorosis	Aug 23, 2021
2.72	Tomato	Chlorosis	Aug 23, 2021
2.73	Tomato	Chlorosis	Aug 23, 2021
2.74	Tomato	Leafroll	Aug 23, 2021
2.75	Tomato	Interveinal chlorosis	Aug 23, 2021
2.76	Tomato	Chlorosis and leafroll	Aug 23, 2021
2.77	Tomato	Chlorosis	Aug 23, 2021
2.78	Tomato	No symptoms	Aug 23, 2021
2.79	Tomato	Chlorosis	Aug 23, 2021
2.80	Tomato	No symptoms	Aug 23, 2021
2.81	Tomato	No symptoms	Aug 23, 2021
2.82	Tomato	No symptoms	Aug 23, 2021
2.83	Tomato	No symptoms	Aug 23, 2021
2.84	Tomato	No symptoms	Aug 23, 2021
2.85	Tomato	No symptoms	Aug 23, 2021
2.86	Tomato	No symptoms	Aug 23, 2021
2.87	Tomato	No symptoms	Aug 23, 2021
2.88	Tomato	No symptoms	Aug 23, 2021
2.89	Tomato	No symptoms	Aug 23, 2021
2.90	Tomato	No symptoms	Aug 23, 2021
2.91	Tomato	No symptoms	Aug 23, 2021
2.92	Tomato	No symptoms	Aug 23, 2021
2.93	Tomato	No symptoms	Aug 23, 2021
2.94	Tomato	No symptoms	Aug 23, 2021

2.95	Tomato	No symptoms	Aug 23, 2021
2.96	Tomato	No symptoms	Aug 23, 2021
2.97	Tomato	No symptoms	Aug 23, 2021
2.98	Tomato	No symptoms	Aug 23, 2021
2.99	Tomato	No symptoms	Aug 23, 2021
2.100	Tomato	No symptoms	Aug 23, 2021
2.101	Tomato	No symptoms	Aug 23, 2021
2.102	Tomato	No symptoms	Aug 23, 2021
2.103	Tomato	No symptoms	Aug 23, 2021
2.104	Tomato	No symptoms	Aug 23, 2021
2.105	Tomato	No symptoms	Aug 23, 2021
2.106	Tomato	No symptoms	Aug 23, 2021
2.107	Tomato	No symptoms	Aug 23, 2021
2.108	Tomato	No symptoms	Aug 23, 2021
2.109	Tomato	No symptoms	Aug 23, 2021
2.110	Tomato	No symptoms	Aug 23, 2021

Colored lines in red represent positive samples for PVY using dot-ELISA.

Bolded lines represent samples selected for sequencing.

952 **Sup. Table 2.** The longest reads for each virus isolate and the most closely related virus
 953 based on Blast analysis. All sequences shared high identity with PVY sequences.

Virus	Number	Read length	Identity (%)	BLASTn result
PVYCa	1	10,550	88.00	MT200665 [PVY]
PVYCa	2	9,484	91.18	EU563512 [PVY]
PVYCa	3	9,364	89.39	MT200665 [PVY]
PVYCa	4	9,341	88.66	MT200665 [PVY]
PVYCa	5	9,199	91.92	OM056939 [PVY]
PVYSt	1	12,601	94.28	OR479975 [PVY]
PVYSt	2	12,535	95.17	KX756672 [PVY]
PVYSt	3	12,343	95.00	OR480043 [PVY]
PVYSt	4	10,430	88.15	EU563512 [PVY]
PVYSt	5	9,741	95.28	KX756672 [PVY]
PVYSI	1	11,689	86.22	EU563512 [PVY]
PVYSI	2	10,186	86.82	MT200665 [PVY]
PVYSI	3	9,899	90.39	MT200665 [PVY]
PVYSI	4	9,835	89.88	MT200665 [PVY]

PVYSI	5	9,535	94.32	OR479975 [PVY]
-------	---	-------	-------	-------------------

954

1

2

3 **Experimental evolution of host range for two isolates of *Potyvirus*** 4 ***yituberosi***

5

6 **Abstract**

7 Potato virus Y (PVY) is a highly diverse and adaptable plant pathogen with a significant
8 economic impact on solanaceous crops. This study investigates the evolutionary
9 dynamics and host-specific adaptation of two PVY isolates (PVYNb and PVYSt) across
10 three plant species (benthamiana, potato and tomato) through a series of experimental
11 infections and serial passages. Transmission efficiency, viral load, and host-specific
12 adaptation were assessed over 10 mechanical passages using RT-qPCR and
13 high-throughput sequencing. Results demonstrated significant differences in infection
14 efficiency between the two viral strains and across the three host species. PVYNb
15 exhibited higher overall infection efficiency, particularly in benthamiana, whereas
16 PVYSt showed limited infectivity, especially in tomato. Host-dependent variations were
17 observed, with *N. benthamiana* acting as a source host supporting high viral replication,
18 while tomato frequently acting as a sink, hindering sustained infection. Serial passage
19 experiments revealed fluctuating viral loads, with significant interactions between viral
20 isolate, host species, and passage number influencing virus accumulation. Infectivity
21 tests of evolved lineages indicated that viruses passaged in *N. benthamiana* were
22 generally more infectious, whereas those evolved in tomato or mixed hosts showed
23 reduced infectivity. Genome analysis revealed higher population variation in PVYNb
24 that tends to specialize in specific hosts. In contrast, PVYSt has a generalist behavior
25 with lower frequency of fixed SNPs. This study highlights the significant role of host
26 species in shaping PVY adaptation, with implications for understanding virus evolution
27 and developing effective management strategies for PVY in diverse agricultural
28 systems.

29

30 **Keywords:** Emerging virus; *Potyvirus*; Source-sink dynamics; Virulence; Virus
31 evolution

32 Introduction

33

34 Viruses of the *Potyviridae* family are amongst the most prevalent plant pathogens.
35 Specifically, potato virus Y (PVY; species *Potyvirus yituberosi*, genus *Potyvirus*, family
36 *Potyviridae*) was once ranked as the fifth most important plant virus (Scholthof et al.
37 2011). PVY has a positive-sense single-stranded RNA genome about 9.7 kb long, linked
38 at the 5' end to a viral protein (VPg) and featuring a poly(A) tail at the 3' end (Shukla et
39 al. 1994). It translates into a single polyprotein of roughly 3062 amino acids
40 (Inoue-Nagata et al. 2022), which is further processed into 10 mature peptides. An
41 additional peptide is translated from a small open reading-frame that results from a +2
42 read-through within the P3 cistron. The PVY genome is replicated by its own
43 RNA-dependent RNA polymerase, NIb. Due to the low replication fidelity of NIb,
44 potyviruses are known for their high mutation rates, with reports of 2.6×10^{-6} in turnip
45 mosaic virus (de la Iglesia et al. 2012) and 2.9×10^{-5} in tobacco etch virus (Sanjuán et al.
46 2009) substitutions per site per replication event. Such high mutation rates result in the
47 generation of a viral quasispecies population structure of closely related viral genomes
48 that undergo constant genetic variation, competition, and selection of the most fit
49 variants in specific environments (Domingo et al. 2012). The large size of viral
50 populations facilitates competitive as well as cooperative interactions between genetic
51 variants, resulting in a dynamic quasi-equilibrium distribution. The high diversity of
52 PVY allows it to be classified into strains based on biological properties, symptoms in
53 potato and tobacco hosts, and phylogeny.

54 Given its high genomic diversity and evolutionary potential, PVY is expected to
55 easily adapt to new hosts and readapt when returning to previous hosts. However, it
56 remains unclear why some PVY strains appear more adapted to certain plant species
57 and what genomic alterations occur due to host changes. Plant species are likely one of
58 the major drivers of virus evolution by exerting strong selective pressures. In turn, the
59 virus exerts selective pressure on the host, leading to a continuous cycle of reciprocal
60 coevolutionary adaptations, commonly referred to as the Red Queen hypothesis
61 (Whitlock 1996). During coevolution, viruses acquire the ability to encode proteins and
62 regulate various functions within the minimal length of RNA sequences (Belshaw et al.

63 2007), producing multifunctional proteins that play roles in viral infection, from
64 genome replication to interaction with the host plant and vector transmission.

65 An important factor in viral biology is the range of species a virus can infect.
66 Some plant viruses specialize in infecting a few host species, while many are
67 generalists, capable of infecting multiple species across different taxonomic groups.
68 PVY is classified as a generalist virus with a polyphagous vector, allowing infection in
69 diverse hosts and persistence in the environment (Edwardson and Christie 1997; Jeffries
70 1998). PVY is a globally significant plant virus, affecting at least 495 species across 72
71 genera in 31 families (Edwardson and Christie 1997). It infects economically relevant
72 solanaceous crops such as potato (*Solanum tuberosum*), tomato (*S. lycopersicum*),
73 pepper (*Capsicum* spp.), and tobacco (*Nicotiana tabacum*) and is spread by at least 70
74 aphid species in a non-persistent manner (Kerlan et al. 2008).

75 Emerging viruses face significant ecological challenges. With low initial
76 abundance and limited within-host fitness, their persistence depends on how and how
77 often they are transmitted, which can be affected by the proximity of alternative host
78 populations in space or time (Gandon et al. 2013). If transmission is insufficient, the
79 virus population cannot sustain its growth, leading to extinction before it can genetically
80 adapt to the new host (Morse 1995; Antia et al. 2003; Gandon 2004). Therefore, the
81 transmission rate is a crucial component of fitness at the between-host scale. The initial
82 persistence of a viral population is determined by its fitness at both within- and
83 between-host scales. A new host species acts as a “source” if within-host growth
84 compensates for the population bottleneck during transmission, and as a “sink” if the
85 growth rate or transmission is too low for the population to sustain itself (Dennehy et al.
86 2006, 2007). When only a single host is available, the virus becomes a specialist,
87 increasing replicative fitness in the new host but decreasing it in the original one, *i.e.*,
88 antagonistic pleiotropy (Elena et al. 2009). However, antagonistic pleiotropy is not
89 universal. For instance, tomato spotted wilt virus can adapt to new hosts and expand its
90 host range through positive pleiotropy (Ruark-Seward et al. 2020). Some interactions
91 and adaptations do not incur any cost to generalist viruses or generate fitness trade-offs
92 between hosts (Bedhomme et al. 2012). Instead, ecological fitting, due to the
93 phenotypic plasticity of the viral quasispecies, occurs when viruses colonize new niches
94 without undergoing adaptive evolution (Peláez et al. 2021). Generalist viruses, due to

95 their broader host range, are more likely to cross species boundaries and infect new
96 hosts (Woolhouse and Gowtage-Sequeria 2005).

97 Experimental evolution studies, in which the same virus isolate or genotype is
98 repeatedly passed through different hosts (either various species within the host range or
99 sequential hosts in the infection cycle), typically reveal a pattern of specialization
100 (Elena 2017). Virus lineages evolved in one host tend to perform better in that host
101 compared to lineages evolved in other hosts, though this often comes at the cost of
102 reduced fitness in alternative hosts (Wallis et al. 2007; Agudelo-Romero et al. 2008;
103 Bedhomme et al. 2012b; Hillung et al. 2014). Despite some studies performed on a few
104 potyviruses, no work has yet been done using PVY. It remains unclear if fitness
105 trade-offs across host species may arise in PVY, and what the limits of adaptation in
106 different hosts are from a molecular and phenotypical perspective. To address these
107 questions, we experimentally infected three host species under five distinct conditions
108 with two PVY strains, originally isolated from different hosts, and performed an
109 evolution experiment that spanned ten sequential passages. We measured fluctuations in
110 viral titer using RT-qPCR and sequenced the genomes by high-throughput sequencing
111 (HTS) at different passages. Additionally, we assessed the impact of both viruses on
112 symptomatology and plant height, correlating genome modifications with virus
113 evolution and virulence across generations.

114

115 **Materials and methods**

116

117 **Plants and growth environment**

118 In this study, we used three plant species in the passage experiments: *Nicotiana*
119 *benthamiana*, *S. lycopersicum* cv. Marmande, and *S. tuberosum* cv. Kennebec. Plants
120 were maintained in a growth chamber, with a light period of 16 h at 24 °C (LED tubes
121 at PAR 90 - 100 $\mu\text{mol m}^{-2} \text{s}^{-1}$), a dark period of 8 h at 20 °C, and 40% relative humidity.

122 Individual plants were transplanted into pots, with each pot containing two plants,
123 except for the potato tubers, which were cultivated in separate pots. The soil substrate
124 comprised a mixture of DSM WNR1 R73454 substrate (Kekkilä Professional, Vantaa,
125 Finland), grade 3 vermiculite, and 3-6 mm perlite in a ratio of 2:1:1.

126 Prior to the experiment, the batch of potato tubers were tested by RT-PCR to
127 ensure the absence of PVY infection. Infection of the tuber by other viruses is not
128 expect, since all tubers used are certified as free from viral infections. The potato tubers
129 were cut into two or three sections, each containing at least one eye, and submerged in a
130 2-ppm gibberellic acid solution for approximately one hour before planting. To
131 standardize the experimental conditions, only one potato stem was retained for each
132 plant before the inoculation process, with additional stems removed. This approach
133 aimed to minimize variability and ensure the uniformity of the experimental setup.

134

135 **Isolates, inoculation and collection**

136 Throughout the experiments, we used two isolates of PVY: PVYSt from the N-Wi
137 strain, which was collected in potato field and propagated in potato plants, and PVYNb
138 that belongs to the O strain, which was maintained continuously in *N. benthamiana*
139 through several generations. The strains were defined by visualizing the formation of
140 clades in a maximum-likelihood (ML) phylogenetic tree constructed using iqtree2
141 (Minh et al. 2020), with 10,000 bootstraps. This analysis utilized a dataset of 447
142 representative PVY haplotypes downloaded from GenBank (download on the
143 25-12-2023), along with the consensus sequences of PVYNb and PVYSt (Sup. Fig. 1),
144 determined by HTS, described below.

145 For mechanical inoculation, we utilized a phosphate inoculation buffer, pH 7, with
146 3% polyethylene glycol (PEG), and 1:100 diluted of 100mg Carborundum. For
147 inoculation, 20 μ L inoculum were deposited per leaf on two leaves per plant.
148 Inoculation was done manually.

149 Ten days post-inoculation (dpi), the three superior leaves of the plants were
150 harvested, excluding the inoculated leaves. Subsequently, these plant tissues were
151 rapidly frozen in liquid N₂, powdered, and homogenized. All collected samples were
152 preserved at -80 °C to maintain their molecular integrity and ensure the preservation of
153 viral particles for subsequent analyses.

154

155 **Primer design and RNA amplification**

156 In our study, we employed two approaches depending on the objectives. The first aimed
157 to quantify viral RNA using quantitative reverse transcription polymerase chain reaction

158 (RT-qPCR), while the second focused on detecting the virus using standard RT-PCR.
159 We designed two sets of primers for these purposes.

160 The RT-PCR primer set targeted a PVY-specific region with the following
161 sequences: Forward 5'-ACTATGATTTTCGTCGAGAACAA-3' (Universal PVY
162 Primer Forward, UYF) and Reverse 5'-CGCGAGGTTCCATTTTCAATGC-3'
163 (Universal PVY Primer Reverse, UYR), as described in Chapter II. Total RNA
164 extractions were performed using the NZY Plant/Fungi RNA Isolation Kit (Tech
165 MB45601, NZYtech). RT-PCR was carried out using NZYSupreme One-step RT-qPCR
166 Probe Master Mix 2x (NZYtech) under the following conditions: 50 °C for 20 min, 95
167 °C for 5 min, followed by 40 cycles of 95 °C for 5 s, 60 °C for 40 s.

168 On the other hand, the RT-qPCR primer set targeted a conserved region of the *CP*
169 gene of the virus (qYF, 5'-CAATCACAGTTTGATACGTGG-3' and qYR
170 5'-GGCGAGGTTCCATTTTCAATGC-3') and a common housekeeping gene, the
171 glyceraldehyde-3-phosphate dehydrogenase (GAPDH), highly conserved among plant
172 taxa (Martin and Cerff 1986) (qGAPDHF 5'-CTGTAACCCCAAYTCGTTGTC-3' and
173 qGAPDHR 5'-GTKGKTCMAMWGAYTTTGTKGG-3').

174 To generate the standard curves, a series of cDNA dilutions of PVY ranging from
175 50 ng/μL to 0.005 ng/μL was prepared. Each dilution was tested in triplicate. The
176 standard curves were used to calculate the qPCR reaction efficiency and the accuracy of
177 the quantification, utilizing the linear regression equations derived from the C_T values
178 versus the logarithm of the initial RNA concentration. The amplification efficiencies
179 (%) were calculated based on the slope (s) of the standard curves using the expression
180 $\text{efficiency} = 100 \times (10^{-1/s} - 1)$. The efficiency of PVY primers for the amplification of the
181 portion of PVYNb and PVYSt genome was 94% ($R^2 = 99.9\%$) and 104% ($R^2 = 99.1\%$),
182 respectively. For the GAPDH primers, the amplification efficiency was 89% for
183 benthamiana ($R^2 = 99.3\%$) and tomato ($R^2 = 98.4\%$), and 91% ($R^2 = 99.9\%$) for potato
184 (Sup. Fig. 2). Thus, the RT-qPCR method was validated for adequate quantification of
185 PVY RNA in the plant samples.

186 RNA extraction for this set was conducted using Sigma STRN250 Spectrum Plant
187 Total RNA Kit with DNase treatment (Invitrogen TURBO DNA-free Kit AM1907).
188 The samples were checked for concentration and quality using Nanodrop and
189 normalized to 50 ng/μL. RT-qPCR was performed using qPCRBIO SyGreen 1-Step Go

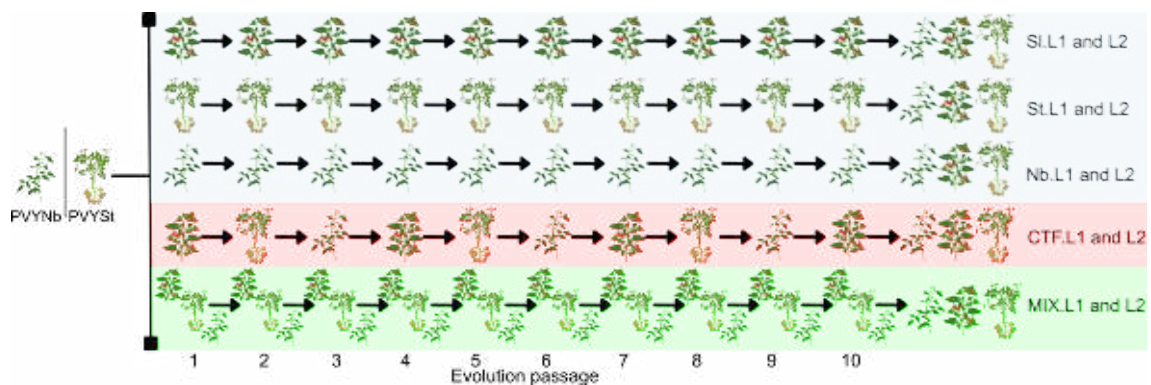
190 Hi-Rox (PCR BIOSYSTEMS) with at least three replicates for each sample. The
191 conditions included 45 °C for 10 min, 95 °C for 2 min, followed by 40 cycles of 95 °C
192 for 5 s and 60 °C for 30 s. All RT-qPCR results were filtered based on quality, using C_T
193 cut-off values of 5 and 35, and with a maximum deviation between replicates of 0.3.
194 The data were analyzed using qRAT (Flatschacher et al. 2022). Viral loads were then
195 obtained using the $\Delta\Delta C_T$ method (Schmittgen and Livak 2008).

196

197 Evolution experiment

198 Twenty evolution experiments were simultaneously initiated, each with a total of ten
199 serial passages; half were started with PVYNb and the other half with PVYSt. Five
200 treatments were tested differing in their host plant composition as follows: (Sl) viruses
201 only inoculated to tomato plants; (St) only to potato plants; or (Nb) only to benthamiana
202 plants; (Correlated temporal fluctuations, CTF) viruses alternating inoculations among
203 the three host species in the tomato-potato-benthamiana sequence; and (MIX) at each
204 passage, viruses were inoculated into a mixture of the three plant species at equal
205 proportions. Two independent evolution lineages per treatment were generated (L1 and
206 L2). At each passage, the host population size was 16 plants. A full experiment design
207 can be seen in the Fig. 1, totaling 20 experimental lines, 10 for each PVY isolate.

208



209

210 **Fig 1.** Schematic illustration of the passage experiment for analysis of the evolution of
211 PVY according to the host. The founder population of two isolates, PVYNb from
212 benthamiana and PVYSt from potato, were used to inoculate the 5 plant sets, in 2
213 replicates, totaling 10 Lines (Sl.L1, Sl.L2; St.L1, St.L2; Nb.L1, Nb.L2; CTF.L1,
214 CTF.L2; MIX.L1, MIX.L2). The inoculation scheme for the passages in the same plant
215 species are presented in the blue background, while the sequential scheme with

216 switching hosts is shown in red. In green, inoculations were performed in a mixture of
217 different plants. Each plant in the scheme represents 16 inoculated plants, with MIX
218 being the exception in which each plant represents 6 inoculated plant. The arrow
219 represents mechanical inoculation from the previous passage. Using the last positive
220 sample, 10 plants of each species were inoculated with the immediately preceding
221 positive infection from the negative infection passage. A list of the last positive line is
222 available at Sup. Table 1.

223

224 All evolving lineages underwent simultaneous inoculation on the same day, and
225 the plant symptoms were daily monitored until 10 dpi. Then, the 16 plants were pooled
226 and representative samples were collected. The tissue was powdered in liquid N₂, a
227 portion used for inoculation of the next passage, and another portion was used for RNA
228 extraction. Following quantification via relative RT-qPCR, only the positive lineages
229 were continued. For those negative lineages, the inoculation process was repeated again
230 using tissue from the previous positive passage to minimize potential inoculation error.
231 Importantly, no previously negative lineage yielded a positive result after the second
232 trial, ensuring the reliability of the experimental outcomes.

233 In each passage, six plants from each species served as mock controls, inoculated
234 only with phosphate buffer. In addition, six plants of each species were employed as
235 negative controls.

236 For the evaluation of disease phenotypic effects, the plant height was measured
237 from the base of the plant to the apical meristem. Measurements were taken one day
238 before inoculation and one day before collection (9 dpi).

239 At the end of passages and using the last positive passage available, all lineages
240 were subjected to inoculation in the three different hosts, 10 plants of each. At this
241 point, we applied an individual RT-PCR in order to detect the number of positive
242 samples. Negative and mock controls were used during the inoculation and detection
243 steps.

244

245 **Transmission rate experiment**

246 In the passage experiment, we recognized the potential for a loss of quantification
247 accuracy due to pooling all 16 plants during collection and further inoculation. To

248 address this issue, we devised a transmission rate quantification experiment. In this
249 setup, we inoculated 50 benthamianas, 50 potatoes, and 50 tomatoes using PVYNb or
250 PVYSt. Each plant was individually collected to quantify the number of positive plants.

251 For this analysis, we employed an individual standard RT-PCR, and the samples
252 were subjected to 1% agarose gel electrophoresis with SYBR green. Among the positive
253 samples, we randomly selected three samples, with the exception of tomatoes infected
254 with PVYSt, for which only two positive plants were obtained. Subsequently, each
255 selected positive sample was used to inoculate another set of 50 plants for each species.

256 This process allowed us to assess the likelihood of a virus passing through the
257 same host. Utilizing the same approach of RT-PCR and gel electrophoresis, we
258 systematically analyzed the infection rates and dynamics within each host species. This
259 individualized sampling strategy aimed to provide a more accurate and detailed
260 understanding of virus transmission patterns among the different plant species.

261

262 **HTS and sequence analyses**

263 To determine the genome changes of the virus during the passage experiment, we
264 employed Illumina HTS on three time points, in (1) the initial PVYNb and PVYSt
265 inoculum source, in (2) the fourth passage ($n = 12$), and in (3) the latest available
266 passage of each line ($n = 17$) (the list of the last available passage is available in Sup
267 Table 1). Total RNA was extracted from fresh or dried leaf tissue using Sigma
268 STRN250 Spectrum Plant Total RNA Kit (Invitrogen TURBO DNA-free Kit AM1907),
269 then they were treated with DNase. The RNA concentration and the ratio absorbance at
270 260/230 and 260/280 nm quality was checked using Nanodrop before being sent for
271 sequencing at Macrogen Inc. (Seoul, South Korea). GenTegra RNA GTR5001-S
272 screwcap microtubes ensured secure sample storage and transportation during
273 sequencing. Paired-end reads was prepared using TruSeq Stranded Total RNA Library
274 Plant Kit library kit with TrueSeq Stranded Total RNA Reference Guide protocol in
275 Illumina plataform.

276 To generate a consensus sequence for each sample ($n = 31$), reads were trimmed
277 with BBDuk (<https://sourceforge.net/projects/bbmap/>), assembled with MEGAHIT
278 (Martin and Cerff 1986; Li et al. 2015) and subjected to diamond blastx (Buchfink et al.
279 2015) searches against the non-redundant NCBI database (download on the

280 2024-06-24). The longest contigs identified as PVY for each sample were then
281 subjected to BLASTn searches against the nucleotide database to identify their closest
282 isolate (HM367076 and MW685829 for PVYNb and PVYSt, respectively). Then, reads
283 were aligned against their respective reference sequence with BBMap v39.01
284 (<https://sourceforge.net/projects/bbmap/>) and a consensus sequence for each isolate was
285 generated with Geneious Prime build 2022-03-15. Reads were aligned to the
286 corresponding consensus sequence of PVY with BBmap with the vslow option. Base
287 recalibration was then performed with GATK v4.0.5.1 (Van der Auwera and O'Connor
288 2020).

289 The diversity of each sequenced line was calculated as the sum of the Shannon
290 entropy of each polymorphic site divided by the genome length using the aligned reads
291 against the genome, resulting in a normalized quantity that varies between 0 (no
292 polymorphic site) and 2 (all sites have an equal proportion of A, C, U and G). The
293 genetic distance between population was calculated from the allele frequency difference
294 (AFD) (Berner 2019). We also constructed the ML-tree using iqtree2 with 10,000
295 bootstrap replications with all consensus generate sequences.

296

297

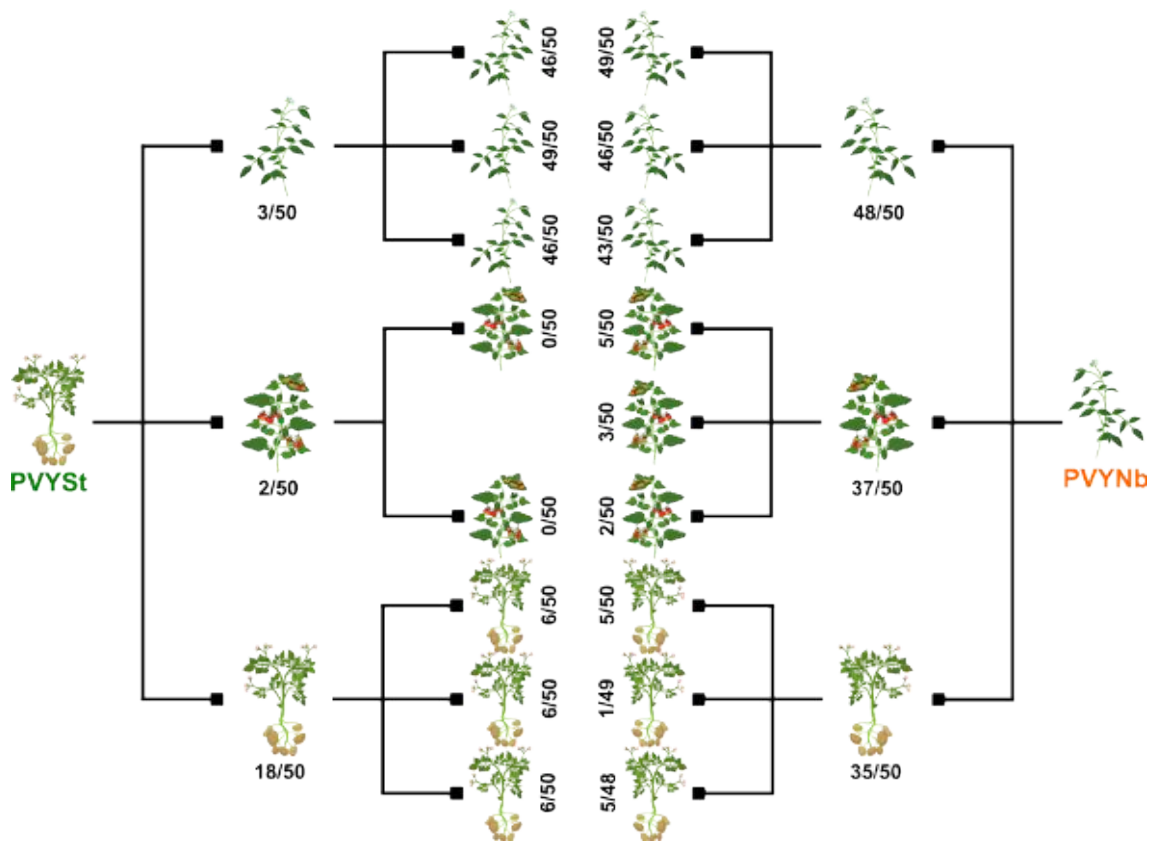
298 **Results**

299

300 **Test of transmission efficiency across host species**

301 Initially, we examined the potential constraints imposed by the hosts on the adaptation
302 of the PVY isolates and evaluated which of the three plant species may act as source or
303 sink for the virus, by evaluating the probabilities of successfully infecting each of the
304 three selected hosts with each of the two viral isolates. Fifty plants per host species were
305 inoculated with the initial PVYNb and PVYSt isolates and analyzed individually by
306 RT-PCR as illustrated in the experimental design shown in Fig. 2.

307



308

309 **Fig 2.** Infection rate evaluation according to the host, in which PVYSt and PVYNb
 310 were inoculated in 50 plants of each species and then reinoculated in the same host. The
 311 numbers below or at the side of each plant represent the infected and inoculated plants,
 312 respectively. The infection status of each plant was individually evaluated using
 313 RT-PCR.

314

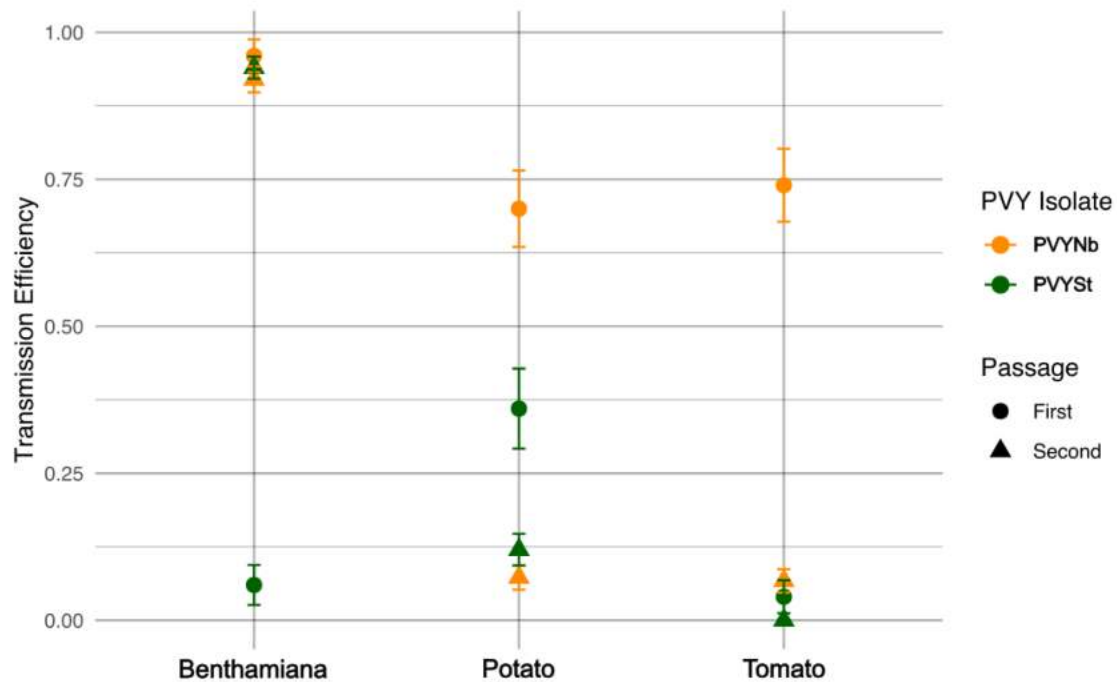
315 Data shown in Fig. 3 were fitted to a logistic-regression using a generalized linear
 316 model (GLM) with a Binomial distribution probability and logit link function. Firstly,
 317 this analysis confirmed the high significant differences between the two viral isolates (χ^2
 318 = 154.204, 1 d.f., $P < 0.001$), with PVYNb transmission efficiency across hosts being
 319 0.844 ± 0.037 (± 1 SE), while it was 8.2-fold lower (0.103 ± 0.030) for PVYSt.
 320 Differences in transmissibility among plant species was also observed ($\chi^2 = 9.821$, 2
 321 d.f., $P = 0.007$), with benthamiana (0.553 ± 0.116) and potato (0.534 ± 0.053) showing
 322 similar average PVY transmission efficiencies while tomato was about one-half less
 323 susceptible to infection (0.256 ± 0.075). More interestingly, a significant interaction
 324 between viral isolate and host species was found ($\chi^2 = 30.608$, 2 d.f., $P < 0.001$),

325 confirming that the transmission efficiency actually depended on the combination of
326 viral genotype and host species: in the first round of inoculation, maximum
327 transmissibility of PVYNb was shown in benthamiana (0.960 ± 0.028) and minimum in
328 potato (0.700 ± 0.065) while maximum transmissibility for PVYSt was observed in
329 potato (0.360 ± 0.068) and minimum in tomato (0.040 ± 0.028).

330 Following this first experiment, we randomly selected three positive plants
331 (except for PVYSt in tomatoes with only two positive samples), prepared new
332 independent inocula and reinoculated 50 plants of the same host. Differences among the
333 two viral isolates remained significant in this second infection ($\chi^2 = 4.001$, 1 d.f., $P =$
334 0.045), although in this case the average transmission efficiency for the PVYNb-derived
335 samples was 0.287 ± 0.037 but null for the PVYSt-derived ones. The transmission
336 efficiency results were strongly variable across host species ($\chi^2 = 707.822$, 2 d.f., $P <$
337 0.001), being 0.931 ± 0.015 for benthamiana, 0.094 ± 0.017 for potato and null for
338 tomato. Finally, as observed in the first transmission trial, the outcome of this second
339 one also depended on the interaction between the origin of the inoculum and the host
340 species being inoculated ($\chi^2 = 12.770$, 2 d.f., $P = 0.002$). In this second case,
341 PVYNb-derived inocula from benthamiana had a transmission efficiency of 0.920
342 ± 0.022 in benthamiana, while inocula from tomato and potato were much less
343 transmissible when inoculated again in the same host (0.067 ± 0.020 and 0.073 ± 0.021 ,
344 respectively). Likewise, PVYSt-derived inocula from benthamiana also had a high
345 transmission efficiency in benthamiana (0.940 ± 0.022), inocula from potato had a lower
346 transmissibility in potato (0.120 ± 0.027) while inocula from tomato failed to be
347 transmitted to other tomatoes.

348 Based on the transmission efficiencies obtained at the first and second events, we
349 can now evaluate the sign and magnitude of the observed changes in transmission
350 efficiencies (Fig. 3). In the case of PVYNb, a host-species dependent reduction in
351 transmission efficiency has been observed ($\chi^2 = 6.946$, 2 d.f., $P = 0.031$). While no
352 significant reduction was observed for benthamiana plants (0.960 ± 0.028 vs 0.920
353 ± 0.022 ; sequential Bonferroni *post hoc* test, $P = 0.779$), significant reductions were
354 observed for tomato (0.740 ± 0.062 vs 0.067 ± 0.020 ; $P < 0.001$) and potato (0.700
355 ± 0.065 vs 0.073 ± 0.021 ; $P < 0.001$). A host-dependent change in the transmission
356 efficiency between sequential inoculation experiments was observed for PVYSt ($\chi^2 =$

357 123.735, 2 d.f., $P < 0.001$). In the case of benthamiana plants, transmission efficiency
 358 largely improved in the second transmission event compared to the first one (0.060
 359 ± 0.034 vs 0.940 ± 0.019 ; $P < 0.001$). In sharp contrast, no change in efficiency was
 360 observed for tomato (0.040 ± 0.028 vs 0.000 ± 0.000 ; $P = 0.447$) and a significant
 361 reduction in potato (0.360 ± 0.068 vs 0.120 ± 0.027 ; $P = 0.006$) was found.
 362



363
 364 **Fig 3.** Transmission efficiencies of PVYNb and PVYSt in benthamiana, tomato and
 365 potato plants based on the results of the infection rate experiment during two sequential
 366 passages using the same host. The data were fitted to a logistic-regression using a
 367 generalized linear model (GLM) with a Binominal distribution probability and logit link
 368 function.

369
 370 In conclusion, our study shows that the transmission efficiency of PVY isolates is
 371 highly dependent on both the viral genotype and host species. PVYNb exhibited higher
 372 transmissibility across all hosts compared to PVYSt, with benthamiana being the most
 373 susceptible. Sequential inoculations revealed that PVYNb transmission efficiency
 374 decreased significantly in potato and tomato, while remaining stable in benthamiana. In
 375 contrast, PVYSt improved its transmission in benthamiana but struggled in tomato and

376 potato. These results suggest that different plant species can act as either facilitators or
377 barriers to viral adaptation and transmission.

378

379 **Variation of viral loads along the passage through the plants**

380 Our aim was to understand the host effect in the variation on the genome of PVY
381 through serial passages. Closely related plants were used as test hosts, all in the family
382 *Solanaceae*. In the passage experiment (Fig. 1), the isolates PVYSt and PVYNb were
383 inoculated in five plant groups, tomato, benthamiana, potato, sequential switching hosts
384 and mixed plants, through ten passages by mechanical inoculation. Viral load was taken
385 as a proxy to within-host fitness. Fig. 4 shows the evolution of viral loads, measured by
386 relative qPCR, for both PVY isolates under each of the five experimental host
387 treatments. Data were fitted to a GLM with a Gamma probability function and a
388 log-link function; viral isolate, experimental treatment and passage were included in the
389 model as orthogonal factors and lineage was nested within the interaction of viral isolate
390 and experimental treatment.

391 Firstly, a net effect of passage was observed ($\chi^2 = 3984.677$, 9 d.f., $P < 0.001$) due
392 to fluctuations and an overall tendency towards decreasing values in most of the
393 conditions (Fig. 4). Secondly, net differences exist between both PVY isolates ($\chi^2 =$
394 1691.114 , 1 d.f., $P < 0.001$), with PVYNb, on average, accumulating orders of
395 magnitude more than PVYSt (292.354 ± 15.505 vs. 0.023 ± 0.002 , respectively).

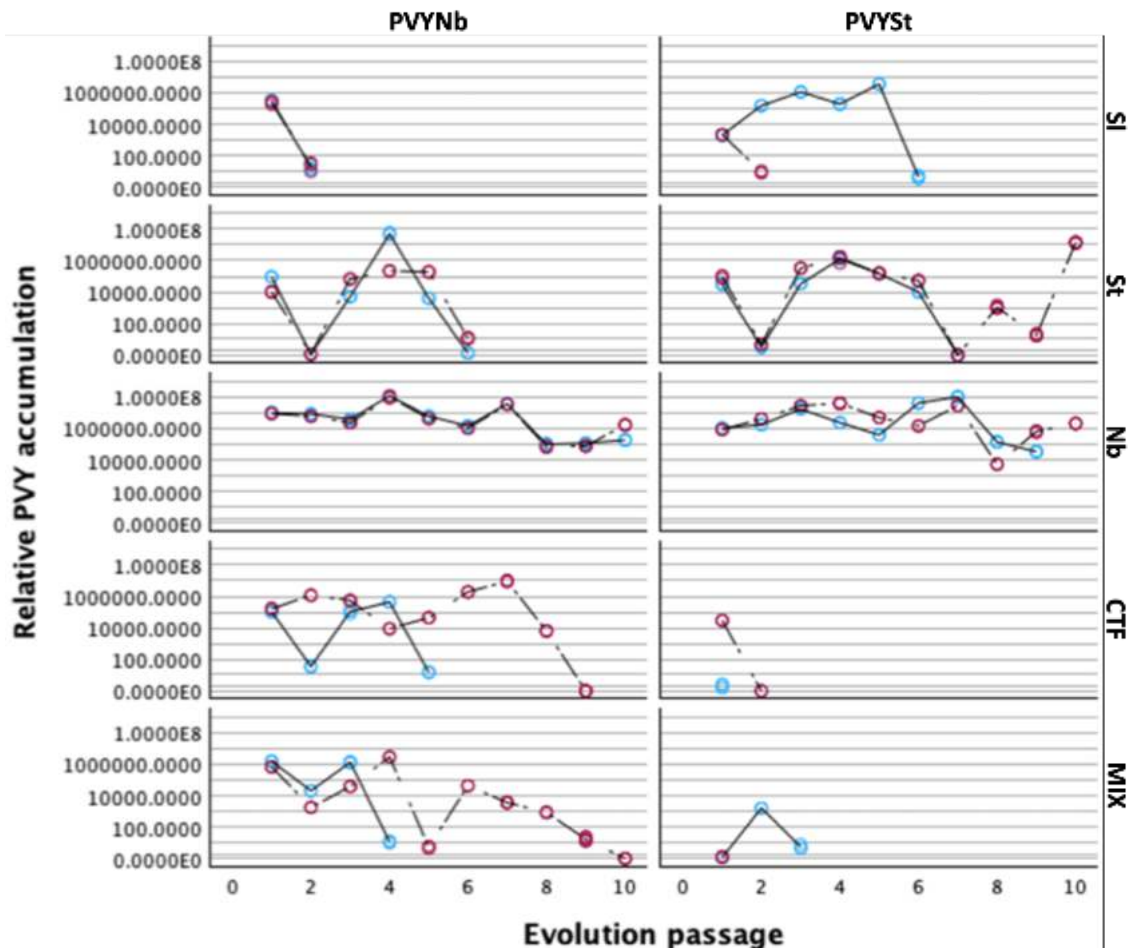
396 Thirdly, differences exist between the five host treatments ($\chi^2 = 5682.249$, 4 d.f., P
397 < 0.001). Overall, the most permissive host for virus replication was benthamiana (Nb)
398 (average accumulation $2.334 \pm 0.032 \cdot 10^6$) distantly followed by tomatoes (Sl) (161.143
399 ± 18.076) and potatoes (St) (12.985 ± 0.820). Viral loads estimated for the two
400 mixed-hosts treatments (CTF and MIX) were low and hardly distinguishable from
401 noise.

402 Interestingly, a significant interaction between PVY isolate and experimental
403 conditions was observed ($\chi^2 = 2532.462$, 4 d.f., $P < 0.001$), indicating that the
404 accumulation of each isolate actually depended on the particular host in which it was
405 measured. Furthermore, this effect also depends on passage number ($\chi^2 = 1498.356$, 9
406 d.f., $P < 0.001$). For both isolates, benthamiana showed the highest accumulations,
407 confirming its role as source host ($2.750 \pm 0.049 \cdot 10^6$ for PVYNb and $1.981 \pm 0.041 \cdot 10^6$

408 for PVYSt). However, in the case of PVYNb CTF showed the second largest
409 accumulation ($2.139 \pm 0.107 \cdot 10^3$), while for PVYSt in potato (St) ranked second (1.028
410 $\pm 0.003 \cdot 10^3$). The lowest accumulation of PVYNb was observed in St (0.164 ± 0.019)
411 while for PVYSt it was in CTF, and MIX values were indistinguishable from noise. In
412 tomatoes (Sl), PVYNb was unable to infect plants in the second passage after an initial
413 infection, being restricted to the first passage (Fig. 4). PVYSt also showed difficulty in
414 infecting tomatoes, but PVYSt/Sl.L1 was maintained in tomatoes for five serial
415 passages (Fig. 4). Interestingly, PVYSt/Sl.L1 showed an increase in viral RNA during
416 the passages, but after the peak of virus abundance, it failed to infect the plants in the
417 next passage. This result is in line with the evidences that tomato is a less permissive
418 sink host for the propagation of the two used PVY isolates. In potatoes (St), both PVY
419 isolates could infect systemically and be passed through at least five passages. The viral
420 RNA contents variation during passages did not follow a consistent pattern. PVYNb
421 lines infected potatoes for five passages, showing a similar infection pattern except for
422 the fourth passage, which decreased dramatically and resulted in absence of infection in
423 the next passage. PVYSt/St.L1 could infect potato plants for six passages and
424 PVYSt/St.L2 for ten passages. PVYSt/St.L2 exhibited a significant increase in virus
425 RNA after the eighth passage, suggesting adaptation to the host. In benthamiana (Nb),
426 both PVYNb/Nb.L1 and PVYNb/Nb.L2 and PVYSt/Nb.L1 and PVYSt/Nb.L2 exhibited
427 high viral RNA contents compared to other lines (Fig. 4). The viral RNA amount was
428 high from the first passage and remained high throughout all passages. The four
429 experimental lineages reached 10 passages. Both PVYNb lineages had a close detection
430 pattern and constant virus amount with minimal variation. In contrast, PVYSt lineages
431 displayed more variation but seemed to have adapted to the host in the last two
432 passages. For the host switching treatment (CTF), starting with tomatoes and then
433 passing to potatoes and benthamiana, PVYSt/CTF.L1 could not infect tomato plants,
434 while in PVYSt/CTF.L2 only the first passage contained infected plants, but failed to
435 infect potato plants in the next passage. PVYNb had an initial low infection ability in
436 tomatoes but it increased in subsequent passages with potatoes and benthamiana,
437 decreasing again when returning to tomatoes. PVYNb/CTF.L1 reached the fourth
438 passage but could not infect potatoes after being inoculated in tomatoes, while
439 PVYNb/CTF.L2 stopped at the eighth passage, unable to pass from potatoes to

440 benthamiana. In mixed host treatment (MIX), PVYSt/MIX.L1 was terminated at the
 441 second passage with a low viral load, and PVYSt/MIX.L2 caused no infection. PVYNb
 442 was detected until the third passage, with similar virus load in both lineages. Lineage
 443 PVYNb/MIX.L2 reached the ninth passage with significant variation between passages.
 444 It was unclear which host contributed to virus replication as plants were pooled during
 445 RNA extraction and virus detection.

446



447

448 **Fig 4.** Relative quantification of the PVY RNA at each passage ($\Delta\Delta C_T$ method; see
 449 Materials and Methods section). Data are organized by PVY isolate (columns) and
 450 passage treatment (rows). Independent evolutionary lineages are indicated by different
 451 colors.

452

453 The observed effects of passages on virus titer did not necessarily represent an
 454 overall trend of increase or decrease in virus accumulation, but simply uncorrelated

455 significant differences among passages. Indeed, for lineages evolved in host
456 environments Sl (partial correlation coefficient controlling for viral strain and lineage: r
457 = 0.289, 34 d.f., $P = 0.088$), Nb ($r = -0.121$, 130 d.f., $P = 0.167$) and CTF ($r = 0.156$, 53
458 d.f., $P = 0.254$), there was no significant correlation between the number of the passage
459 and the virus titer. A weak positive yet significant correlation ($r = 0.208$, 108 d.f., $P =$
460 0.029) was found for viral lineages evolved in St, while a significant negative
461 correlation was found for lineages evolved in MIX ($r = -0.360$, 59 d.f., $P = 0.004$).

462 Based on this evolution experiment, we concluded that host species significantly
463 influence the pace of PVY adaptation. The permissiveness of different hosts varied
464 widely, with benthamiana plants demonstrating their role as source host supporting high
465 viral replication and efficient transmission across passages, while tomato plants acting
466 as sink hosts, often failing to support the virus beyond the initial passages. Host
467 switching revealed that initial low infection rates in less permissive hosts could improve
468 in more permissive hosts, and mixed host lines showed varied infection outcomes.

469

470 **Infectivity of evolved lineages depends on both the evolved environment and the** 471 **test host**

472 Using the last positive sample of PVYNb as inoculum, 10 plants of each host were
473 inoculated and their infection status determined by RT-PCR detection (Sup. Table 1).
474 Fitting these infectivity data to a logistic-regression, the analysis confirmed a significant
475 effect of the host compositions during serial passages ($\chi^2 = 35.722$, 4 d.f., $P < 0.001$),
476 with viruses passaged in benthamiana being, on average, the most infectious, followed
477 by those evolved in potato. No net significant effect was observed for the host in which
478 the infectivity of the evolved lineages was tested ($\chi^2 = 0.000$, 2 d.f., $P = 1.000$),
479 although a significant interaction existed between the evolved host and the test host (χ^2
480 = 33.915, 8 d.f., $P < 0.001$). PVYNb/Sl.L1 could not infect any hosts, while
481 PVYNb/Sl.L2 infectivity of benthamiana plants was 0.167 ± 0.215 (LaPlace estimator of
482 the binomial parameter with 95% adjusted Wald CI). After five passages in potatoes,
483 PVYNb/St.L1 could not infect any hosts, but PVYNb/St.L2 infectivity in benthamiana
484 was 0.750 ± 0.237 , 0.833 ± 0.215 in tomato and 0.250 ± 0.237 in potato plants. After ten
485 passages in benthamiana, PVYNb/Nb.L1 infectivity in benthamiana was 0.750 ± 0.237
486 and 0.917 ± 0.142 tomato plants but no potatoes could be infected. PVYNb/Nb.L2

487 infectivity in benthamiana and tomatoes was 0.917 ± 0.142 but dropped down to 0.167
488 ± 0.215 in potatoes. After four passages, switching hosts and ending in tomatoes,
489 PVYNb/CTF.L1 infectivity in benthamiana was zero, 0.500 ± 0.263 in tomato and 0.333
490 ± 0.252 in potato plants. PVYNb/CTF.L2, after eight passages, ending in potato plants,
491 could not infect any hosts. After three passages, PVYNb/MIX.L1 infectivity in
492 benthamiana was 0.833 ± 0.215 and 0.750 ± 0.237 in tomato plants but no potatoes, and
493 PVYNb/MIX.L2, after nine passages, could not infect any hosts.

494 Following the same approach with the PVYSt isolate, we also found significant
495 effects of the host composition during serial passages in the infectivity of the evolved
496 viruses ($\chi^2 = 58.871$, 4 d.f., $P < 0.001$), with again lineages evolved in benthamiana
497 plants being the most infectious. However, for this viral isolate, significant differences
498 among the three test hosts were observed ($\chi^2 = 17.708$, 2 d.f., $P < 0.001$), with tomato
499 showing more infected plants than the other two hosts. A significant interaction between
500 evolution conditions and test host was also observed ($\chi^2 = 35.799$, 8 d.f., $P < 0.001$).
501 PVYSt/Sl.L1 could not establish infection in any host, while PVYSt/Sl.L2, after one
502 passage, infectivity in benthamiana was 0.250 ± 0.237 and 0.750 ± 0.237 in tomato plants
503 but null in potatoes. PVYSt/St.L1 reached six passages and could not infect
504 benthamiana but had an infectivity of 0.417 ± 0.261 in tomatoes and of 0.250 ± 0.237 in
505 potatoes. PVYSt/St.L2 reached ten passages but had an infectivity of 0.167 ± 0.215 in
506 potato plant not the other two hosts. In benthamiana, PVYSt/Nb.L1 and PVYSt/Nb.L2
507 reached ten passages. Lineage PVYSt/Nb.L1 infectivity in benthamiana was 0.833
508 ± 0.215 , 0.917 ± 0.142 in tomato and 0.167 ± 0.215 in potato plants, while lineage
509 PVYSt/Nb.L2 infectivity in benthamiana was 0.917 ± 0.142 , 0.917 ± 0.142 in tomato and
510 0.250 ± 0.237 in potatoes plants. In switching hosts, only PVYSt/CTF.L2 achieved one
511 passage and had infectivity 0.250 ± 0.237 in tomato and in potato plants. Lineage
512 PVYSt/MIX.L1 achieved the second passage and showed infectivity 0.167 ± 0.215 in
513 benthamiana and in potato plants.

514 All together, these observations suggest that benthamiana is the most permissive
515 host for PVY strains evolution, allowing sustained virus replication across multiple
516 passages. Potato served as an intermediate host with variable viral replication patterns,
517 while tomato was the least permissive of the three tested hosts, often failing to support
518 continued virus passages. Notably, PVYNb struggled to infect tomatoes beyond the

519 initial passage, while PVYSt showed limited but more sustained replication in certain
520 lines. The mixed host lines indicated the complexity of host-virus interactions and
521 potential adaptation mechanisms. These findings highlight the importance of host
522 species in virus replication dynamics.

523

524 **Changes in virulence and symptomatology**

525 Next, we sought to evaluate the virulence of the PVY evolving lineages. As a first
526 measure of virulence on each host species, we evaluated the effect of viral infection in

527 plant growth relative to the mean growth of mock inoculated plants, $V = 1 - \frac{\Delta L_{infected}}{\langle \Delta L_{mock} \rangle}$,

528 where L is the plant height measured at the time of inoculation and 9 dpi. $V < 0$ indicate

529 a reduction in growth while $V > 0$ indicates infection enabled growth compared to

530 noninfected plants. Virulence was measured after each of the 10 serial passages. Data

531 are shown in Fig. 5. Data were fitted to a complex GLM with a Normal probability

532 distribution and identity link function. Viral isolate, experimental passage, host

533 treatment, and test host were used as orthogonal main factors, while experimental

534 lineage was nested within the interaction between viral isolate and host treatment.

535 Focusing in the main factors, overall significant differences were found between the two

536 viral isolates ($\chi^2 = 4.680$, 1 d.f., $P = 0.031$), being the mean virulence for PVYNb (0.040

537 ± 0.029 ; ± 1 SE) 8.6-fold larger than for PVYSt (0.005 ± 0.084) and positive in both

538 cases, suggesting plant elongation was a common symptom of infection. No main

539 effects were associated for the host environment in which lineages evolved ($\chi^2 = 7.488$,

540 4 d.f., $P = 0.112$) nor for the host in which virulence was tested ($\chi^2 = 3.542$, 2 d.f., $P =$

541 0.170). However, significant differences among viral lineages evolved in a particular

542 host environment and the host species in which virulence was evaluated have been

543 found ($\chi^2 = 8.441$, 2 d.f., $P = 0.015$), confirming that virulence indeed dependent on the

544 interaction between viral strain, host environment and test host. For example, the largest

545 reduction in growth induced by PVYNb infection was observed for lineages evolved in

546 potatoes and tested in the same host (-0.133 ± 0.078), while the smallest virulence was

547 observed for lineages evolved in potato but tested in tomato (0.018 ± 0.104). In contrast,

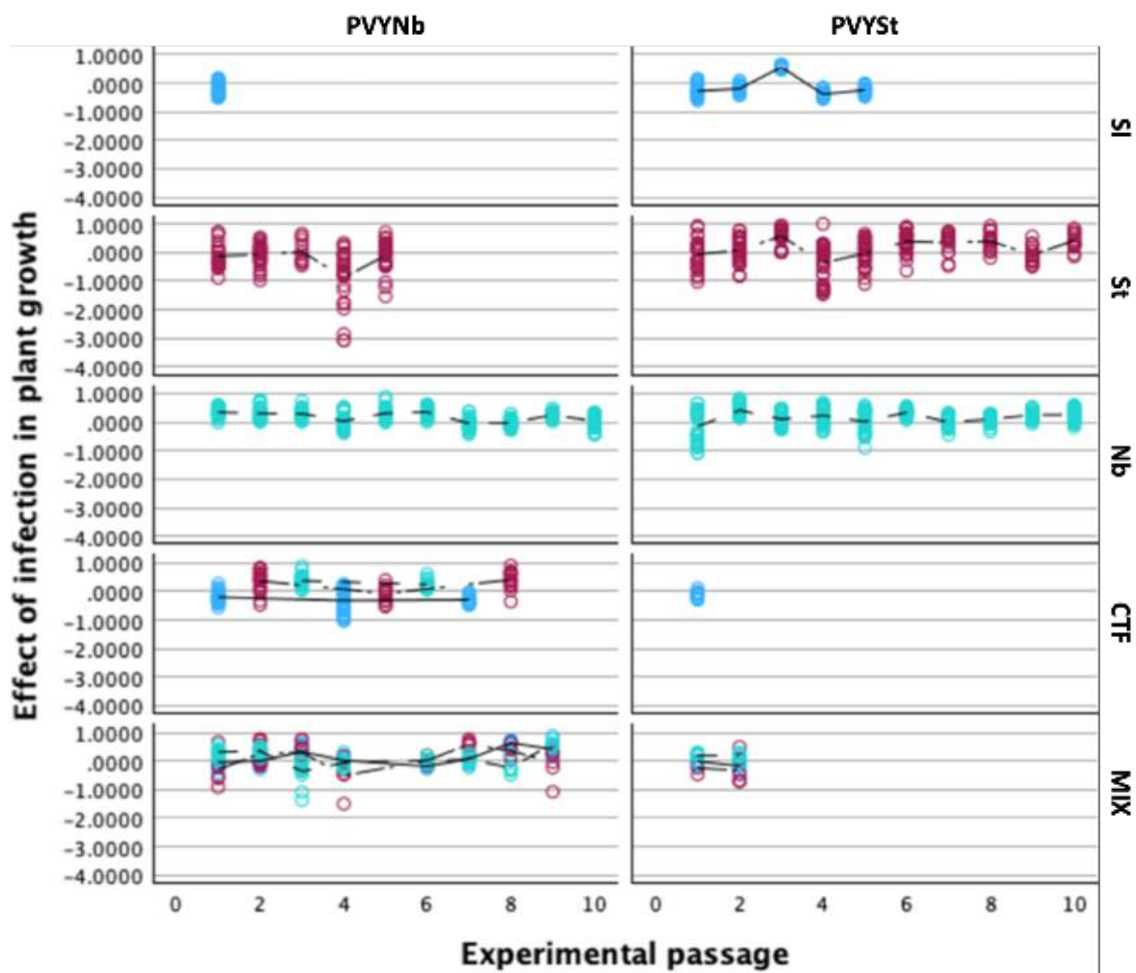
548 in the case of PVYSt infections, the largest effect was observed for lineages evolved in

549 tomatoes and tested in potato (-0.699 ± 0.178) and the smallest for lineages evolved in

550 the mixed host populations and tested in the most permissive host, benthamiana (0.011
551 ± 0.166).

552 Next, we decided to evaluate the possible effect of the source host on the
553 evolution of symptoms in the most permissive host, *i.e.*, benthamiana. To do so, we
554 monitored the presence or absence of symptoms in inoculated plants over 9 dpi. Mean
555 time to the appearance of first visible symptoms was calculated using the Kaplan-Meier
556 regression of the number of infected plants to days after inoculation. Fig. 6 shows the
557 evolution of this mean time along the passage experiment. Remarkably, only the
558 lineages evolved in benthamiana (Nb) plants, and that of MIX.L2 evolved in the mixed
559 population were able to generate visible symptoms along all the passages. Indeed, for
560 these lineages, a significant negative correlation exists between mean time to symptoms
561 and passage number (partial correlation coefficient controlling for viral isolate and
562 lineage: $r = -0.601$, 34 d.f., $P < 0.001$), indicating that symptoms tend to appear faster
563 in benthamiana plants as the virus was evolving in this plant species. In other instances,
564 symptoms appeared only sporadically (*e.g.*, lineage PVYNb/CTF.L2 recovered from
565 benthamiana plants or early passages of PVYSt/MIX.L1), making additional statistical
566 analyses unreliable.

567



569

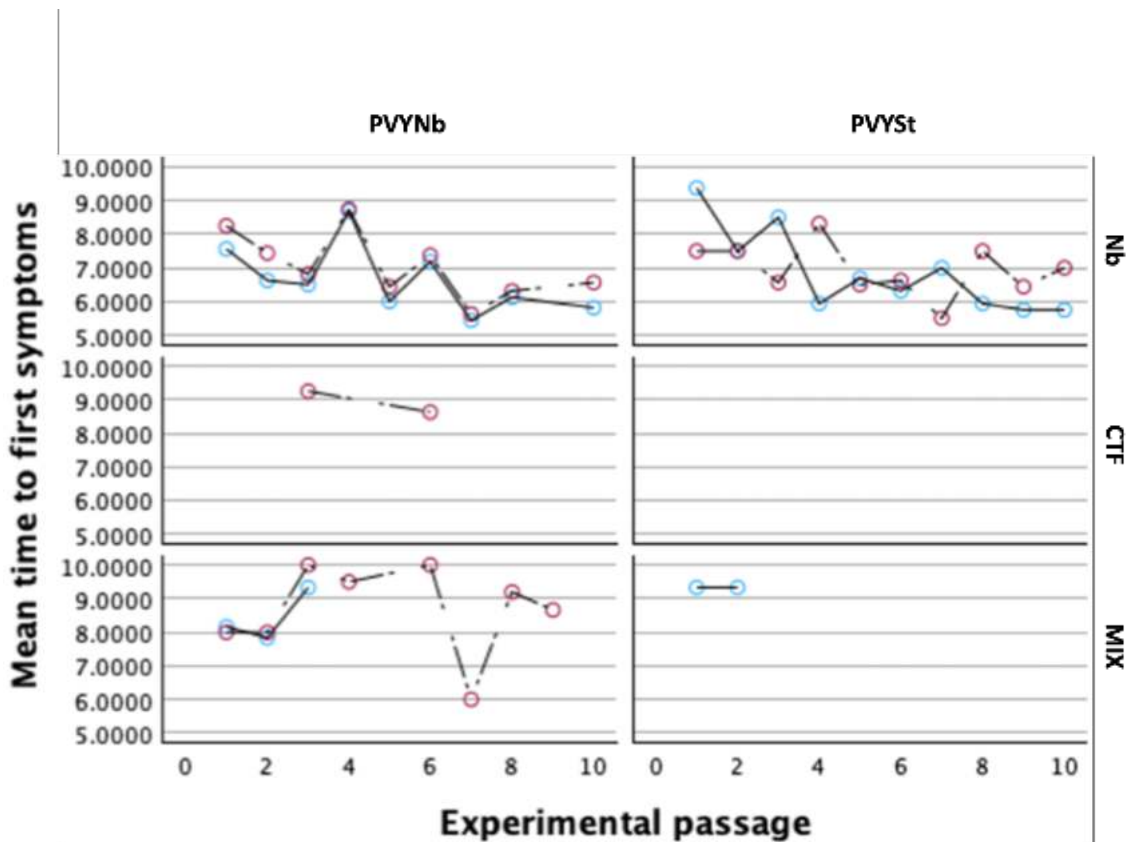
570 **Fig 5.** Evolution of virulence (relative effect of infection in plant growth). Data are
 571 organized by PVY isolate (columns) and passage treatment (rows). Plant species in
 572 which virulence was evaluated are indicated by colors: blue: tomato, red: potato, green:
 573 benthamiana. Viral lineages evolved in CTF were tested on the plant species
 574 corresponding to each passage. Viral lineages evolved in MIX were tested in all three
 575 plant species.

576

577 Taken together, these findings highlight the multifaceted nature of viral infection
 578 on plant growth, emphasizing the importance of considering various factors and their
 579 interactions in understanding the impact of viral infections on plant phenotypes.

580

581



582

583 **Fig 6.** Evolution of the mean time for the appearance of the first symptoms in *N.*
584 *benthamiana* plants inoculated with the different evolving lineages (indicated by
585 colors), divided by treatment (Nb, CTF and MIX).

586

587 **Genome alterations**

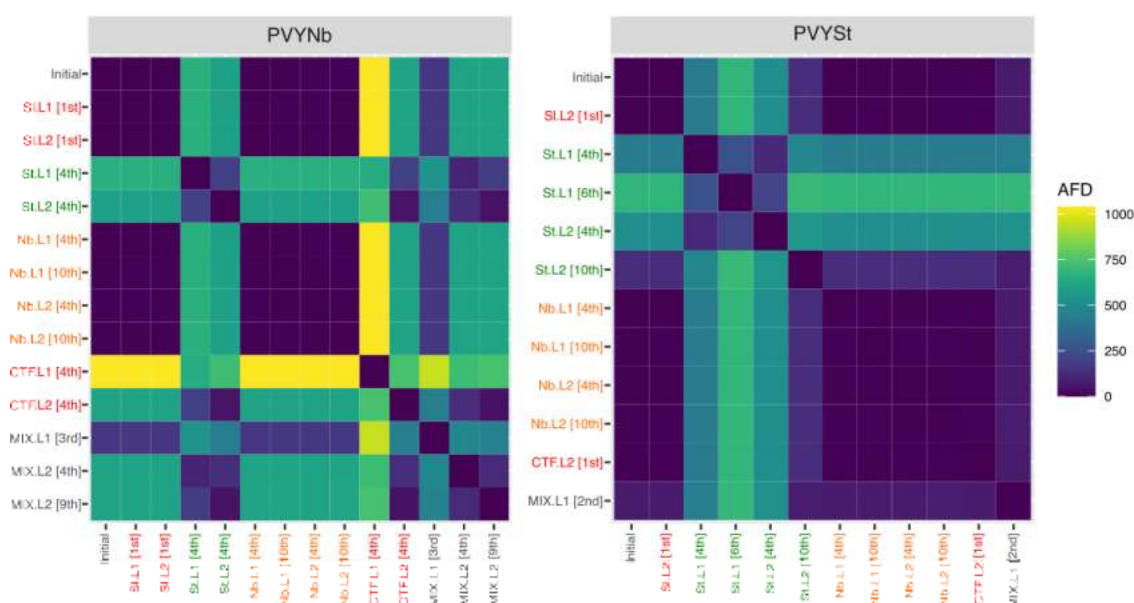
588 We observed clear alterations in virus accumulation, infection rate and symptom
589 induction throughout the passages, and now we were interested in understanding the
590 genome modifications observed in selected time points. Sequencing was based on HTS
591 from the original isolates, then those of the 4th passage and the latest viable passage for
592 all the 20 lines. Firstly, the coverage along the genome differed between samples (Sup.
593 Fig. 3). Five samples did not meet our threshold of 50× average coverage across the
594 genome and were excluded from further analysis due to potential biases. The excluded
595 samples were PVYNb/St.L1 and PVYNb/St.L2 (both 5th passage), PVYNb/CTF.L2 (8th
596 passage), PVYSt/Sl.L1 (4th passage), and PVYSt/Sl.L1 (5th passage). Their low

109

597 coverage could lead to reduced accuracy in variant calling and lower confidence in
598 quantitative analyses, thereby introducing uncertainty.

599 Using the reliable dataset, we calculated genetic differentiation between
600 populations using allele frequency difference (AFD) (Fig. 7). The AFD measures the
601 genetic difference between populations and how these changes are related to viral
602 fitness. In our case, AFD allows to compare both PVY isolates under similar
603 environmental conditions, helping to track if the population is undergoing genetic drift
604 or natural selection.

605



606

607 **Fig 7.** Allele frequency difference (AFD) analysis for genetic differentiation between
608 PVY populations (treatments and lineage of the selected passage) based on sequences
609 generated by Illumina sequencing of total RNA. The colors applied on sample column
610 (y-axis) indicate the plant species: orange for benthamiana, green for potato and red for
611 tomato.

612

613 Although PVYNb can infect a broad range of hosts, its population variation was
614 higher (AFD = 1040) compared to PVYSt (AFD = 701), with PVYNb also exhibiting
615 greater variation between samples (mean AFD \pm 1 SD: 388 \pm 335) than PVYSt (235
616 \pm 255).

617 PVYNb AFD can be divided into three clusters: (i) the first cluster, which
618 includes the initial population, was closely related to tomato populations Si.L1 and
619 Si.L2 at the 1st passage, as well as benthamiana populations Nb.L1 and Nb/L2 at the 4th

620 and 10th passages. For both tomato (Sl) and benthamiana (Nb), L1 and L2 were very
621 closely related, with conserved AFD between passages; (ii) the second cluster
622 comprises potato (St) and mixed lines (MIX), which were closely related and presented
623 fewer differences compared to all samples. An exception was MIX.L1 at the 3rd passage,
624 which was closer to the first cluster; (iii) the third cluster is represented by the CTF
625 alternating line at the 4th passage (tomato), which showed a very distinct pattern, with
626 the highest AFD for L1. Although L2 was similar to St and MIX, L1 presented
627 significant genetic differences, suggesting limited gene flow, potential barriers to gene
628 exchange, or a distinct evolutionary history.

629 In contrast, the PVYSt populations are more closely related but they could be
630 divided into two clusters: (i) the first cluster includes the initial PVYSt, tomato Sl/L2,
631 benthamiana populations Nb.L1 and Nb.L2 (4th to 10th passages), CTF.L2 (1st passage),
632 and mixed population MIX.L1 (2nd passage). Additionally, the potato St.L2 at the 10th
633 passage became much closer to the initial population than at the 4th passage; (ii) the
634 second cluster includes the potato St.L1 at the 4th and 6th passages and St.L2 at the 4th
635 passage. This suggest that the passage through potato plants filter some haplotypes, and
636 that these plants may exert a selective pressure that reduces genetic diversity by filtering
637 some haplotypes. In contrast, this filtering effect was not observed after passage through
638 benthamiana and tomato plants, for which the virus populations tended to maintain
639 greater genetic diversity and remained more closely related to the initial population.

640 The number of SNPs differed between populations, impacting the number of fixed
641 synonymous and non-synonymous SNPs (Table 1). Comparing to the initial population
642 (PVYNb time 0), PVYNb/Sl.L1 and Sl.L2 retained 18% of the SNPs in the 1st passage,
643 while St and MIX lines presented none. SNP percentages in Nb.L1 decreased from 36%
644 at the 4th passage to 9% at the 10th, while Nb.L2 remained stable at 27%. CTF.L1
645 preserved 9% of SNPs. For PVYSt, 5% of SNPs were preserved in Sl.L2 at the 1st
646 passage, while St.L1 retained 22% from the 4th to 6th passage, and St.L2 decreased from
647 22% to 11%. SNP percentages in Nb.L1 decreased from 11% to 5%, and in Nb.L2 from
648 16% to 11% from the 4th to 10th passage. MIX.L1 had 11% at the 2nd passage, and
649 CTF.L2 had zero at the 1st passage. This variability in SNP underscored the dynamic
650 nature of viral evolution, reflecting how specific host environments influenced the
651 genetic stability and adaptation of the virus.

652 The observed differences in the number of fixed SNPs between PVYNb and
653 PVYSt highlighted significant distinctions in the evolutionary dynamics of both PVY
654 isolates (Table 1). PVYNb populations exhibited a generally higher number of fixed
655 SNPs compared to PVYSt, reflecting greater genetic variability and potentially more
656 extensive adaptation within these populations. For example, St.L2 and CTF.L1 and
657 CTF.L2 accumulated substantial numbers of fixed SNPs, with St.L2 reaching 414 fixed
658 SNPs, including a significant proportion of non-synonymous changes. This suggests
659 that PVYNb underwent considerable selective pressures or mutational events,
660 particularly during passages through potato plants.

661 In contrast, PVYSt lines showed lower numbers of fixed SNPs, with several lines,
662 including Sl, Nb and CTF, retaining no fixed SNPs throughout their passages. The
663 minimal accumulation of fixed SNPs in PVYSt might indicate a more stable or
664 conserved genetic profile, potentially due to less intense selective pressures or a more
665 uniform host environment. However, St.L1 displayed a marked increase in fixed SNPs
666 from the 4th to 6th passage, accumulating 192 fixed SNPs, which included a substantial
667 number of synonymous changes. This suggests that while PVYSt generally exhibited
668 less genetic divergence, specific conditions or passages could still drive significant
669 genetic variation.

670 Overall, the greater variability in PVYNb suggests it may be more prone to
671 genetic changes under different selective pressures, potentially allowing it to adapt more
672 rapidly to new hosts or environmental conditions. In contrast, PVYSt relatively stable
673 SNP profile could indicate greater selection pressure in its host environment, leading to
674 the elimination of less adapted variants and consequently a lower genotypic diversity.
675 This suggests that while PVYNb might be more flexible in its evolution, PVYSt
676 evolutionary strategy might be more focused on optimizing fitness within a specific
677 host, leading to a more conserved genetic makeup.

678 Genetic diversity, measured by Shannon Entropy (SH) (Table 1), fluctuated
679 depending on the host and passage. Both initial populations had low SH, which can
680 indicate genetic stability at the initial inoculum. For PVYNb, SH decreased in tomato
681 Sl.L1 and Sl.L2 and benthamiana Nb.L1 and Nb.L2 at the 4th passage but slightly
682 increased at the 10th passage. Other populations showed higher SH compared to the

683 initial population, with St.L1 (4th passage) and MIX.L1 (3rd passage) having the highest
 684 SH.

685

686 **Table 1.** Population genetic analyses of all last positive samples divided by treatment
 687 (T) and lineage (L1 or L2) and passage number.

Sample	Passage	% SNPs*	Fixed SNPs	Synonymous fixed SNPs	Nonosynonymous fixed SNPs	SH (×1000)
PVYNb	0	-	-	-	-	0.363
		0.181				
PVYNb/Sl.L1	1	8	0	0	0	0.116
		0.181				
PVYNb/Sl.L2	1	8	0	0	0	0.116
		0.000				
PVYNb/St.L1	4	0	23	14	9	37.602
		0.000				
PVYNb/St.L2	4	0	414	300	102	1.750
		0.363				
PVYNb/Nb.L1	4	6	0	0	0	0.271
		0.090				
PVYNb/Nb.L1	10	9	0	0	0	0.480
		0.272				
PVYNb/Nb.L2	4	7	0	0	0	0.620
		0.272				
PVYNb/Nb.L2	10	7	0	0	0	1.026
		0.090				
PVYNb/CTF.L1	4	9	382	282	98	5.405
		0.000				
PVYNb/CTF.L2	4	0	233	158	67	2.833
		0.000				
PVYNb/MIX.L 1	3	0	0	0	0	47.110
		0.000				
PVYNb/MIX.L 2	4	0	96	61	35	2.093
		0.000				
PVYNb/MIX.L 2	9	0	24	11	13	5.796

PVYSt	0	-	-	-	-	0.361
		0.055				
PVYSt/T1.L2	1	6	0	0	0	0.063
		0.222				
PVYSt/St.L1	4	2	0	0	0	62.550
		0.222				
PVYSt/St.L1	6	2	192	147	32	3.677
		0.222				
PVYSt/St.L2	4	2	0	0	0	56.470
PVYSt/St.L2	10	0.1111	1	0	0	1.222
PVYSt/Nb.L1	4	0.1111	0	0	0	0.201
		0.055				
PVYSt/Nb.L1	10	6	0	0	0	0.750
		0.166				
PVYSt/Nb.L2	4	7	0	0	0	0.404
PVYSt/Nb.L2	10	0.1111	0	0	0	1.240
		0.000				
PVYSt/CTF.L2	1	0	0	0	0	0.112
PVYSt/MIX.L1	2	0.1111	2	0	0	12.812

*Number of SNPs from the initial PVY that are present in the population

SH = Shannon Entropy

The colors applied on sample column indicate the plant species: orange for benthamiana, green for potato and red for tomato.

688

689 Notable increases in SH observed in PVYNb/St.L1 (0.037) and PVYSt St.L1/L2
690 at the 4th passage might reflect the isolate adaptative response to potato plants, driving
691 the generation of new variants that can better exploit the host environment. Curiously,
692 the SH decreased in later passages in potato plants. The PVYSt/St.L1 at the 6th and
693 St.L2 at the 10th passage showed a reduction in the genetic diversity, potentially
694 indicating fixation of specific mutations, population homogenization or stabilization of
695 the virus within the host environment. In contrast, the SH slightly increased in
696 benthamiana populations from 4th to 10th passages to both isolates. This suggest a slight
697 increase of genetic variability, indicating that over the time, viral populations might be

698 experiencing less bottleneck effects or more balanced selective pressures, allowing a
699 broader range of genetic variants to coexist.

700 Although the number of SNPs in PVYNb CTF.L1/L2 was high, the SH did not
701 necessarily increase proportionally, indicating that these SNPs may be clustered in
702 specific regions of the genome rather than being spread evenly. This suggests that the
703 observed genetic changes might be concentrated in particular genomic areas, which can
704 influence measures of genetic diversity differently than simply counting SNPs.

705 In summary, comparing PVYNb with PVYSt, based on the AFD analysis, the
706 results suggest that the PVYNb population may be more diverse and more specialized to
707 certain hosts, whereas PVYSt appears more versatile and generalist. Host species seems
708 to influence the evolutionary process, with a lower need to fix SNPs when infecting
709 benthamiana, a permissive host. However, adaptation is required when transitioning to a
710 different host environment. When infecting the same host, the virus tends to reduce the
711 number of fixed SNPs. The exception was PVYSt/St.L1 from the 4th to 6th passage, from
712 which the number of SNPs increased. Both synonymous and non-synonymous SNPs
713 were present, with synonymous SNPs being more frequent. A host species change
714 appeared to create a bottleneck effect, which is dependent on the PVY isolate. PVYSt,
715 being more versatile, experiences high gene flow and low selective pressure,
716 maintaining higher genetic diversity with fewer fixed SNPs. Conversely, populations
717 struggling to adapt to new host environments tend to have a higher number of SNPs.

718 As a final step, a ML-tree was constructed using all consensus genomes, as
719 depicted in Sup. Fig 4. Notably, sequences that were previously excluded due to not
720 meeting the 50× average coverage threshold were included in this analysis. Despite the
721 lower coverage, the consensus sequences still reflect the dominant viral population,
722 allowing us to construct a phylogeny that may help understanding the relationships
723 among the PVY populations. The tree shows well-structured group formations with
724 highly intriguing clades. PVYNb and PVYSt isolates tended to cluster with isolates
725 derived from the same initial virus. Additionally, the host played a significant role in
726 shaping the phylogenetic structure, as seen in benthamiana isolates from both viruses,
727 which showed to be closely related to the initial population and to each other. Indeed,
728 the initial PVYNb clustered with all the benthamiana treatments (Nb.L1/L2 4th and 10th
729 passage) and tomato isolates in the first generation, a pattern also observed for PVYSt.

730 This demonstrated multiple passages in a permissive host like benthamiana, and also in
731 tomato, the most non-permissive host, produced similar effects. It may explain why
732 tomato plants in general behaved as the dead-end host of PVYNb and PVYSt, since
733 these isolates were not adapted to tomato plants, and new variants were not easily
734 produced.

735 Another notable aspect is the tendency of potato isolates to remain grouped
736 together, often forming a distinct clade separate from other isolates. This observation
737 highlights the potato as a host that can rapidly induce and fix genome alterations within
738 a shorter time frame. These alterations result in isolates that cluster differently from the
739 initial population. For example, while PVYSt St.L2 in the 4th passage appears
740 significantly distinct from the original population, by the 10th generation, this
741 difference diminishes. This shift underscores the strong bottleneck effects during
742 passage in the potato host, where isolates with new genomic characteristics can emerge.
743 This clustering pattern reflects the influence of the host and passage number on the
744 phylogenetic relationships among virus populations, particularly given the high number
745 of SNPs observed, many of which were fixed during the passage experiment.

746

747

748 Discussion

749 Understanding the ecology, evolution, and population biology of viruses, their hosts and
750 vectors, and the communities they inhabit is fundamental for thoroughly analyzing the
751 conditions for disease emergence in new plant hosts (Morse 1995; Jones 2009; Lefevre
752 et al. 2019). Emerging plant viruses, such as tomato torrado virus, tomato brown rugose
753 fruit virus, cassava brown streak virus, rice stripe virus or cucumber green mottle
754 mosaic virus, have caused significant damage over the past decades. The growing
755 impact of these viruses on agricultural crops and wild plant populations underscores the
756 urgent need to comprehend the ecological dynamics behind plant viral emergence
757 (Jones 2009; Lefevre et al. 2019).

758 Viral emergence often occurs in multiple stages. Initially, virus fitness is typically
759 lower on a new host compared to an original host due to the lack of adaptation. The
760 virus must establish and maintain a population in the new host and then further
761 dissemination (Morse 1995). To study the early phase of a plant viral emergence, we

762 have used PVY as a model, in its native host, potato, and included two new hosts,
763 tomato and benthamiana. Our research focused on how PVY establishes persistent
764 populations on these hosts.

765 The implications of source-sink dynamics for viral emergence depend on a
766 pathogen's pattern of exposure to a given host. Broadly, a pathogen may encounter a
767 novel host in two ways: homogeneously or heterogeneously. In the homogeneous case, a
768 pathogen population initially contacts the novel host and is then isolated from the
769 original host. If the novel host is of low quality, leading to the pathogen's absolute
770 fitness being well below one, the pathogen is likely to go extinct before it can adapt
771 (Holt and Gaines 1992; Gomulkiewicz and Holt 1995; Morse 1995; Antia et al. 2003).
772 In the heterogeneous case, the pathogen intermittently encounters both hosts across
773 different times or locations. This heterogeneous exposure can be coarse-grained or
774 fine-grained in space, time, or both, and may facilitate initial persistence on the novel
775 host. Our study examined various situations, including an extreme case of
776 coarse-grained temporal heterogeneity, where the virus alternated between host
777 environments with each passage, mimicking 100% dispersal between source and sink.
778 This scenario is akin to a pathogen facing seasonal or annual host availability changes,
779 like an agricultural pest infecting rotated crops. We hypothesized that intermittent
780 exposure to the original host could act as a "rescue" mechanism for emerging PVY
781 populations on novel hosts, potentially enhancing their chances of adaptation and
782 persistence. This could provide insights into how viruses might exploit familiar host
783 environments to overcome challenges in new hosts, offering information for predicting
784 and managing viral outbreaks in agricultural settings. Understanding these dynamics is
785 crucial for developing strategies to mitigate the impact of emerging plant viruses. Future
786 research will explore other heterogeneous host use patterns, such as spatiotemporal
787 variations in a metacommunity or fine-grained variation in well-mixed host
788 communities.

789 The persistence of the virus with alternating host exposure suggests that a
790 temporally heterogeneous host regime might provide emerging viruses time to adapt to
791 novel hosts, facilitating this shift by affecting viral population size. However, whether
792 this leads to host expansion or a host shift remains to be seen. The extensive literature
793 on evolution in heterogeneous environments will not be covered in depth here, as our

794 focus is on the initial ecological challenges before adaptation. It is noteworthy that
795 pathogens may persist on novel hosts despite low fitness, allowing new genes and gene
796 combinations to arise through mutation and recombination. The success of new genes or
797 combinations depends on their effects (Kawecki 2000). Holt and Gomulkiewicz (1997)
798 suggested adaptation in a sink require a mutant capable of persisting on the novel host
799 without immigration from the original host. This stringent “absolute fitness criterion” is
800 rarely met when transmission is low and the novel host is a strong sink (*i.e.*,
801 PVYSt/CTF.L1 and L2 from the 4th to 5th passage). However, this assumes a negative
802 correlation of mutant fitness on the two hosts and unidirectional immigrant flow. Our
803 research shows that alternating host exposure can select for mutations enhancing PVY
804 growth on both hosts, as evidenced in PVYNb/CTF Lines. Positive correlations in
805 selection responses increase emergence likelihood (Gandon 2004), and bidirectional
806 transmission may enhance adaptation probability to the novel host (Kawecki and Holt
807 2002).

808 The primary aim of emerging disease research is to pinpoint the crucial ecological
809 factors that drive the emergence of new plant viral diseases. By identifying these
810 factors, we can improve our ability to predict which host populations are at greatest risk
811 of future infections by emerging plant viruses (Lefeuvre et al. 2019). Our research has
812 demonstrated that the persistence of a virus in a homogeneous environment can be
813 predicted based on its growth and transmission rates. However, these metrics are less
814 effective for predicting outcomes in more complex host exposure scenarios, which are
815 more representative of real-world emergence events.

816 Plant virus populations are genetically heterogeneous, meaning each combination
817 of host and virus is unique. The genetic diversity in RNA virus populations is governed
818 by interactions between host and viral factors (Schneider and Roossinck 2001), and the
819 population structure of plant viruses varies across different hosts (Huang et al. 2015). In
820 our study, we found that benthamiana is a permissive host for PVY, while tomato acts as
821 a sink for the PVY population. But it is important to highlight the source of the virus,
822 while PVYSt was collected in potato field, PVYNb was maintained in laboratory in
823 benthamiana.

824 Our results suggest that PVYNb is a more dynamic virus in terms of its ability to
825 adapt to different host environments, likely due to its higher genetic variability. This

826 could make PVYNb more versatile but also potentially more prone to developing
827 virulence or resistance to host defenses. In contrast, PVYSt, while generally more
828 stable, can still exhibit significant diversity under certain conditions. This stability
829 might make it less likely to evolve quickly, which could be advantageous in a consistent
830 environment but might limit its adaptability to new or changing conditions. These
831 results may indicate that in more restrictive hosts, such as potato, viral populations
832 evolve more slowly, in contrast to that has observed for strain YC5 of *Potyvirus rapae*
833 in *Arabidopsis thaliana* (Navarro et al. 2022). The bottleneck effect during host change
834 was more pronounced in the PVYNb population, indicating that PVYNb has adapted
835 more specifically to hosts, such as benthamiana, potentially limiting its adaptability to
836 other host environments. When transmitted to different plant species, the ratio of
837 synonymous to non-synonymous substitutions tends to increase, indicating that both
838 types of substitutions are crucial for virus-host interactions (Huang et al. 2015). This
839 increase in the ratio of synonymous to non-synonymous substitutions was more
840 pronounced in the PVYNb population, highlighting its greater specialization to specific
841 hosts. This suggests that PVYNb evolution involves more precise adaptation to host
842 interactions. In response to virus replication and movement, the host can activate
843 various defense mechanisms, such as innate immunity, autophagy, and gene silencing.
844 Permissive hosts provide essential components needed for the virus to replicate within
845 the cell (Kushner et al. 2003; Panavas et al. 2005) and in the absence of these factors,
846 virus accumulation can reduce due the deficiency in replication or movement. The SNPs
847 decrease in later lines, i.e. PVYNb/Nb.L1 and L2, can represent an adaptation of the
848 population to the host environment. On the other hand, populations with high genetic
849 diversity can activate plants defense factors that can repress the virus, i.e.,
850 PVYNb/CTF.L1 that was unavailable to infect the next generation.

851 As mentioned, tomato acted as a sink crop in our experiment, but this does not
852 imply that tomato cannot be infected by PVY. Recent outbreaks of PVY in tomato crops
853 in Brazil demonstrate that this virus remains present and capable of causing agronomic
854 damage (Lucena et al. 2024). It is important to acknowledge that our study did not
855 include PVY isolates obtained from tomato crops, and different isolates might exhibit
856 varying behavior when infecting tomato plants. Specifically, isolates adapted to
857 tomatoes might show different infectivity patterns compared to those from other

858 sources. Additionally, the host from which the virus was originally isolated plays a
859 crucial role in determining the virus's behavior and adaptability. Future research using a
860 broader range of isolates, including those adapted to different hosts, will be essential to
861 fully understand the variability in virus-host interactions. Our findings highlight that
862 PVYNb and PVYSt exhibit distinct transmission dynamics across different hosts, and
863 the emergence of different viral populations, as observed through allele frequency
864 differences in potato treatments St.L1 and L2, further supports this variability. This is
865 consistent with previous studies showing that different PVY isolates can lead to diverse
866 responses in various hosts, including the ability to complete the replicative cycle in
867 resistant cultivars (Morais et al. 2024).

868 In conclusion, our study underscores the complexity and variability of plant virus
869 emergence and adaptation across different hosts. By examining the behavior of PVY in
870 different host species, we revealed critical insights into the dynamics of viral persistence
871 and genetic differentiation. The observed specialization of PVYNb in specific host
872 environments and the relatively stable genetic diversity of PVYSt across different hosts
873 underscore how host conditions can significantly influence viral evolution. These
874 findings illustrate that the host environment plays a crucial role in shaping the genetic
875 and adaptive responses of plant viruses. The implications of source-sink dynamics,
876 particularly in heterogeneous host exposure scenarios, suggest that viruses can persist
877 and adapt to novel hosts through intermittent exposure to native hosts, potentially
878 facilitating host expansion or shifts. These findings contribute to a broader
879 understanding of the ecological and evolutionary factors driving the emergence of new
880 plant viral diseases. Future research should focus on diverse host exposure patterns and
881 their effects on viral adaptation, ultimately aiming to predict and mitigate the risks of
882 emerging plant viruses in agricultural and wild populations. Understanding these
883 dynamics is crucial for developing effective strategies to manage and prevent viral
884 epidemics, ensuring the stability and productivity of global agriculture.

885 It is important to note that the experimental approach was focused on the
886 detection of the early stages of interaction of virus and the host. A prolonged incubation
887 time would produce additional factors leading to complex interpretations. On the other
888 hand, it could also enable a buildup of fitter virus populations. This issue must be
889 addressed in future studies.

890 One of the questions we wanted to answer was whether PVY evolved in a specific
891 host could easily adapt to a closely related but distinct host, such as potato and tomato.
892 Our findings indicate that PVY exhibits distinct evolutionary patterns depending on the
893 host, with PVYNb adapting more rapidly and showing higher genetic diversity, while
894 PVYSt demonstrated greater stability, underscoring the complex interplay between host
895 environments and viral evolution.

896 References

897

898 Agudelo-Romero P, de la Iglesia F, Elena SF (2008) The pleiotropic cost of
899 host-specialization in Tobacco etch potyvirus. *Infection, Genetics and Evolution*
900 8:806–814. <https://doi.org/10.1016/j.meegid.2008.07.010>

901

902 Antia R, Regoes RR, Koella JC, Bergstrom CT (2003) The role of evolution in the
903 emergence of infectious diseases. *Nature* 426:658–661.
904 <https://doi.org/10.1038/nature02104>

905

906 Bedhomme S, Lafforgue G, Elena SF (2012) Multihost experimental evolution of a
907 plant RNA virus reveals local adaptation and host-specific mutations. *Molecular*
908 *Biology and Evolution* 29:1481–1492. <https://doi.org/10.1093/molbev/msr314>

909

910 Belshaw R, Pybus OG, Rambaut A (2007) The evolution of genome compression and
911 genomic novelty in RNA viruses. *Genome Research* 17:1496–1504.
912 <https://doi.org/10.1101/gr.6305707>

913

914 Berner D (2019) Allele Frequency Difference AFD: an intuitive alternative to F_{ST} for
915 quantifying genetic population differentiation. *Genes (Basel)* 10:308.
916 <https://doi.org/10.3390/genes10040308>

917

918 Buchfink B, Xie C, Huson DH (2015) Fast and sensitive protein alignment using
919 DIAMOND. *Nature Methods* 12:59–60. <https://doi.org/10.1038/nmeth.3176>

920

921 de la Iglesia F, Martínez F, Hillung J, et al (2012) Luria-delbrück estimation of turnip
922 mosaic virus mutation rate *in vivo*. *Journal of Virology* 86:3386–3388.
923 <https://doi.org/10.1128/JVI.06909-11>

924

925 Dennehy JJ, FriedenberG NA, Holt RD, Turner PE (2006) Viral ecology and the
926 maintenance of novel host use. *The American Naturalist* 167:429–439.
927 <https://doi.org/10.1086/499381>

928

929 Dennehy JJ, FriedenberG NA, Yang YW, Turner PE (2007) Virus population extinction
930 via ecological traps. *Ecology Letters* 10:230–240.
931 <https://doi.org/10.1111/j.1461-0248.2006.01013.x>

932

933 Domingo E, Sheldon J, Perales C (2012) Viral quasispecies evolution. *Microbiology
934 and Molecular Biology Reviews* 76:159–216. <https://doi.org/10.1128/MMBR.05023-11>

935

936 Edwardson JR, Christie RG (1997) Viruses infecting peppers and other solanaceous
937 crops. Agricultural Experiment Station, University of Florida, Gainesville.

938

939 Elena SF (2017) Local adaptation of plant viruses: lessons from experimental evolution.
940 *Molecular Ecology* 26:1711–1719. <https://doi.org/10.1111/mec.13836>

941

942 Elena SF, Agudelo-Romero P, Lalic J (2009) The evolution of viruses in multi-host
943 fitness landscapes. *The Open Virol Journal* 3:1–6.
944 <https://doi.org/10.2174/1874357900903010001>

945

946 Flatschacher D, Speckbacher V, Zeilinger S (2022) qRAT: an R-based stand-alone
947 application for relative expression analysis of RT-qPCR data. *BMC Bioinformatics*
948 23:286. <https://doi.org/10.1186/s12859-022-04823-7>

949

950 Gandon S (2004) Evolution of multihost parasites. *Evolution (NY)* 58:455–469.

951

952 Gandon S, Hochberg ME, Holt RD, Day T (2013) What limits the evolutionary
953 emergence of pathogens? *Philosophical Transactions of the Royal Society B: Biological
954 Sciences* 368:20120086. <https://doi.org/10.1098/rstb.2012.0086>

955

956 Gomulkiewicz R, Holt RD (1995) When does Evolution by Natural Selection Prevent
957 Extinction? *Evolution (NY)* 49:201. <https://doi.org/10.2307/2410305>

958

959 Hillung J, Cuevas JM, Valverde S, Elena SF (2014) experimental evolution of an
960 emerging plant virus in host genotypes that differ in their susceptibility to infection.
961 *Evolution* 68:2467–2480. <https://doi.org/10.1111/evo.12458>
962

963 Holt RD, Gaines MS (1992) Analysis of adaptation in heterogeneous landscapes:
964 implications for the evolution of fundamental niches. *Evolutionary Ecology* 6:433–447.
965 <https://doi.org/10.1007/bf02270702>
966

967 Holt RD, Gomulkiewicz R (1997) How does immigration influence local adaptation? A
968 Reexamination of a Familiar Paradigm. *The American Naturalist* 149:563–572.
969

970 Huang L, Li Z, Wu J, et al (2015) Analysis of genetic variation and diversity of rice
971 stripe virus populations through high-throughput sequencing. *Frontiers in Plant Science*
972 6. <https://doi.org/10.3389/fpls.2015.00176>
973

974 Inoue-Nagata AK, Jordan R, Kreuze J, et al (2022) ICTV Virus Taxonomy Profile:
975 Potyviridae 2022. *Journal of General Virology* 103:001738.
976 <https://doi.org/10.1099/jgv.0.001738>
977

978 Jeffries CJ (1998) FAO/IPGRI Technical guidelines for the safe movement of potato
979 germplasm. Food and Agriculture Organization of the United Nations,
980 Rome/International Plant Genetic Resources Institute, Rome, Italy 19.
981

982 Jones RAC (2009) Plant virus emergence and evolution: Origins, new encounter
983 scenarios, factors driving emergence, effects of changing world conditions, and
984 prospects for control. *Virus Research* 141:113–130.
985 <https://doi.org/10.1016/j.virusres.2008.07.028>
986

987 Kawecki TJ (2000) Adaptation to marginal habitats: contrasting influence of the
988 dispersal rate on the fate of alleles with small and large effects. *Proceedings of the*
989 *Royal Society of London B Biology Science* 267:1315–1320.
990 <https://doi.org/10.1098/rspb.2000.1144>

991

992 Kawecki TJ, Holt RD (2002) Evolutionary Consequences of Asymmetric Dispersal
993 Rates. *The American Naturalist* 160:333–347. <https://doi.org/10.1086/341519>

994

995 Kerlan C, Moury B, Granoff A, Webster RG (2008) *Encyclopedia of virology*.
996 Association of Applied Biologists 287–296.

997

998 Kushner DB, Lindenbach BD, Grdzlishvili VZ, et al (2003) Systematic, genome-wide
999 identification of host genes affecting replication of a positive-strand RNA virus.
1000 *Proceedings of the National Academy of Sciences* 100:15764–15769.
1001 <https://doi.org/10.1073/pnas.2536857100>

1002

1003 Lefeuvre P, Martin DP, Elena SF, et al (2019) Evolution and ecology of plant viruses.
1004 *Nature Reviews Microbiology* 17:632–644. <https://doi.org/10.1038/s41579-019-0232-3>

1005

1006 Li D, Liu C-M, Luo R, et al (2015) MEGAHIT: an ultra-fast single-node solution for
1007 large and complex metagenomics assembly via succinct de Bruijn graph. *Bioinformatics*
1008 31:1674–1676. <https://doi.org/10.1093/bioinformatics/btv033>

1009

1010 Lucena VS, Nakasu EYT, Pereira JL, et al (2024) Emergence of potato virus Y
1011 outbreaks in tomatoes in Brazil, the disease and spread. *bioRxiv*. <https://doi.org/10.1101/2024.05.17.594728>

1013

1014 MARTIN W, CERFF R (1986) Prokaryotic features of a nucleus-encoded enzyme.
1015 cDNA sequences for chloroplast and cytosolic glyceraldehyde-3-phosphate
1016 dehydrogenases from mustard (*Sinapis alba*). *European Journal of Biochemistry*
1017 159:323–331. <https://doi.org/10.1111/j.1432-1033.1986.tb09871.x>

1018

1019 Minh BQ, Schmidt HA, Chernomor O, et al (2020) IQ-TREE 2: New Models and
1020 Efficient Methods for Phylogenetic Inference in the Genomic Era. *Molecular Biology*
1021 and Evolution 37:1530–1534. <https://doi.org/10.1093/molbev/msaa015>

1022

1023 Morais IJ, Silva DYM, Camargo BM, et al (2024) Unraveling the dynamics of host
1024 specificity and resistance responses to potato virus Y, and implications for crop
1025 management. bioRxiv.

1026

1027 Morse SS (1995) Factors in the Emergence of Infectious Diseases. *Emerging Infectious*
1028 *Diseases* 1:7–15. <https://doi.org/10.3201/eid0101.950102>

1029

1030 Navarro R, Ambrós S, Butković A, et al (2022) Defects in plant immunity modulate the
1031 rates and patterns of RNA virus evolution. *Virus Evolution* 8.
1032 <https://doi.org/10.1093/ve/veac059>

1033

1034 Panavas T, Serviene E, Brasher J, Nagy PD (2005) Yeast genome-wide screen reveals
1035 dissimilar sets of host genes affecting replication of RNA viruses. *Proceedings of the*
1036 *National Academy of Sciences* 102:7326–7331.
1037 <https://doi.org/10.1073/pnas.0502604102>

1038

1039 Peláez A, McLeish MJ, Paswan RR, et al (2021) Ecological fitting is the forerunner to
1040 diversification in a plant virus with broad host range. *Journal of Evolutionary Biology*
1041 34:1917–1931. <https://doi.org/10.1111/jeb.13672>

1042

1043 Ruark-Seward CL, Bonville B, Kennedy G, Rasmussen DA (2020) Evolutionary
1044 dynamics of Tomato spotted wilt virus within and between alternate plant hosts and
1045 thrips. *Scientific Reports* 10:. <https://doi.org/10.1038/s41598-020-72691-3>

1046

1047 Sanjuán R, Agudelo-Romero P, Elena SF (2009) Upper-limit mutation rate estimation
1048 for a plant RNA virus. *Biology Letters* 5:394–396.
1049 <https://doi.org/10.1098/rsbl.2008.0762>

1050

1051 Schmittgen TD, Livak KJ (2008) Analyzing real-time PCR data by the comparative CT
1052 method. *Nature Protocols* 3:1101–1108. <https://doi.org/10.1038/nprot.2008.73>

1053

1054 Schneider WL, Roossinck MJ (2001) Genetic diversity in RNA virus quasispecies is
1055 controlled by host-virus interactions. *Journal of Virology* 75:6566–6571.
1056 <https://doi.org/10.1128/JVI.75.14.6566-6571.2001>

1057

1058 Scholthof KBG, Adkins S, Czosnek H, et al (2011) Top 10 plant viruses in molecular
1059 plant pathology. *Molecular Plant Pathology* 12:938–954. [https://doi.org/](https://doi.org/10.1111/j.1364-3703.2011.00752.x)
1060 [10.1111/j.1364-3703.2011.00752.x](https://doi.org/10.1111/j.1364-3703.2011.00752.x)

1061

1062 Shukla DD, Ward CW, Brunt AA (1994) *The Potyviridae*. Cambridge: CAB
1063 International.

1064

1065 Van der Auwera GA, O'Connor BD (2020) *Genomics in the Cloud: using Docker,*
1066 *GATK, and WDL in Terra*. O'Reilly Media, Inc.

1067

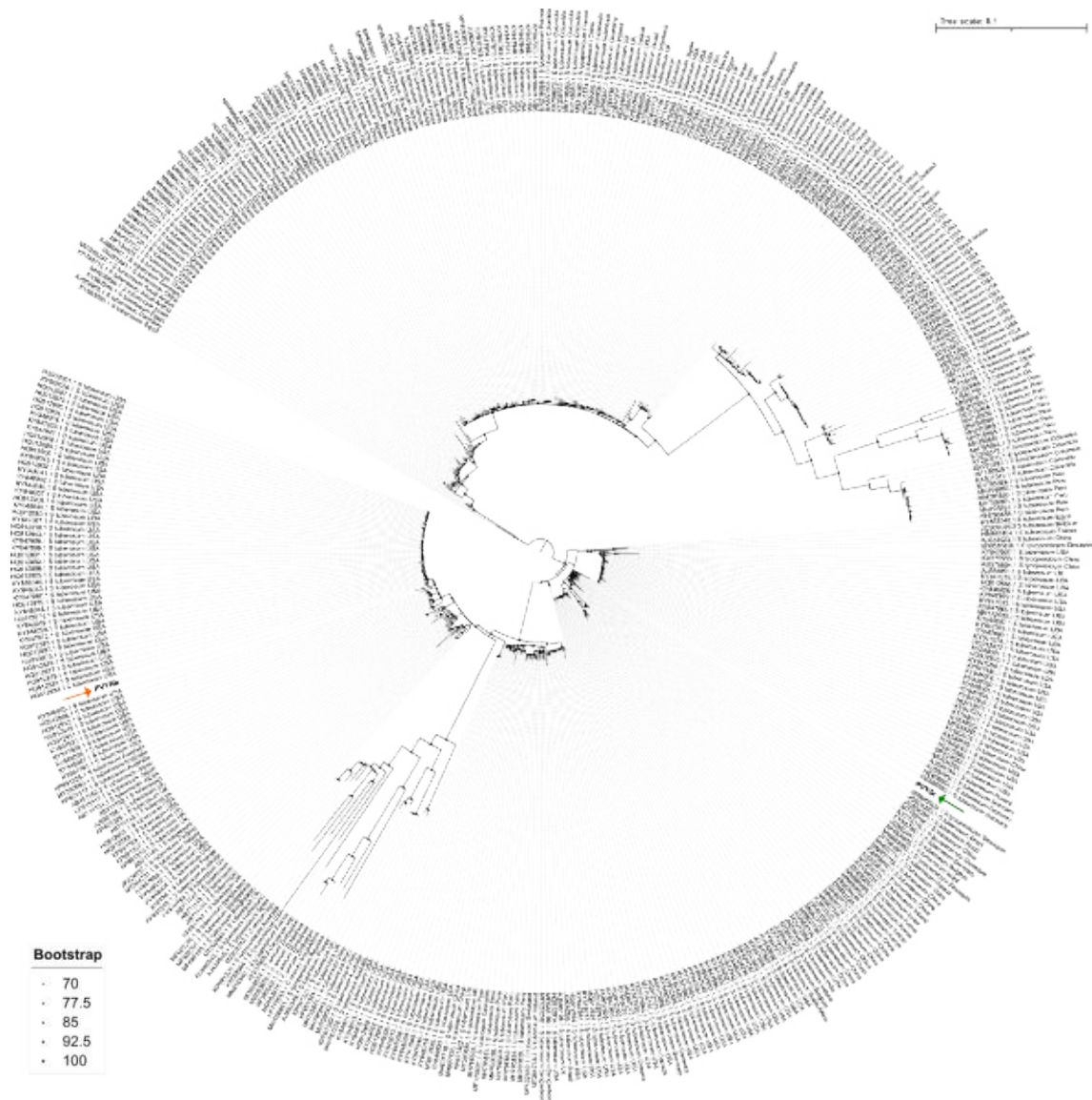
1068 Wallis CM, Stone AL, Sherman DJ, et al (2007) Adaptation of plum pox virus to a
1069 herbaceous host (*Pisum sativum*) following serial passages. *Journal of General Virology*
1070 88:2839–2845. <https://doi.org/10.1099/vir.0.82814-0>

1071

1072 Whitlock MC (1996b) The Red Queen beats the jack-of-all-trades: the limitations on the
1073 evolution of phenotypic plasticity and niche breadth. *The American Naturalist*
1074 148:S65–S77. <https://doi.org/10.1086/285902>

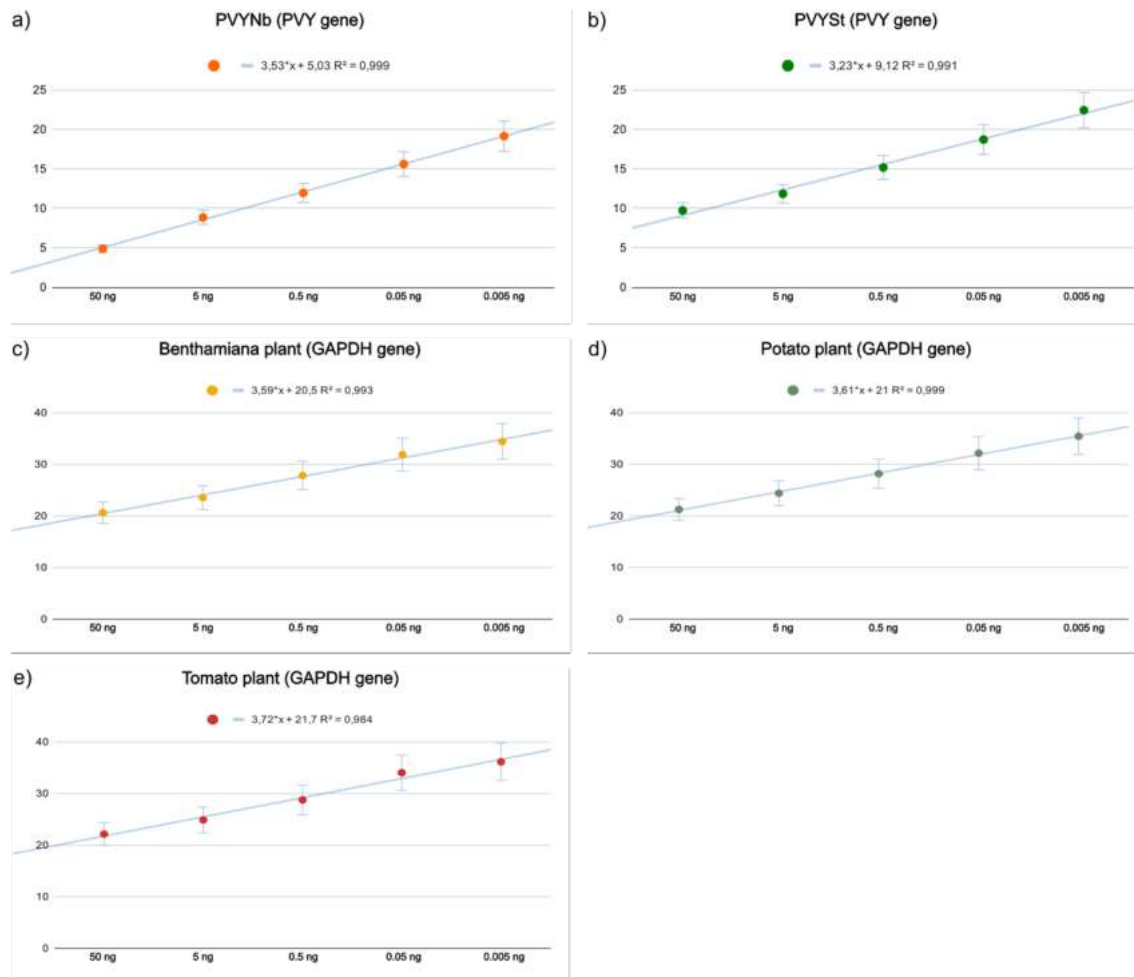
1075

1076 Woolhouse MEJ, Gowtage-Sequeria S (2005) Host range and emerging and reemerging
1077 pathogens. *Emerging Infectious Diseases* 11:1842–1847.
1078 <https://doi.org/10.3201/eid1112.050997>



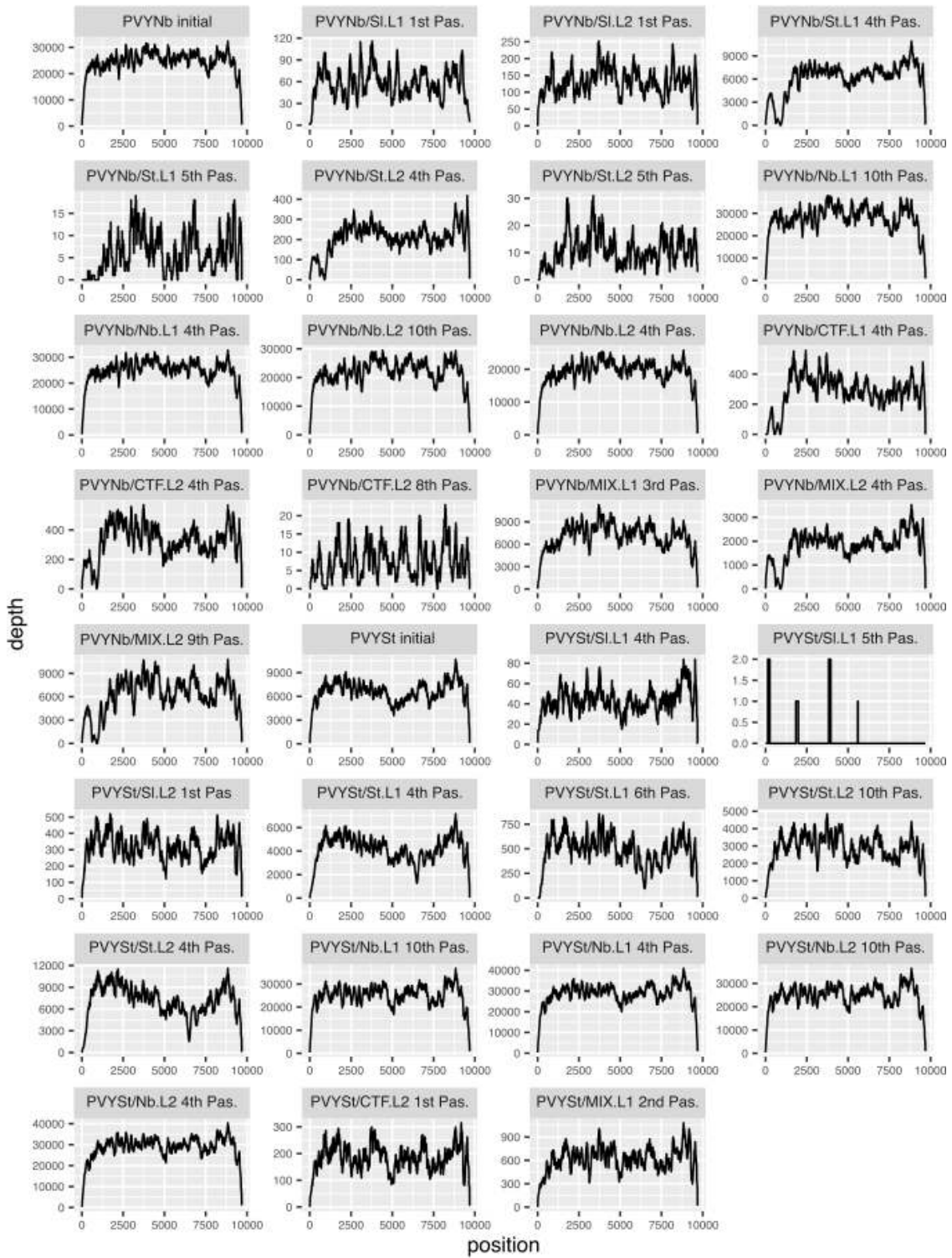
1079

1080 **Sup Fig 1.** ML-tree constructed by iqtree2 using 447 PVY isolates retrieved from
 1081 GenBank together with PVYNb and PVYSt consensus sequence with 10,000 bootstrap
 1082 replications. An arrow indicates the PVYNb (orange) and PVYSt (green) isolates.



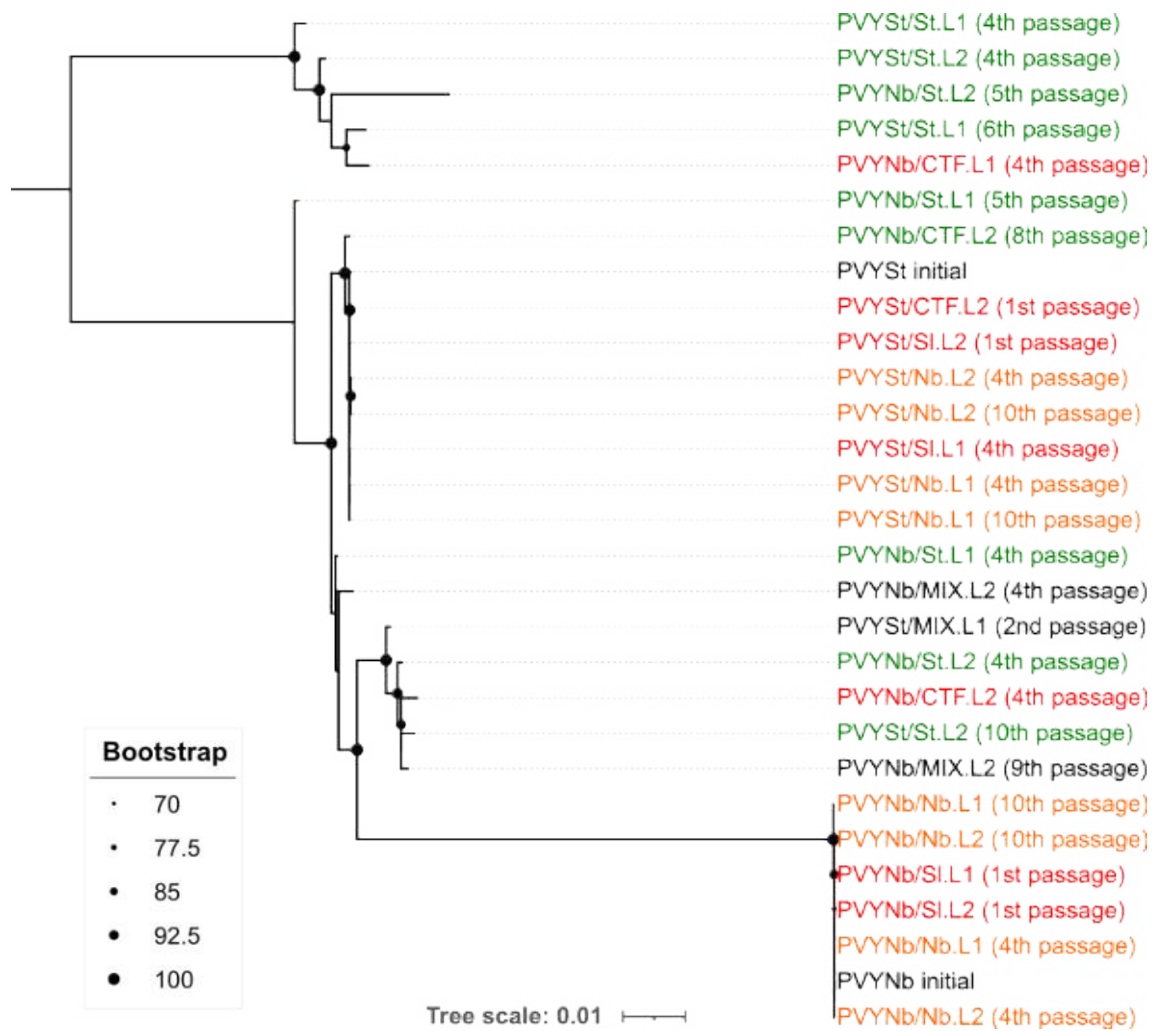
1083

1084 **Sup Fig 2.** Efficiency of qPCR primers targeting PVYNb (a) and PVYSt (b) and
 1085 GAPDH to benthamiana (c), potato (d) and tomato (e) plants. The regression equation
 1086 and the R^2 are shown above the curve. The Eff was calculated using five dilutions
 1087 ranging from 50 to 0.005 ng of initial RNA. The optimal qRT-PCR conditions were
 1088 previously defined.



1089

1090 **Sup Fig 3.** Reads coverage along the genome. Sequencing was performed from total
 1091 RNA in the Illumina platform.



1092

1093 **Sup Fig 4.** ML-tree constructed by iqtree2 using all Illumina consensus genomes with
 1094 10,000 bootstrap replications. The colors applied on sample labels indicate the plant
 1095 species: orange for benthamiana, green for potato and red for tomato. The initial PVY
 1096 sources and the mixed MIX treatment are shown in black.

1097 **Sup Table 1.** Final inoculation results of the passage experiment, in which the last
 1098 positive sample of each line was used to inoculate ten plants of each species followed
 1099 by individual PVY detection by RT-PCR.

Virus	Line	Passage	Host	Total # of plants	Infected plants
PVYNb	Sl.L1	1	Benthamiana	10	0
PVYNb	Sl.L1	1	Potato	10	0
PVYNb	Sl.L1	1	Tomato	10	0
PVYNb	Sl.L2	1	Benthamiana	10	1
PVYNb	Sl.L2	1	Potato	10	0
PVYNb	Sl.L2	1	Tomato	10	0
PVYNb	St.L1	5	Benthamiana	10	0
PVYNb	St.L1	5	Potato	10	0
PVYNb	St.L1	5	Tomato	10	0
PVYNb	St.L2	5	Benthamiana	10	8
PVYNb	St.L2	5	Potato	10	2
PVYNb	St.L2	5	Tomato	10	9
PVYNb	Nb.L1	10	Benthamiana	10	8
PVYNb	Nb.L1	10	Potato	10	0
PVYNb	Nb.L1	10	Tomato	10	10
PVYNb	Nb.L2	10	Benthamiana	10	10
PVYNb	Nb.L2	10	Potato	10	1
PVYNb	Nb.L2	10	Tomato	10	10
PVYNb	CTF.L1	4	Benthamiana	10	0
PVYNb	CTF.L1	4	Potato	10	3

PVYNb	CTF.L1	4	Tomato	10	5
PVYNb	CTF.L2	8	Benthamiana	10	0
PVYNb	CTF.L2	8	Potato	10	0
PVYNb	CTF.L2	8	Tomato	10	0
PVYNb	MIX.L1	3	Benthamiana	10	9
PVYNb	MIX.L1	3	Potato	10	0
PVYNb	MIX.L1	3	Tomato	10	8
PVYNb	MIX.L2	9	Benthamiana	10	0
PVYNb	MIX.L2	9	Potato	10	0
PVYNb	MIX.L2	9	Tomato	10	0
PVYSt	Sl.L1	5	Benthamiana	10	0
PVYSt	SL.L1	5	Potato	10	0
PVYSt	Sl.L1	5	Tomato	10	0
PVYNb	Sl.L2	1	Benthamiana	10	2
PVYSt	Sl.L2	1	Potato	10	0
PVYSt	Sl.L2	1	Tomato	10	8
PVYSt	St.L1	6	Benthamiana	10	0
PVYNb	St.L1	6	Potato	10	2
PVYSt	St.L1	6	Tomato	10	4
PVYSt	St.L2	10	Benthamiana	10	0
PVYSt	St.L2	10	Potato	10	1
PVYNb	St.L2	10	Tomato	10	0
PVYSt	Nb.L1	10	Benthamiana	10	9

PVYSt	Nb.L1	10	Potato	10	1
PVYSt	Nb.L1	10	Tomato	10	10
PVYSt	Nb.L2	10	Benthamiana	10	10
PVYSt	Nb.L2	10	Potato	10	2
PVYSt	Nb.L2	10	Tomato	10	10
PVYSt	CTF.L2	1	Benthamiana	10	0
PVYNb	CTF.L2	1	Potato	10	2
PVYSt	CTF.L2	1	Tomato	10	2
PVYSt	MIX.L1	2	Benthamiana	10	1
PVYSt	MIX.L1	2	Potato	10	0
PVYNb	MIX.L1	2	Tomato	10	1

1100 PVYNb treatments are shown in orange and PVYSt in green.

1

2

3 ***In silico* evidences for the presence of defective viral genomes (DVGs)**

4 **in potato virus Y-infected plants**

5

6

7 **Abstract**

8 Defective viral genomes (DVGs) are frequently found in RNA virus populations due to
9 the error-prone nature of the viral replicases, in addition to other factors. DVGs are
10 generated during the replication of the wild-type (WT) viral genome because the
11 replicase detaches from the template it is copying and, in some cases, reattaches to a
12 different region of the genome. DVGs can be classified into six types: 3' copy-back (cb)
13 or snap-back (sb), 5' cb/sb, deletion forward, deletion reverse, insertion forward, and
14 insertion reverse. To date, no DVGs have been described for members of the
15 *Potyviridae* family. This study investigates the diversity and dynamics of DVGs
16 generation in potato virus Y (species *Potyvirus yituberosi*) populations. Two datasets
17 were analyzed: the first involving PVY strains (N, O and N-Wi) in potato plants,
18 passage modes, types of transmission, and plant organ, and the second involving
19 PVYNb (isolated from benthamiana) and PVYSt (isolated from potato) in different host
20 plants. High-throughput sequencing data were analyzed to detect and categorize DVGs,
21 using DVGFinder and custom filtering approaches. Principal Component Analysis
22 (PCA) was employed to investigate clustering patterns of DVG types across samples.
23 Furthermore, we explored the diversity of DVG formation and calculated population
24 diversity using Shannon Entropy (SH). DVGs were consistently detected across all
25 PVY samples, with strain-specific variations. Strain O exhibited the highest number of
26 unique DVGs, while strains N and N-Wi showed lower but notable counts. DVG
27 populations varied significantly by transmission mode and host plant. Indeed, potato
28 tubers harbored more unique DVGs than leaves. The second dataset revealed
29 host-specific DVG profiles, with benthamiana showing high DVG diversity, while
30 tomato and potato plants demonstrated more restrictive environments. PCA highlighted
31 distinct clustering patterns of DVG types, but very consistent with all populations. SH

32 analysis revealed that forward deletion and insertion DVGs exhibit high conservation
33 across PVY strains, while reverse deletion DVGs show greater variability. Also,
34 deletion-type DVGs are the most diverse when different hosts were examined with
35 benthamiana populations demonstrating the highest overall DVG diversity. These
36 findings underscore the complex interplay between viral strain, transmission mode,
37 passage and host plant in shaping DVG diversity and distribution. The results suggest
38 that host species play a critical role in DVG formation and evolution, with implications
39 for understanding PVY variability and optimizing management strategies.

40

41 **Key-words:** DVG diversity, DVG dynamics, Defective RNAs, *in silico* analysis,
42 *Potyvirus*

43 Introduction

44

45 Viruses are among the smallest replicative forms found in almost all environments.
46 However, even smaller entities, known as sub-viral agents, have been identified. These
47 include satellite viruses (200-1800 nucleotides long), which require a helper virus for
48 replication, viroids (200-400 nucleotides), which do not encode proteins nor need a
49 helper virus, virophages (15-30 kbp), which parasitize giant viruses like mimiviruses
50 (La Scola et al. 2008), which are composed solely of proteins and lack nucleic acids.

51 The concept of "replicators" was introduced by Richard Dawkins in 1976 in "The
52 Selfish Gene". Replicators are entities that pass on their structure largely intact through
53 generations and can be copied or replicated, propagating their form or information
54 (Dawkins 2016). This concept encompasses a wide range of replicators, including
55 inteins, introns, mini-inteins, plasmids, quasi-replicators, retrotransposons, and
56 transposons (Koonin and Starokadomskyy 2016). From unicellular to multicellular
57 organisms, a complex and interconnected network of replicators highlights the
58 evolutionary dynamics of parasite-host coevolution (Koonin and Starokadomskyy
59 2016).

60 In 1947, Preben von Magnus described non-infectious, incomplete forms of the
61 influenza A virus, leading to the discovery of defective RNAs (DRNAs) or defective
62 viral genomes (DVGs) (Gard and von Magnus 1947; von Magnus 1954). Although
63 DVGs are versions of the wild-type (WT) viral genome that cannot replicate
64 autonomously, they can form heterogeneous or homogeneous subpopulations
65 (Budzyńska et al. 2020). DVGs represent a complex and nuanced form of replicator,
66 fitting into the broader conceptual framework that includes genes, memes, and other
67 entities capable of replication and evolution. Despite having lost the ability to replicate
68 autonomously, DVGs can propagate and be subject to evolutionary forces. Although
69 they are not fully autonomous, they can still be replicated and passed on to successive
70 generations of viral particles during co-infections with the WT virus.

71 Certain DVGs can interfere with the production of the WT virus, critically
72 influencing infection outcomes, and are referred to as defective interfering particles
73 (DIPs) (von Magnus 1954). Only DVGs that interfere with WT virus accumulation are

74 termed DIPs or defective interfering RNAs (DI-RNAs), a subclass of D-RNAs (Huang
75 and Baltimore 1970).

76 The formation of DVGs is often attributed to the template switching of viral
77 RNA-dependent RNA polymerase (RdRp), known as the copy-choice mechanism
78 (Lazzarini et al. 1981). This process involves the premature dissociation of the viral
79 RNA polymerase and the nascent strand from the RNA template, followed by the
80 reinitiation of replication at a different site, resulting in incomplete RNA strands
81 (Lazzarini et al. 1981). Thus, DVGs originate from the WT genome and often require
82 co-infection with the WT virus to express all necessary viral proteins and package the
83 DVG progeny (Lazzarini et al. 1981).

84 DVGs can be categorized into three types: (i) those with single or multiple
85 internal deletions, (ii) those with mosaic genomes, which include insertions and
86 deletions, and (iii) copy-back (or snap-back) genomes (Beauclair et al. 2018). Although
87 initially detected in animal viruses, DVGs are also present in plant viruses. For instance,
88 DVGs have been identified in *Bromovirus* (Damayanti et al. 1999; Llamas et al. 2004),
89 *Closterovirus* (Che et al. 2002), *Crinivirus* (Rubio et al. 2000, 2002), *Cucumovirus*
90 (Graves and Roossinck 1995), *Nepovirus* (Hasiów-Jaroszewska et al. 2012),
91 *Orthospovirus* (de Oliveira Resende et al. 1991, 1992), *Pomovirus* (Torrance et al.
92 1999), *Potexvirus* (White et al. 1992; Calvert et al. 1996), *Tobravirus* (Visser et al.
93 1999), and *Tombusvirus* (Burgyan et al. 1989; Knorr et al. 1991; Chang et al. 1995),
94 mostly through serial passage experiments. However, their detection has been elusive
95 for members of the *Potyviridae* family.

96 The mechanisms shaping the DVG population are host-specific, as evidenced by
97 the formation, maintenance, and accumulation of DVGs in tomato bushy stunt virus
98 (TBSV) populations in *Nicotiana benthamiana* but not in pepper plants (Omarov et al.
99 2004). These mechanisms can be expanded to other viral families. Although some plant
100 viruses exhibit DVG formation, this field remains underexplored with significant
101 potential for discovery. Given that DVGs have not been found in the *Potyviridae*, we
102 investigated an agriculturally important virus, potato virus Y (PVY), the type member
103 of the *Potyvirus* genus, responsible for substantial crop production losses. PVY has a
104 single-strand positive sense RNA of approximately 9-10kb in length that encode a
105 polyprotein that suffer autoproteolysis (Inoue-Nagata et al. 2022).

106 PVY is an ideal subject for studying DVGs due to its high mutation and
107 recombination rates and fast replication cycle (Tromas et al 2014; Sanjuán et al. 2009).
108 Furthermore, PVY can be classified in strains (Singh et al. 2008), based on symptoms
109 expression in specific hosts and phylogeny.

110 Though often considered insignificant non-infectious byproducts in typical or
111 infectious virus cultures, virus-like particles can engage in various biological processes.
112 These processes include disrupting standard infections, initiating apoptosis or
113 destroying host cells, and activating innate immune responses (Vignuzzi and López
114 2019). Here, we use an *in silico* approach to explore the formation of DVGs through
115 two passage experiments of PVY: one using potato plants with different strains and
116 transmission modes and another using mechanical inoculation with different host
117 combinations.

118

119

120 **Materials and methods**

121

122 **Datasets**

123 In our study, we utilized two datasets to investigate the presence of DVGs in PVY
124 populations. The first one, obtained from an online source (da Silva et al. 2020), was
125 divided into subsets according to different criteria outlined in the original paper. These
126 subsets included three PVY strains (N, N-Wi and O), inoculation methods (mechanical
127 (MI), aphid-mediated (AT), or infected tuber (IT) transmission), plant organ (leaf or
128 tuber), and passage number (1 to 5). It is important to note that passage 4 was not
129 available to download and was excluded from the analysis. The raw sequencing reads
130 were downloaded from the NCBI BioProject database (PRJNA601749). To generate the
131 dataset, the potato plants were cultivated in a greenhouse and harvested 14 weeks after
132 planting. The three strains were collected from Wisconsin (PVY^O), Minnesota
133 (PVY^{N-Wi}), and Montana (PVY^N), all in the USA. The isolates were maintained in
134 lyophilized tobacco tissue and used to inoculate a single founding plant. Then, three
135 source plants were mechanically inoculated using the founding plant, and each source
136 plant was used for each transmission mode (MI, AT, or IT).

137 The second dataset (author's dataset) was generated from a passage experiment
138 involving two PVY isolates collected from different hosts: *Solanum tuberosum* (potato)
139 (PVYSt) and *Nicotiana benthamiana* (PVYNb). These isolates were passed through
140 three different hosts (benthamiana, potato and tomato) using various combinations over
141 ten passages. The experiment consisted of five treatments: (i) Sl: viruses passed through
142 tomato plants exclusively; (ii) St: viruses passed exclusively through potato plants; (iii)
143 Nb: viruses passed exclusively through benthamiana plants; (iv) CTF (correlated
144 temporal fluctuations): hosts alternated starting with tomato, followed by potato,
145 benthamiana, and back to tomato; (v) MIX: a mix of all three hosts was used during
146 inoculation and collection. Each treatment (T) had two independent lineages (L1 and
147 L2). Each passage lasted ten days. Initial viruses (PVYNb and PVYSt), and different
148 points of passages (ranging from 1st to 10th) to each treatment and respectively lineages
149 were also sequenced using high-throughput sequencing (HTS) Illumina, as for the first
150 dataset (a list of all samples used can be found at Sup. Table 1). Unlike the first dataset,
151 the second dataset involved collecting a pool of 16 mechanically inoculated plants per
152 lineage rather than individual plant. The plants were cultivated in growing chambers
153 with a controlled environment. PVYNb was maintained repeatedly in benthamiana
154 plants, and PVYSt was collected from a potato production field.

155

156 **DVGs identification**

157 To detect the presence of DVGs, we employed DVGFinder (Olmo-Uceda et al. 2022), a
158 metasearch tool designed for Illumina data. DVGFinder integrates ViReMa-a (Routh
159 and Johnson 2014) and DI-tector (Beauclair et al. 2018), two algorithms specifically
160 developed for DVG detection. We applied DVGFinder to the entire first dataset and
161 each subset individually, including all three strains data and its subdivisions by
162 transmission type, plant organ, and number of passages. The same conditions were
163 applied to the second dataset, using the original dataset divisions by treatment, line, and
164 passage. The standard command line of DVGFinder was used. The DVGFinder
165 algorithm requires a reference genome to map the reads. The consensus genome of each
166 sample was mapped against the NCBI database using BLASTn (Johnson et al. 2008),
167 and the genome with the greatest identity was used as the reference genome for the
168 analysis.

169 The output table from DVGFinder was further analyzed in R (R Core Team 2022).
170 To refine the results and reduce false positives, we added new columns to the data
171 frame: a 'start' column with the minimum values between the breakpoint (BP) and the
172 reinitiating point (RI), and an 'end' column with the maximum values of BP and RI. The
173 difference between 'end' and 'start' was calculated and stored in a 'delta' column.
174 Additionally, a 'total reads' column was created by summing the read counts from
175 ViReMa-a and DI-tector. Data preprocessing involved filtering out rows that did not
176 meet the criteria of a delta greater than one and ViReMa-a read counts greater than 10,
177 ensuring the remaining data was relevant and meaningful. This filter imposed a strong
178 threshold on both datasets, greatly reducing the number of DVGs found but ensuring
179 reliability.

180

181 **DVG analysis**

182 The analysis of high-throughput sequencing data was conducted to evaluate DVG
183 diversity and distribution across various PVY populations.

184 Principal Component Analysis (PCA) was performed to explore patterns in DVG
185 distribution and simplify the data by reducing the number of variables, making it easier
186 to interpret complex relationships. PCA helps to identify clusters of samples or DVGs
187 with similar characteristics, revealing underlying structures in the dataset that might not
188 be immediately apparent. To perform PCA, the R stats package version 4.5.0 was used
189 on original read counts.

190 Normalization of read counts was essential for accurate comparison across
191 samples. Reads per million (RPM) were calculated for each sample using the dplyr
192 (<https://dplyr.tidyverse.org/>) and tidyr (<https://tidyr.tidyverse.org/>) R packages.
193 Normalization corrects for differences in sequencing depth, allowing for a fair
194 comparison of DVG abundance across samples. To visualize DVG abundance, a
195 heatmap of normalized read counts for the top found DVGs was generated. The top
196 DVGs criterion refers to selecting the most abundant DVGs based on their read counts
197 in the dataset. This approach is used to focus on DVGs that are most prevalent across
198 samples, which are often of greater interest for analysis due to their higher abundance
199 and potential biological significance.

200 Shannon Diversity Index (SH) was calculated using vegan R package
201 (10.32614/CRAN.package.vegan) to measure the diversity of DVGs within each
202 sample. SH accounts for both the number of DVG types and their relative abundance,
203 providing a comprehensive measure of diversity.

204 All used packages were employed using RStudio version 2024.4.1.748 (Posit
205 Team 2024), and all plots were generated using ggplot2 (Wickham 2016).

206

207

208 **Results**

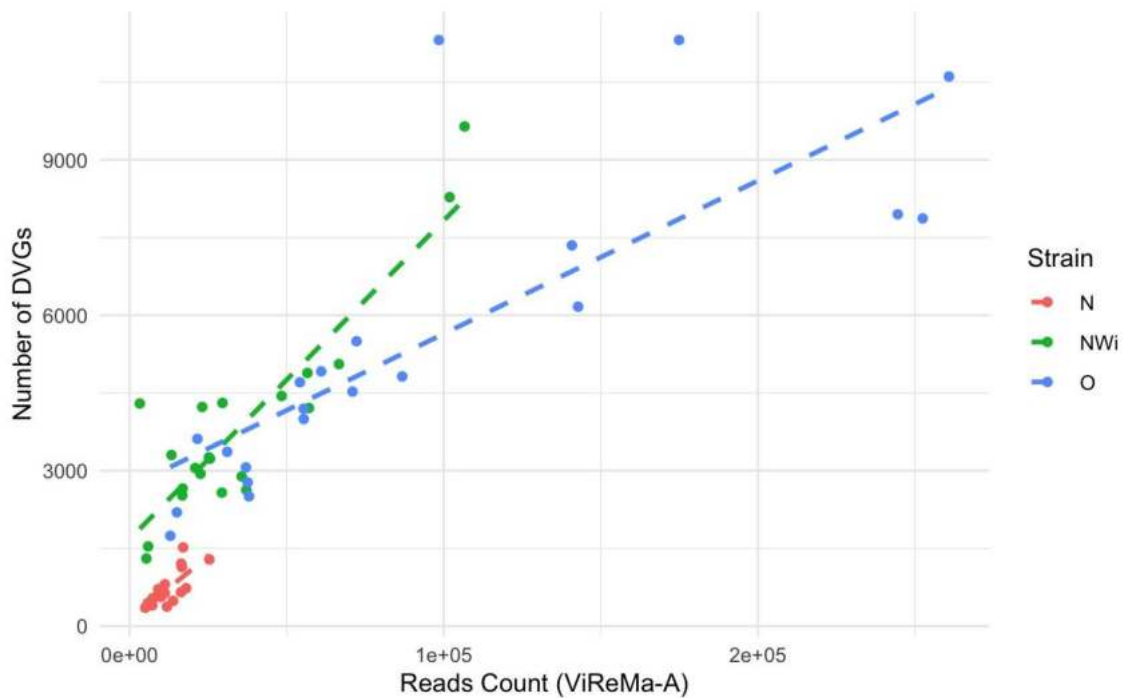
209

210 **DVGs profile**

211 The analysis of the first dataset considered various populations. Initially, we focused on
212 two main populations: the founding population and the source plants. The founding
213 population comprised lyophilized PVY-infected tobacco tissue mechanically inoculated
214 into potato plants, which were then divided by strain to initiate the experiment. The
215 source plants, derived from these plants, were further categorized based on inoculation
216 via leaf or tuber to begin the passage experiments. Using the source plants, five
217 passages were conducted, with leaves divided by transmission modes: aphid-mediated
218 transmission (AT), mechanical inoculation (MI), and two passages using infected tuber
219 transmission (IT). Additionally, files containing strain-specific information were
220 grouped into populations corresponding to the N, N-Wi and O strains, which were
221 further subdivided by the plant organ collected in each sample: leaves (L) or tuber (T).

222 Despite the variations in read numbers across populations and subpopulations, a
223 significant finding was the consistent detection of DVGs across all PVY samples, even
224 when stringent threshold filters were applied. The initial analysis revealed a high
225 number of DVGs without filtering, but applying the filters improved the visualization
226 and removed poorly represented DVGs. In general, the number of DVGs varied
227 significantly among the viral strains. Strain O exhibited the highest number of reads
228 mapped to the reference genome (X12456) using ViReMa-a, as well as the largest
229 number of unique DVGs (Fig. 1). In contrast, strain N-Wi had a smaller number of
230 mapped reads but a DVG count close to that of strain O. Strain N, on the other hand,
231 showed both a low number of mapped reads and a low number of DVGs.

232



233

234 **Fig 1.** Number of reads mapped against the reference genome using ViReMa-A (x-axis)
235 against the number of distinct DVGs detected in each PVY strain to the first dataset.
236 Each point represents a population.

237

238 Representative figures for each population are provided in Sup. Fig. 1 and Sup.
239 Table 1. The DVG population varied depending on the dataset, indicating that DVG
240 formation is influenced by multiple factors. When considering all strains together, the
241 foundation populations exhibited fewer DVGs compared to later passages, although
242 some patterns of DVG formation emerged between populations.

243 The different founding populations of the strains exhibited distinct groupings and
244 formations of DVGs, yet all classes of DVGs were present in these populations. In the
245 first passage to the source plants, a noticeable change in behavior was observed. The
246 number of DVGs in source plants was higher than in the foundation plants for all
247 strains, maintaining diversity. However, when analyzed by plant organ, all strains had
248 more unique DVGs in tubers than in leaves. For example, even though strain O had 4.6
249 times more mapped reads in leaves than in tubers, the number of unique DVGs was
250 higher in the latter. Given the differences in mapped reads across samples, the number
251 of unique DVGs per sample was considered in the analysis.

252 During aphid transmission, all strains exhibited a similar pattern, with the number
253 of unique DVGs in leaves decreasing from the first to the fourth passage. In tubers, two
254 patterns emerged: strain N showed a decrease in DVGs, while strains N-Wi and O
255 showed an increase in DVGs with successive viral passages. For tuber transmission, the
256 number of unique DVGs remained relatively constant for strain N, regardless of the
257 organ analyzed. For strain N-Wi, the DVG population in leaves remained stable, while
258 it increased from the first to the second passage in tubers. A similar increase was
259 observed in strain O tubers, though the number of DVGs decreased sharply between the
260 first and second passage when analyzing infected leaves. MI yielded results similar to
261 aphid transmission. For all strains, the number of unique DVGs in leaves tended to
262 decrease over the five viral passages. An exception was noted for strain O, where a
263 significant increase occurred from the first to the second passage, followed by a
264 decrease in subsequent passages. As with AT, the opposite trend was observed in tubers,
265 where unique DVGs tended to increase with viral passages.

266 The results demonstrate that DVG populations in PVY are highly dependent on
267 the virus strain, transmission mode, and the number of passages. Notably, bottlenecks
268 were observed in some conditions, particularly in leaves during AT and MI, where the
269 number of unique DVGs decreased over time. However, tubers, which exhibited more
270 unique DVGs despite fewer mapped reads, appeared to reduce or mitigate these
271 bottlenecks, suggesting a more permissive environment for viral replication and DVG
272 formation. Strain-specific effects were also evident: strain O, with the highest number of
273 reads and unique DVGs, showed intermittent bottleneck effects, especially in leaves,
274 while tubers maintained or increased DVG diversity. In contrast, strain N exhibited
275 more pronounced bottlenecks in both leaves and tubers, while strain N-Wi showed an
276 intermediate behavior.

277 The analysis of the second dataset revealed that some populations were devoid of
278 DVGs. Specifically, for PVYNb, DVGs were absent in Sl.L1 and Sl.L2 (both at the first
279 passage), St.L1 and St.L2 (both at the fifth passage), Nb.L1 (at the fourth and tenth
280 passages), CTF.L2 (at the eighth passage), and MIX.L2 (at the ninth passage). For
281 PVYSt, DVGs were absent in Sl.L1 (fifth passage), Sl.L2 (first passage), St.L1 (sixth
282 passage), St.L2 (tenth passage), Nb.L1 (tenth passage), CTF.L2 (first passage), and

283 MIX.L1 (second passage). Although 97 unique DVGs were detected in
284 PVYNb/CTF.L1, this sample did not pass the threshold filtering and was discarded.

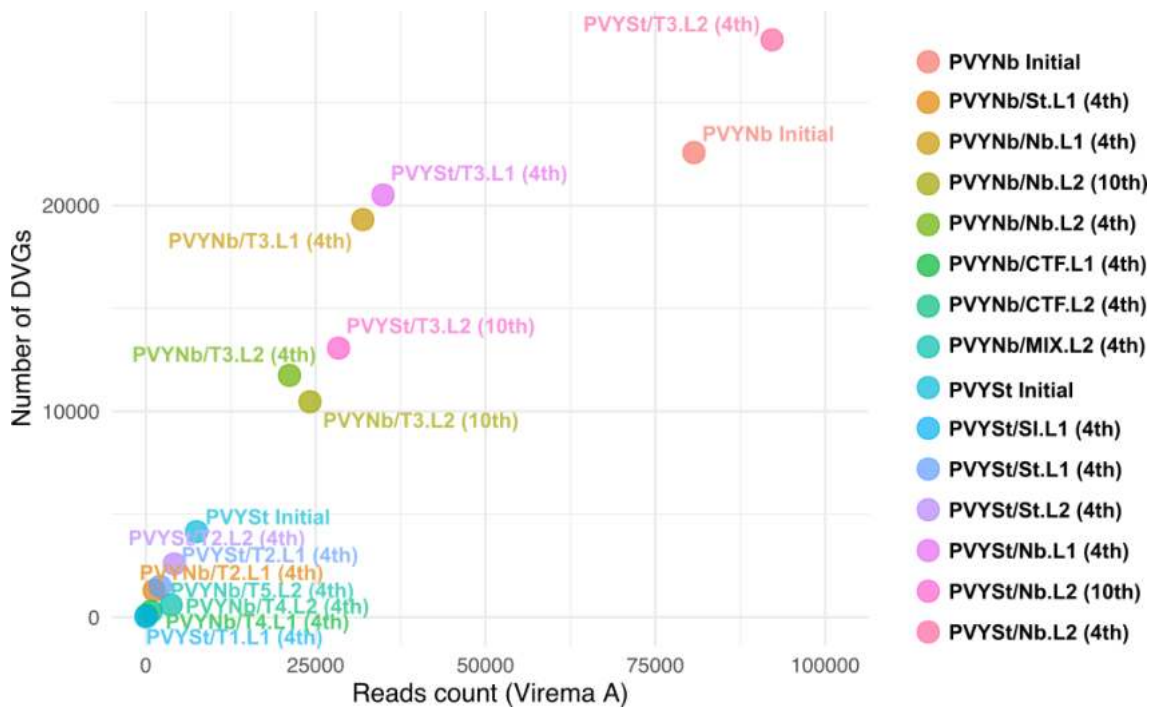
285 Initially, both PVYNb and PVYSt samples exhibited DVG formation. However,
286 the number of unique DVGs in the PVYNb population ($n = 22,557$) was substantially
287 higher compared to the initial PVYSt ($n = 4,154$) (Fig. 2, Sup. Table 2). Despite some
288 samples having a low number of mapped reads, unique DVGs were still found.

289 This dataset highlights the critical role of the host in DVG formation (Sup. Table
290 2). Despite the initial population of unique DVGs of PVYNb in benthamiana, this
291 population remained stable in intermediate and advanced. Similarly, benthamianas
292 infected with PVYSt exhibited a significant increase in the number of unique DVGs,
293 even though the initial PVYSt population was smaller. This indicates the permissiveness
294 of benthamiana in the DVG formation process. Although fewer reads were mapped to
295 St (potatoes), the ratio of reads to unique DVGs was considerably high (1.06 for
296 PVYNb/St.L1, 0.72 for PVYSt/St.L1, and 0.62 for PVYSt/St.L2). Therefore, the
297 number of unique DVGs in potatoes was even greater than in benthamiana for both
298 isolates.

299 In PVYSt/Sl.L1, only 19 unique DVGs were found among 23 mapped reads,
300 indicating poor sampling but suggesting a highly restrictive environment for DVG
301 generation in tomato plants. For PVYNb, treatments that involved host alternation
302 (CTF) and mixing (MIX) showed a decrease in the number of DVGs relative to the
303 initial population, likely due to the presence of tomato plants during viral passages.

304 Representative figures for each population and subpopulation are provided in Sup.
305 Fig. 2. Notably, none of the PVYNb subpopulations presented 5' copy back/snap
306 back-type DVGs, which were exclusive to some PVYSt populations. Interestingly,
307 different types of DVGs were present in early PVYNb, but only deletion-type DVGs
308 were found in PVYSt. However, as PVYSt replicated in benthamiana, it recovered all
309 DVG types, increasing diversity. In PVYNb, the same DVG formation pattern was
310 observed in intermediate and final passages in benthamiana, demonstrating DVG
311 stability in this host.

312



313

314 **Fig 2.** Number of reads mapped against the reference genome using ViReMa-A (x-axis)
 315 against the number of distinct DVGs detected in each PVY strain. Each point represents
 316 a subpopulation.

317

318 Curiously, although the number of DVGs decreased drastically when PVYNb
 319 transitioned to different hosts from benthamiana, different patterns were observed in
 320 different treatments. For example, in PVYNb/St.L1, only reverse deletion-type DVGs
 321 were maintained in potatoes. Conversely, in the alternating host treatment (CTF.L2),
 322 only insertion-type DVGs persisted. In the mixing hosts treatment, forward deletion and
 323 reverse insertion-type DVGs were maintained. Even more intriguingly, despite the
 324 significant decrease in DVG numbers, treatments using only potato plants presented
 325 exactly the same DVG types as the initial PVYSt, even after four passages.

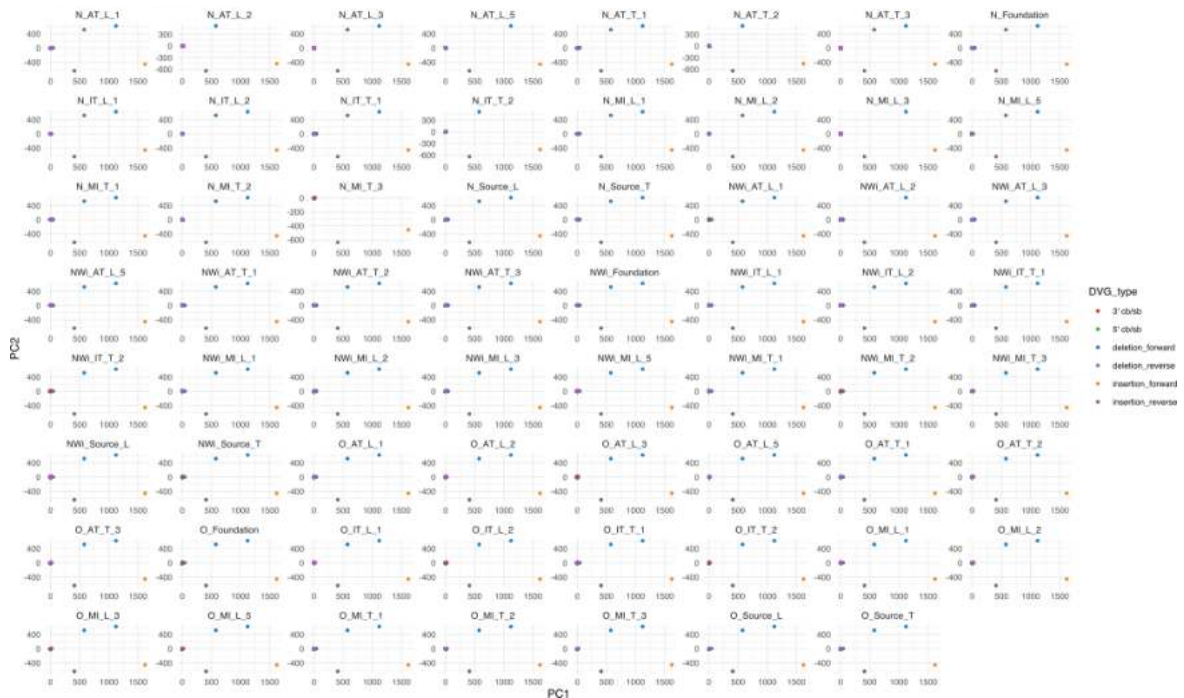
326 This dataset underscores the influence of the host on DVG formation, with
 327 benthamiana showing high permissiveness and stability in DVG populations. The
 328 restrictive environment in tomato plants and the variable patterns observed in different
 329 treatments highlight the complexity of host-virus interactions in DVG dynamics.

330

331 Clustering DVGs

332 In this analysis, PCA was applied to all mapped reads with the goal of simplifying
333 our dataset by focusing on DVG types. The results, illustrated in Fig. 3, reveal
334 intriguing patterns across different datasets and subpopulations.

335



336

337 **Fig 3.** Clustering of DVGs type using PCA to first dataset. The “N, NWi or O” value is
338 referenced to the PVY strain, followed by the type of transmission (AT to
339 aphid-transmission, IT to infected tuber and MI to mechanical infection), the plant
340 organ (L to leaf or T to tuber) and passage number.

341

342 For the first dataset, the PCA results show a consistent clustering pattern among
343 the various DVG types across all samples. While small differences are evident between
344 samples, these become more pronounced in later generations. An example is the
345 subpopulation of the PVY^N transmitted by aphids in leaves, where a clear distinction
346 emerges between the 1st and 2nd passages. However, this difference seems to be more
347 related to the reduction in DVGs in the 2nd passage rather than any inherent change in
348 the DVG types themselves.

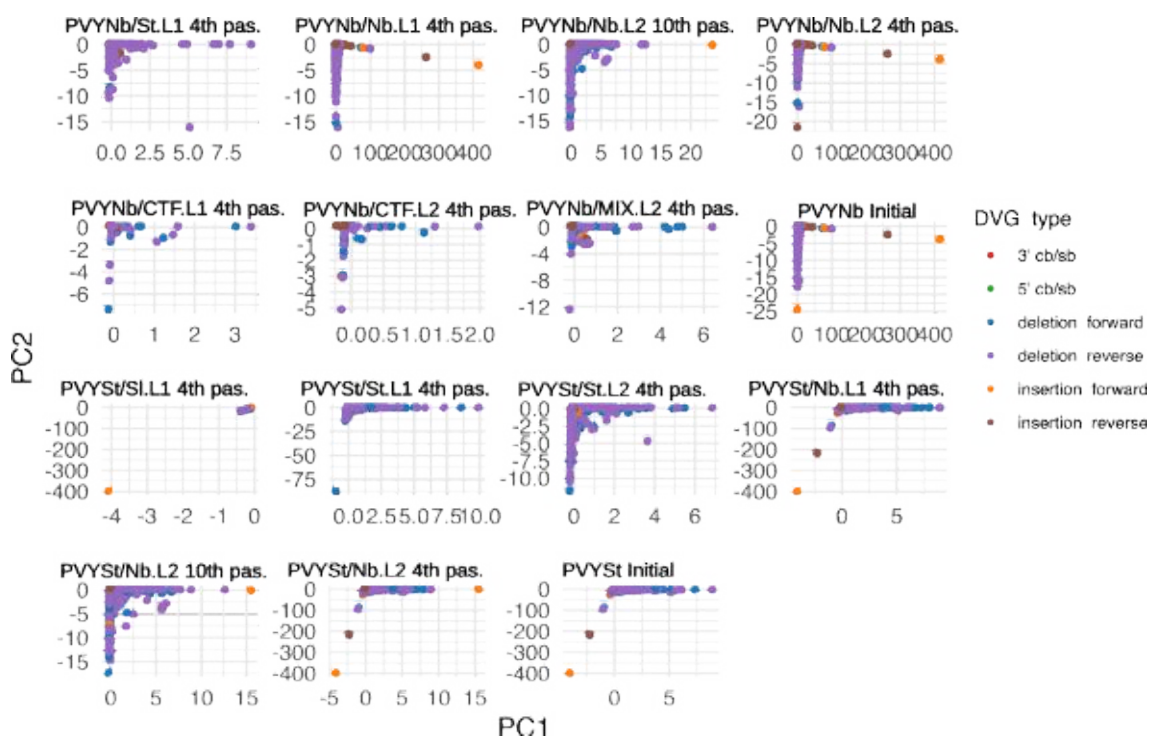
349 A key observation is the distinct clustering of specific DVG types. For instance,
350 DVGs formed by 3' and 5' cb/sb are closely grouped together, often alongside DVGs

351 created by reverse deletion. This pattern is consistent across most populations. In some
 352 cases, such as in the PVY^{N-Wi}-infected tubercles during the 2nd passage, two groups of
 353 reverse insertion DVGs are formed, with one group clustering closely with the 3', 5'
 354 cb/sb, and reverse deletion types. In contrast, forward insertion DVGs are clearly
 355 differentiated, consistently clustering far from the other DVG types. Additionally,
 356 forward deletion DVGs tend to form two distinct groups within nearly all populations.

357 The PCA analysis across both datasets underscores the complexity and variability
 358 of DVG formation and maintenance in PVY populations. The consistent clustering of
 359 certain DVG types, such as the 3' and 5' cb/sb (grouped on axis 0 along with reverse
 360 deletion), across different subpopulations suggests that some DVG types are inherently
 361 more stable or prevalent. However, the distinct clustering of forward insertion DVGs
 362 and the variability in forward deletion DVGs indicate that other types of DVGs may be
 363 more sensitive to factors such as viral passage, transmission mode, and host plant.

364 The PCA results for the second dataset reveal similar clustering patterns, with
 365 some nuances and slight variations in grouping, as shown in Fig. 4. Like the first
 366 dataset, the 3' and 5' cb/sb DVGs consistently cluster closely together across all
 367 populations. However, forward insertion DVGs again stand out by forming distinct
 368 clusters, separate from other DVG types.

369



370

371 **Fig 4.** PCA analysis of DVGs using PCA to the second dataset, in which each dot
372 represents a unique DVG separated by different colors by type.

373

374 Within the second dataset, there are several noteworthy observations. For
375 example, the initial PVYNb and intermediate generations of CTF show high PC values,
376 indicating a strong influence or differentiation along the main component. As these
377 populations advance, such as in PVYSt Nb.L2 by the 10th generation, the PC values
378 decrease significantly, suggesting reduced differentiation between the various DVG
379 types formed. In benthamiana populations (Nb) infected with PVYSt, the clustering
380 pattern remains similar to the initial isolate, but like PVYNb, this pattern only persists
381 through intermediate generations. By the 10th generation in Nb.L2, the DVGs begin to
382 form tighter clusters, indicating less variation in PVYSt population.

383 The PVYSt Sl.L1 tomato lineage presents a unique cluster, with forward insertion
384 DVGs clearly distinct from the other DVG types within this subpopulation.
385 Interestingly, when host alternation (CTF) or mixing (MIX) is applied, the established
386 DVG patterns are disrupted, leading to distinct clusters that differ both from the initial
387 PVYNb and from each other.

388 Furthermore, the influence of the host plant on DVG formation is particularly
389 evident in the second dataset, where host-specific clusters emerge, and the introduction
390 of host alternation or mixing disrupts established DVG patterns. This highlights the
391 importance of the host environment in shaping DVG diversity and evolution.

392 Overall, these findings suggest that DVG populations in PVY are dynamic and
393 could be influenced by multiple factors, including virus strain, transmission mode,
394 passage number, and host plant.

395

396 **DVGs formation and distribution**

397 By filtering the most frequently observed DVGs by type, we were able to analyze their
398 formation and distribution across different subpopulations. The results are detailed in
399 Fig. 5.

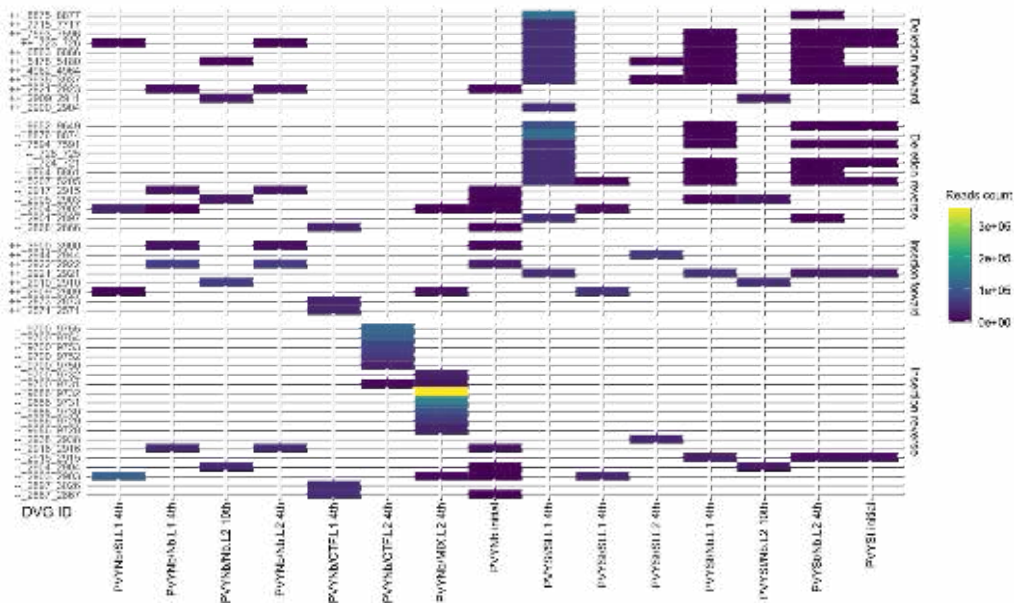
400 The first dataset reveals a strikingly similar pattern of DVG formation between
401 the N-Wi and O strains. Many DVGs appear consistently across all populations, with
402 the forward insertion DVG (ID: ++2973-2973) being the most prevalent. However, not

423 lost, leading to a reduction in DVG diversity and selection of fewer DVGs. This
 424 selective reduction does not occur in the N-Wi and O strains, where subpopulations
 425 maintain a consistent pattern despite some specific differences.

426 The second dataset does not exhibit a clear pattern of DVG formation (Fig. 6).
 427 Each population seems to possess unique DVGs with minimal similarity to other
 428 populations, and no DVGs are widely found across all samples. Notably, none of the 3'
 429 or 5' cb/sb DVGs met the threshold for inclusion in this analysis.

430 Despite the lack of a clear formation pattern, some trends are observed. In
 431 PVYNb, DVGs present in the initial population are filtered out in subsequent passages.
 432 Consecutive passages in the same host (*e.g.*, St and Nb) appear to refine the DVGs
 433 compared to the initial population. However, when hosts are alternated (CTF) or mixed
 434 (MIX), the DVG profile changes markedly, for example, eliminating all forward
 435 deletion DVGs and favoring the formation of reverse insertion DVGs.

436



437

438 **Fig 6.** Heatmap showing the most found unique DVGs, divided by type and to number
 439 of reads count to the second dataset. Each different population can be found in the
 440 abscissa and each unique DVG ID in the ordinate, divided by type.

441

442 For PVYSt, there is a tendency to retain DVGs from the initial population in
 443 intermediate benthamiana passages (Nb.L1 and L2). Yet, by the 10th passage in the

444 advanced Nb.L2 population, the DVG profile undergoes significant filtering, drastically
 445 altering its composition. This filtering is also evident in potato populations (St). In
 446 contrast, the DVG diversity increases sharply in tomato (Sl) compared to the initial
 447 population, forming distinct patterns while still preserving some original DVGs.

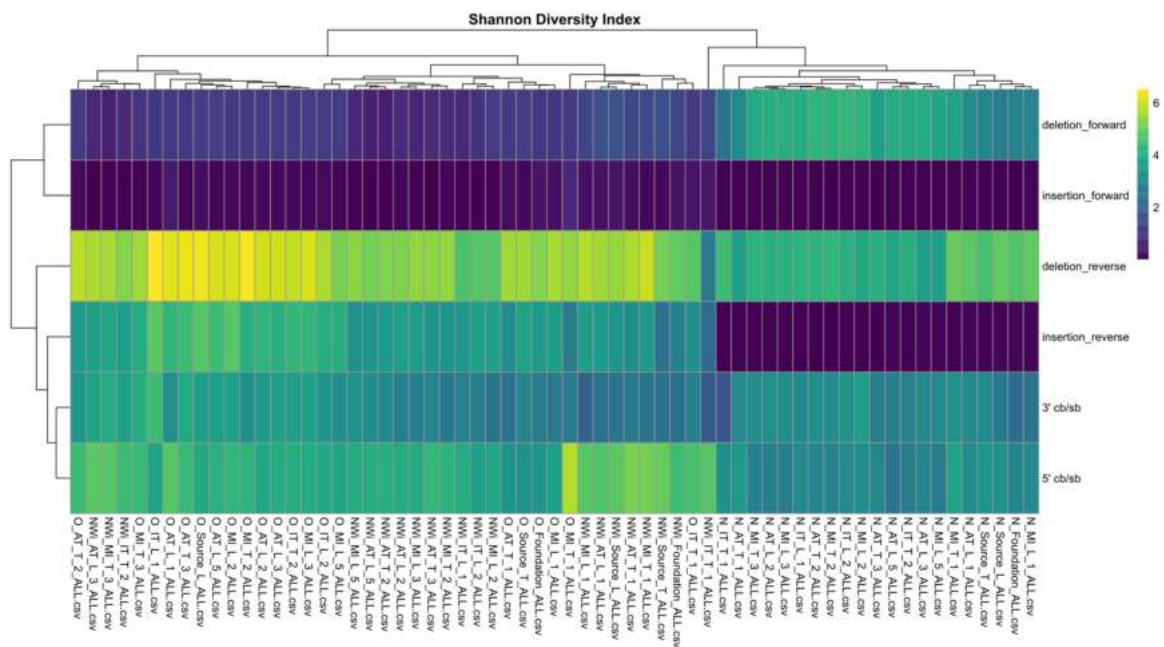
448 The analysis of DVG formation across different strains and subpopulations
 449 reveals distinct patterns in DVG types and their persistence over successive passages.
 450 While N-Wi and O strains show a consistent DVG formation pattern, the N strain
 451 diverges significantly, particularly in its reverse insertion DVG prevalence. The second
 452 dataset highlights the impact of host consistency on DVG selection, with alternating or
 453 mixed hosts resulting in a more diverse DVG profile. These findings underscore the
 454 complex dynamics of DVG formation and selection, influenced by both viral strain and
 455 host interaction.

456

457 DVGs diversity

458 In our analysis, we calculated SH for all populations to directly compare the diversity of
 459 different types of DVGs. The results for the first dataset are presented in Fig. 7.

460



461

462 **Fig 7.** Shannon-Entropy graph to the first dataset, in which the bluer color represents
 463 less diversity and the yellow more diversity between each population, represented by
 464 each square.

465

466 To the first dataset, when examining diversity across samples, there is a noticeable
467 similarity in diversity among the same types of DVGs. Forward deletion and insertion
468 DVGs exhibit similar diversity levels, showing a high degree of conservation across all
469 populations. A similar trend is observed for 3' and 5' cb/sb DVGs. Interestingly, the
470 diversity of reverse insertion DVGs is more closely aligned with the 3' and 5' cb/sb
471 group than with reverse deletion DVGs, which tend to show greater variability
472 compared to other DVG types.

473 Diversity patterns also tend to cluster by strain, with some exceptions, such as the
474 blending of diversity between PVY^O and PVY^{N-Wi}. Despite this, PVY^N generally
475 displays a unique diversity pattern, distinct from the other strains, with the exception of
476 PVY^{N-Wi} IT from tubers in the 1st passage. Notably, the diversity of forward deletion
477 DVGs is lower in PVY^O and PVY^{N-Wi}, while this trend is inversely proportional to the
478 reverse insertion DVGs when compared to the N strain.

479 In PVY^{N-Wi} and O, diversity is predominantly concentrated in reverse deletion
480 DVGs, with lower diversity observed in forward deletion DVGs. Conversely, PVY^N
481 shows lower overall diversity, but reverse deletion DVGs still tend to exhibit greater
482 diversity among samples. An interesting contrast is evident between the diversity
483 patterns of PVY^{N-Wi} and O compared to PVY^N. Forward deletion DVGs are less diverse
484 in N-Wi and O but show increased diversity in N. On the other hand, reverse insertion
485 DVGs are highly conserved in PVYN but exhibit greater diversity in the other two
486 strains.

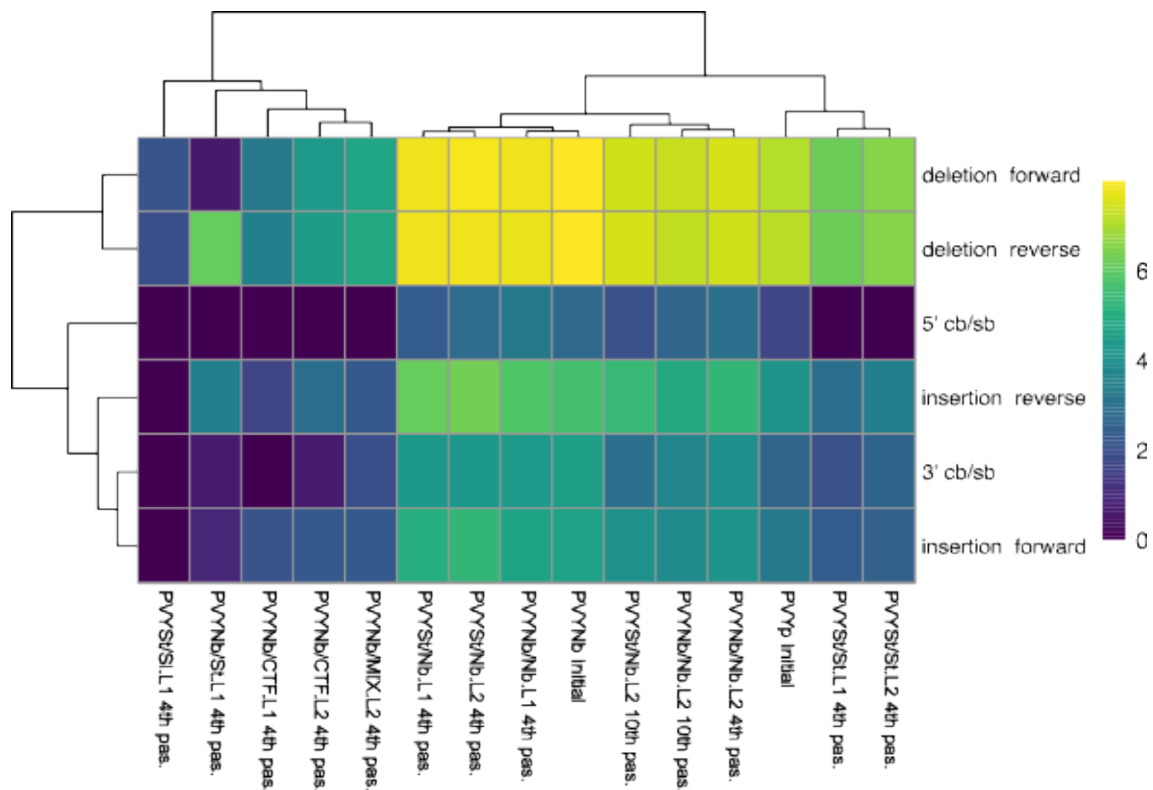
487 The diversity patterns in the second dataset differ from those observed in the first
488 (Fig. 8). Deletion-type DVGs generally show higher diversity similarity, making them
489 the most diverse DVG type across all samples. Insertion and 3' cb/sb DVGs have similar
490 diversity levels, while 5' cb/sb DVGs are the most conserved type among all samples.

491 Significant differences are also noted between samples. While there is a general
492 tendency for clusters to originate from the same viral isolate, exceptions exist. For
493 instance, DVG diversity is relatively conserved in tomato (PVYSt/Sl.L1), potatoes
494 inoculated with PVYNb (St.L1), and in the alternate (CTF) and mix (MIX) treatments.
495 However, diversity increases in the remaining populations. Populations found in
496 benthamiana exhibit greater diversity compared to others, clustering together regardless

497 of the virus or passage. This suggests that benthamiana's more permissive cellular
498 environment may promote higher DVG diversity. In support of this observation,
499 correlation analysis shows a strong positive relationship between the number of DVGs
500 and the reads count in benthamiana (correlation coefficient of 0.929), indicating that as
501 viral replication increases, so does DVG diversity. The linear model further supports
502 this, revealing a significant positive association between the number of DVGs and reads
503 count across all samples, with an R-squared value of 0.6914, highlighting that a
504 substantial proportion of the variability in DVG numbers can be explained by variations
505 in viral replication levels. Thus, the increased diversity observed in benthamiana likely
506 reflects the host ability to support more extensive viral replication and a higher
507 likelihood of replication errors, resulting in greater accumulation of DVGs. This
508 suggests that the more permissive nature of benthamiana cellular environment may
509 facilitate the generation and persistence of a wider range of DVGs. Additionally, a more
510 conserved diversity pattern is observed starting from the initial PVYSt, where both St
511 lines tend to maintain the diversity conformation of the initial population. This finding
512 suggests that DVG diversity formation is more dependent on the host species than on
513 viral passage.

514 The analysis of DVG diversity across different strains and subpopulations reveals
515 distinct patterns influenced by both DVG type and host-virus interactions. In the first
516 dataset, diversity tends to cluster by strain, with forward deletion and insertion DVGs
517 showing high conservation, while reverse deletion DVGs display more variability. The
518 second dataset highlights the role of host species in shaping DVG diversity, with
519 deletion-type DVGs being the most diverse and benthamiana populations exhibiting the
520 greatest overall diversity. These findings underscore the complex interplay between
521 viral strain, DVG type, and host species in determining the diversity of DVGs.

522



523

524 **Fig 8.** Shannon-entropy graph to the second dataset, in which the bluer color represents
 525 less diversity and the yellow more diversity between each population, represented by
 526 each square.

527

528

529 Discussion

530

531 The viral RdRp naturally introduces errors during replication, leading to high variability
 532 in viral genomes. This variability can result in the formation of DVGs, which coexist
 533 with WT genomes in infected cells (Vignuzzi and López 2019). Our detection approach
 534 successfully identified DVGs across nearly all PVY samples, even with stringent filters.
 535 The number of detected DVGs varied by viral strain: PVY^O exhibited the highest
 536 number of mapped reads and unique DVGs, while PVY^{N-Wi} had fewer reads but a
 537 similar number of DVGs. PVY^N had the lowest counts for both metrics. Additionally,
 538 PVY accumulation in potato cultivars varies by strain and plant stage, which could
 539 affect DVG generation (Mondal et al. 2023). Higher viral accumulation often correlates
 540 with increased DVG numbers.

541 The DVG population also varied with virus strain, transmission mode (AT, IT, or
542 MI), and plant organ (leaves or tubers). During AT, DVGs in leaves decreased with
543 successive passages, while tubers showed variable trends depending on the strain. In
544 MI, similar trends to AT were observed, with a general decrease in DVGs in leaves over
545 time and an increase in tubers for some strains. This suggests an organ-specific
546 influence on DVG dynamics. Although DVGs typically increase with multiple passages
547 (Pogany et al. 1995; Hasiów-Jaroszewska et al. 2012), our results indicated a decrease
548 in DVGs in potato leaves and an increase in tubers during sequential passages. This is
549 important as DVG generation is not always random; virus-encoded sequences can
550 actively promote specific DVGs (Vignuzzi and López 2019), indicating that host-virus
551 interactions are specific.

552 These findings align well with the diversity analyses, showing high diversity in
553 insect transmission, medium in mechanical inoculation, and low in tuber transmission
554 due to bottlenecks (da Silva et al. 2020). Tubers generally exhibit higher diversity (π)
555 than leaves for tuber and mechanical inoculation (da Silva et al. 2020), suggesting that
556 increased diversity is related to higher DVG numbers. Metabolic activities,
557 development, hormonal responses, and gene expression differences between potato
558 tuber and leaf cells (Taiz et al. 2015) that likely contribute to these variations.

559 Host factors play a critical role in DVG formation. In benthamiana, the DVG
560 population remained stable for PVYNb and increased significantly for PVYSt,
561 indicating the plant's permissiveness (*discussed in Chapter III*). Conversely, potato
562 samples showed a higher ratio of reads to unique DVGs, suggesting robust DVG
563 formation even with fewer mapped reads. The formation of DVGs depends on both host
564 factors and environmental conditions, such as temperature (Llamas et al. 2004). In this
565 work, we used two datasets, the first one was entirely produced under greenhouse
566 conditions, subject to environmental variations. On the other hand, the second dataset
567 was conducted entirely under artificial conditions (*M&M from Chapter III*), which may
568 have influenced the divergence between both datasets as well. Importantly, no work has
569 yet addressed the issue of environmental factors that can shape the population of DVGs
570 in plants. Host alternation or mixing disrupted established DVG patterns, leading to
571 distinct clusters, further emphasizing the complex interaction between host and

572 environment. Additionally, DVG formation often results in the loss of specific DVG
573 types and the emergence of new ones in mixed or alternate host passages.

574 DVGs can interfere with WT viruses, potentially reducing virulence, protecting
575 the host, or generating an immune response (Rabinowitz and Huprikar 1979; Barrett and
576 Dimmock 1984). Recent studies have demonstrated the efficacy of DVGs in treating
577 viral infections in animals (also known as therapeutic interfering particles, TIPs) (Rezelj
578 et al. 2021; Xiao et al. 2021). Studies using this strategy in planta are non-existent,
579 although interfering DVGs has been previously reported to for others virus genera
580 (Graves et al. 1996; Hasiów-Jaroszewska et al. 2018) and DVGs construction was done
581 using plant hosts (Pathak and Nagy 2009; Lee and White 2014). But unlike the use of
582 animal cells that can generate different DVGs *in vitro* and *in vivo* (Li et al. 2024), the
583 use of plants for such studies may simplify testing and yield results closer to real-world
584 conditions. This strategy holds potential for a non-transgenic and efficient viral control
585 method. However, further research is necessary for effective implementation.

586 A major challenge in utilizing DVGs as therapeutic agents lies in isolating those
587 with antiviral properties from the broader array of defective genomes produced during
588 WTV replication. Three primary mechanisms through which DI RNAs interfere with
589 viral processes have been identified: (i) competing with the virus and host for resources,
590 thereby hindering viral replication and reducing symptom severity; (ii) inducing
591 posttranscriptional gene silencing (PTGS), leading to gene silencing; and (iii) altering
592 the functions of viral factors (Szittyá et al. 2002; Pathak and Nagy 2009; Lukhovitskaya
593 et al. 2013). Methodologies for interrogating DVGs and identifying potential
594 therapeutic candidates have been explored (Rezelj et al. 2021). Our study revealed
595 consistent clustering patterns of specific DVG types across various samples, with 5'
596 DVGs showing a preference in therapeutic applications (Li et al 2024) due to their
597 retention of essential replication regions and their ability to induce strong antiviral
598 immune responses interfering the WT-virus replication. Additionally, 5' DVGs are less
599 likely to revert to fully functional viruses, reducing the risk of generating pathogenic
600 viruses during therapy. Despite the preliminary results found, our *in silico* methodology
601 seeks to understand the formation of DVGs in different virus-host-environment
602 interactions that still need to be validated in the future in bench work.

603 In conclusion, this study provides valuable insights into the diversity and
604 evolution of DVGs within PVY populations, revealing patterns that reflect the complex
605 interplay between viral genetics, host factors, and evolutionary pressures. Further
606 research into the mechanisms driving these patterns and the functional consequences of
607 different DVG types will be essential for a deeper understanding of DVG biology and
608 its implications for viral fitness, pathogenicity, and host interactions. DVGs, particularly
609 those retaining the 5' end of the viral genome, hold promise as therapeutic agents.
610 Although preliminary, our findings suggest that DVGs could serve as a basis for
611 developing novel antiviral strategies, particularly in plant systems. Further research is
612 needed to validate the therapeutic potential of DVGs and to explore their application in
613 viral control. Investigating the specific mechanisms driving DVG formation and their
614 effects on viral fitness and host interactions will be crucial for advancing this area.

615 References

616

617 Barrett ADT, Dimmock NJ (1984) Modulation of semliki forest virus-induced infection
618 of mice by defective-interfering virus. *Journal of Infectious Diseases* 150:98–104.

619 <https://doi.org/10.1093/infdis/150.1.98>

620

621 Beauclair G, Mura M, Combredet C, et al (2018) DI-tector: defective interfering viral
622 genomes detector for next-generation sequencing data. *RNA* 24:1285–1296.

623 <https://doi.org/10.1261/rna.066910.118>

624

625 Budzyńska D, Minicka J, Hasiów-Jaroszewska B, Elena SF (2020) Molecular evolution
626 of tomato black ring virus and *de novo* generation of a new type of defective RNAs
627 during long-term passaging in different hosts. *Plant Pathology* 69:1767–1776.

628 <https://doi.org/10.1111/ppa.13258>

629

630 Burgyan J, Grieco F, Russo M (1989) A defective interfering RNA molecule in
631 cymbidium ringspot virus infections. *Journal of General Virology* 70:235–239.

632 <https://doi.org/10.1099/0022-1317-70-1-235>

633

634 Calvert LA, Cuervo MI, Ospina MD, et al (1996) Characterization of cassava common
635 mosaic virus and a defective RNA species. *Journal of General Virology* 77:525–530.

636 <https://doi.org/10.1099/0022-1317-77-3-525>

637

638 Chang YC, Borja M, Scholthof HB, et al (1995) Host effects and sequences essential for
639 accumulation of defective interfering RNAs of cucumber necrosis and tomato bushy
640 stunt tomosviruses. *Virology* 210:41–53. <https://doi.org/10.1006/viro.1995.1315>

641

642 Che X, Mawassi M, Bar-Joseph M (2002) A novel class of large and infectious
643 defective RNAs of citrus tristeza virus. *Virology* 298:133–145.

644 <https://doi.org/10.1006/viro.2002.1472>

645

646 da Silva W, Kutnjak D, Xu Y, et al (2020) Transmission modes affect the population
647 structure of potato virus Y in potato. *PLoS Pathology* 16:e1008608.
648 <https://doi.org/10.1371/journal.ppat.1008608>
649

650 Damayanti TA, Nagano H, Mise K, et al (1999) Brome mosaic virus defective RNAs
651 generated during infection of barley plants. *Journal of General Virology* 80:2511–2518.
652 <https://doi.org/10.1099/0022-1317-80-9-2511>
653

654 Dawkins R (2016) *The selfish gene, 40th anniversary*. Oxford University Press
655

656 de Oliveira Resende R, de Haan P, de Avila AC, et al (1991) Generation of envelope
657 and defective interfering RNA mutants of tomato spotted wilt virus by mechanical
658 passage. *Journal of General Virology* 72:2375–2383.
659 <https://doi.org/10.1099/0022-1317-72-10-2375>
660

661 de Oliveira Resende R, de Haan P, van de Vossen E, et al (1992) Defective interfering L
662 RNA segments of tomato spotted wilt virus retain both virus genome termini and have
663 extensive internal deletions. *Journal of General Virology* 73:2509–2516.
664 <https://doi.org/10.1099/0022-1317-73-10-2509>
665

666 Gard S, von Magnus P (1947) Studies on interference in experimental influenza:
667 purification and centrifugation experiments. *Ark Kemi Mineral Geologi* 24:1–4.
668

669 Graves MV, Pogany J, Romero J (1996) Defective interfering RNAs and defective
670 viruses associated with multipartite RNA viruses of plants. *Seminars in Virology*
671 7:399–408. <https://doi.org/10.1006/smvv.1996.0048>
672

673 Graves MV, Roossinck MJ (1995) Characterization of defective RNAs derived from
674 RNA 3 of the Fny strain of cucumber mosaic cucumovirus. *Journal of Virology*
675 69:4746–4751. <https://doi.org/10.1128/jvi.69.8.4746-4751.1995>
676

677 Hasiów-Jaroszewska B, Borodynko N, Figlerowicz M, Pospieszny H (2012) Two types
678 of defective RNAs arising from the tomato black ring virus genome. Archives of
679 Virology 157:569–572. <https://doi.org/10.1007/s00705-011-1200-z>
680

681 Hasiów-Jaroszewska B, Minicka J, Zarzyńska-Nowak A, et al (2018) Defective RNA
682 particles derived from Tomato black ring virus genome interfere with the replication of
683 parental virus. Virus Research 250:87–94.
684 <https://doi.org/10.1016/j.virusres.2018.04.010>
685

686 Huang AS, Baltimore D (1970) Defective viral particles and viral disease processes.
687 Nature 226:325–327. <https://doi.org/10.1038/226325a0>
688

689 Inoue-Nagata AK, Jordan R, Kreuze J, et al (2022) ICTV Virus Taxonomy Profile:
690 *Potyviridae* 2022. Journal of General Virology 103:001738.
691 <https://doi.org/10.1099/jgv.0.001738>
692

693 Johnson M, Zaretskaya I, Raytselis Y, et al (2008) NCBI BLAST: a better web interface.
694 Nucleic Acids Research 36. <https://doi.org/10.1093/nar/gkn201>
695

696 Karasev AV, Gray SM (2013) Continuous and emerging challenges of potato virus Y in
697 potato. Annual Review of Phytopathology 51:571–586.
698 <https://doi.org/10.1146/annurev-phyto-082712-102332>
699

700 Karasev AV, Hu X, Brown CJ, et al (2011) Genetic diversity of the ordinary strain of
701 Potato virus Y (PVY) and origin of recombinant PVY strains. Phytopathology
702 101:778–785. <https://doi.org/10.1094/phyto-10-10-0284>
703

704 Knorr DA, Mullin RH, Hearne PQ, Morris TJ (1991) *De novo* generation of defective
705 interfering RNAs of tomato bushy stunt virus by high multiplicity passage. Virology
706 181:193–202. [https://doi.org/10.1016/0042-6822\(91\)90484-S](https://doi.org/10.1016/0042-6822(91)90484-S)
707

708 Koonin EV, Starokadomskyy P (2016) Are viruses alive? The replicator paradigm sheds
709 decisive light on an old but misguided question. *Studies in History and Philosophy of*
710 *Science Part C: Studies in History and Philosophy of Biological and Biomedical*
711 *Sciences* 59:125–134. <https://doi.org/10.1016/j.shpsc.2016.02.016>
712

713 La Scola B, Desnues C, Pagnier I, et al (2008) The virophage as a unique parasite of the
714 giant mimivirus. *Nature* 455:100–104. <https://doi.org/10.1038/nature07218>
715

716 Lazzarini RA, Keene JD, Schubert M (1981) The origins of defective interfering
717 particles of the negative-strand RNA viruses. *Cell* 26:145–154.
718 [https://doi.org/10.1016/0092-8674\(81\)90298-1](https://doi.org/10.1016/0092-8674(81)90298-1)
719

720 Lee PKK, White KA (2014) Construction and characterization of an Aureusvirus
721 defective RNA. *Virology* 452–453:67–74. <https://doi.org/10.1016/j.virol.2013.12.033>
722

723 Li X, Ye Z, Plant EP (2024) 5' copyback defective viral genomes are major component
724 in clinical and non-clinical influenza samples. *Virus Research* 339:199274.
725 <https://doi.org/10.1016/j.virusres.2023.199274>
726

727 Llamas S, Sandoval C, Babin M, et al (2004) Effect of the host and temperature on the
728 formation of defective RNAs associated with broad bean mottle virus infection.
729 *Phytopathology* 94:69–75. <https://doi.org/10.1094/phyto.2004.94.1.69>
730

731 Lukhovitskaya NI, Thaduri S, Garushyants SK, et al (2013) Deciphering the mechanism
732 of defective interfering RNA (DI RNA) biogenesis reveals that a viral protein and the
733 DI RNA act antagonistically in virus infection. *Journal of Virology* 87:6091–6103.
734 <https://doi.org/10.1128/jvi.03322-12>
735

736 Mondal S, Wintermantel WM, Gray SM (2023) Infection dynamics of potato virus Y
737 isolate combinations in three potato cultivars. *Plant Disease* 107:157–166.
738 <https://doi.org/10.1094/pdis-09-21-1980-re>
739

740 Olmo-Uceda MJ, Muñoz-Sánchez JC, Lasso-Giraldo W, et al (2022) DVGfinder: a
741 metasearch tool for identifying defective viral genomes in RNA-seq data. *Viruses* 14.
742 <https://doi.org/10.3390/v14051114>
743

744 Omarov RT, Rezende JAM, Scholthof HB (2004) Host-specific generation and
745 maintenance of tomato bushy stunt virus defective interfering RNAs. *molecular*
746 *plant-microbe interactions* 17:195–201. <https://doi.org/10.1094/mpmi.2004.17.2.195>
747

748 Pathak KB, Nagy PD (2009) Defective Interfering RNAs: foes of viruses and friends of
749 virologists. *Viruses* 1:895–919. <https://doi.org/10.3390/v1030895>
750

751 Pogany J, Romero J, Huang Q, et al (1995) *De novo* generation of defective
752 interfering-like RNAs in broad bean mottle bromovirus. *Virology* 212:574–586.
753 <https://doi.org/10.1006/viro.1995.1515>
754

755 Posit team (2024) RStudio: integrated development environment for R. Posit Software,
756 PBC, Boston, MA.
757

758 Rabinowitz SG, Huprikar J (1979) The influence of defective-interfering particles of the
759 PR-8 strain of influenza A virus on the pathogenesis of pulmonary infection in mice.
760 *Journal of Infectious Diseases* 140:305–315. <https://doi.org/10.1093/infdis/140.3.305>
761

762 Rezelj VV, Carrau L, Merwaiss F, et al (2021) Defective viral genomes as therapeutic
763 interfering particles against flavivirus infection in mammalian and mosquito hosts.
764 *Nature Communications* 12:2290. <https://doi.org/10.1038/s41467-021-22341-7>
765

766 Roossinck MJ (1997) Mechanisms of plant virus evolution. *Annual Review of*
767 *Phytopathology* 35:191–209. <https://doi.org/10.1146/annurev.phyto.35.1.191>
768

769 Routh A, Johnson JE (2014) Discovery of functional genomic motifs in viruses with
770 ViReMa—a Virus Recombination Mapper—for analysis of next-generation sequencing
771 data. *Nucleic Acids Research* 42:e11–e11. <https://doi.org/10.1093/nar/gkt916>

772

773 Rubio L, Tian T, Yeh H, et al (2002) *De novo* generation of lettuce infectious yellows
774 virus defective RNAs in protoplasts. *Molecular Plant Pathology* 3:321–327.
775 <https://doi.org/10.1046/j.1364-3703.2002.00125.x>

776

777 Rubio L, Yeh H-H, Tian T, Falk BW (2000) A heterogeneous population of defective
778 RNAs is associated with lettuce infectious yellows virus. *Virology* 271:205–212.
779 <https://doi.org/10.1006/viro.2000.0318>

780

781 Sanjuán R, Agudelo-Romero P, Elena SF (2009) Upper-limit mutation rate estimation
782 for a plant RNA virus. *Biology Letters* 5:394–396.
783 <https://doi.org/10.1098/rsbl.2008.0762>

784

785 Sanjuán R, Domingo-Calap P (2021) Genetic diversity and evolution of viral
786 populations. In: *Encyclopedia of Virology*. Elsevier, pp 53–61

787

788 Singh RP, Valkonen JPT, Gray SM, et al (2008) Discussion paper: the naming of Potato
789 virus Y strains infecting potato. *Archives of Virology* 153:1–13.
790 <https://doi.org/10.1007/s00705-007-1059-1>

791

792 Szittyá G, Molnár A, Silhavy D, et al (2002) Short defective interfering RNAs of
793 tombusviruses are not targeted but trigger post-transcriptional gene silencing against
794 their helper virus. *Plant Cell* 14:359–372. <https://doi.org/10.1105/tpc.010366>

795

796 Taiz L, Zeiger E, Møller IM, Murphy AS (2015) *Plant physiology and development*, 6th
797 ed. Sinauer Associates, Incorporated, Publishers.

798

799 Torrance L, Cowan GH, Sokmen MA, Reavy B (1999) A naturally occurring deleted
800 form of RNA 2 of potato mop-top virus. *Journal of General Virology* 80:2211–2215.
801 <https://doi.org/10.1099/0022-1317-80-8-2211>

802

803 Tromas N, Zwart MP, Maïté P, Elena, SF (2014) Estimation of the *in vivo* recombination
804 rate for a plant RNA virus. *Journal of General Virology* 95:724-732. [https://doi.org/](https://doi.org/10.1099/vir.0.060822-0)
805 10.1099/vir.0.060822-0

806

807 Vignuzzi M, López CB (2019) Defective viral genomes are key drivers of the virus–host
808 interaction. *Nature Microbiology* 4:1075–1087.
809 <https://doi.org/10.1038/s41564-019-0465-y>

810

811 Visser PB, Brown DJF, Brederode FTh, Bol JF (1999) Nematode transmission of
812 tobacco rattle virus serves as a bottleneck to clear the virus population from defective
813 interfering RNAs. *Virology* 263:155–165. <https://doi.org/10.1006/viro.1999.9901>

814

815 von Magnus P (1954) Incomplete Forms of Influenza Virus. *Advances in Virus*
816 *Research* 2:59-79. [https://doi.org/ 10.1016/s0065-3527\(08\)60529-1](https://doi.org/10.1016/s0065-3527(08)60529-1)

817

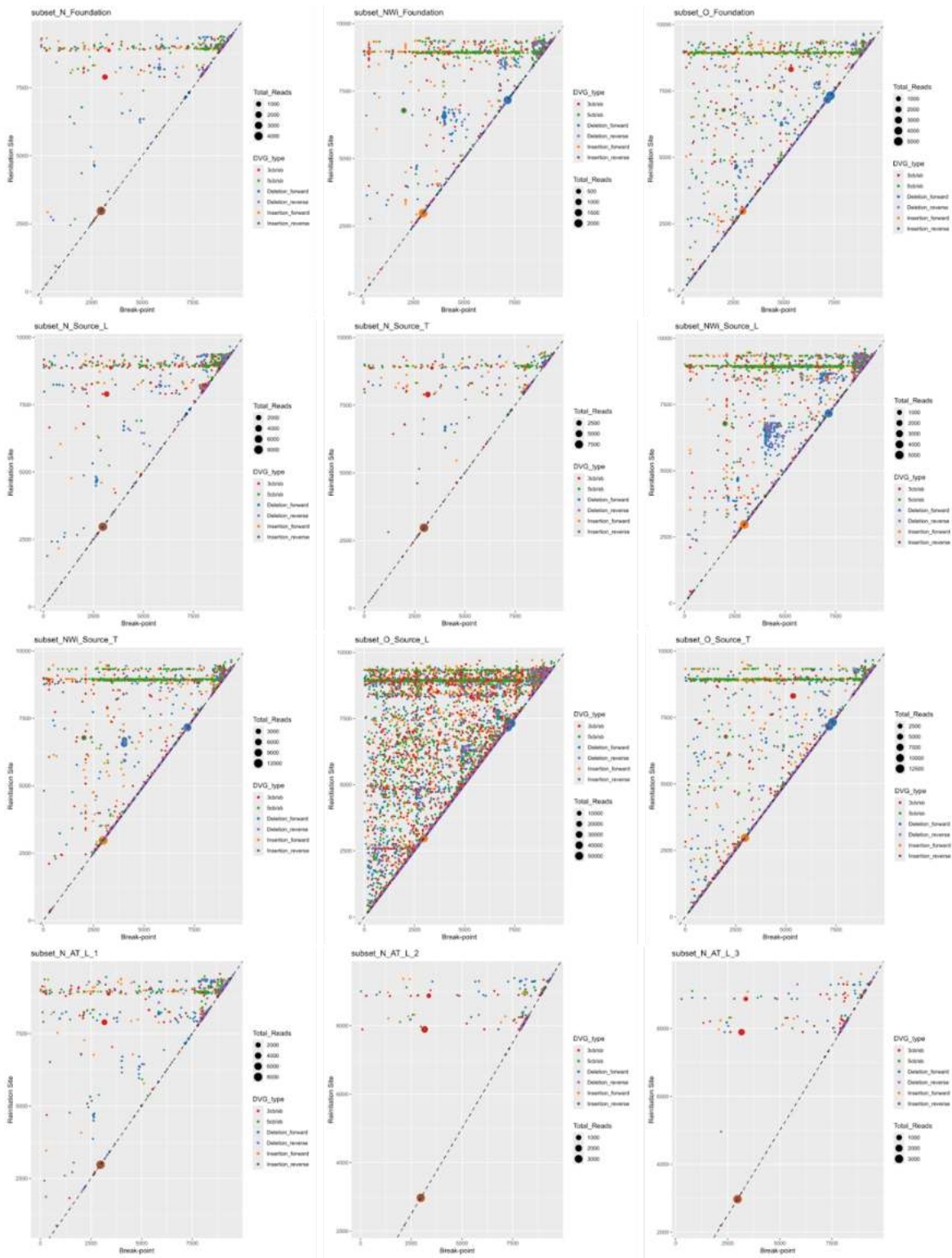
818 White KA, Bancroft JB, Mackie GA (1992) Coding capacity determines *in vivo*
819 accumulation of a defective RNA of clover yellow mosaic virus. *Journal of Virology*
820 66:3069–3076. <https://doi.org/10.1128/jvi.66.5.3069-3076.1992>

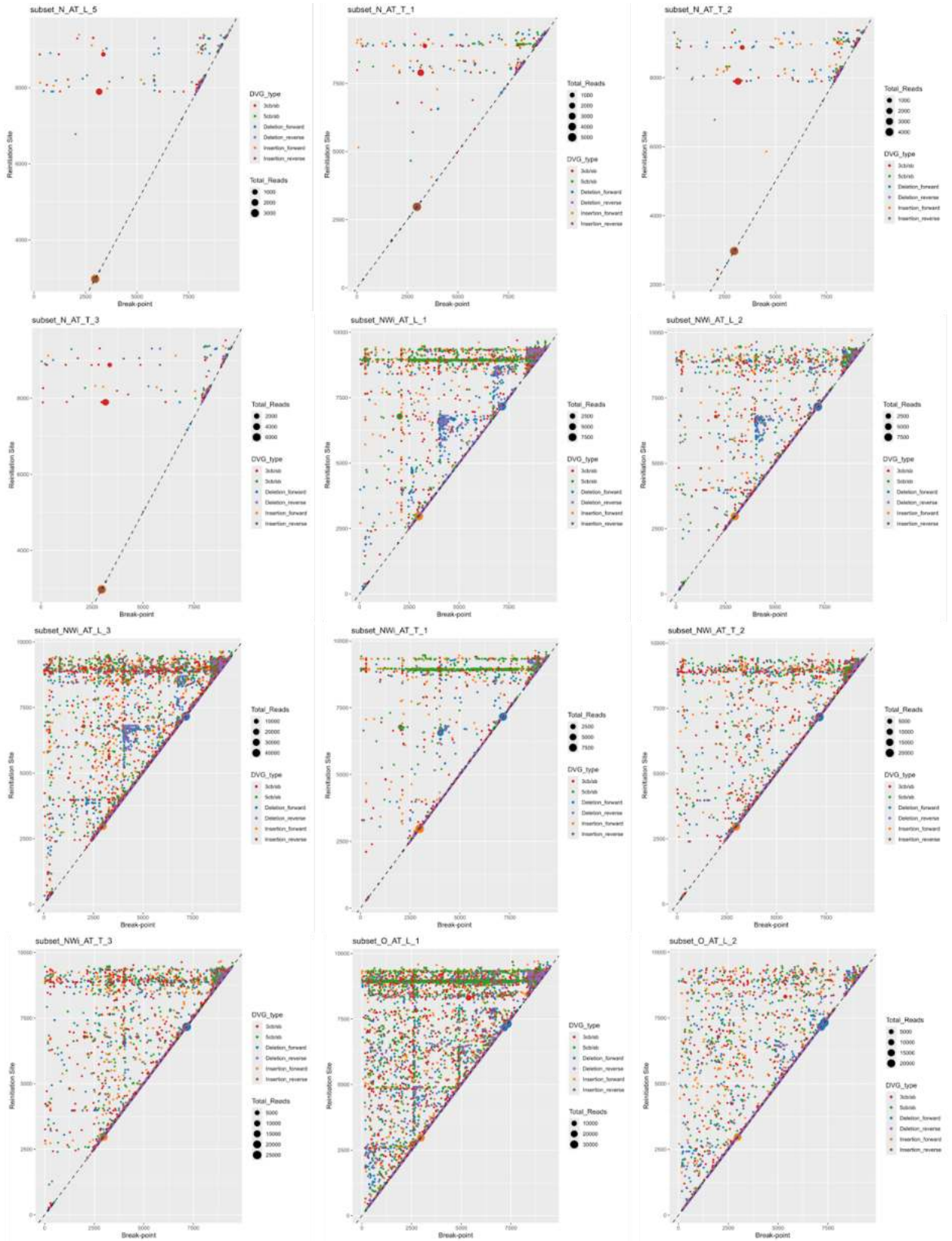
821

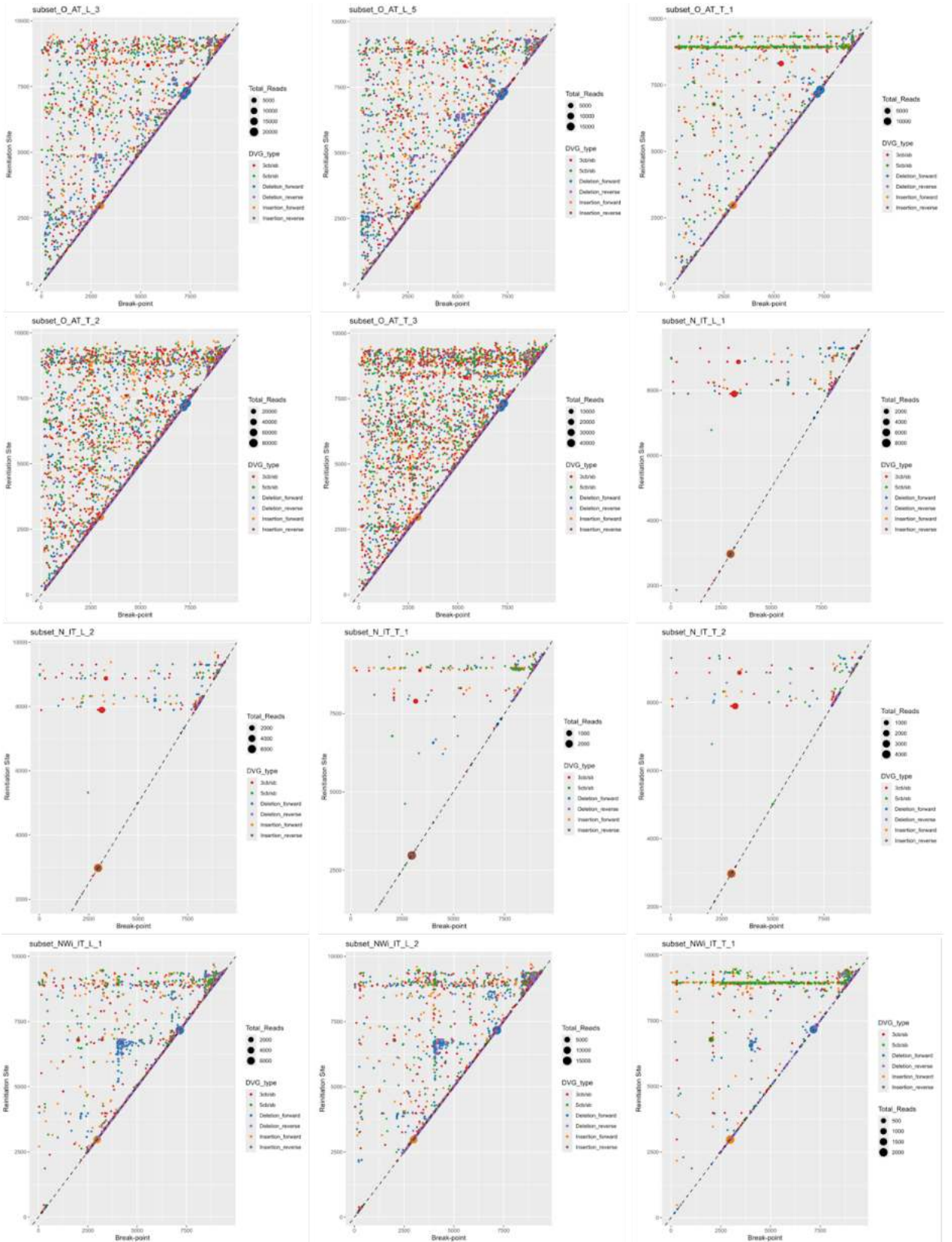
822 Wickham H (2016) *Ggplot2: elegant graphics for data analysis*, 2nd ed. Springer
823 International Publishing, Cham, Switzerland.

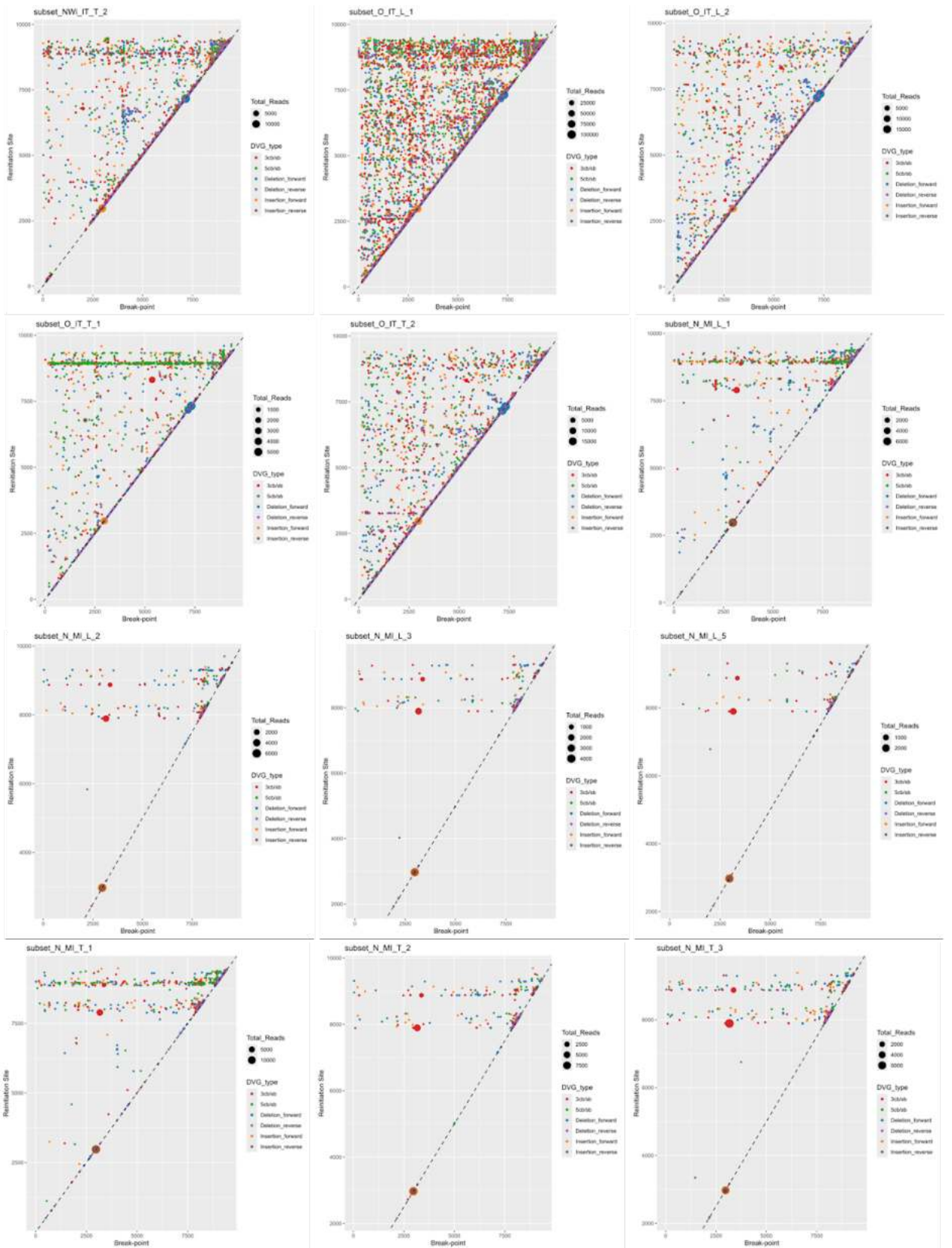
824

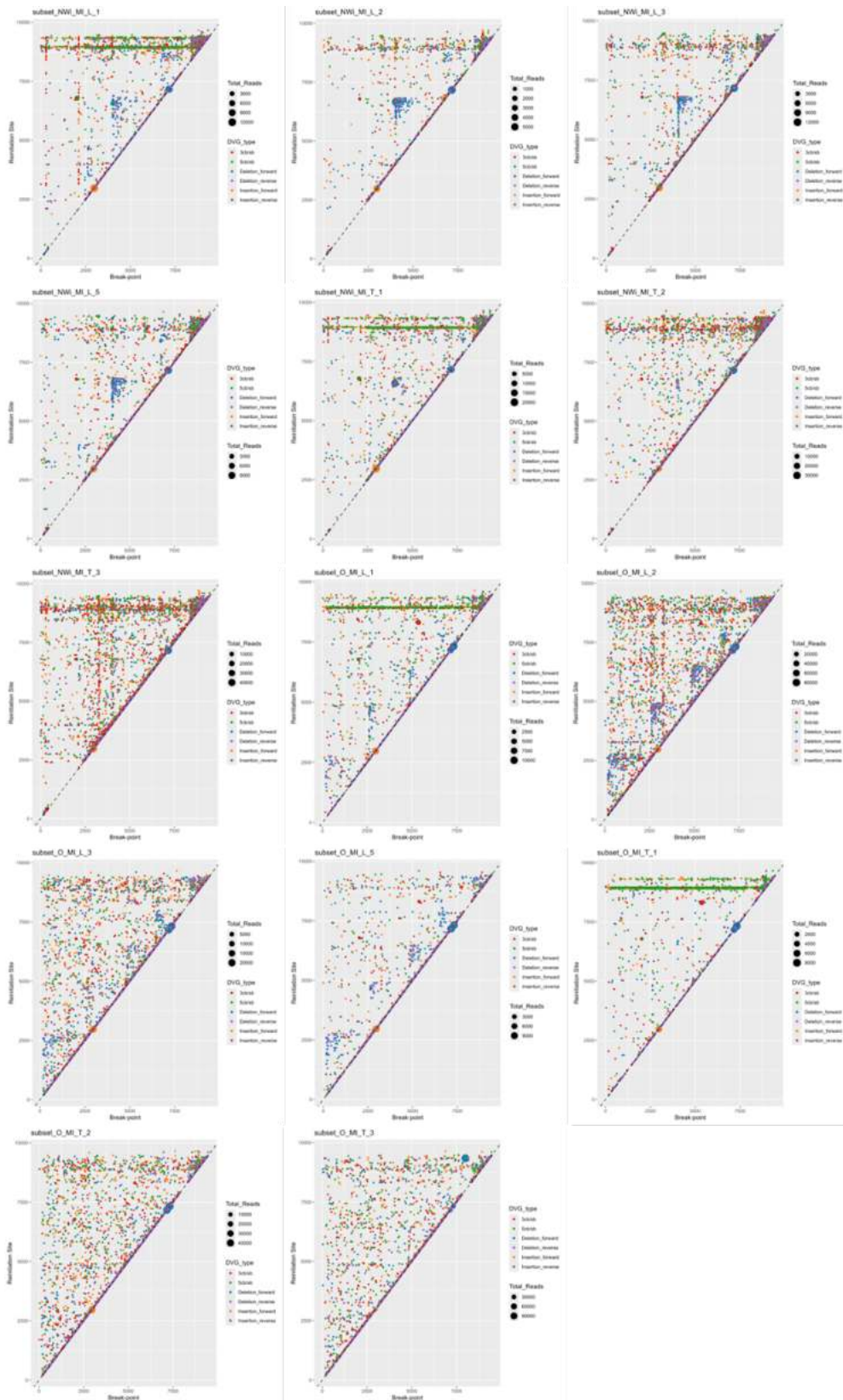
825 Xiao Y, Lidsky PV., Shirogane Y, et al (2021) A defective viral genome strategy elicits
826 broad protective immunity against respiratory viruses. *Cell* 184:6037-6051.e14.
827 <https://doi.org/10.1016/j.cell.2021.11.023>







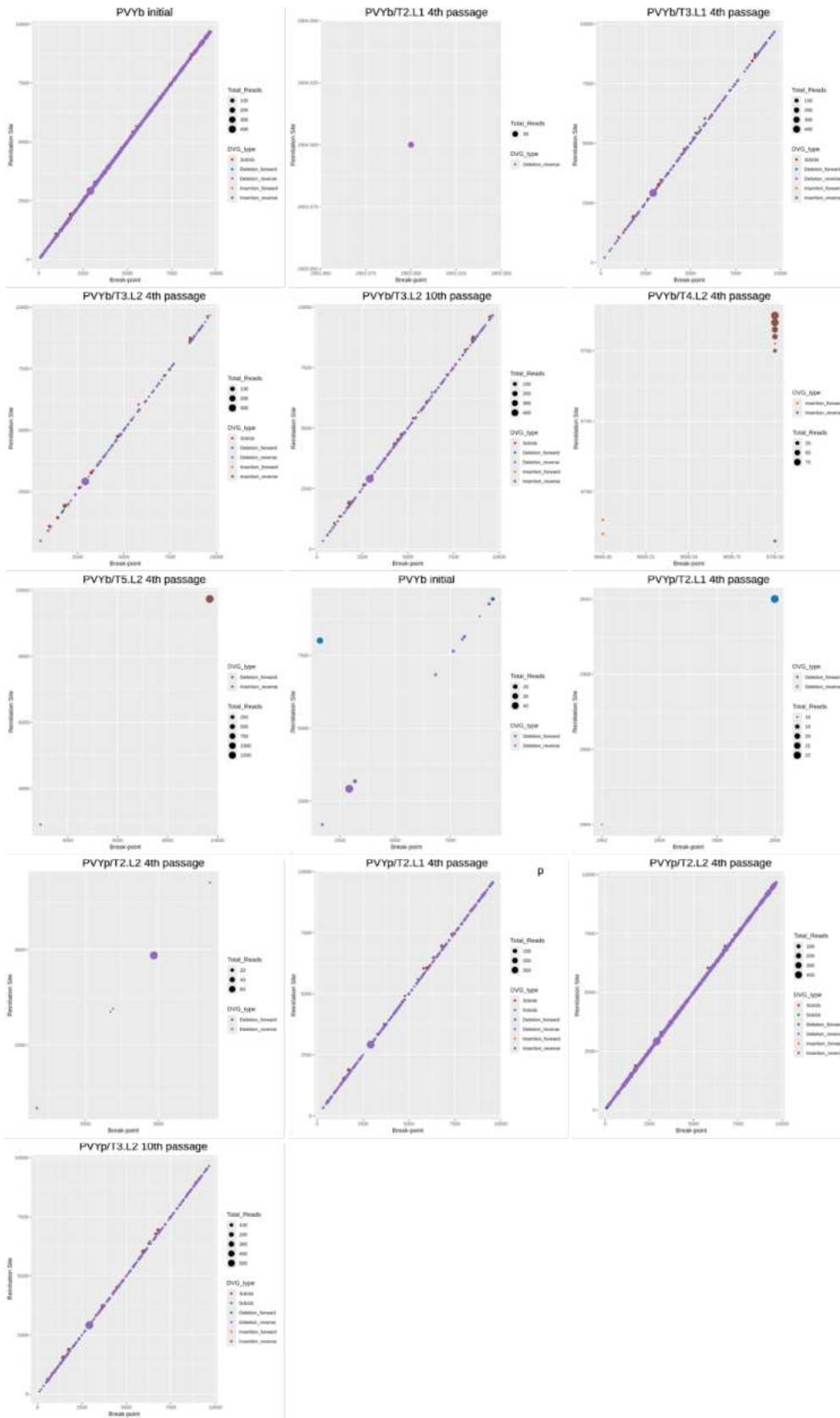




833

834 **Sup Fig 1.** DVGs conformation to each population, divided by strain (O, N or NWi),
 835 type of transmission (AT, MI or IT), plant organ (L or T) and passage (1-5) of first

836 dataset, obtained in (da Silva, 2020). Each point represents a mapped read against the
837 reference genome of PVY (X12456).



839 **Sup Fig 2.** DVGs conformation to each population, divided by two PVY isolates
840 (PVYNb and PVYSt), treatment (Sl, St, Nb, CTF and MIX) and number of passages (1st
841 to 10th) of second dataset, same as used in the Chapter III. Each point represents a
842 mapped read.

843 **Sup. Table 1.** Total number of reads that mapped against the PVY reference genome
844 using ViReMa-A and the number of DVGs found in each population to the first dataset.

Virus	Strain	Transmission			Reads count	
		mode	Organ	Passage	ViReMa-A	Number of DVGs
PVY	N			Foundation	9078	714
PVY	N		L	Source	16409	1206
PVY	N		T	Source	17974	731
PVY	N	AT	L	1	16608	1140
PVY	N	AT	L	2	6959	453
PVY	N	AT	L	3	5717	401
PVY	N	AT	L	5	6098	414
PVY	N	AT	T	1	10421	645
PVY	N	AT	T	2	8421	567
PVY	N	AT	T	3	11858	376
PVY	N	IT	L	1	13814	487
PVY	N	IT	L	2	11225	635
PVY	N	IT	T	1	5787	446
PVY	N	IT	T	2	7209	400
PVY	N	MI	L	1	17014	1519
PVY	N	MI	L	2	9947	563
PVY	N	MI	L	3	7320	537
PVY	N	MI	L	5	4958	354
PVY	N	MI	T	1	25376	1287
PVY	N	MI	T	2	16323	655
PVY	N	MI	T	3	11216	809
PVY	N-Wi			Foundation	5883	1538
PVY	N-Wi		L	Source	13290	3302
PVY	N-Wi		T	Source	29333	2577
PVY	N-Wi	AT	L	1	23094	4230
PVY	N-Wi	AT	L	2	20875	3052
PVY	N-Wi	AT	L	3	106606	9642
PVY	N-Wi	AT	L	5	37130	2630

PVY	N-Wi	AT	T	1	22524	2939
PVY	N-Wi	AT	T	2	48376	4441
PVY	N-Wi	AT	T	3	56586	4886
PVY	N-Wi	IT	L	1	16762	2521
PVY	N-Wi	IT	L	2	35662	2889
PVY	N-Wi	IT	T	1	5325	1305
PVY	N-Wi	IT	T	2	3220	4296
PVY	N-Wi	MI	L	1	29545	4307
PVY	N-Wi	MI	L	2	16878	2656
PVY	N-Wi	MI	L	3	25552	3231
PVY	N-Wi	MI	L	5	25227	3256
PVY	N-Wi	MI	T	1	57056	4210
PVY	N-Wi	MI	T	2	66610	5056
PVY	N-Wi	MI	T	3	101846	8278
PVY	O			Foundation	12939	1743
PVY	O		L	Source	174904	11311
PVY	O		T	Source	37556	2773
PVY	O	AT	L	1	98431	11310
PVY	O	AT	L	2	70946	4526
PVY	O	AT	L	3	60976	4917
PVY	O	AT	L	5	54190	4706
PVY	O	AT	T	1	37980	2505
PVY	O	AT	T	2	244520	7948
PVY	O	AT	T	3	140772	7348
PVY	O	IT	L	1	260815	10606
PVY	O	IT	L	2	55415	3998
PVY	O	IT	T	1	15016	2196
PVY	O	IT	T	2	55350	4196
PVY	O	MI	L	1	31045	3363
PVY	O	MI	L	2	252454	7868
PVY	O	MI	L	3	72229	5498
PVY	O	MI	L	5	37005	3063

PVY	O	MI	T	1	21571	3613
PVY	O	MI	T	2	142749	6165
PVY	O	MI	T	3	86750	4818

845

846 **Sup Table 2.** Total number of reads that mapped against the PVY reference genome
847 using ViReMa-A and the number of DVGs found in each population to the second
848 dataset.

Virus	Treatment	Line	Passage	Host	Reads	count
					ViReMa-A	Number of DVGs
PVYN				Benthamian		
b	Initial			a	80679	22557
PVYN						
b	St	L1	4	Potato	1231	1312
PVYN				Benthamian		
b	Nb	L1	4	a	31936	19304
PVYN				Benthamian		
b	Nb	L2	4	a	21145	11744
PVYN				Benthamian		
b	Nb	L2	10	a	24171	10464
PVYN						
b	CTF	L1	4	Tomato	92	97
PVYN						
b	CTF	L2	4	Tomato	758	280
PVYN						
b	MIX	L2	4	Mix	3728	594
PVYSt	Initial			Potato	7454	4154
PVYSt	Sl	L1	4	Tomato	23	19
PVYSt	St	L1	4	Potato	2094	1501
PVYSt	St	L2	4	Potato	4192	2592
				Benthamian		
PVYSt	Nb	L1	4	a	34921	20503
				Benthamian		
PVYSt	Nb	L2	4	a	92179	28032
				Benthamian		
PVYSt	Nb	L2	10	a	28378	13067

849

1 **Concluding remarks**

2

3 As the global population grows, so does the need for increased food production.
4 However, various factors can affecting the productivity of cultivated plants, with viruses
5 posing a significant challenge. PVY has long been known as an obstacle to sustainable
6 agriculture, and addressing the development of crops with high resistance to PVY
7 infection was always one of the top priorities. The most relevant challenges though are
8 the lack of resistance sources for a specific crop (*e.g.*, potatoes) and the emergence of
9 the so-called resistance-breaking isolates.

10 Our research employed diverse approaches to uncover the genetic variations and
11 phenotypic impacts of different PVY isolates on various hosts. We focused on
12 understanding the importance of identifying isolates from different crops, as even
13 isolates of the same species can yield vastly different results in experimental settings.
14 While genetic differences in PVY are influenced by multiple factors, we were
15 specifically interested on the role of the host. From some advances in these aspects,
16 future research should aim to unravel the molecular mechanisms that determine an
17 isolate's ability to infect a particular host. This knowledge is vital for crafting effective
18 resistance strategies.

19 In addition to exploring PVY genetic diversity, we wanted to facilitate generation
20 of genome data by producing an easy and fast protocol. We found out that Nanopore
21 sequencing technology offers a promising alternative, providing rapid, cost-effective,
22 and accurate results comparable to Illumina sequencing.

23 There are still unresolved questions that need further investigation, such as
24 identifying the most affected genomic regions during host switching and understanding
25 the molecular interactions between viral and host factors. This includes studying the
26 structural roles of proteins and intrinsically disordered proteins, as well as assessing the
27 current level of protection in potato cultivars against PVY. These insights may be gained
28 through a deeper analysis of the genome. Notably, we have detected the formation of
29 DVGs in PVY populations for the first time. While this discovery requires further
30 validation, it may represent the first step for developing new non-transgenic control
31 strategies, which is one of our goals.

32 We have not yet answered all the questions posed at the outset of this research, but
33 we believe our findings provide a crucial foundation for understanding and mitigating
34 the impact of PVY on agriculture. Our study lays the groundwork for future research
35 and control measures, including the development of resistant cultivars, targeted antiviral
36 treatments, and integrated pest management strategies.